Oxidant production and disinfection by-product formation during chlorine photolysis

By

Devon Marie Manley Bulman

A dissertation submitted in partial fulfillment of

the requirements for the degree of

Doctor of Philosophy

(Environmental Chemistry and Technology Program)

at the

UNIVERSITY OF WISCONSIN-MADISON

2020

Date of final oral examination: 07/23/2020

The dissertation is approved by the following members of the Final Oral Committee:
Christina K. Remucal, Associate Professor, Civil and Environmental Engineering
Matthew Ginder-Vogel, Associate Professor, Civil and Environmental Engineering
James P. Hurley, Professor, Civil and Environmental Engineering
Greg Harrington, Professor, Civil and Environmental Engineering
Joel A. Pedersen, Professor, Soil Science

Abstract

Oxidant production and disinfection by-product formation during chlorine photolysis

By

Devon Marie Manley Bulman

Doctor of Philosophy - Environmental Chemistry and Technology Program

University of Wisconsin-Madison

Associate Professor Christina K. Remucal

Chlorine photolysis is an advanced oxidation process used to degrade organic contaminants in water. Ultraviolet photolysis of free chlorine (i.e., the mixture of hypochlorous acid and hypochlorite) results in the formation of a suite of reactive oxidants including hydroxyl radical, chlorine radical, and ozone. The photochemistry of hypochlorous acid and hypochlorite impacts the distribution of reactive oxidants formed under different treatment conditions. Observed chlorine loss rate constants increase with pH during irradiation with long wavelengths due to the higher molar absorptivity of hypochlorite. The steady-state concentration of the two primary oxidants, hydroxyl radical and chlorine radical, is highest at low pH and wavelength. Ozone generation is observed under all conditions, despite the assumption in previous studies that ozone does not form during photolysis at 254 nm. A comprehensive kinetic model is compared against experimental data and generally predicts the trends in chlorine loss and oxidant concentrations. However, a comparison of previously published kinetic models demonstrates the challenges of modeling this complex system.

Light, free chlorine, and reactive oxidants can react with naturally occurring dissolved organic matter to form potentially harmful disinfection by-products. Chlorine loss rate constants

increase in the presence of dissolved organic matter due to the formation of carbon-centered radicals. Oxidant steady-state concentrations decrease in natural waters due to radical scavenging by organic and inorganic carbon. High-resolution mass spectrometry shows that chlorine photolysis produces dissolved organic matter that is more aliphatic in nature and contains novel high molecular weight chlorinated disinfection by-products. The high molecular weight chlorinated disinfection by-products form via direct halogenation by reactive chlorine species and from dissolved organic matter transformation, primarily due to direct photolysis, that produces dissolved organic matter that is more reactive with chlorine. Quenching experiments demonstrate that reactive chlorine species are partially responsible for the formation of halogenated DOM, haloacetic acids, and haloacetonitriles. Trihalomethane concentrations decrease relative to dark chlorination due to decreased chlorine contact time.

The presence of bromide in this system could result in the formation of brominated disinfection by-products, which are more toxic than their chlorinated analogues. Therefore, research is proposed for the investigation of the impact of bromide on disinfection by-product formation during chlorine photolysis. Probe measurements of reactive oxidants, measurement of small aliphatic and inorganic disinfection by-products, and bulk and molecular measurements of dissolved organic matter will be used to determine the impact of bromide on oxidant and disinfection by-product formation during chlorine photolysis.

Acknowledgements

Though this dissertation carries my name alone, nothing happens in a vacuum. I would like to take the space here to thank and acknowledge all those who have helped me get to this point.

To my advisor, Christy Remucal, a simple “thanks” is not enough for all of the support and help you have given to me, and to all of your students, throughout the years. You are the intimidating kind of smart. That combined with your incredible kindness, efficiency, ability to balance life’s many challenges, and unyielding support of the Oxford comma make you the person I want to be when I grow up. I truly believe that you are the perfect advisor, you see each student as an important individual and tailor your support and advising style to them.

I would like to thank my committee for their insight and support. To Matt Ginder-Vogel for always keeping me honest, and for making me feel heard. To Jim Hurley for always putting my work in a broader context, and for believing in the value of this program. To Joel Pedersen for reminding me to think about the fundamental chemistry, and for being interested in the person behind the student. To Greg Harrington for reminding me to think about where the water goes next and reminding me that it is all connected, and for travelling across campus with a broken foot to start up your treatment plant whenever I needed more sample.

Thanks to Steve Mezyk for inviting me to the Notre Dame Radiation Laboratory and teaching me all about pulse radiolysis and reminding me that I deserve to be here in a time when I doubted myself.

The community at the Water Science and Engineering Laboratory is unique, people like each other and support each other, and we celebrate victories together because we are a family. The relationships I have built there and the laughs we have shared are some of my most treasured

memories from my time in Madison. I hope that I am always able to work with a group of people like you, who I so genuinely enjoy spending time with.

Chris Worley and James Lazarcik deserve a special thanks. They deal with so much every day, from flooding basements to overheating rooms, but they will still drop anything to help a student. James, I have particularly enjoyed working with you. You are the only other person who loves taking things apart as much as I do.

These past five years have been hard, and without the support of my family and friends I am not confident that I would have made it through. Emma, Steph, and Sarah, between random twenty-minute conversations in the halls to Friday night happy hours you have helped me grow both as a person and as a scientist. Sarah, Elle, and Eden, you remind me that there is a world outside of grad school and outside of Madison, thank you for keeping me grounded. Anthony, Tylor, Emma, and Becca never has a group of people made me feel so comfortable being myself.

To my family, especially my parents and grandparents. You have made me the person I am today. You have always believed in me and supported me. I never even considered that there was anything I couldn't do because you raised me to be sure of my abilities.

To my teammate, partner, best friend, and husband. Jeremy you are essential to me. You encourage me to grow, but accept me as I am. I can't imagine the last nine years without you. This hasn't been easy for either of us, but every moment of joy and every struggle have made us more confident in each other. After this I know that we can do anything together.

Table of Contents

List of Figures

List of Tables

List of Schematics

List of Symbols and Abbreviations

AOP	advanced oxidation process
$^{\bullet}OH$	hydroxyl radical
HOCl	hypochlorous acid
OCl^-	hypochlorite
DBP	disinfection by-product
DOM	dissolved organic matter
k	rate constant
H_2O_2	hydrogen peroxide
O_3	ozone
pK_a	acid dissociation constant
ε	molar absorptivity
$O(^1D)$	excited state oxygen atom
$O(^3P)$	excited state oxygen atom
$Cl_2^{\bullet-}$	dichloride radical anion
RCS	reactive chlorine species
RHS	reactive halogen species
RBS	reactive bromine species
$Cl^{\bullet}$	chlorine radical
λ	wavelength
hν	photolysis
FAC	free available chlorine
PPCPs	pharmaceuticals and personal care products
LP UV	monochromatic light at 254 nm
MP UV	polychromatic light ranging from 200 - 400 nm
Φ	quantum yield
HOBr	hypobromous acid
OBr^-	hypobromite
[DOC]	concentration of dissolved organic carbon
THMs	trihalomethanes
HAAs	haloacetic acids
HANs	haloacetonitriles
TOX	total organic halide
MCL	maximum contaminant level
N-DBP	nitrogen-containing disinfection by-product
$[^{\bullet}OH]_{ss}$	hydroxyl radical steady-state concentration
$[Cl^{\bullet}]_{ss}$	chlorine radical steady-state concentration
FT-ICR MS	Fourier-transform ion cyclotron resonance mass spectrometry
TMW	treated Mendota water
$SUVA_{254}$	ratio of specific UV absorbance at 254 nm and dissolved organic carbon concentration
H:C	hydrogen to carbon ratio
O:C	oxygen to carbon ratio
$H:C_w$	relative intensity weighted hydrogen to carbon ratio
$O:C_w$	relative intensity weighted oxygen to carbon ratio
DBE/C_w	relative intensity weighted double bond equivalents per carbon
PCA	principle component analysis

$k_{obs,FAC}$, $k_{obs,chlorine}$	observe chlorine loss rate constant
TMB	1,3,5-trimethoxybenzene

Chapter 1

Introduction

1.1 Motivation

Organic contaminants such as pharmaceuticals, pesticides, and personal care products are common in drinking water sources around the world.[1–6] These contaminants present a threat to human[7–9] and ecosystem[10–12] health and are not removed by conventional drinking water[1–6] or wastewater[13–16] treatment. Advanced oxidation processes (AOPs), such as chlorine photolysis, are designed to remove organic contaminants and may be applied in conventional treatment trains.

Chlorine photolysis degrades organic contaminants through the production of hydroxyl radical ($^{\bullet}OH$) and a suite of other reactive oxidants.[17–21] Chlorine, which is the mixture of hypochlorous acid (HOCl) and hypochlorite (OCl^-), commonly referred to as free available chlorine and is frequently used for disinfection in the U.S. Previous investigations of this system have focused primarily on contaminant degradation[17–19,21–24] with some measurement of small aliphatic disinfection by-product (DBP) formation.[25–36] The numerous contaminant degradation studies typically use light in the UV-C region (i.e., 254 nm) and do not provide mechanistic information on oxidant production or subsequent reaction with naturally occurring dissolved organic matter (DOM) to form halogenated DBPs. The work presented in this dissertation evaluates how solution pH and irradiation wavelength affect the formation of reactive oxidants during chlorine photolysis and how free available chlorine, free available bromine, light, and reactive halogen species transform DOM and form DBPs.

1.*2 Contaminants in Drinking Water*

Organic contaminants are released into the environment through urban and agricultural runoff,[15,37,38] landfill leachate,[39] and intentional application.[40,41] Additionally, many organic compounds that enter into wastewater treatment plants are not removed and are released in secondary effluent.[13–16,37,42–46] Many organic contaminants are not readily degraded in the environment[43,47,48] and, as a result, are found in both surface water and groundwater.[15,49] Organic contaminants have even been detected in rainwater.[50]

Organic contaminants fall into many classes of compounds including pharmaceuticals, pesticides, and personal care products, and have important implications for human and ecosystem health. Many pharmaceutical compounds, particularly antibiotics, can change the dynamics of stream ecosystems even at low concentrations.[10–12] Even the compounds that are not toxic at low concentrations can impact organisms higher in the food chain as some organic contaminants biomagnify.[51] The risk to human health is poorly understood due to the vast number of organic contaminants, but pharmaceutical compounds present in drinking water have a possible toxicity risk.[7,45] Even if the toxicity risk of an individual contaminant is generally low, many researchers are concerned with the synergistic effects of so many compounds present together.[7–9]

Although some organic contaminants can react with chlorine[52–57] or sorb to activated carbon filters,[11,58] other compounds are not readily removed by drinking water treatment and [11,52]are still found in drinking water.[5] Hundreds of organic contaminants have been found in treated drinking water through the distribution system and out the tap across the U.S. and Europe.[1–6] While only a small number of organic chemicals are currently regulated in drinking water in the U.S., many researchers are investigating ways to remove organic contaminants from drinking water due to anticipated future regulations.

1.3 Advanced Oxidation Processes

Advanced oxidation processes are designed to remove organic contaminants through the production of •OH. •OH oxidizes organic contaminants through multiple mechanisms including hydroxylation, H-atom abstraction, electron-transfer, and ring cleavage reactions.[14,59–62] Many studies have demonstrated removal of organic contaminants through reaction with •OH as this oxidant is unselective and reacts quickly with many organic compounds (k = 10^9 - 10^{10} M^{-1} s^{-1}).[14,21,59,60,63–68] There are many different methods for generating •OH in water treatment applications, including mixed oxidant methods, electrochemical generation, photocatalysis, and oxidant photolysis.

Mixed oxidant AOPs generate hydroxyl radical after addition of two oxidants into the drinking water. Fenton's reaction is a well-established process where the reaction of iron(II) and hydrogen peroxide (H_2O_2) generates •OH under acidic conditions.[69,70] The other primary mixed oxidant AOP is ozone (O_3)/H_2O_2, which is effective[71,72] but requires on-site O_3 generation and runs the risk of *N*-nitrosodimethylamine (NDMA) formation.[72] Photocatalytic AOPs utilize photolysis of a metal oxide particle or nanoparticle, such as titanium dioxide (TiO_2)[73,74] or bismuth phosphate,[75] but recent work highlights the limitations in applying this approach to municipal water treatment.[76] Electrochemical AOPs are currently limited to bench-scale applications and can degrade organic contaminants through direct electron transfer or by generating radical species, namely •OH.[65,77–82 73,75]

Photochemical AOPs[17,19,21,24,25,62,83–88] generate reactive oxidant such as •OH or sulfate radical ($SO_4^{\bullet-}$) through photolysis of oxidants such as chlorine,[17,19,21,24,25,62,83–88] chloramine (NH_3Cl),[17,22,89] H_2O_2,[63,66,68,71,72,89–92] or persulfate.[85,89] Chlorine photolysis was selected as AOP of interest for this research because free chlorine is cost effective and could easily be applied after

conventional disinfection using chlorine.[72,93] Additionally, chlorine photolyzes at wavelengths in the solar spectrum making solar treatment applications feasible.[23,94–99]

1.4 Chlorine Photolysis Chemistry

1.4.1 Chlorine Speciation

Free available chlorine is the mixture of hypochlorous acid (HOCl) and hypochlorite (OCl^-) and is generated by reacting Cl_2 gas with water. Hypochlorous acid has an acid dissociation constant (pK_a) of 7.5 (Reaction 1.1), meaning both the acid and base forms of the molecule are present under most water treatment applications. HOCl is a stronger oxidant and is capable of degrading more organic contaminants than OCl^-.[13]

$$HOCl \leftrightharpoons OCl^- + H^+ \qquad (1.1)$$

1.4.2 Homolytic Cleavage of Chlorine

Photolysis of free available chlorine results in the homolytic cleavage of hypochlorous acid or hypochlorite.[87,100–102] Photochemistry is driven by molar absorptivity (ε) and quantum yield, which are both wavelength dependent. Molar absorptivity defines much light is absorbed by a molecule, while quantum yield is the efficiency of undergoing a particular reaction per photon of light absorbs. OCl^- has a higher molar absorptivity than HOCl at wavelengths longer than 254 nm, while the molar absorptivity is roughly equivalent at 254 nm ($\varepsilon_{HOCl,254}$ = 59 M^{-1} cm^{-1}, $\varepsilon_{OCl^-,254}$ = 66 M^{-1} cm^{-1}).[99,102] HOCl produces hydroxyl radical and chlorine radical with a wavelength-dependent quantum yield (Reaction 1.2).[17,87,103] OCl^- undergoes more complex chemistry and photolyzes to form either the oxide radical anion ($O^{\bullet-}$; Reaction 1.3) or one of two excited states of oxygen (i.e.,

$O(^1D)$ or $O(^3P)$; Reactions 1.4 and 1.5) in addition to chlorine radical.[101] The dominant OCl^- photolysis pathway varies with wavelength.[17,101]

$$HOCl + h\nu \leftrightharpoons {}^{\bullet}OH + Cl^{\bullet} \quad (1.2)$$

$$OCl^- + h\nu \leftrightharpoons O^{\bullet-} + Cl^{\bullet} \quad (1.3)$$

$$OCl^- + h\nu \leftrightharpoons O(^1D) + Cl^{\bullet} \quad (1.4)$$

$$OCl^- + h\nu \leftrightharpoons O(^3P) + Cl^{\bullet} \quad (1.5)$$

1.4.3 Formation of Secondary Oxidants

The primary oxidants generated by chlorine photolysis can undergo subsequent reactions to form secondary oxidants. These secondary oxidants are $^{\bullet}OH$, dichloride radical anion ($Cl_2^{\bullet-}$), and hypochlorite radical ($ClO^{\bullet}$), along with O_3, which is understudied compared with the $^{\bullet}OH$, $Cl^{\bullet}$, $Cl_2^{\bullet-}$, and $ClO^{\bullet}$.[19,21,97] $^{\bullet}OH$ is both a primary oxidant, formed from the homolytic cleavage of free chlorine, and a secondary oxidant formed from the reaction of $O(^1D)$ with water (Reaction 1.6). $Cl_2^{\bullet-}$ forms from reaction of $Cl^{\bullet}$ with Cl^- (Reaction 1.7) and is more selective than $Cl^{\bullet}$, but can react quickly with some organic contaminants ($k_{Cl} = 10^9$ - 10^{10} M^{-1} s^{-1}, $k_{Cl2\bullet-} = 10^6$ - 10^9 M^{-1} s^{-1}).[104] $ClO^{\bullet}$ radical can form through reaction of another radical with free chlorine (Reactions 1.8 and 1.9).[99] This radical can degrade some organic contaminants via hydroxylation[62] and has been reported to dominate degradation of a limited number of contaminants, particularly at high pH.[21,105] O_3 is formed from reaction of $O(^3P)$ with dissolved oxygen (Reaction 1.10)[97,101,106] and is capable of degrading organic contaminants with rate constants of 10^{-1} – 10^9 M^{-1} s^{-1}.[107–110] O_3 can also inactivate chlorine resistant pathogens, and is sometimes applied as an oxidant in drinking and wastewater treatment. [97]

$$O(^1D) + H_2O \leftrightharpoons 2\ {}^{\bullet}OH \quad (1.6)$$

$$Cl^{\bullet} + Cl^{-} \leftrightharpoons Cl_2^{\bullet-} \quad (1.7)$$

$$^{\bullet}OH + HOCl \leftrightharpoons ClO^{\bullet} + H_2O \quad (1.8)$$

$$^{\bullet}OH + OCl^{-} \leftrightharpoons ClO^{\bullet} + OH^{-} \quad (1.9)$$

$$O(^3P) + O_2 \leftrightharpoons O_3 \quad (1.10)$$

1.4.4 Subsequent Radical Reactions

Chlorine photolysis is a highly complex system with hundreds of radical reactions. In addition to the formation of secondary oxidants, there are many other oxidants and compounds formed from subsequent radical reactions including H_2O_2, HO_2^-, $HOCl^{\bullet-}$, ClO_2^-, and ClO_3^-.[17,28,99] Most of the subsequent reactions produce radicals that have such low concentrations they do not participate meaningfully in contaminant degradation, but as a whole these lesser radicals and compounds can impact the steady-state concentrations of important radicals, such as $^{\bullet}OH$.[99] In order to describe this system more accurately many researchers have used kinetic models.[17,19,21–23,97] These kinetic models are built with second order reactions and should be verified against experimental data.

1.5 Measuring Reactive Oxidant Species

The reactive oxidants produced during chlorine photolysis cannot be directly measured because they do not have long enough lifetimes in solution. Therefore, the steady-state concentration of these reactive oxidants is measured using probe compounds. Probe compounds react selectively with the oxidants in a known way to allow for quantification. Nitrobenzene is used to measure $^{\bullet}OH$ because it is a selective compound that does not photodegrade or react with chlorine.[25,87,111] Benzoate reacts with $^{\bullet}OH$, $Cl^{\bullet}$, and $Cl_2^{\bullet-}$ and can be used to determine the

concentrations of $Cl^{\bullet}$ and $Cl_2^{\bullet-}$ using a system of equations developed in Chapter 3.[19,99,112–114] Cinnamic acid reacts with ozone to form benzaldehyde, which can be used to measure the cumulative concentration of ozone.[115] 1,3,5-Trimethoxybenzene has recently been introduced as a way to measure free chlorine and free bromine in solution.[116] Standard methods such as the *N,N*-diethyl-*p*-phenylenediamine colorimetric method cannot differentiate between free chlorine and free bromine.[117]

1.6 Dissolved Organic Matter Transformation During Water Treatment

Naturally occurring dissolved organic matter can react with light, chlorine, and reactive oxidants.[118–121] DOM undergoes transformation during photolysis during UV irradiation and in sunlit surface waters to become smaller and more aliphatic in nature as the chromophoric moieties in the DOM absorb light and degrade.[122–124] This transformation in DOM can result in removal of disinfection by-product precursors.[124] Direct reaction of DOM with free chlorine also transforms DOM. Chlorine reacts with DOM through electron transfer and chlorine addition reactions.[13,26,122] The formation of high molecular weight DBPs during chlorine photolysis has not been investigated, but has been demonstrated during conventional chlorine disinfection.[125,126] These halogenated compounds are important because they represent around 50% of total organic halogens,[127,128] and some studies demonstrate that they are more toxic than the regulated DBPs, such as trihalomethanes and haloacetic acids.[125,126,129,130]

1.7 Identified Research Needs

There are many unanswered questions about chlorine photolysis despite the growing interest in this AOP. First, there has been no mechanistic investigation of the formation of different

reactive oxidant species under different treatment conditions. This is of interest because the pK_a of chlorine is 7.5,[87] which falls in the range of the pH of natural waters and the distinct photochemistry of HOCl and OCl^- results in the formation of different oxidants.[99] Additionally, the impact of chlorine photolysis on the nature of DOM is understudied and there is no mechanistic information available about how the reactive oxidants produced during chlorine photolysis will transform the DOM or participate in halogenation reactions, potentially forming novel high-molecular weight DBPs. Finally, previous work has demonstrated that the presence of bromide can form more toxic DBPs during dark chlorination,[129,131,132] but there has been no investigation of the impact of bromide on the formation of regulated and novel DBPs during chlorine photolysis.

1.8 Research Objectives

The goals of this dissertation are to determine what reactive oxidants are present during chlorine photolysis under different treatment conditions, investigate the transformation of dissolved organic matter and formation of disinfection by-products, and to determine the impact of bromide and reactive bromine species on the formation of halogenated by-products. The research chapters (Chapter 3 - Chapter 5) focus on the questions about chlorine photolysis set forth in this chapter and Chapter 2. The final chapter is a summary of the research described in Chapters 3 - 5.

Chapter 2 is a literature review summarizing chlorine photolysis research up to early 2016. Research conducted between 2016 and 2020 is discussed in previous sections of this chapter. The purpose of this review was to summarize the state of knowledge on chlorine photolysis and to the identify gaps in the literature; this chapter guides the research directions of the three research

chapters. This chapter was published in *Environmental Science: Water Research and Technology* in 2016.

Chapter 3 focuses on the fundamental oxidant chemistry of chlorine photolysis. The formation of reactive oxidants is quantified for a range of solution and irradiation conditions. A kinetic model containing over 200 reactions is presented and compared to both experimental results and literature kinetic models. This chapter was published in *Environmental Science and Technology* in 2019.

Chapter 4 investigates the effect of chlorine photolysis on dissolved organic matter and the formation of disinfection by-products. This chapter uses ultrahigh resolution mass spectrometry to investigate the transformation of dissolved organic matter at the molecular level. This chapter was published in *Environmental Science and Technology* in 2020.

Chapter 5 is a description of proposed research to investigate the impact of bromide on the formation of halogenated disinfection by-products during chlorine photolysis.

Chapter 6 is a summary of the major findings of this dissertation, along with suggestions for future research.

1.9 References

(1) Benotti, M. J.; Trenholm, R. A.; Vanderford, B. J.; Holady, J. C.; Stanford, B. D.; Snyder, S. A.; Pharmaceuticals and endocrine disrupting compounds in U.S. Drinking water. *Environ. Sci. Technol.* **2009**, 43(3), 597-603.

(2) Karakurt, S.; Schmid, L.; Hübner, U.; Drewes, J. E.; Dynamics of wastewater effluent contributions in streams and impacts on drinking water supply via riverbank filtration in Germany- A national reconnaissance. *Environ. Sci. Technol.* **2019**, 53(11), 6154-6161.

(3) Kleywegt, S.; Pileggi, V.; Yang, P.; Hao, C.; Zhao, X.; Rocks, C.; Thach, S.; Cheung, P.; Whitehead, B.; Pharmaceuticals, hormones and bisphenol a in untreated source and finished drinking water in Ontario, Canada — occurrence and treatment efficiency. *Sci. Total Environ.* **2011**, 409(8), 1481-1488.

(4) Mompelat, S.; Thomas, O.; Le Bot, B.; Contamination levels of human pharmaceutical compounds in French surface and drinking water. *J. Environ. Monitor.* **2011**, 13(10), 2929-2939.

(5) Padhye, L. P.; Yao, H.; Kung'u, F. T.; Huang, C.-H.; Year-long evaluation on the occurrence and fate of pharmaceuticals, personal care products, and endocrine disrupting chemicals in an urban drinking water treatment plant. *Water Res.* **2014**, 51, 266-276.

(6) Valcárcel, Y.; González Alonso, S.; Rodríguez-Gil, J. L.; Gil, A.; Catalá, M.; Detection of pharmaceutically active compounds in the rivers and tap water of the Madrid region (Spain) and potential ecotoxicological risk. *Chemosphere* **2011**, 84(10), 1336-1348.

(7) Mompelat, S.; Le Bot, B.; Thomas, O.; Occurrence and fate of pharmaceutical products and by-products, from resource to drinking water. *Environ. Int.* **2009**, 35(5), 803-814.

(8) Schwarzenbach, R. P.; Escher, B. I.; Fenner, K.; Hofstetter, T. B.; Johnson, C. A.; von Gunten, U.; Wehrli, B.; The challenge of micropollutants in aquatic systems. *Science* **2006**, 313(5790), 1072-1077.

(9) Kuehn, B. M.; Traces of drugs found in drinking water. *J. Am. Med. Assoc.* **2008**, 299(17), 2011-2013.

(10) Lee, S. S.; Paspalof, A. M.; Snow, D. D.; Richmond, E. K.; Rosi-Marshall, E. J.; Kelly, J. J.; Occurrence and potential biological effects of amphetamine on stream communities. *Environ. Sci. Technol.* **2016**, 50(17), 9727-9735.

(11) Ma, X. Y.; Wang, Y.; Dong, K.; Wang, X. C.; Zheng, K.; Hao, L.; Ngo, H. H.; The treatability of trace organic pollutants in WWTP effluent and associated biotoxicity reduction by advanced treatment processes for effluent quality improvement. *Water Res.* **2019**, 159, 423-433.

(12) Martin, J. M.; Bertram, M. G.; Saaristo, M.; Fursdon, J. B.; Hannington, S. L.; Brooks, B. W.; Burket, S. R.; Mole, R. A.; Deal, N. D. S.; Wong, B. B. M.; Antidepressants in surface waters: Fluoxetine influences mosquitofish anxiety-related behavior at environmentally relevant levels. *Environ. Sci. Technol.* **2019**, 53(10), 6035-6043.

(13) Acero, J. L.; Benitez, F. J.; Real, F. J.; Roldan, G.; Kinetics of aqueous chlorination of some pharmaceuticals and their elimination from water matrices. *Water Res.* **2010**, 44(14), 4158-4170.

(14) An, T.; Yang, H.; Li, G.; Song, W.; Cooper, W. J.; Nie, X.; Kinetics and mechanism of advanced oxidation processes (AOPs) in degradation of ciprofloxacin in water. *Appl. Catal. B* **2010**, 94(3-4), 288-294.

(15) Reemtsma, T.; Berger, U.; Arp, H. P. H.; Gallard, H.; Knepper, T. P.; Neumann, M.; Quintana, J. B.; Voogt, P.; Mind the gap: Persistent and mobile organic compounds-water contaminants that slip through. *Environ. Sci. Technol.* **2016**, 50(19), 10308-10315.
(16) Been, F.; Bastiaensen, M.; Lai, F. Y.; Libousi, K.; Thomaidis, N. S.; Benaglia, L.; Esseiva, P.; Delémont, O.; Van Nuijs, A. L. N.; Covaci, A.; Mining the chemical information on urban wastewater: Monitoring human exposure to phosphorus flame retardants and plasticizers. *Environ. Sci. Technol.* **2018**, 52(12), 6996-7005.
(17) Chuang, Y.-H.; Chen, S.; Chinn, C. J.; Mitch, W. A.; Comparing the UV/monochloramine and UV/free chlorine advanced oxidation processes (AOPs) to the UV/hydrogen peroxide AOP under scenarios relevant to potable reuse. *Environ. Sci. Technol.* **2017**, 51(23), 13859-13868.
(18) Chan, P. Y.; Gamal El-Din, M.; Bolton, J. R.; A solar-driven UV/chlorine advanced oxidation process. *Water Res.* **2012**, 46(17), 5672-5682.
(19) Fang, J.; Fu, Y.; Shang, C.; The roles of reactive species in micropollutant degradation in the UV/free chlorine system. *Environ. Sci. Technol.* **2014**, 48(3), 1859-1868.
(20) Remucal, C. K.; Manley, D.; Emerging investigators series: The efficacy of chlorine photolysis as an advanced oxidation process for drinking water treatment. *Environ. Sci.: Water Res. Technol.* **2016**, 2(4), 565-579.
(21) Guo, K.; Wu, Z.; Shang, C.; Yao, B.; Hou, S.; Yang, X.; Song, W.; Fang, J.; Radical chemistry and structural relationships of PPCP degradation by UV/chlorine treatment in simulated drinking water. *Environ. Sci. Technol.* **2017**, 51(18), 10431-10439.
(22) Li, W.; Jain, T.; Ishida, K.; Remucal, C. K.; Liu, H.; A mechanistic understanding of the degradation of trace organic contaminants by UV/hydrogen peroxide, UV/persulfate and UV/free chlorine for water reuse. *Environ. Sci.: Water Res. Technol.* **2017**, 3(1), 128-138.
(23) Sun, P.; Lee, W.-N.; Zhang, R.; Huang, C.-H.; Degradation of DEET and caffeine under UV/chlorine and simulated sunlight/chlorine conditions. *Environ. Sci. Technol.* **2016**, 50(24), 13265-13273.
(24) Hua, Z.; Guo, K.; Kong, X.; Lin, S.; Wu, Z.; Wang, L.; Huang, H.; Fang, J.; PPCP degradation and DBP formation in the solar/free chlorine system: Effects of pH and dissolved oxygen. *Water Res.* **2019**, 150, 77-85.
(25) Nowell, L. H.; Hoigné, J.; Photolysis of aqueous chlorine at sunlight and ultraviolet wavelengths. 2. Hydroxyl radical production. *Water Res.* **1992**, 26(5), 599-605.
(26) Liu, W.; Cheung, L. M.; Yang, X.; Shang, C.; THM, HAA and CNCl formation from UV irradiation and chlor(am)ination of selected organic waters. *Water Res.* **2006**, 40(10), 2033-2043.
(27) Pisarenko, A. N.; Stanford, B. D.; Snyder, S. A.; Rivera, S. B.; Boal, A. K.; Investigation of the use of chlorine based advanced oxidation in surface water: Oxidation of natural organic matter and formation of disinfection byproducts. *J. Adv. Oxid. Technol.* **2013**, 16(1), 137-150.
(28) Wang, D.; Bolton, J. R.; Andrews, S. A.; Hofmann, R.; Formation of disinfection by-products in the ultraviolet/chlorine advanced oxidation process. *Sci. Total Environ.* **2015**, 518-519, 49-57.
(29) Zhang, X.; Li, W.; Blatchley, E. R.; Wang, X.; Ren, P.; UV/chlorine process for ammonia removal and disinfection by-product reduction: Comparison with chlorination. *Water Res.* **2015**, 68, 804-811.

(30) Zhao, Q.; Shang, C.; Zhang, X.; Effects of bromide on UV/chlorine advanced oxidation process. *Water Sci. Technol. Water Supply* **2009**, 9(6), 627-634.
(31) Zhao, Q.; Shang, C.; Zhang, X.; Ding, G.; Yang, X.; Formation of halogenated organic byproducts during medium-pressure UV and chlorine coexposure of model compounds, nom and bromide. *Water Res.* **2011**, 45(19), 6545-6554.
(32) Plewa, M. J.; Wagner, E. D.; Metz, D. H.; Kashinkunti, R.; Jamriska, K. J.; Meyer, M.; Differential toxicity of drinking water disinfected with combinations of ultraviolet radiation and chlorine. *Environ. Sci. Technol.* **2012**, 46(14), 7811-7817.
(33) Ben, W.; Sun, P.; Huang, C.-H.; Effects of combined UV and chlorine treatment on chloroform formation from triclosan. *Chemosphere* **2016**, 150, 715-722.
(34) Liu, J.; Zhang, X.; Li, Y.; Photoconversion of chlorinated saline wastewater DBPs in receiving seawater is overall a detoxification process. *Environ. Sci. Technol.* **2017**, 51(1), 58-67.
(35) Lu, J.; Yang, P.; Dong, W.; Ji, Y.; Huang, Q.; Enhanced formation of chlorinated disinfection byproducts in the UV/chlorine process in the presence of benzophenone-4. *Chem. Eng. J.* **2018**, 351, 304-311.
(36) Dong, H.; Qiang, Z.; Hu, J.; Qu, J.; Degradation of chloramphenicol by UV/chlorine treatment: Kinetics, mechanism and enhanced formation of halonitromethanes. *Water Res.* **2017**, 121, 178-185.
(37) Kerrigan, J. F.; Sandberg, K. D.; Engstrom, D. R.; Lapara, T. M.; Arnold, W. A.; Sedimentary record of antibiotic accumulation in Minnesota lakes. *Sci. Total Environ.* **2018**, 621, 970-979.
(38) Fairbairn, D. J.; Arnold, W. A.; Barber, B. L.; Kaufenberg, E. F.; Koskinen, W. C.; Novak, P. J.; Rice, P. J.; Swackhamer, D. L.; Contaminants of emerging concern: Mass balance and comparison of wastewater effluent and upstream sources in a mixed-use watershed. *Environ. Sci. Technol.* **2016**, 50(1), 36-45.
(39) Masoner, J. R.; Kolpin, D. W.; Furlong, E. T.; Cozzarelli, I. M.; Gray, J. L.; Landfill leachate as a mirror of today's disposable society: Pharmaceuticals and other contaminants of emerging concern in final leachate from landfills in the conterminous United States. *Environ. Toxicol. Chem.* **2016**, 35(4), 906-918.
(40) McConville, M. B.; Hubert, T. D.; Remucal, C. K.; Direct photolysis rates and transformation pathways of the lampricides TFM and niclosamide in simulated sunlight. *Environ. Sci. Technol.* **2016**, 50(18), 9998-10006.
(41) Netherland, M. D.; Jones, J. D.; A three-year evaluation of triclopyr for selective whole-bay management of Eurasian watermilfoil on lake Minnetonka, Minnesota. *Lake Reserv. Manage.* **2015**, 31(4), 306-323.
(42) Kolpin, D. W.; Furlong, E. T.; Meyer, M. T.; Thurman, E. M.; Zaugg, S. D.; Barber, L. B.; Buxton, H. T.; Pharmaceuticals, hormones, and other organic wastewater contaminants in U.S. streams, 1999−2000: A national reconnaissance. *Environ. Sci. Technol.* **2002**, 36(6), 1202-1211.
(43) Li, Z.; Sobek, A.; Radke, M.; Fate of pharmaceuticals and their transformation products in four small European rivers receiving treated wastewater. *Environ. Sci. Technol.* **2016**, 50(11), 5614-5621.
(44) Löve, A. S. C.; Baz-Lomba, J. A.; Reid, M. J.; Kankaanpää, A.; Gunnar, T.; Dam, M.; Ólafsdóttir, K.; Thomas, K. V.; Analysis of stimulant drugs in the wastewater of five Nordic capitals. *Sci. Total Environ.* **2018**, 627, 1039-1047.

(45) Kostich, M. S.; Batt, A. L.; Lazorchak, J. M.; Concentrations of prioritized pharmaceuticals in effluents from 50 large wastewater treatment plants in the us and implications for risk estimation. *Environmental Pollution* **2014**, 184, 354-359.
(46) Brooker, M. R.; Longnecker, K.; Kujawinski, E. B.; Evert, M. H.; Mouser, P. J.; Discrete organic phosphorus signatures are evident in pollutant sources within a lake Erie tributary. *Environ. Sci. Technol.* **2018**, 52(12), 6771-6779.
(47) McEachran, A. D.; Hedgespeth, M. L.; Newton, S. R.; McMahen, R.; Strynar, M.; Shea, D.; Nichols, E. G.; Comparison of emerging contaminants in receiving waters downstream of a conventional wastewater treatment. *Environ. Sci. Pollut. Res.* **2018**, 25(13), 12451-12463.
(48) Provini, A.; Galassi, S. Organic micropollutants in lake sediments. In *Handbook of Hazardous Materials*. **1993**, 491-504.
(49) Bexfield, L. M.; Toccalino, P. L.; Belitz, K.; Foreman, W. T.; Furlong, E. T.; Hormones and pharmaceuticals in groundwater used as a source of drinking water across the United States. *Environ. Sci. Technol.* **2019**, 53(6), 2950-2960.
(50) Bossi, R.; Vejrup, K. V.; Mogensen, B. B.; Asman, W. A. H.; Analysis of polar pesticides in rainwater in Denmark by liquid chromatography–tandem mass spectrometry. *J. Chromatogr. A* **2002**, 957(1), 27-36.
(51) Walters, D. M.; Jardine, T. D.; Cade, B. S.; Kidd, K. A.; Muir, D. C.; Leipzig-Scott, P.; Trophic magnification of organic chemicals: A global synthesis. *Environ. Sci. Technol.* **2016**, 50(9), 4650-4658.
(52) Kennedy Neth, N. L.; Carlin, C. M.; Keen, O. S.; Emerging investigator series: Transformation of common antibiotics during water disinfection with chlorine and formation of antibacterially active products. *Environ. Sci.: Water Res. Technol.* **2019**, 5(7), 1222-1233.
(53) Deborde, M.; Rabouan, S.; Gallard, H.; Legube, B.; Aqueous chlorination kinetics of some endocrine disruptors. *Environ. Sci. Technol.* **2004**, 38(21), 5577-5583.
(54) Gallard, H.; von Gunten, U.; Chlorination of phenols: kinetics and formation of chloroform. *Environ. Sci. Technol.* **2002**, 36(5), 884-890.
(55) Dodd, M. C.; Huang, C.-H.; Aqueous chlorination of the antibacterial agent trimethoprim: Reaction kinetics and pathways. *Water Res.* **2007**, 41(3), 647-655.
(56) Dodd, M. C.; Huang, C.-H.; Transformation of the antibacterial agent sulfamethoxazole in reactions with chlorine: kinetics, mechanisms, and pathways. *Environ. Sci. Technol.* **2004**, 38(21), 5607-5615.
(57) Deborde, M.; von Gunten, U.; Reactions of chlorine with inorganic and organic compounds during water treatment-kinetics and mechanisms: A critical review. *Water Res.* **2008**, 42(1-2), 13-51.
(58) Cuthbertson, A. A.; Kimura, S. Y.; Liberatore, H. K.; Summers, R. S.; Knappe, D. R. U.; Stanford, B. D.; Maness, J. C.; Mulhern, R. E.; Selbes, M.; Richardson, S. D.; Does granular activated carbon with chlorination produce safer drinking water? From disinfection byproducts and total organic halogen to calculated toxicity. *Environ. Sci. Technol.* **2019**, 53(10), 5987-5999.
(59) Cai, M.; Sun, P.; Zhang, L.; Huang, C.-H.; UV/peracetic acid for degradation of pharmaceuticals and reactive species evaluation. *Environ. Sci. Technol.* **2017**, 51(24), 14217-14224.
(60) Lian, L.; Yao, B.; Hou, S.; Fang, J.; Yan, S.; Song, W.; Kinetic study of hydroxyl and sulfate radical-mediated oxidation of pharmaceuticals in wastewater effluents. *Environ. Sci. Technol.* **2017**, 51(5), 2954-2962.

(61) Luo, S.; Gao, L.; Wei, Z.; Spinney, R.; Dionysiou, D. D.; Hu, W. P.; Chai, L.; Xiao, R.; Kinetic and mechanistic aspects of hydroxyl radical–mediated degradation of naproxen and reaction intermediates. *Water Res.* **2018**, 137, 233-241.

(62) Kong, X.; Wu, Z.; Ren, Z.; Guo, K.; Hou, S.; Hua, Z.; Li, X.; Fang, J.; Degradation of lipid regulators by the UV/chlorine process: Radical mechanisms, chlorine oxide radical ($ClO^{\bullet}$)-mediated transformation pathways and toxicity changes. *Water Res.* **2018**, 137, 242-250.

(63) Baeza, C.; Knappe, D. R.; Transformation kinetics of biochemically active compounds in low-pressure UV photolysis and UV/H_2O_2 advanced oxidation processes. *Water Res.* **2011**, 45(15), 4531-4543.

(64) Luo, S.; Wei, Z.; Spinney, R.; Villamena, F. A.; Dionysiou, D. D.; Chen, D.; Tang, C.-J.; Chai, L.; Xiao, R.; Quantitative structure-activity relationships for reactivities of sulfate and hydroxyl radicals with aromatic contaminants through single-electron transfer pathway. *J. Hazard. Mater.* **2018**, 344, 1165-1173.

(65) Barazesh, J. M.; Prasse, C.; Sedlak, D. L.; Electrochemical transformation of trace organic contaminants in the presence of halide and carbonate ions. *Environ. Sci. Technol.* **2016**, 50(18), 10143-10152.

(66) Gerrity, D.; Lee, Y.; Gamage, S.; Lee, M.; Pisarenko, A. N.; Trenholm, R. A.; von Gunten, U.; Snyder, S. A.; Emerging investigators series: Prediction of trace organic contaminant abatement with UV/H_2O_2: Development and validation of semi-empirical models for municipal wastewater effluents. *Environ. Sci.: Water Res. Technol.* **2016**, 2(3), 460-473.

(67) Grebel, J. E.; Pignatello, J. J.; Mitch, W. A.; Effect of halide ions and carbonates on organic contaminant degradation by hydroxyl radical-based advanced oxidation processes in saline waters. *Environ. Sci. Technol.* **2010**, 44(17), 6822-6828.

(68) García Einschlag, F. S.; Carlos, L.; Capparelli, A. L.; Competition kinetics using the UV/H_2O_2 process: A structure reactivity correlation for the rate constants of hydroxyl radicals toward nitroaromatic compounds. *Chemosphere* **2003**, 53(1), 1-7.

(69) Miralles-Cuevas, S.; Oller, I.; Agüera, A.; Pérez, J. A. S.; Sánchez-Moreno, R.; Malato, S.; Is the combination of nanofiltration membranes and aops for removing microcontaminants cost effective in real municipal wastewater effluents. *Environ. Sci.: Water Res. Technol.* **2016**, 2(3), 511-520.

(70) Bossmann, S. H.; Oliveros, E.; Göb, S.; Siegwart, S.; Dahlen, E. P.; Payawan, L.; Straub, M.; Wörner, M.; Braun, A. M.; New evidence against hydroxyl radicals as reactive intermediates in the thermal and photochemically enhanced Fenton reactions. *J. Phys. Chem. A* **1998**, 102(28), 5542-5550.

(71) Lee, M.; Merle, T.; Rentsch, D.; Canonica, S.; Von Gunten, U.; Abatement of polychoro-1,3-butadienes in aqueous solution by ozone, UV photolysis, and advanced oxidation processes (O_3/H_2O_2 and UV/H_2O_2). *Environ. Sci. Technol.* **2017**, 51(1), 497-505.

(72) Lee, Y.; Gerrity, D.; Lee, M.; Gamage, S.; Pisarenko, A.; Trenholm, R. A.; Canonica, S.; Snyder, S. A.; von Gunten, U.; Organic contaminant abatement in reclaimed water by UV/H_2O_2 and a combined process consisting of O_3/H_2O_2 followed by UV/H_2O_2: Prediction of abatement efficiency, energy consumption, and byproduct formation. *Environ. Sci. Technol.* **2016**, 50(7), 3809-3819.

(73) Li, S.; Hu, J.; Transformation products formation of ciprofloxacin in UVA/LED and UVA/LED/TiO_2 systems: Impact of natural organic matter characteristics. *Water Res.* **2018**, 132, 320-330.

(74) Chen, Y.; Ye, J.; Li, C.; Zhou, P.; Liu, J.; Ou, H.; Degradation of 1H-benzotriazole by UV/H_2O_2 and UV/TiO_2: Kinetics, mechanisms, products and toxicology. *Environ. Sci.: Water Res. Technol.* **2018**, 4(9), 1282-1294.
(75) Liu, G.; You, S.; Tan, Y.; Ren, N.; In situ photochemical activation of sulfate for enhanced degradation of organic pollutants in water. *Environ. Sci. Technol.* **2017**, 51(4), 2339-2346.
(76) Loeb, S. K.; Alvarez, P. J. J.; Brame, J. A.; Cates, E. L.; Choi, W.; Crittenden, J.; Dionysiou, D. D.; Li, Q.; Li-Puma, G.; Quan, X.; Sedlak, D. L.; David Waite, T.; Westerhoff, P.; Kim, J. H.; The technology horizon for photocatalytic water treatment: Sunrise or sunset. *Environ. Sci. Technol.* **2019**, 53(6), 2937-2947.
(77) Cho, K.; Qu, Y.; Kwon, D.; Zhang, H.; Cid, C. A.; Aryanfar, A.; Hoffmann, M. R.; Effects of anodic potential and chloride ion on overall reactivity in electrochemical reactors designed for solar-powered wastewater treatment. *Environ. Sci. Technol.* **2014**, 48(4), 2377-2384.
(78) Divišek, J.; Kastening, B.; Electrochemical generation and reactivity of the superoxide ion in aqueous solutions. *J. Electroanal. Chem.* **1975**, 65, 603-621.
(79) Jasper, J. T.; Shafaat, O. S.; Hoffmann, M. R.; Electrochemical transformation of trace organic contaminants in latrine wastewater. *Environ. Sci. Technol.* **2016**, 50(18), 10198-10208.
(80) Jasper, J. T.; Yang, Y.; Hoffmann, M. R.; Toxic byproduct formation during electrochemical treatment of latrine wastewater. *Environ. Sci. Technol.* **2017**, 51(12), 7111-7119.
(81) Jing, Y.; Chaplin, B. P.; Mechanistic study of the validity of using hydroxyl radical probes to characterize electrochemical advanced oxidation processes. *Environ. Sci. Technol.* **2017**, 51(4), 2355-2365.
(82) Wang, X.; Sun, M.; Zhao, Y.; Wang, C.; Ma, W.; Wong, M. S.; Elimelech, M.; In situ electrochemical generation of reactive chlorine species for efficient ultrafiltration membrane self-cleaning. *Environ. Sci. Technol.* **2020**, 54(11), 6997-7007.
(83) Kwon, M.; Yoon, Y.; Kim, S.; Jung, Y.; Hwang, T.-M.; Kang, J.-W.; Removal of sulfamethoxazole, ibuprofen and nitrobenzene by UV and UV/chlorine processes: A comparative evaluation of 275 nm LED-UV and 254 nm LP-UV. *Sci. Total Environ.* **2018**, 637-638, 1351-1357.
(84) Li, M.; Qiang, Z.; Hou, P.; Bolton, J. R.; Qu, J.; Li, P.; Wang, C.; VUV/UV/chlorine as an enhanced advanced oxidation process for organic pollutant removal from water: Assessment with a novel mini-fluidic VUV/UV photoreaction system (MVPS). *Environ. Sci. Technol.* **2016**, 50(11), 5849-5856.
(85) Lu, X.; Shao, Y.; Gao, N.; Chen, J.; Deng, H.; Chu, W.; An, N.; Peng, F.; Investigation of clofibric acid removal by UV/persulfate and UV/chlorine processes: Kinetics and formation of disinfection byproducts during subsequent chlor(am)ination. *Chem. Eng. J.* **2018**, 331, 364-371.
(86) Nowell, L. H.; Hoigné, J.; Photolysis of aqueous chlorine at sunlight and ultraviolet wavelengths. 1. Degradation rates. *Water Res.* **1992**, 26(5), 593-598.
(87) Watts, M. J.; Linden, K. G.; Chlorine photolysis and subsequent $^{\bullet}$OH radical production during UV treatment of chlorinated water. *Water Res.* **2007**, 41(13), 2871-2878.
(88) Watts, M. J.; Rosenfeldt, E. J.; Linden, K. G.; Comparative $^{\bullet}$OH radical oxidation using UV-Cl_2 and UV-H_2O_2 processes. *J. Water Supply Res. T.* **2007**, 56(8), 469-477.
(89) Li, W.; Xu, E.; Schlenk, D.; Liu, H.; Cyto- and geno-toxicity of 1,4-dioxane and its transformation products during ultraviolet-driven advanced oxidation processes. *Environ. Sci.: Water Res. Technol.* **2018**, 4(9), 1213-1218.

(90) Li, M.; Li, W.; Wen, D.; Bolton, J. R.; Blatchley, E. R.; Qiang, Z.; Micropollutant degradation by the UV/H_2O_2 process: Kinetic comparison among various radiation sources. *Environ. Sci. Technol.* **2019**, 53(9), 5241-5248.
(91) Luo, J.; Liu, T.; Zhang, D.; Yin, K.; Wang, D.; Zhang, W.; Liu, C.; Yang, C.; Wei, Y.; Wang, L.; Luo, S.; Crittenden, J. C.; The individual and co-exposure degradation of benzophenone derivatives by UV/H_2O_2 and UV/PDS in different water matrices. *Water Res.* **2019**, 159, 102-110.
(92) Miklos, D. B.; Hartl, R.; Michel, P.; Linden, K. G.; Drewes, J. E.; Hübner, U.; UV/H_2O_2 process stability and pilot-scale validation for trace organic chemical removal from wastewater treatment plant effluents. *Water Res.* **2018**, 136, 169-179.
(93) Yin, R.; Zhong, Z.; Ling, L.; Shang, C.; The fate of dichloroacetonitrile in UV/Cl_2 and UV/H_2O_2 processes: Implications on potable water reuse. *Environ. Sci.: Water Res. Technol.* **2018**, 4(9), 1295-1302.
(94) Duan, X.; Sanan, T.; De La Cruz, A.; He, X.; Kong, M.; Dionysiou, D. D.; Susceptibility of the algal toxin microcystin-LR to UV/chlorine process: Comparison with chlorination. *Environ. Sci. Technol.* **2018**, 52(15), 8252-8262.
(95) Morgan, M. S.; Van Trieste, P. F.; Garlick, S. M.; Mahon, M. J.; Smith, A. L.; Ultraviolet molar absorptivities of aqueous hydrogen peroxide and hydroperoxyl ion. *Analytica Chimica Acta* **1988**, 215, 325-329.
(96) Buck, R. P.; Singhadeja, S.; Rogers, L. B.; Ultraviolet absorption spectra of some inorganic ions in aqueous solutions. *Anal. Chem.* **1954**, 26(7), 1240-1242.
(97) Forsyth, J. E.; Zhou, P.; Mao, Q.; Asato, S. S.; Meschke, J. S.; Dodd, M. C.; Enhanced inactivation of *bacillus subtilis* spores during solar photolysis of free available chlorine. *Environ. Sci. Technol.* **2013**, 47(22), 12976-12984.
(98) Young, T. R.; Li, W.; Guo, A.; Korshin, G. V.; Dodd, M. C.; Characterization of disinfection byproduct formation and associated changes to dissolved organic matter during solar photolysis of free available chlorine. *Water Res.* **2018**, 146, 318-327.
(99) Bulman, D. M.; Mezyk, S. P.; Remucal, C. K.; The impact of pH and irradiation wavelength on the production of reactive oxidants during chlorine photolysis. *Environ. Sci. Technol.* **2019**, 53(8), 4450-4459.
(100) Buxton, G. V.; Subhani, M. S.; Radiation chemistry and photochemistry of oxychlorine ions. Part 1. Radiolysis of aqueous solutions of hypochlorite and chlorite ions. *J. Chem. Soc., Faraday Trans. 1* **1972**, 68, 947-957.
(101) Buxton, G. V.; Subhani, M. S.; Radiation chemistry and photochemistry of oxychlorine ions. Part 2. Photodecomposition of aqueous solutions of hypochlorite ions. *J. Chem. Soc., Faraday Trans. 1* **1972**, 68, 958-969.
(102) Feng, Y.; Smith, D. W.; Bolton, J. R.; Photolysis of aqueous free chlorine species (HOCl and OCl^-) with 254 nm ultraviolet light. *J. Environ. Eng. Sci.* **2007**, 6(3), 277-284.
(103) Molina, M. J.; Ishiwata, T.; Molina, L. T.; Production of hydroxyl radical from photolysis of hypochlorous acid at 307-309 nm. *J. Phys. Chem.* **1980**, 84(8), 821-826.
(104) Lei, Y.; Cheng, S.; Luo, N.; Yang, X.; An, T.; Rate constants and mechanisms of the reactions of $Cl^•$ and $Cl_2^{•-}$ with trace organic contaminants. *Environ. Sci. Technol.* **2019**, 53(19), 11170-11182.
(105) Wu, Z.; Guo, K.; Fang, J.; Yang, X.; Xiao, H.; Hou, S.; Kong, X.; Shang, C.; Yang, X.; Meng, F.; Chen, L.; Factors affecting the roles of reactive species in the degradation of micropollutants by the UV/chlorine process. *Water Res.* **2017**, 126, 351-360.

(106) Kläning, U. K.; Sehested, K.; Wolff, T.; Ozone formation in laser flash photolysis of oxoacids and oxoanions of chlorine and bromine. *J. Chem. Soc., Faraday Trans. 1* **1984**, 80, 2969-2979.
(107) von Gunten, U.; Ozonation of drinking water: Part 1. Oxidation kinetics and products formation. *Water Res.* **2003**, 37, 1443-1467.
(108) Dodd, M. C.; Kohler, H.-P. E.; von Gunten, U.; Oxidation of antibacterial compounds by ozone and hydroxyl radical: Elimination of biological activity during aqueous ozonation processes. *Environ. Sci. Technol.* **2009**, 43(7), 2498-2504.
(109) Dodd, M. C.; Buffle, M.-O.; von Gunten, U.; Oxidation of antibacterial molecules by aqueous ozone: moiety-specific reaction kinetics and application to ozone-based wastewater treatment. *Environ. Sci. Technol.* **2006**, 40(6), 1969-1977.
(110) Dai, N.; Mitch, W. A.; Controlling nitrosamines, nitramines, and amines in amine-based CO_2 capture systems with continuous ultraviolet and ozone treatment of washwater. *Environ. Sci. Technol.* **2015**, 49(14), 8878-8886.
(111) Buxton, G. V.; Greenstock, C. L.; Helman, W. P.; Ross, A. B.; Critical review of rate constants for reactions of hydrated electrons, hydrogen atoms and hydroxyl radicals ($^{\bullet}OH/O^{\bullet-}$) in aqueous solution. *J. Phys. Chem. Ref Data* **1988**, 17(2), 513-886.
(112) Oliver, B. G.; Carey, J. H.; Photochemical production of chlorinated organics in aqueous solutions containing chlorine. *Environ. Sci. Technol.* **1977**, 11(9), 893-895.
(113) Ashton, L.; Buxton, G. V.; Stuart, C. R.; Temperature dependence of the rate of reaction of oh with some aromatic compounds in aqueous solution. *J. Chem. Soc., Faraday Trans.* **1995**, 91(11), 1631-1633.
(114) Mártire, D. O.; Rosso, J. A.; Bertolotti, S.; Le Roux, G. C.; Braun, A. M.; Gonzalez, M. C.; Kinetic study of the reactions of chlorine atoms and $Cl_2^{\bullet-}$ radical anions in aqueous solutions. II. Toluene, benzoic acid, and chlorobenzene. *J. Phys. Chem. A* **2001**, 105(22), 5385-5392.
(115) Leitzke, A.; Reisz, E.; Flyunt, R.; von Sonntag, C.; The reactions of ozone with cinnamic acids: Formation and decay of 2-hydroperoxy-2-hydroxyacetic acid. *J. Chem. Soc., Perkin Trans. 2* **2001**, (5), 793-797.
(116) Lau, S. S.; Dias, R. P.; Martin-Culet, K. R.; Race, N. A.; Schammel, M. H.; Reber, K. P.; Roberts, A. L.; Sivey, J. D.; 1,3,5-trimethoxybenzene (TMB) as a new quencher for preserving redox-labile disinfection byproducts and for quantifying free chlorine and free bromine. *Environ. Sci.: Water Res. Technol.* **2018**, 4(7), 926-941.
(117) Eaton, A. D.; Clesceri, L. S.; Greenberg, A. E., Eds. *Standard Methods for the Examination of Water and Wastewater*, ed.; United Book Press, Inc., Baltimore, 1995.
(118) Phungsai, P.; Kurisu, F.; Kasuga, I.; Furumai, H.; Changes in dissolved organic matter composition and disinfection byproduct precursors in advanced drinking water treatment processes. *Environ. Sci. Technol.* **2018**, 52(6), 3392-3401.
(119) Xu, J.; Kralles, Z. T.; Dai, N.; Effects of sunlight on the trichloronitromethane formation potential of wastewater effluents: Dependence on nitrite concentration. *Environ. Sci. Technol.* **2019**, 53(8), 4285-4294.
(120) Li, C.; Wang, D.; Xu, X.; Wang, Z.; Formation of known and unknown disinfection by-products from natural organic matter fractions during chlorination, chloramination, and ozonation. *Sci. Total Environ.* **2017**, 587-588, 177-184.
(121) Kamath, D.; Minakata, D.; Emerging investigators series: Ultraviolet and free chlorine aqueous-phase advanced oxidation process: Kinetic simulations and experimental validation. *Environ. Sci.: Water Res. Technol.* **2018**, 4(9), 1231-1238.

(122) Varanasi, L.; Coscarelli, E.; Khaksari, M.; Mazzoleni, L. R.; Minakata, D.; Transformations of dissolved organic matter induced by UV photolysis, hydroxyl radicals, chlorine radicals, and sulfate radicals in aqueous-phase UV-based advanced oxidation processes. *Water Res.* **2018**, 135, 22-30.
(123) Maizel, A. C.; Remucal, C. K.; Molecular composition and photochemical reactivity of size-fractionated dissolved organic matter. *Environ. Sci. Technol.* **2017**, 51(4), 2113-2123.
(124) Du, Y.; Wu, Q.-Y.; Lv, X.-T.; Ye, B.; Zhan, X.-M.; Lu, Y.; Hu, H.-Y.; Electron donating capacity reduction of dissolved organic matter by solar irradiation reduces the cytotoxicity formation potential during wastewater chlorination. *Water Res* **2018**, 145, 94-102.
(125) Gonsior, M.; Schmitt-Kopplin, P.; Stavklint, H.; Richardson, S. D.; Hertkorn, N.; Bastviken, D.; Changes in dissolved organic matter during the treatment processes of a drinking water plant in Sweden and formation of previously unknown disinfection byproducts. *Environ. Sci. Technol.* **2014**, 48(21), 12714-12722.
(126) Lavonen, E. E.; Gonsior, M.; Tranvik, L. J.; Schmitt-Kopplin, P.; Köhler, S. J.; Selective chlorination of natural organic matter: Identification of previously unknown disinfection byproducts. *Environ. Sci. Technol.* **2013**, 47(5), 2264-2271.
(127) Krasner, S. W.; The formation and control of emerging disinfection by-products of health concern. *Phil. Trans. R. Soc. A* **2009**, 367(1904), 4077-4095.
(128) Ziegler, G.; Gonsior, M.; Fisher, D. J.; Schmitt-Kopplin, P.; Tamburri, M. N.; Formation of brominated organic compounds and molecular transformations in dissolved organic matter (DOM) after ballast water treatment with sodium dichloroisocyanurate dihydrate (DICD). *Environ. Sci. Technol.* **2019**, 53(14), 8006-8016.
(129) Plewa, M. J.; Wagner, E. D.; Richardson, S. D.; TIC-tox: A preliminary discussion on identifying the forcing agents of DBP-mediated toxicity of disinfected water. *J. Environ. Sci.* **2017**, 58, 208-216.
(130) Richardson, S. D.; Ternes, T. A.; Water analysis: Emerging contaminants and current issues. *Analytical Chemistry* **2018**, 90(1), 398-428.
(131) Allard, S.; Tan, J.; Joll, C. A.; von Gunten, U.; Mechanistic study on the formation of $Cl^-/Br^-/I^-$ trihalomethanes during chlorination/chloramination combined with a theoretical cytotoxicity evaluation. *Environ. Sci. Technol.* **2015**, 49(18), 11105-11114.
(132) Daiber, E. J.; Demarini, D. M.; Ravuri, S. A.; Liberatore, H. K.; Cuthbertson, A. A.; Thompson-Klemish, A.; Byer, J. D.; Schmid, J. E.; Afifi, M. Z.; Blatchley, E. R.; Richardson, S. D.; Progressive increase in disinfection byproducts and mutagenicity from source to tap to swimming pool and spa water: Impact of human inputs. *Environ. Sci. Technol.* **2016**, 50(13), 6652-6662.

Chapter 2

The efficacy of chlorine photolysis as an advanced oxidation process for drinking water treatment[1]

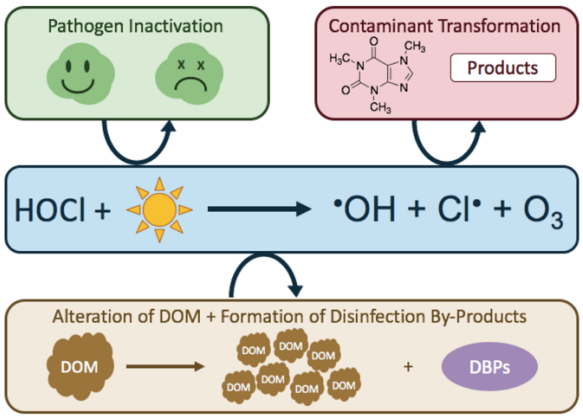

2.1 Abstract

The photolysis of hypochlorous acid (HOCl) and hypochlorite (OCl^-) produces a suite of reactive oxidants, including hydroxyl radical (•OH), chlorine radical (Cl•), and ozone (O_3). Therefore, the addition of light to chlorine disinfection units could effectively convert existing drinking water treatment systems into advanced oxidation processes. This review critically examines existing studies on chlorine photolysis as a water treatment process. After describing the fundamental chemistry of chlorine photolysis, we evaluate the ability of chlorine photolysis to transform model probe compounds, target organic contaminants, and chlorine-resistant microorganisms. The efficacy of chlorine photolysis to produce reactive oxidants is dependent on solution and irradiation conditions (e.g., pH and irradiation wavelength). For example, lower pH values result in higher steady-state concentrations of •OH and Cl•, resulting in enhanced

[1] Reproduced with permission from *Environmental Science: Water Research and Technology.* Remucal, C. K.; Manley, D. 2016, 2(4), 565-579. Copyright 2016, Royal Society of Chemistry.

contaminant removal. We also present the current state of knowledge on the alteration of dissolved organic matter and subsequent formation of disinfection by-products (DBPs) during chlorine photolysis. Although the relative yields of DBPs during chlorine photolysis are also dependent on solution conditions (e.g., higher organic DBP yields at low pH values), there is conflicting evidence on whether chlorine photolysis increases or decreases DBP production compared to thermal reactions between chlorine and dissolved organic matter in the dark. We conclude the review by identifying knowledge gaps in the current body of literature.

2.2 Introduction

Conventional drinking water treatment systems are primarily designed to remove particles and pathogens.[1] The majority of drinking water utilities in the United States utilize chlorine-based disinfection systems, in which free chlorine is added as chlorine gas (Cl_2) or sodium hypochlorite (NaOCl) to form hypochlorous acid (HOCl) and hypochlorite (OCl^-).[2,3] The use of free available chlorine (FAC; referred to as "chlorine" in this manuscript) has several advantages compared to other disinfectants; chlorine is inexpensive, effective against many waterborne pathogens, and provides residual disinfectant in the distribution system.[1] However, concerns about the formation of disinfection by-products (DBPs) during chlorine disinfection, as well as the presence of chlorine-resistant pathogens and emerging chemical contaminants, have led utilities to consider alternative treatment approaches.[2,4-6]

Chlorine-resistant pathogenic microorganisms include oocysts of protozoan parasites (e.g., *Cryptosporidium parvum*) and spores of vegetative bacteria (e.g., *Bacillus subtilis*).[2,7-9] These organisms cannot be effectively inactivated using chlorine-based disinfectants under the conditions encountered in most treatment facilities. The use of sequential disinfectants is

considered to be a viable treatment option to inactivate chlorine-resistant pathogens because it results in enhanced disinfection compared to chlorine alone.[7-11] During sequential disinfection, a primary disinfectant (e.g., ozone, chlorine dioxide, or ultraviolet (UV) irradiation) is applied to achieve partial inactivation followed by the application of a chlorine-based secondary disinfectant to achieve additional inactivation and to provide residual disinfection in the water distribution system.[2,7-13] Although this approach is effective against many recalcitrant pathogens, it requires additional infrastructure and can alter the yield of DBPs in the treated water.[4,12-15]

Emerging chemical contaminants of concern in drinking water include pharmaceuticals and personal care products (PPCPs). Many of these compounds are poorly retained in wastewater treatment systems and can be found at low levels in the environment, including in drinking water sources.[6,16-19] Although some PPCPs are oxidized in chlorine-based disinfection systems through direct reaction with HOCl or Cl_2,[20-26] many compounds are not removed by conventional treatment processes and can be found in treated water.[17,18,27-36] While the toxicological effects of constant exposure to low levels of PPCPs are unknown, the presence of these compounds is of concern.

One potential solution to remove trace organic contaminants, such as PPCPs, from drinking water is the use of advanced oxidation processes (AOPs). Conventional AOPs, such as UV/hydrogen peroxide (H_2O_2), UV/ozone (O_3), H_2O_2/O_3, and Fenton-based (i.e., iron/H_2O_2) systems, rely on the formation of hydroxyl radical ($^{\bullet}OH$).[37-42] The production of $^{\bullet}OH$ is desirable because the non-selective radical reacts at near diffusion-controlled rates with many organic compounds, including organic contaminants and biomolecules (e.g., proteins, nucleic acids).[43,44] Although the low selectivity of $^{\bullet}OH$ means that other compounds typically present in water (e.g., dissolved organic matter (DOM) and bicarbonate) can compete with contaminants for $^{\bullet}OH$, its rapid reactivity facilitates its use in the remediation of numerous types of recalcitrant compounds.

However, the inclusion of conventional AOPs in existing drinking water treatment facilities requires costly retrofits, increases the physical size of the plant, and can be expensive to operate due to high energy costs.

The combination of chlorine and light during water treatment could effectively turn existing chlorine-based disinfection systems into AOPs. The photolysis of HOCl and OCl^- produces a suite of reactive oxidants, including $^{\bullet}OH$, O_3, and chlorine radical ($Cl^{\bullet}$).[45-47] Chlorine photolysis could be applied to simultaneously inactivate chlorine-resistant pathogens and transform organic contaminants of concern by combining multiple mechanisms: (1) direct reaction with HOCl/OCl^-, (2) direct photolysis by UV irradiation, and (3) reactive species-mediated indirect photolysis (i.e., reaction with $^{\bullet}OH$, O_3, and/or $Cl^{\bullet}$ produced during chlorine photolysis).[39-42,48-54] In the case of municipal drinking water treatment systems, this approach would utilize existing infrastructure and require only the addition of a suitable light source (i.e., either UV-A light-emitting diodes or higher energy UV-C lamps).[52,53] Additional applications include solar-based point-of-use water treatment in decentralized systems,[52,55] pump-and-treat groundwater remediation,[56] treatment of ballast water,[57] and point-of-use treatment to remove chlorine off-flavors.[58] The fundamental chemistry of this process is also relevant to chlorine photolysis in uncovered chlorine disinfection contact basins in wastewater treatment plants[59,60] and swimming pools.[59,61]

The overall aim of this manuscript is to critically review existing studies on chlorine photolysis as a water treatment application. After describing the fundamental chemistry of chlorine photolysis, we evaluate the ability of chlorine photolysis to transform model probe compounds, target organic contaminants, and chlorine-resistant microorganisms. We also present the current state of knowledge on the alteration of DOM and the formation of DBPs during chlorine

photolysis. Our review focuses on the effect of solution and irradiation conditions (e.g., pH and irradiation wavelengths) on the efficacy of chlorine photolysis because the formation of reactive oxidants is dependent on these parameters. Most studies utilized low pressure-UV (LP UV; a monochromatic light source at 254 nm) or medium pressure-UV (MP UV; a polychromatic light source with wavelengths ranging from 200-400 nm) light sources. Studies conducted with alternate light sources (e.g., light in the UV-A region or the complete solar spectrum) are included when available. We limit our discussion to combined chlorine and irradiation applications, rather than sequential treatment (i.e., UV irradiation followed by chlorine addition). Studies on chloramine photolysis, which is not as photoactive as $HOCl/OCl^-$,[39,57,58,62] are not included.

2.3 Chemistry of Chlorine Photolysis

The rate of chlorine photolysis is pH and wavelength (**λ**) dependent. Solution pH is critical because the acid dissociation constant (pK_a) of hypochlorous acid is approximately 7.5 (Reaction 2.5), which is near the pH of many natural waters. As a result, the dominant chlorine species can shift between HOCl and OCl^- over the pH range expected in water treatment applications (Figure 2.1). The two chlorine species have different UV-visible absorption spectra (Figure 2.2); HOCl has a maximum absorption coefficient of 98-101 M^{-1} cm^{-1} at 235 nm, while OCl^- has a maximum absorption coefficient of 359-365 M^{-1} cm^{-1} at 292 nm.[41,63] Therefore, the effect of pH on chlorine photolysis rate depends on the light source used for irradiation. The photolysis rate of chorine is generally independent of pH using a LP UV light source because both species have similar absorptivities at 254 nm (Figure 2.2).[64] When UV-A, UV-B, or polychromatic (i.e., MP UV) light sources are used, the photodecomposition of chlorine is faster at higher pH values because OCl^- absorbs more light at $\lambda > 254$ nm (Figure 2.2).[59]

The products of chlorine photolysis are also pH and wavelength dependent. The irradiation of HOCl at $\lambda < 400$ nm produces $^{\bullet}OH$ and $Cl^{\bullet}$ via homolytic cleavage (Reaction 2.1 in Table 2.1).[47,59,65] $Cl^{\bullet}$ can react with water to produce $HOCl^{\bullet-}$ (Reaction 2.16 in Table 2.2), which can decompose to form additional $^{\bullet}OH$ (Reaction 2.20). At $\lambda < 320$ nm, the irradiation of OCl^- produces predominantly $O^{\bullet-}$ (Reaction 2.2) or excited singlet state oxygen atoms ($O(^1D)$) (Reaction 2.3). $O^{\bullet-}$ is the conjugate base of $^{\bullet}OH$ (Reaction 2.6; $pK_a = 11.9$), while $O(^1D)$ can produce $^{\bullet}OH$ through reaction with water (Reaction 2.7).[66] At $\lambda > 320$ nm, OCl^- photolysis produces ground state oxygen atoms ($O(^3P)$) (Reaction 2.4),[45,69] which react with O_2 to form O_3 (Reaction 2.8).[46,70,71]

The photochemical efficiency of chlorine photolysis can be described in three ways (Table 2.1). First, the quantum yield of chlorine loss (Φ_{HOCl} and Φ_{OCl^-} in Table 2.1) is most commonly reported. This quantum yield is equal to the moles of free chlorine lost per mole of photons absorbed. The quantum yield of chlorine loss is dependent on solution conditions and often has a value greater than 1.0 due to radical chemistry (e.g., additional chlorine loss via Reactions 2.10, 2.11, 2.13, and 2.14).[39,40] Second, the quantum yield of $^{\bullet}OH$ formation (Φ_{OH}) represents the moles of $^{\bullet}OH$ produced per mole of photons absorbed. This parameter represents the true quantum yield of Reactions 2.1 and 2.2. Finally, the production of $^{\bullet}OH$ may be represented by the yield factor (η_{OH}),[50] which is defined as the moles of $^{\bullet}OH$ produced per mole of free chlorine decomposed. Although these three parameters are sometimes compared within the literature, it is important to note that they represent different processes and cannot be used interchangeably.

The available quantum yields for Reactions 2.1 - 2.4 are summarized in Table 2.1. Although OCl^- can absorb more light (Figure 2.2), the production of $^{\bullet}OH$ is more efficient at low pH (i.e., when HOCl is the dominant species) and at $\lambda < 320$ nm because the quantum yield of $^{\bullet}OH$ production by HOCl is higher than that of OCl^-.[39,59,63,72] To date, most of the studies focusing on

contaminant transformation utilized wavelengths in the UV-C range (i.e., LP and MP UV sources) and focused on the generation of •OH. At higher irradiation wavelengths, HOCl photolysis becomes less important because the compound no longer absorbs light. Under these conditions, the photolysis products of OCl^- shift from $O^{\bullet-}$ and $O(^1D)$ (i.e., which subsequently generate •OH) to $O(^3P)$ (i.e., leading to O_3 generation).[46,70]

The numerous reactive oxidants produced during chlorine photolysis include •OH, Cl•, dichloride radical anion ($Cl_2^{\bullet-}$), and O_3. The most important reactions involved in the formation of these species are summarized in Table 2.2, along with the range of experimentally determined rate constants. Of the oxidants produced during the AOP, •OH is the least selective and most reactive species, reacting at near diffusion-controlled rates with many organic and inorganic compounds.[44,73] The radical reacts with organic compounds via H-atom abstraction, electron transfer, or OH addition.[73] While the high reactivity of •OH radical makes it ideal for degrading a wide range of contaminants, it is also inefficient as it reacts quickly with many compounds present in natural waters such as DOM, carbonate/bicarbonate, and other molecules.[44,59]

The reactive halogen species formed during chlorine photolysis include Cl• and $Cl_2^{\bullet-}$. Cl• forms directly from HOCl and OCl^- photolysis (Reactions 2.1 and 2.2). Although the reactivity of Cl• with many compounds is similar to •OH, it is generally more selective and therefore less desirable as an AOP oxidant. This radical generally reacts via H-atom abstraction or Cl addition, with rate constants near diffusion-controlled limit in some cases (i.e., 10^8 - 10^{10} M^{-1} s^{-1}).[80] Cl• radical can also react with Cl^- to form $Cl_2^{\bullet-}$ (Reaction 2.15) in aqueous solutions.[82] Like Cl•, $Cl_2^{\bullet-}$ can react via H-atom abstraction or Cl addition. Rate constants of $Cl_2^{\bullet-}$ are on the order of 10^2 - 10^6 M^{-1} s^{-1} for H-atom abstraction,[82] while reaction via Cl addition is generally noted to be faster.[80,82]

The production of O_3 in the AOP is desirable because the oxidant can lead to contaminant oxidation or pathogen inactivation through direct reaction or through the generation of $^{\bullet}OH$.[84] Rate constants for the oxidation of organic compounds by ozone vary widely (i.e., 10^{-2} - 10^{9} M^{-1} s^{-1})[84] and are generally four orders of magnitude faster than those for HOCl.[67,85]

In water containing bromide (Br^-), chlorine photolysis can result in the production of hypobromous acid (HOBr), hypobromate (OBr^-), and a series of bromine radicals.[86-88] The photolysis of HOBr and OBr^- produce $^{\bullet}OH$ and O_3 via similar pathways as their chlorinated analogues.[46,64,69,71,89] Bromine radicals such as $Br^{\bullet}$, $^{\bullet}BrO_3$, $Br_2^{\bullet-}$, $^{\bullet}BrO$, and $^{\bullet}BrO_2$ form via a series of electron transfer reactions when $^{\bullet}OH$ and $Cl^{\bullet}$ are present.[46,66,69,71,90] The oxidizing strength of the bromine radicals follows the general trend $^{\bullet}BrO_3 > Br^{\bullet} > Br_2^{\bullet-} > {}^{\bullet}BrO > {}^{\bullet}BrO_2$.[71,91] Bromine radicals are generally more reactive than their chlorine counterparts but are found in lower concentrations and therefore are less important in organic oxidation. Note that this review focuses on chlorine photolysis of freshwater and the chemistry of bromine radicals is not discussed in detail.

2.4 Applications of Chlorine Photolysis

2.4.1 Probe Compounds

A variety of model probe compounds have been used to quantify the formation of selected radicals and to assess the trends in radical formation under different experimental conditions (Table 2.3). An ideal probe compound should meet three criteria in order to be used during chlorine photolysis. First, the probe should react slowly with chlorine in the absence of light.[49,50,53] Second, the probe should undergo minimal direct photolysis under experimental conditions.[39,50,53] Rapid thermal oxidation by chlorine or rapid direct photolysis (e.g., *p*-chlorobenzoate photolysis at 254

nm)[92] complicates interpretation of experimental results. Finally, the probe compound should react with the specific reactive species through known mechanisms at known rates. For example, nitrobenzene is an ideal •OH probe because the compound does not react quickly with Cl• or $Cl_2^{\bullet-}$.[39,50] Conversely, many commonly used probes (e.g., benzoate and *p*-chlorobenzoate) react with both •OH and Cl• at comparable rates (Table 2.3).[39,49,50] Due to the formation of multiple reactive species during chlorine photolysis, the use of multiple probes (i.e., an •OH-specific probe and one that reacts with both •OH and Cl•) is a good approach to assess the yields of each species.

The relative importance of •OH and reactive halogen species (i.e., Cl• and $Cl_2^{\bullet-}$) as oxidants in the chlorine photolysis system has not been resolved. Multiple studies suggest that •OH is the dominant oxidant based on kinetic arguments. For example, experimental results obtained with both 1-chlorobutane and nitrobenzene were consistent with •OH as the only rate-controlling oxidant for the elimination of the probe molecules, despite the fact that 1-chlorobutane is also susceptible to reaction with Cl•.[50] Similarly, accurate prediction of *p*-chlorobenzoate (*p*-CBA) loss based on the results of nitrobenzene transformation supported the conclusion that •OH is the primary oxidant.[39] Conversely, a comprehensive kinetic model of chlorine photolysis indicated that both •OH and Cl• contributed to the degradation of benzoate during the photolysis of chlorine at 254 nm.[53] Reaction with Cl• was estimated to be more important because the bimolecular reaction rate between Cl• and benzoate is higher than that of •OH, assuming that benzoate reacts with Cl• at a similar rate to benzoic acid (Table 2.3). Although the limited ability of *t*-butanol to quench benzoate oxidation was reported as further evidence of the importance of non-•OH oxidants,[53] it is important to note that *t*-butanol and many other commonly used •OH quenchers also react with Cl• at near diffusion-controlled rates (Table 2.3). More research is needed to

conclusively demonstrate the relative importance of reactive halogen species compared to •OH during chlorine photolysis.

Quantification of the transformation products of probe compounds could provide needed insight into the contribution of Cl• as an oxidant. However, the probe experiments listed in Table 2.3 simply quantified the loss of the probe compounds and did not identify relative yields of transformation products, with the exception of methanol oxidation to formaldehyde. Aromatic probe compounds are likely to form different products depending on the oxidant with which they react. For example, benzoate reacts with •OH to form hydroxybenzoate isomers[101,102] and with Cl• to form chlorobenzoate isomers;[49,94] therefore, different yields of products could be used to investigate the relative yields of •OH and Cl•. However, it should be noted that the presence of halogenated products may not be due to direct reaction with Cl• or $Cl_2^{\bullet-}$ in the chlorine photolysis system. Phenols produced by •OH attack to the aromatic ring (e.g., nitrophenols produced by nitrobenzene oxidation) are more amenable to direct oxidation by free chlorine compared to the parent probe compound, leading to the production of halogenated products.[49,98] The formation of multiple products, including 2-chloro-4-nitrophenol, and the absence of chloronitrobenzene isomers as products of nitrobenzene oxidation during one chlorine photolysis study[39] demonstrates the relevance of this mechanism. Therefore, the role of reactive halogen species in the generation of chlorinated products from probe compounds must be interpreted carefully.

Despite the limitations in existing probe compound studies, the available data provides insight into the formation of reactive species during chlorine photolysis. Most probe studies of chlorine photolysis systems focused on the formation of •OH, in part because generation of the radical is critical for applications of the AOP. Reported steady-state concentrations of •OH ($[^{\bullet}OH]_{ss}$) range from 10^{-14} to 10^{-12} M, with most measured values on the order of 10^{-13} M.[39,41,52,53,64]

Details on the trends in $[^{\bullet}OH]_{ss}$ with respect to pH and wavelength are discussed below. Although limited data is available on the steady-state concentrations of reactive halogen species, $[Cl^{\bullet}]_{ss}$ and $[Cl_2^{\bullet-}]_{ss}$ on the order of 10^{-14} M and 10^{-14} to 10^{-13} M, respectively, were estimated using a kinetic model.[53]

Degradation rates of probe compounds and reported $[^{\bullet}OH]_{ss}$ values are consistently higher at lower pH values.[39,50,53,64,92,98] For example, the $[^{\bullet}OH]_{ss}$ at pH 6 - 6.5 is generally 2 - 4 times the $[^{\bullet}OH]_{ss}$ at pH 8.5 - 9.[53,64] Although OCl^- absorbs more light than HOCl (Figure 2.2),[59] it is less efficient at producing $^{\bullet}OH$ (Table 2.1).[39,50,64] Additionally, OCl^- reacts more quickly with $^{\bullet}OH$ compared to HOCl (Reactions 2.10 and 2.11) and the ability of free chlorine to scavenge $^{\bullet}OH$ increases at higher pH values.[39] Production of $^{\bullet}OH$ increases with chlorine concentration at pH values $\leq$ 6,[39,53] but is independent of chlorine concentration at circumneutral pH values due to enhanced scavenging of $^{\bullet}OH$ by OCl^-.[39] Collectively, these factors result in a lower apparent $^{\bullet}OH$ yield at higher pH values. Similarly, predicted steady-state concentrations of $Cl^{\bullet}$ and $Cl_2^{\bullet-}$ are both approximately four times higher at pH 6 compared to pH 9[53] and yields of chlorinated products from *n*-butanol transformation increased with decreasing pH values.[49]

The trends in $^{\bullet}OH$ and $Cl^{\bullet}$ production during chlorine photolysis due to irradiation wavelengths are less clear. At pH values > 8.5, similar $^{\bullet}OH$ yields were reported using a 254 nm lamp and a Hg lamp (λ > 300 nm)[50] and consistent $[^{\bullet}OH]_{ss}$ values were observed using both narrow-band LP UV and polychromatic MP UV irradiation sources.[64] Production of $^{\bullet}OH$ appears to be wavelength dependent at pH values < 6.5 (i.e., when HOCl is dominant); both Hg lamps[50] and MP UV lamps[64] produced higher $^{\bullet}OH$ yields than LP UV light sources. Limited data suggests

that production of $Cl^{\bullet}$ may also be wavelength dependent; higher yields of chlorinated *n*-butanol products were observed using 254 nm light compared to 365 nm light at pH 10.[49]

Numerous compounds typically present in natural waters can decrease loss rates of probe compounds by scavenging $^{\bullet}OH$ and $Cl^{\bullet}$, as is true for all $^{\bullet}OH$-based AOPs. Natural scavengers shown to affect probe compound degradation during chlorine photolysis include DOM, bicarbonate/carbonate, and bromide.[39,53,64,98] Additionally, scavengers that trigger chain reactions (e.g., methanol)[40] can lead to enhanced chlorine consumption while decreasing the oxidation rate of probe compounds. Based on relative rates of reaction, DOM preferentially scavenges $^{\bullet}OH$, while HCO_3^- preferentially scavenges $Cl^{\bullet}$.[53]

The generation of O_3 during chlorine photolysis (e.g., via Reaction 2.8) has received minimal attention in the literature, likely because the generation of O_3 is favored when higher wavelengths of light are used and most studies utilize light in the UV-C region (Tables 2.1 and 2.4). However, O_3 can form under some conditions.[52,55] For example, O_3 concentrations up to 1.8 μM were quantified when 10 mg Cl_2/L was irradiated in a solar simulator ($\lambda > 290$ nm) at pH 8.[52] O_3 is a potent oxidant and can undergo further reaction to form $^{\bullet}OH$;[84] therefore, the conditions under which chlorine photolysis results in enhanced O_3 generation warrants further investigation.

2.4.2 Organic Contaminants

The chlorine photolysis-based AOP is capable of transforming a wide range of target organic contaminants (Table 2.4). The process has been investigated in lab-, pilot-,[42,108,114] and full-scale treatment reactors,[56,108] with most studies utilizing LP and MP UV irradiation sources. Chlorine photolysis is able to remove recalcitrant organic compounds through three mechanisms: direct reaction with chlorine, direct photolysis, and reaction with reactive oxidants (e.g., $^{\bullet}OH$).

Different transformation products may be produced through each mechanism. For example, ronidazole forms chlorinated products through thermal reactions with HOCl, hydroxylated products during direct photolysis, and a combination of products during chlorine photolysis.[110] Therefore, contaminant transformation may result in a wide range of products (Table 2.4), including the formation of chlorinated products[48,54,103,107,110,112,115] and mineralization to CO_2 in some cases.[48,92,103,105,107,110,112,115] Although degradation of many compounds is generally very efficient,[42] some compounds are relatively less susceptible to oxidation in the AOP (e.g., carbamazepine,[42] cyclohexanoic acid,[40] desethylatrazine,[42] and TCE[56]).

Rates of contaminant removal are dependent on experimental conditions (e.g., pH, the concentration of chlorine, and irradiation intensity) and follow the trends expected based on the probe compound experiments described above. In general, the oxidation rates of target contaminants increase with decreasing pH values[41,56,105-111,114,115] and with increasing chlorine concentrations.[51,54,56,106,107,109-111,115] However, high concentrations of chlorine can result in decreased contaminant transformation rates due to scavenging of $^{\bullet}OH$, primarily at higher pH values when OCl^- is the dominant species.[51] Additionally, contaminant transformation product distributions can be dependent on initial chlorine concentrations, with a shift from organic products to mineralization observed at very high chlorine concentrations.[48,103,107,110,112] Finally, contaminant transformation rates are also dependent on light intensity,[107,109] but the effect of irradiation wavelength on organic compound removal has not been systematically investigated.

The role of reactive species in enhanced contaminant degradation rates during chlorine photolysis warrants further investigation. In most cases, $^{\bullet}OH$ is assumed to be the dominant oxidant based on the seminal work by Hoigné discussed above.[41,50,51,107,110,113] For example, a kinetic model developed for TCE oxidation assumed that the dominant loss pathways were through

direct photolysis and reaction with •OH.[41] One study provided mechanistic evidence for •OH by demonstrating that nitrobenzene (i.e., an •OH-specific scavenger) was able to quench oxidation of naphthenic acids.[106] Conversely, the formation of chlorinated metoprolol products was attributed to reaction with Cl• and ClO• radicals.[109] However, as discussed above, the presence of chlorinated products does not necessarily indicate direct reaction with halogen radicals; it is likely that hydroxylated products formed through •OH attack are more susceptible to oxidation by HOCl. Therefore, more mechanistic evidence is needed to conclusively rule out reactive halogen species as oxidants during chlorine photolysis.

Direct comparison between the UV/chlorine AOP and the commonly used UV/H_2O_2 AOP shows that UV/chlorine is more effective on the basis of contaminant removal, •OH yield, chemical costs, and energy usage under some conditions. HOCl and OCl^- are more efficient at producing •OH because the chlorine species absorb more light and have higher quantum yields than H_2O_2.[39,113,114] Additionally, the scavenging rate of •OH by HOCl (Reaction 2.10) is lower than that of H_2O_2 ($k_{H2O2} = 2.7 \times 10^7\ M^{-1}\ s^{-1}$).[39,114] However, OCl^- is much more reactive with •OH (Reaction 2.11) than either HOCl or H_2O_2 and the UV/chlorine AOP becomes less competitive at higher pH values.[114] In waters with low concentrations of dissolved organic carbon (DOC), UV/chlorine is more effective at producing •OH and at degrading target contaminants than UV/H_2O_2 only at slightly acidic pH values (i.e., pH ≤ 6.5).[41,108,113,114] However, UV/chlorine can be as effective as UV/H_2O_2 at circumneutral pH values in waters with [DOC] > 2 mg C/L.[41,113] The chemical costs of chlorine are up to 50% lower than that of H_2O_2[39,56,114] and the UV/chlorine AOP could result in a 30-75% energy savings compared to UV/H_2O_2, depending on the target contaminant and the pH of the treated water.[42,108]

2.4.3 Chlorine-resistant Microorganisms

Limited data is available on the inactivation of microorganisms during simultaneous exposure to chlorine and light. Photolysis of chlorine by simulated and real sunlight enhances the inactivation of chlorine-resistant microorganisms, including the model spore *Bacillus subtilis*[52] and the pathogenic oocyst *Cryptosporidium parvum*.[55] Inactivation of *B. subtilis* with chlorine in the dark was faster at pH 6 than at pH 8 because HOCl is a more potent disinfectant than OCl^-. However, the relative enhancement of inactivation due to chlorine photolysis was greater at higher pH values; *B. subtilis* inactivation rates increased by a factor of 1.2 and 2.3 at pH 6 and 8, respectively.[52] Increased inactivation of *B. subtilis* and *C. parvum* was observed in natural waters and in pure buffered waters, indicating that increased alkalinity and DOM did not play a major role in hindering inactivation.[52,55] The results from probe and quencher experiments demonstrate that both $^{\bullet}OH$ and O_3 have complementary roles in the inactivation of *B. subtilis* and *C. parvum*, possibly by sensitizing the organisms to further oxidative attack by HOCl or O_3.[52,55] More research is needed on the mechanism and rates of inactivation of other chlorine-resistant microorganisms during chlorine photolysis, as well as inactivation rates under different conditions (e.g., UV-C irradiation).

2.5 Formation of Disinfection By-products

2.5.1 Alteration of Bulk DOM Properties

The reaction of DOM with chlorine is the major source of DBPs during conventional water disinfection.[4-6] Therefore, investigating the effect of chlorine photolysis on the concentration and composition of DOM is essential to understanding the effect of the AOP on DBP production. During chlorine photolysis, DOM could react directly with $HOCl/OCl^-$, undergo photobleaching

via direct photolysis, or react with reactive oxidants (e.g., $^{\bullet}OH$, O_3, or $Cl^{\bullet}$). Each of these processes may change the molecular composition of DOM and alter its reactivity with chlorine, leading to changes in DBP formation.[39,92,98,116] Furthermore, the reaction of $Cl^{\bullet}$ or $Cl_2^{\bullet-}$ with DOM could produce novel DBPs.[116]

The combination of chlorine and light can alter treated waters by affecting the concentration of DOM compared to water that has only been exposed to chlorine in the dark. Chlorine photolysis of natural waters consistently results in enhanced loss of absorbance in the UV-C region (i.e., absorbance at 254 nm).[62,92,98] Loss of absorbance at 254 nm is greater under UV-C irradiation compared to UV-A irradiation, and is greater at lower pH values.[92] Loss of absorbance is coupled to enhanced mineralization (i.e., loss of DOC) in most cases using MP UV,[117] UV-C,[62,118] and UV-A[119] light sources at circumneutral pH values and free chlorine concentrations as low as 1.5 mg/L. The loss of absorbance and extent of mineralization is higher for solutions exposed to both chlorine and light compared to light alone[98,119] or chlorine alone.[62,97,98]

Additionally, chlorine photolysis can alter the composition of DOM by changing its structure. The irradiation of natural water in the presence of chlorine results in a loss of chromophoric moieties (i.e., preferential loss of absorbance in the visible and UV-A regions)[92,98] and a decrease in fluorescence;[92] losses were greater for solutions simultaneously exposed to both chlorine and light relative to chlorine and light separately. This preferential loss of high-molecular weight chromophoric moieties can result in a decrease in the molecular weight of DOM.[98] Irradiation of DOM in the presence of chlorine also decreases the specific absorbance at 254 nm ($SUVA_{254}$), which corresponds to a decrease in aromaticity.[92] Similar trends have been observed for DOM exposed to UV irradiation in the absence of chlorine.[12,13,88,120]

2.5.2 Organic DBPs

The interaction of chlorine with light will alter the concentration and distribution of organic DBPs formed by DOM during the advanced oxidation process. Chlorine photolysis could potentially decrease DBPs by decreasing the concentration of DOM and by allowing for a shorter contact time compared to traditional chlorine disinfection systems.[42,52] However, the benefits of a short contact time may be offset by the need for higher chlorine concentrations because depletion of the concentration of chlorine via photolysis (Reactions 2.1-2.4)[39,113,116] and by chain reactions between chlorine and carbon-centered radicals[63,121] increases chlorine demand. Finally, the changes in DOM composition (i.e., the decrease in chromophoric, fluorescent, and aromatic moieties) observed during chlorine photolysis will alter the reactivity of DOM with chlorine.

The formation of trihalomethanes (THMs), haloacetic acids (HAAs), haloacetonitriles (HANs), and total organic halides (TOX) from DOM during chlorine photolysis has been investigated in multiple studies. It is challenging to make broad conclusions about the trends in DBP formation during chlorine photolysis due to variability in experimental conditions across studies. Variables include the use of different light sources (LP UV, MP UV, UV-A, and Hg lamps), different pH values (6.5-8.5), different chlorine concentrations (1.5-10 mg/L as Cl_2), and different water sources with a wide range of DOC concentrations (1.5-5 mg C/L). Available data for experiments in which DBP concentrations change due to reaction of chlorine with DOM in the presence and absence of light are summarized in Figure 2.3 and in Tables A1-A4. The difference between [DBP] measured with chlorine in the light and [DBP] produced by chlorine in the dark enables visualization of the relative increase or decrease in each DBP class. Data points with values < 0 represent experiments in which DBP concentrations decreased in the AOP relative to reaction

of the same DOM with the same chlorine concentration in the dark, while data points with values > 0 represent experiments in which DBP concentrations increased. Note that DBP concentrations increase with time of reaction with chlorine (i.e., post-photolysis); all chlorine reaction times, which range from < 1 min to 3 days, are included in the figure to show the relative changes in DBP yield. The trends in DBP formation with respect to concentration, pH, and wavelength are described for individual organic DBP classes below.

The effect of chlorine photolysis on THM yields relative to reaction with chlorine in the dark is highly variable (Figure 2.3a; Table A1). Irradiation of DOM with MP UV[14,116] and UV-A[92] light in the presence of chlorine generally resulted in higher concentrations of THMs relative to dark controls, while irradiation with an Hg lamp (λ > 300 nm) resulted in lower THM concentrations.[50] The use of LP UV light sources both increased[14] and decreased[62,92] relative THM yields. Despite possible increases in THM production, the reported THM concentrations due to irradiation with chlorine and subsequent reaction with chlorine for up to two hours were always below the maximum contaminant level (MCL) of 80 μg/L.[122,123] Similarly low levels of THM production were observed in additional chlorine photolysis studies that did not report the concentration of THMs in dark reactions.[42,113,114] Limited data suggests less THM formation during chlorine photolysis at higher pH values[50,116] and with lower wavelengths of light.[92] However, these general trends do not hold across all of the available studies, possibly due to differences in experimental parameters or DOM sources.

The production of HAAs during chlorine photolysis is also sensitive to experimental parameters (Figure 2.3b; Table A2). Note that Figure 2.3 includes data on the sum of the five regulated HAAs (HAA_5), as well as the sum of nine frequently studied HAAs (HAA_9 = HAA_5 + bromochloro-, bromodichloro-, dibromochloro- and tribromoacetic acid). Total HAA

concentrations during chlorine photolysis have been reported to increase,[14,92,116] decrease,[14,62] or stay the same[14] relative to reaction with chlorine in the absence of light. Production of HAAs immediately after chlorine addition was always below the MCL of 60 μg/L.[62,92,113,114,116,122,123] HAA yields in chlorine photolysis systems appear to decrease with increasing pH values.[116] With respect to wavelength, UV-C light produced higher yields of HAA_5, but lower yields of HAA_9 relative to UV-A light.[92] However, experiments with four different DOM sources irradiated with LP and MP UV using the same chlorine concentration at the same pH value produced conflicting trends in HAA formation potential, further highlighting the importance of DOM composition in DBP formation potential.[14] A limited amount of data is available for nitrogen-containing DBPs (N-DBPs). Two studies on haloacetonitrile (HAN) formation during chlorine photolysis indicate that production of this class of DBPs is enhanced using LP and MP UV (Figure 2.3c; Table C3).[62,116] The yield of HANs during chlorine photolysis was higher at pH 6.5 compared to pH 8.5 and increased with increasing chlorine concentrations.[116] *N*-Nitrosodimethylamine (NDMA) was not observed in a LP UV-based chlorine photolysis AOP, which is unsurprising given that NDMA is most commonly associated with disinfection by chloramine.[42] Finally, elevated levels of cyanogen chloride, dichloroacetonitrile, and chloropicrin were produced during UV-C irradiation of chlorine, but these studies used model amine precursors which may not be representative of DOM in drinking water sources.[107,110,125-127]

The production of TOX, the total organic halogenated material formed during chlorination, was also quantified during chlorine photolysis in several studies (Figure 2.3d; Table A4). In most cases, TOX decreased or stayed the same in studies using LP UV,[64,92,124] MP UV,[64,98] or UV-A[92] irradiation. Conversely, TOX increased during photolysis relative to dark controls in a limited number of studies using LP UV,[64] MP UV,[116,124] and UV-A irradiation.[49] Yields of TOX during

chlorine photolysis were typically lower at higher pH values.[64,98,116] Overall, the reported changes in TOX yields were fairly modest (Figure 2.3d), suggesting that chlorine photolysis may change the distribution of organic halogens without changing bulk TOX concentrations.

While the above discussion considers the possibility of chlorine photolysis altering DBP production due to changes in DOM reactivity, it is also possible that photolysis could lead to degradation of DBPs after they have formed either through direct or indirect photodegradation. For example, chlorinated THMs and HAAs were predominant in waters irradiated using UV-C light, while their brominated analogues were present in much higher levels in UV-A light and in dark control reactions.[92] Similarly, chloroform was the only THM formed in a UV-C/HOCl experiment, while both chloroform and bromodichloromethane were formed with HOCl alone.[62] The decreased yield of brominated organics might be due to direct photolysis by UV-C light,[92] in agreement with the observation of direct photolysis of brominated THMs and HAAs using a MP UV (i.e., polychromatic) light source.[128] Several classes of N-DBPs (e.g., nitrosamines and halonitromethanes) are amenable to direct photolysis[129-131] and could also be potentially degraded in the AOP. Additionally, $^{\bullet}OH$ formed during chlorine photolysis could lead to the degradation of DBPs;[98] this area of research warrants further investigation.

2.5.3 Inorganic DBPs

Chlorine photolysis can produce numerous inorganic products, including chloride (Cl^-), chlorate (ClO_3^-), perchlorate (ClO_4^-), chlorite (ClO_2^-), chlorine dioxide (ClO_2), and bromate (BrO_3^-) via $O(^3P)$- and O_3-mediated pathways in the presence of chlorine and bromide.[45,46,52,87,132,133] With the exception of Cl^-, these species are either currently regulated or under consideration for regulation in drinking water by the U.S. Environmental Protection

Agency.[122,123,134] The major stable inorganic products of chlorine photolysis are Cl^- and ClO_3^-, with yields of free chlorine conversion ranging from 50-91% and 2-30%, respectively.[116,121,135,136] Higher yields of chlorate were observed using narrow-band UV-A, -B, and -C irradiation sources[121,135,136] compared to polychromatic MP UV light.[116] Additionally, the highest yields of chlorate were reported at circumneutral pH values over the pH range 3-10 using UV-B light.[136] The rate of chlorate production is first order with respect to [Cl_2] and is yield independent of light intensity.[136]

The photolysis of chlorine can produce low levels of ClO_4^- under some conditions. Reported yields of free chlorine conversion to perchlorate range from 0.09 x 10^{-3} to 9.2 x 10^{-3} % using a range of chlorine concentrations (70 - 10,000 mg/L Cl_2), pH values (3 - 10), and irradiation wavelengths (254, 311, and 365 nm).[136] The maximum concentration of perchlorate expected from 7 mg/L Cl_2, a typical concentration used in the AOP, is on the order of 0.1 μg/L.[136] A second study reported elevated ClO_4^- generation during OCl^- photolysis using 254 nm light relative to dark controls only at very high concentrations of OCl^- (i.e., 10,000 mg/L Cl_2).[135] Experimental evidence exists for two proposed mechanisms of perchlorate production which involve either chlorite[136] or chlorine dioxide[135,137] as intermediates. The underprediction of ClO_4^- production by a ClO_3^--dependent kinetic model in UV-A irradiation experiments,[136] as well as enhanced production of ClO_4^- from ClO_2^- photolysis at higher wavelengths,[135] suggests that multiple intermediates could be responsible for ClO_4^- production under some conditions. Although two additional studies did not detect ClO_4^- as a product of chlorine photolysis,[116,121] the expected concentrations of ClO_4^- are very low and it is possible that the anion was below the analytical detection limit.

Chlorine photolysis can also generate ClO_2^- (Reaction 2.9) and ClO_2 (Reaction 2.23), but these species are photolabile and are not expected to accumulate in solution. For example,

photoproduction of ClO_2^- has only been quantified using UV-A irradiation of chlorine (i.e., compared to analogous experiments using UV-B and UV-C irradiation), where it behaved as a transient intermediate.[136] This observation is supported by studies on the photolysis of chlorite using 254 nm light, which produces Cl^- (68%) and ClO_3^- (32%) as the major stable species[135] and ClO_2 as a photolabile intermediate.[137] The absence of chlorite[116,121] and chlorine dioxide[52] in additional studies on chlorine photolysis could be due to either analytical sensitivity issues or the transient nature of the photolabile species.

In bromide-containing waters, the photolysis of chlorine could potentially lead to the production of bromate. There are several possible pathways of bromate formation which require the generation of HOBr or OBr^- as intermediates. HOBr/OBr^- could be formed from the oxidation of bromide by O_3 under conditions in which O_3 is generated,[86,87] or by oxidation of Br^- by free chlorine.[88] HOBr/OBr^- can subsequently react with either $^{\bullet}OH$ or O_3 to yield BrO_3^-, as described in detail by von Gunten.[86,87] Although the possible formation of bromate as a DBP during chlorine photolysis has received minimal attention, the oxyanion was detected in one study using MP UV as an irradiation source.[116] Approximately 0.01-0.05% of the photolyzed chlorine produced BrO_3^-, corresponding to concentrations of 0.1-2 μg/L, with higher formation occurring at lower pH values. The formation of bromate during chlorine photolysis warrants further investigation, particularly in waters with elevated ambient bromide concentrations.

2.5.4 Formation of Novel DBPs

The reaction of photochemically generated $Cl^{\bullet}$ or $Cl_2^{\bullet-}$ with DOM could produce novel DBPs. Trends in the chlorination of model compounds during chlorine photolysis provide some insight into the reactivity of reactive halogen species in the AOP. Although $^{\bullet}OH$ outcompetes $Cl^{\bullet}$

for reaction with many aliphatic compounds (e.g., ethanol and maleic acid),[49,98] chlorine photolysis can lead to the production of halogenated products of some compounds (e.g., *n*-butanol and propionic acid) that do not react with chlorine in the dark.[49,103] For example, up to 16% of *n*-butanol was converted to chlorinated products when the compound was irradiated in the presence of chlorine using UV-A light, with higher yields produced at lower pH values.[49] Lower wavelengths of light also produced higher yields of chlorinated *n*-butanol[49] and propionic acid.[103] Although these studies used high concentrations of chlorine (Table 2.4), they indicate that lower pH values and lower wavelengths of light favor the generation of $Cl^{\bullet}$ and possible production of organohalogens.

The mechanism of halogenated aromatic production during chlorine photolysis is more complex. While chlorinated products of benzoic acid,[49,53,98] nitrobenzene,[39,98] and metoprolol[109] have been observed, the production of organohalogens cannot be solely attributed to reaction with reactive halogen species. As described above, it is also possible for phenolic products generated by $^{\bullet}OH$ attack to undergo thermal reaction with chlorine.[49,98] The latter halogenation mechanism may be dominant for some compounds that are highly resistant to oxidation (e.g., nitrobenzene).[98] Additionally, for compounds that are amenable to direct oxidation by chlorine (e.g., phenol and triclosan), chlorine photolysis can lead to the production of ring cleavage products.[54,98]

The formation of novel DBPs during chlorine photolysis has not yet been investigated. Studies using high-resolution Fourier transform ion cyclotron resonance mass spectrometry (FT-ICR MS) have identified hundreds of molecular formulas with one, two, or three chlorine or bromine atoms following the chlorination of DOM, many of which had not been previously detected.[138-142] Although one study presented the mass spectra of Suwannee River NOM before and after chlorine photolysis,[98] the triple quadrupole MS used to generate the mass spectra did not

provide sufficient resolving power to identify molecular formulas in complex mixtures of organic molecules (i.e., DOM). More research is needed using high-resolution mass spectrometry techniques to assess whether chlorine photolysis generates novel high molecular weight DBPs compared to reaction of DOM with chlorine alone.

2.6 Conclusions and Need for Future Research

This review suggests that photolysis of chlorine could effectively convert existing drinking water treatment systems into advanced oxidation processes. The reaction of HOCl and OCl^- with light produces multiple reactive oxidants, including $^{\bullet}OH$, $Cl^{\bullet}$, and O_3. Chlorine photolysis is able to transform recalcitrant organic compounds through three mechanisms: direct reaction with chlorine, direct photolysis, and reaction with reactive oxidants (e.g., $^{\bullet}OH$). In the case of the two studied chlorine-resistant pathogens, the presence of multiple oxidants can lead to synergistic disinfection mechanisms. Chlorine photolysis is able to outcompete commonly used UV/H_2O_2 AOP on the basis of $^{\bullet}OH$ production, energy usage, and cost under some conditions.

The production of reactive oxidants and transformation of organic compounds during chlorine photolysis is dependent on solution and irradiation conditions. The effect of solution pH on the efficacy of chlorine photolysis is clear; lower pH values result in higher steady-state concentrations of $^{\bullet}OH$, $Cl^{\bullet}$, and $Cl_2^{\bullet-}$, leading to enhanced contaminant removal. This trend can be attributed to the increased efficiency of $^{\bullet}OH$ production by HOCl photolysis and decreased rate of reaction between $^{\bullet}OH$ and HOCl compared to OCl^-. As observed with other AOPs, the presence of other water constituents (e.g., DOM and bicarbonate/carbonate) decreases the efficiency of chlorine photolysis for target contaminant transformation. Finally, the effect of wavelength on oxidant production and contaminant transformation during chlorine photolysis has not been

systematically investigated. Limited data suggests that $^{\bullet}OH$ production is wavelength-dependent at pH < 6.5 and that lower wavelengths of light favor the generation of $Cl^{\bullet}$.

A major concern about the use of chlorine photolysis is its potential impact on organic and inorganic DBP formation. Chlorine photolysis alters the composition and reactivity of DOM by decreasing its concentration and by preferentially removing aromatic and high molecular weight material. The resulting impact on organic DBP yields, such as THMs, HAAs, and HANs, is sensitive to experimental parameters. Although organic DBP yields tend to be lower at higher pH values, it is difficult to compare results across different studies due to differences in experimental conditions. In general, chlorine photolysis can either increase or decrease DBP concentrations compared to reaction with chlorine in the dark, but the effect is modest. The main inorganic products of chlorine photolysis are Cl^- and ClO_3^-, with trace levels of ClO_4^-, ClO_2^-, and ClO_2 observed in some studies.

This systematic review of chlorine photolysis studies for water treatment applications reveals several limitations associated with the current body of knowledge.

(1) Many studies assume that $^{\bullet}OH$ is the dominant oxidant without providing mechanistic evidence. More work is needed to assess the potential importance of reactive halogen species (i.e., $Cl^{\bullet}$ and $Cl_2^{\bullet-}$) and O_3 as oxidants. The role of specific oxidants could be assessed through the careful selection of probes and quenchers, or by identifying and quantifying the products of probe compound transformation.

(2) Fundamental research demonstrates that the quantum yields of Reactions 1-4 are wavelength-dependent. However, most studies utilize light in the UV-C region and the effect of irradiation wavelength on the production of oxidants from chlorine photolysis has not been

comprehensively studied. Consideration of irradiation by wavelengths within the actinic spectrum is critical for certain applications of chlorine photolysis (e.g., enhanced solar disinfection).

(3) Available data on model organism and pathogen inactivation during chlorine photolysis is very limited. This area should be expanded to include both conventional and chlorine-resistant pathogens, both of which are likely to undergo enhanced inactivation.

(4) The effect of chlorine photolysis on DBP yields is unclear; some studies show a modest enhancement in DBP production, while others show a decrease in DBP yields. More systematic work on the effect of experimental parameters on DBP production is needed, with an emphasis on both regulated and unregulated (e.g., N-DBPs) compounds. Analysis for novel DBPs using high-resolution mass spectrometry techniques could provide needed insight into the effect of chlorine photolysis on DOM reactivity with chlorine and subsequent formation of DBPs.

In summary, a complete understanding of the chemistry of chlorine photolysis is necessary to optimize conditions for the AOP in water treatment applications in order to simultaneously enhance pathogen inactivation and contaminant transformation while limiting possible negative effects on DBP yields.

2.7 Acknowledgements

This work was supported by an NSF CAREER award (CBET-1451932).

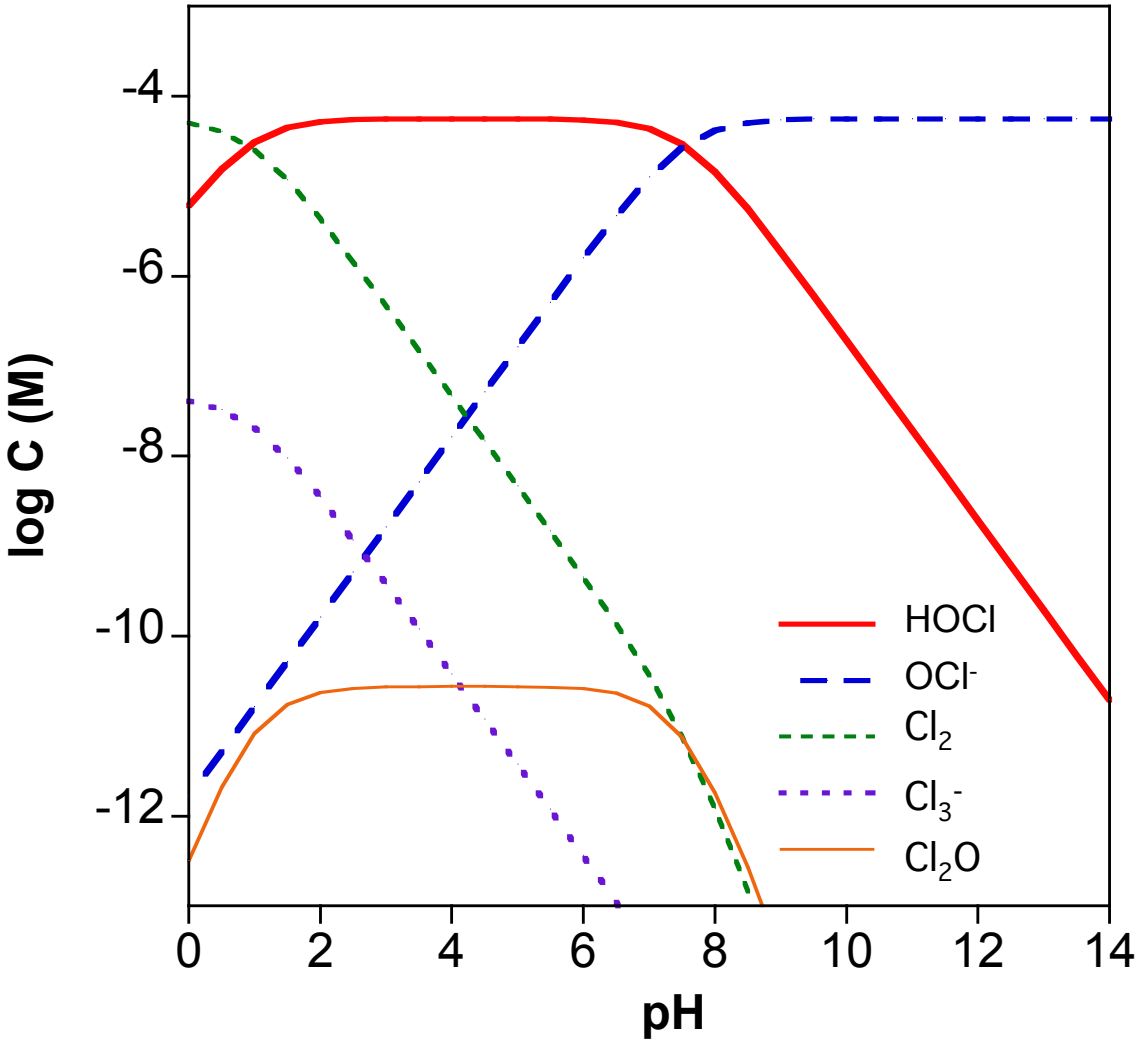

Figure 2.1. Chlorine speciation in 4 mg/L total chlorine and 150 mg/L chloride as a function of pH. Equilibrium constants are from Reference 3.

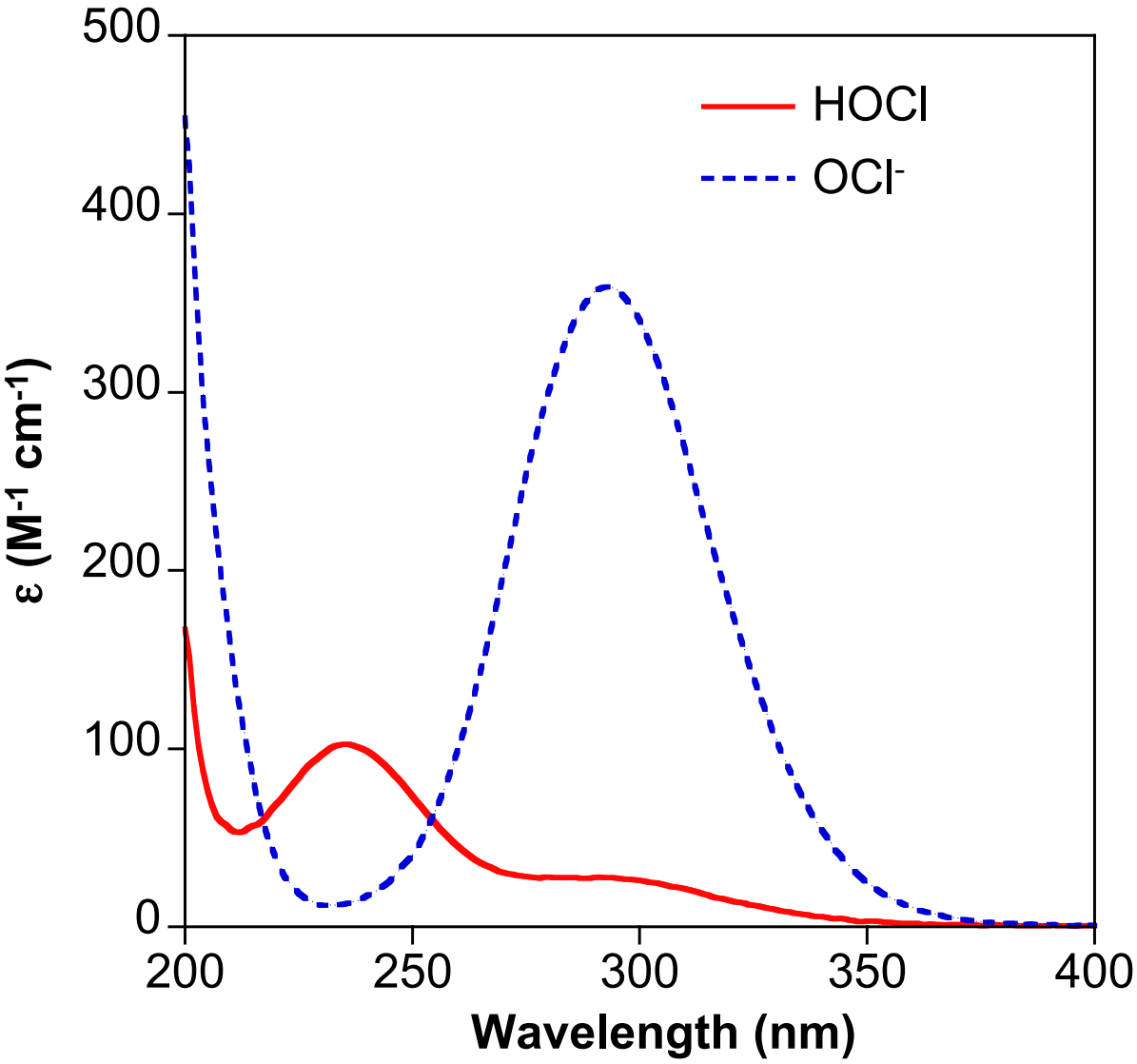

Figure 2.2. The molar absorption coefficients (**ε**) of HOCl and OCl^- as a function of wavelength. The spectra were collected using solutions of free available chlorine in ultrapure water adjusted to pH 6 (HOCl) and pH 9 (OCl^-) using HCl and NaOH, respectively.

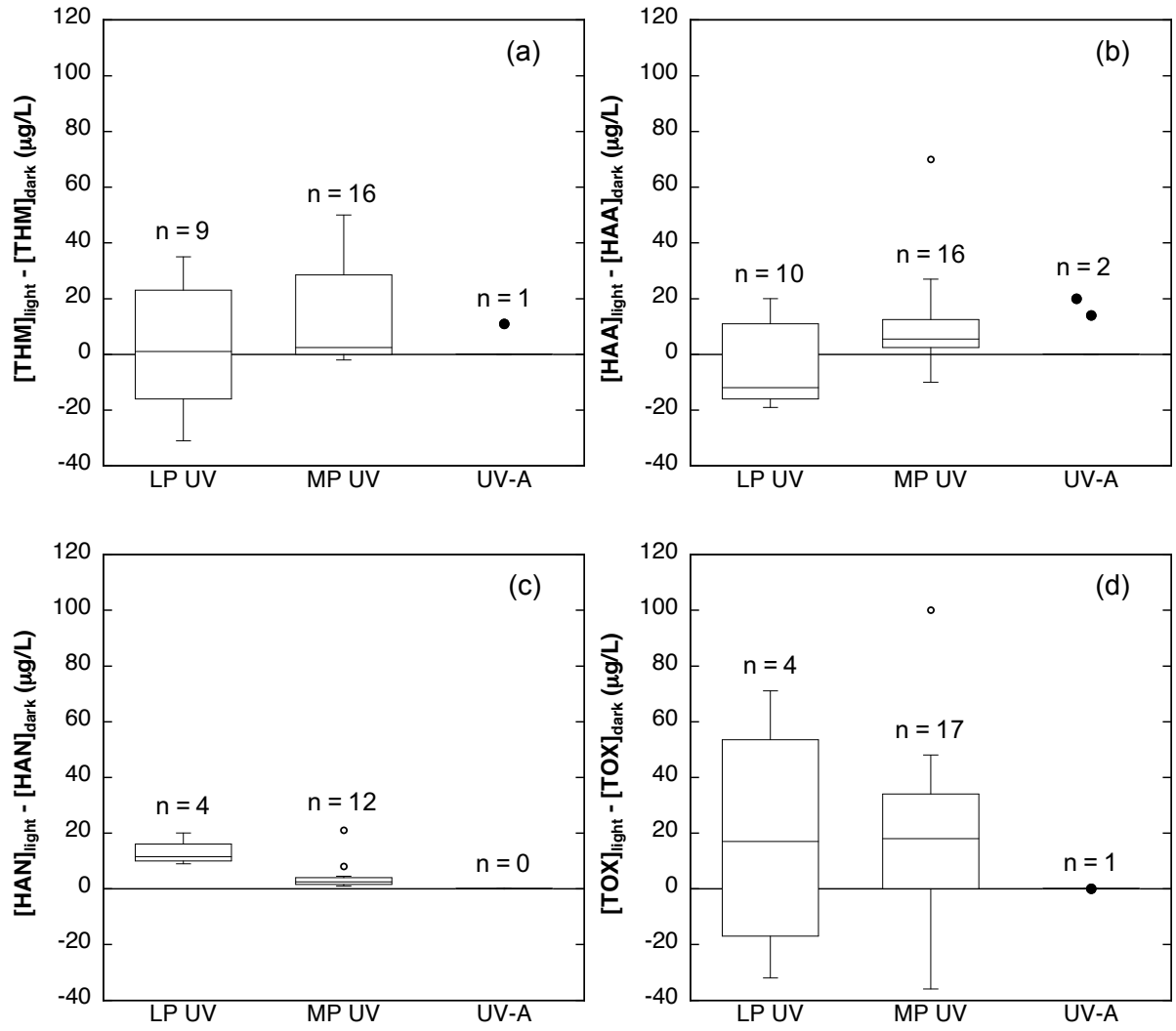

Figure 2.3. Difference between the concentrations of (a) THMs, (b) total HAAs, (c) HANs, and (d) TOX observed during chlorine photolysis and during reaction of the same source water with the same concentration of chlorine in the dark. Box-and-whisker plots were prepared when sufficient data was available ($n \geq 4$). Lines of the boxes represent the first and third quartiles. The line within each box represents the median. Whiskers represent minimum and maximum concentrations. Hollow points represent outliers (i.e., any point less than the lower quartile or greater than the upper quartile by more than 1.5 times the interquartile range). Solid points are individual data points for conditions with insufficient data to construct box-and-whisker plots. Data is summarized from References 14, 62, 64, 92, 116, and 124. Specific experimental conditions for each data point are provided in Tables A1-A4.

Table 2.1. Summary of quantum yields of chlorine decomposition (Φ_{HOCl}, Φ_{OCl^-}), $^{\bullet}OH$ formation (Φ_{OH}), and excited molecular oxygen formation ($\Phi_{O(3P)}$, $\Phi_{O(1D)}$), as well as yield factors of $^{\bullet}OH$ (η_{OH}). Only experiments conducted at pH values < 6.5 (HOCl) or > 8.5 (OCl^-) are included. References are indicated as superscripts.

No.	Reaction	Parameter	254 nm (UV-C)	303-313 nm (UV-B)	355-365 nm (UV-A)	> 300 nm (Hg)	200-400 nm (MP UV)
2.1	$HOCl + h\nu \rightarrow {}^{\bullet}OH + Cl^{\bullet}$	Φ_{HOCl}	1.0 – 2.8[39,40,53,63,64]	N/A	N/A	N/A	1.06 – 3.7[39,41,64]
		Φ_{OH}	1.4[39]	1.0*[65,68]	N/A	N/A	0.79[41]
		η_{OH}	0.46 – 0.85[40,50]	N/A	N/A	0.70[50]	N/A
2.2	$OCl^- + h\nu \rightarrow O^{\bullet-} + Cl^{\bullet}$	Φ_{OCl^-}	0.85 – 2.4[39,40,45,53,63,64]	0.39 – 0.87[45,51]	0.60[45]	N/A	0.9 – 1.7[39,64]
		Φ_{OH}	0.278[45]	0.127[45]	0.08[45]	N/A	N/A
		η_{OH}	0[50]	0.70[51]	N/A	0.10[50]	1.18[41]
2.3	$OCl^- + h\nu \rightarrow Cl^- + O(^1D)$	$\Phi_{O(1D)}$	0.133[45]	0.020[45]	0[45]	N/A	N/A
2.4	$OCl^- + h\nu \rightarrow Cl^- + O(^3P)$	$\Phi_{O(3P)}$	0.074[45]	0.075[45]	0.28[45]	N/A	N/A

* = data collected in the gas phase
N/A = data not available

Table 2.2. Summary of major reactions in the chlorine photolysis AOP in freshwater systems.

No.	Reaction	Rate constant	Reference
2.5	$HOCl \rightleftharpoons H^+ + OCl^-$	$pK_{a2.5}$ = 7.40 - 7.47	3, 74
2.6	$^{\bullet}OH \rightleftharpoons H^+ + O^{\bullet-}$	$pK_{a2.6}$ = 11.9 ± 0.2	44
2.7	$O(^1D) + H_2O \rightarrow 2\ ^{\bullet}OH$	$k_{2.7}$ = 1.2 x 10^{11} $M^{-1}s^{-1}$	65
2.8	$O(^3P) + O_2 \rightarrow O_3$	$k_{2.8}$ = 4 x 10^9 $M^{-1}s^{-1}$	46, 70, 71
2.9	$O(^3P) + OCl^- \rightarrow ClO_2^-$	$k_{2.9}$ = 9.4 x 10^9 M^{-1} s^{-1}	46, 70
2.10	$^{\bullet}OH + HOCl \rightarrow ClO^{\bullet} + H_2O$	$k_{2.10}$ = 8.5 x 10^4 – 2.0 x 10^9 $M^{-1}s^{-1}$	39, 75-77
2.11	$^{\bullet}OH + OCl^- \rightarrow ClO^{\bullet} + OH^-$	$k_{2.11}$ = 8.8 x 10^8 – 9.8 x 10^9 $M^{-1}s^{-1}$	44, 50, 70, 75, 77
2.12	$^{\bullet}OH + Cl^- \rightarrow HOCl^{\bullet-}$	$k_{2.12}$ = 4.3 x 10^9 M^{-1} s^{-1}	69, 73, 78
2.13	$Cl^{\bullet} + HOCl \rightarrow ClO^{\bullet} + H^+ + Cl^-$	$k_{2.13}$ = 3 x 10^9 M^{-1} s^{-1}	69
2.14	$Cl^{\bullet} + OCl^- \rightarrow ClO^{\bullet} + Cl^-$	$k_{2.14}$ = 8.2 x 10^9 M^{-1} s^{-1}	69
2.15	$Cl^{\bullet} + Cl^- \rightarrow Cl_2^{\bullet-}$	$k_{2.15}$ = 6.5 x 10^9 – 2.1 x 10^{10} M^{-1} s^{-1}	69, 73, 78-81
2.16	$Cl^{\bullet} + H_2O \rightarrow HOCl^{\bullet-} + H^+$	$k_{2.16}$ = 3.0 x 10^2 – 1.8 x 10^4 M^{-1} s^{-1}	69, 78, 79
2.17	$Cl_2^{\bullet-} \rightarrow Cl^{\bullet} + Cl^-$	$k_{2.17}$ = 6.0 x 10^4 – 1.1 x 10^5 s^{-1}	73, 78-80
2.18	$Cl_2^{\bullet-} + OH^- \rightarrow Cl^- + HOCl^{\bullet-}$	$k_{2.18}$ = 7.3 x 10^6 – 4.5 x 10^7 s^{-1}	82, 83
2.19	$Cl_2^{\bullet-} + H_2O \rightarrow Cl^- + HOCl^{\bullet-} + H^+$	$k_{2.19}$ = 2.4 x 10^1 $M^{-1}s^{-1}$	73, 79
2.20	$HOCl^{\bullet-} \rightarrow {}^{\bullet}OH + Cl^-$	$k_{2.20}$ = 4.3 x 10^9 $M^{-1}s^{-1}$	69, 73
2.21	$HOCl^{\bullet-} + Cl^- \rightarrow Cl_2^{\bullet-} + OH^-$	$k_{2.21}$ = 1.0 x 10^5 $M^{-1}s^{-1}$	53
2.22	$HOCl^{\bullet-} + H^+ \rightarrow Cl^{\bullet} + H_2O$	$k_{2.22}$ = 2.1 x 10^{10} $M^{-1}s^{-1}$	69
2.23	$O_3 + ClO_2^- \rightarrow ClO_2 + O_3^{\bullet-}$	$k_{2.23}$ = 4 x 10^6 $M^{-1}s^{-1}$	69

Table 2.3. Bimolecular reaction rates between commonly used probe molecules and $^{\bullet}OH$, $Cl^{\bullet}$, and $Cl_2^{\bullet-}$.

Probe	Reaction Rate with $^{\bullet}OH$ (M^{-1} s^{-1})	Ref.	Reaction Rate with $Cl^{\bullet}$ (M^{-1} s^{-1})	Ref.	Reaction Rate with $Cl_2^{\bullet-}$ (M^{-1} s^{-1})	Ref.	Used as a probe in:
benzoate	5.9×10^9	44	N/A		2×10^6	82	49, 53
benzoic acid	1.8×10^9	93	1.8×10^{10} (pH 4)*	94	2×10^5 (pH 4)*	94	
n-butanol	4.2×10^9	44	4.8×10^8 (acetonitrile)**	95	N/A		49
t-butanol	6.0×10^8	44	3×10^8	96	7×10^2	82	
p-chlorobenzoate	5.0×10^9	97	does react at pH<1	39	3×10^6	82	39, 40, 52, 64, 92, 98
1-chlorobutane	3.4×10^9	99	does react at pH<1	50	N/A		50
ethanol	1.9×10^9	44	1.5×10^9	80	4.5×10^4	82	49
methanol	9.7×10^8	44	5.7×10^9 (carbon tetrachloride)**	100	3.5×10^3	82	40, 51
nitrobenzene	3.9×10^9	44	Negligible	39, 50	Negligible	39, 50	39, 50, 53
2-propanol	1.9×10^9	44	6×10^9	96	1.2×10^5	82	

* = Rates were measured at pH 4 (benzoic acid $pK_a = 4.2$).
** = Rates were determined in non-aqueous solvents as indicated.
N/A = data not available.

Table 2.4. Summary of contaminant transformation studies using chlorine photolysis as an advanced oxidation process. Studies that observed an enhanced contaminant degradation rate (i.e., relative to reaction with the same [chlorine] in the dark), as well as studies that identified contaminant transformation products, are noted.

Compound	Light Source	[Free chlorine] (mg Cl_2/L)	pH	References for Chlorine Photolysis	
				Enhanced Degradation Rate	Product Data Available
Acids					
Acetic acid	Hg	30,500	12	103	103
α-Chloropropionic acid	Hg	32,500	12	103	103
β-Chloropropionic acid	Hg	32,500	12	103	103
α-Hydroxypropionic acid	Hg	33,250	12	103	103
β-Hydroxypropionic acid	Hg	32,300	12	103	103
Propionic acid	Hg	31,400	12	103	103
Antibacterial agent					
Triclosan	LP UV	1.4-7	7	54	54
Aromatic sulfonic acids					
p-Cumenesulfonic acid	Hg	710	12	104	104
2-Mesitylenesulfonic acid	Hg	710	12	104	104
1-Napthalenesulfonic acids	Hg	710	12	104	104
2-Napthalenesulfonic acids	Hg	710	12	104	104
Chelating agent					
Ethylenediaminetetraacetic acid (EDTA)	LP UV	0-5.4	5-9	105	105
Corrosion inhibitor					
Benzotriazole	LP UV	1-6	7	42	
Tolyltriazole	LP UV	1-6	7	42	

Table 2.4 continued

Compound	Light Source	[Free chlorine] (mg Cl_2/L)	pH	References for Chlorine Photolysis	
				Enhanced Degradation Rate	Product Data Available
Disinfection by-product					
N-Nitrosodimethylamine (NDMA)	MP UV	0.8-7.7	6.9-7.1	56	
DOM surrogate					
4,6-Dioxoheptanoic acid	LP UV, UV-A	1,000	6, 7.5, 9	92	92
o-Methoxybenzoic acid	LP UV, UV-A	1,000	6, 7.5, 9	92	92
Dye					
Methylene blue	UV-B, sunlight	35-250	10	51	
Napthenic acids and related model compounds					
Cyclohexanoic acid	UV-B, sunlight	35-570	10	51	
	LP UV	50	5	40	
Naphthenic acids in oil sands process-affected water	UV-B, sunlight	200-300	8.3, 10	106	
Pesticides and pesticide degradation products					
Chlortoluron	LP UV	1.8-70.9	5-9	107	107
Desethylatrazine	LP UV	1-6	7	42	
Pharmaceutical and personal care products (PPCPs)					
17α-Ethinylestradiol (EE2)	LP UV	1-6	7	42	
Caffeine	MP UV	2, 6, 10	6.5, 7.5, 8.5	108	
Carbamazepine	LP UV	1-6	7	42	
Diclofenac	LP UV	1-6	7	42	
Metoprolol	LP UV	1-5	2-9	109	109
Ronidazole	LP UV	3.5-210	5-9	110	110
Sulfamethoxazole	LP UV	1-6	7	42	

Table 2.4 continued

Compound	Light Source	[Free chlorine] (mg Cl_2/L)	pH	References for Chlorine Photolysis	
				Enhanced Degradation Rate	Product Data Available
Solvents and related transformation products					
1,1-Dichloroethene (1,1-DCE)	MP UV	0.8-7.7	6.9-7.1	56	
1,2-Dichloroethene (1,2-DCE)	MP UV	0.8-7.7	6.9-7.1	56	
1,4-Dioxane	LP UV	140-890	2.9-9.5	111	
Trichloroethylene (TCE)	MP UV	0.8-7.7	6.9-7.1	56	
	MP UV	10.6	5, 7.5, 10	41	
Surfactants					
Benzenesulfonic acid	Hg	18,300	11	48	48
Diethylene glycol	Hg	16,000	12	112	112
Diethylene glycol dimethyl ether	Hg	16,000	12	112	112
Diethylene glycol monomethyl ether	Hg	16,000	12	112	112
p-Ethylbenzenesulfonic acid	Hg	16,000	11	48	48
Ethylene glycol	Hg	16,000	12	112	112
Ethylene glycol dimethyl ether	Hg	16,000	12	112	112
Ethylene glycol monomethyl ether	Hg	16,000	12	112	112
p-Toluenesulfonic acid	Hg	2,200	11	48	48
Taste and odor compounds					
2-Methylisoborneal	LP UV	8	5-7.6	113	
	MP UV	1-5	6, 7.5	114	
	MP UV	2, 6, 10	6.5, 7.5, 8.5	108	
Geosmin	LP UV	8	5-7.6	113	
	MP UV	2, 6, 10	6.5, 7.5, 8.5	108	
X-ray contrast media					
Iohexol	LP UV	3.5-35	5-9	115	115
Iopamidole	LP UV	1-6	7	42	

2.8 References

(1) Edzwald, J. K.; *Water Quality & Treatment: A Handbook on Drinking Water*, McGraw Hill, 6th edn., **2011**.

(2) *Alternative Disinfectants and Oxidants Guidance Manual*; U.S. Environmental Protection Agency: Washington, DC, **1999**.

(3) Korshin, G. V.; in *Aquatic Redox Chemistry*, eds. P. G. Tratnyek, T. J. Grundl and S. B. Haderlein, American Chemical Society, Washington, DC, **2011**, vol. 1071, ch. 11, pp. 223-245.

(4) Krasner, S. W.; The formation and control of emerging disinfection by-products of health concern. *Phil. Trans. R. Soc. A*, **2009**, 367(1409), 4077-4095.

(5) Richardson, S. D.; The role of GC-MS and LC-MS in the discovery of drinking water disinfection by-products. *J. Environ. Monitor.* **2002**, 4(1), 1-9.

(6) Richardson, S. D.; Ternes, T. A.; Water analysis: Emerging contaminants and current issues. *Anal. Chem.* **2011**, 83(12), 4614-4648.

(7) Rennecker, J. L.; Driedger, A. M.; Rubin, S. A.; Mariñas, B. J.; Synergy in sequential inactivation of *Cryptosporidium parvum* with ozone/free chlorine and ozone/ monochloramine. *Water Res.* **2000**, 34(17), 4121-4130.

(8) Corona-Vasquez, B.; Samuelson, A.; Rennecker, J. L.; Mariñas, B. J.; Inactivation of *Cryptosporidium parvum* oocysts with ozone and free chlorine. *Water Res.* **2002**, 36(16), 4053-4063.

(9) Cho, M.; Kim, J.-H.; Yoon, J.; Investigating synergism during sequential inactivation of *Bacillus subtilis* spores with several disinfectants. *Water Res.* **2006**, 40(15), 2911-2920.

(10) Driedger, A. M.; Rennecker, J. L.; Mariñas, B. J.; Sequential inactivation *Cryptosporidium parvum* oocysts with ozone and free chlorine. *Water Res.* **2000**, 34(14), 3591-3597.

(11) Cho, M.; Gandhi, V.; Hwang, T.-M.; Lee, S.; Kim, J.-H.; Investigating synergism during sequential inactivation of MS-2 phage and *Bacillus subtilis* spores with UV/H_2O_2 followed by free chlorine. *Water Res.* **2011**, 45(3), 1063-1070.

(12) Reckhow, D. A.; Linden, K. G.; Kim, J.; Shemer, H.; Makdissy, G.; Effect of UV treatment on DBP formation. *J. Am. Water Works Assoc.* **2010**, 102(6), 100-113.

(13) Dotson, A. D.; Keen, V. O. S.; Metz, D.; Linden, K. G.; UV/H_2O_2 treatment of drinking water increases post-chlorination DBP formation. *Water Res.* **2010**, 44(12), 3703-3713.

(14) Liu, W.; Cheung, L. M.; Yang, X.; Shang, C.; THM, HAA and CNCl formation from UV irradiation and chlor(am)ination of selected organic waters. *Water Res.* **2006**, 40(10), 2033-2043.

(15) Lyon, B. A.; Milsk, R. Y.; Deangelo, A. B.; Simmons, J. E.; Moyer, M. P.; Weinberg, H. S.; Integrated chemical and toxicological investigation of UV-chlorine/chloramine drinking water treatment. *Environ. Sci. Technol.* **2014**, 48(12), 6743-6753.

(16) Kolpin, D. W.; Furlong, E. T.; Meyer, M. T.; Thurman, E. M.; Zaugg, S. D.; Barber, L. B.; Buxton, H. T.; Pharmaceuticals, hormones, and other organic wastewater contaminants in U.S. streams, 1999−2000: A national reconnaissance. *Environ. Sci. Technol.* **2002**, 36(6), 1202-1211.

(17) Stackelberg, P. E.; Furlong, E. T.; Meyer, M. T.; Zaugg, S. D.; Henderson, A. K.; Reissman, D. B.; Persistence of pharmaceutical compounds and other organic wastewater contaminants in a conventional drinking-water-treatment plant. *Sci. Total Environ.* **2004**, 329(1-3), 99-113.

(18) Mompelat, S.; Le Bot, B.; Thomas, O.; Occurrence and fate of pharmaceutical products and by-products, from resource to drinking water. *Environ. Int.* **2009**, 35(5), 803-814.
(19) Kostich, M. S.; Batt, A. L.; Lazorchak, J. M.; Concentrations of prioritized pharmaceuticals in effluents from 50 large wastewater treatment plants in the U.S. and implications for risk estimation. *Environ. Poll.* **2014**, 184(C), 354-359.
(20) Gallard, H.; Leclercq, A.; Croue, J.-P.; Chlorination of bisphenol A: Kinetics and by-products formation. *Chemosphere* **2004**, 56(5), 465-473.
(21) Deborde, M.; Rabouan, S.; Gallard, H.; Legube, B.; Aqueous chlorination kinetics of some endocrine disruptors. *Environ. Sci. Technol.* **2004**, 38(21), 5577-5583.
(22) Dodd, M. C.; Huang, C.-H.; Transformation of the antibacterial agent sulfamethoxazole in reactions with chlorine: kinetics, mechanisms, and pathways. *Environ. Sci. Technol.* **2004**, 38(21), 5607-5615.
(23) Dodd, M. C.; Shah, A. D.; Von Gunten, U.; Huang, C.-H.; Interactions of fluoroquinolone antibacterial agents with aqueous chlorine: reaction kinetics, mechanisms, and transformation pathways. *Environ. Sci. Technol.* **2005**, 39(18), 7065-7076.
(24) Rule, K. L.; Ebbett, V. R.; Vikesland, P. J.; Formation of chloroform and chlorinated organics by free-chlorine-mediated oxidation of triclosan. *Environ. Sci. Technol.* **2005**, 39(9), 3176-3185.
(25) Dodd, M. C.; Huang, C.-H.; Aqueous chlorination of the antibacterial agent trimethoprim: Reaction kinetics and pathways. *Water Res.* **2007**, 41(3), 647-655.
(26) Wang, P.; He, Y.-L.; Huang, C.-H.; Reactions of tetracycline antibiotics with chlorine dioxide and free chlorine. *Water Res.* **2011**, 45(4), 1838-1846.
(27) Stackelberg, P. E.; Gibs, J.; Furlong, E. T.; Meyer, M. T.; Zaugg, S. D.; Lippincott, R. L.; Efficiency of conventional drinking-water-treatment processes in removal of pharmaceuticals and other organic compounds. *Sci. Total Environ.* **2007**, 377(2-3), 255-272.
(28) Kleywegt, S.; Pileggi, V.; Yang, P.; Hao, C.; Zhao, X.; Rocks, C.; Thach, S.; Cheung, P.; Whitehead, B.; Pharmaceuticals, hormones and bisphenol A in untreated source and finished drinking water in Ontario, Canada - Occurrence and treatment efficiency. *Sci. Total Environ.* **2011**, 409(8), 1481-1488.
(29) Westerhoff, P.; Yoon, Y.; Snyder, S.; Wert, E.; Fate of endocrine-disruptor, pharmaceutical, and personal care product chemicals during simulated drinking water treatment processes. *Environ. Sci. Technol.* **2005**, 39(17), 6649-6663.
(30) Mompelat, S.; Thomas, O.; Le Bot, B.; Contamination levels of human pharmaceutical compounds in French surface and drinking water. *J. Environ. Monitor.* **2011**, 13(10), 2929-2939.
(31) Valcarcel, Y.; Alonso, S. G.; Rodríguez-Gil, J. L.; Gil, A.; Catalá, M.; Detection of pharmaceutically active compounds in the rivers and tap water of the Madrid region (Spain) and potential ecotoxicological risk. *Chemosphere* **2011**, 84(10), 1336-1348.
(32) Benotti, M. J.; Trenholm, R. A.; Vanderford, B. J.; Holady, J. C.; Stanford, B. D.; Snyder, S. A.; Pharmaceuticals and endocrine disrupting compounds in U.S. Drinking water. *Environ. Sci. Technol.* **2009**, 43(3), 597-603.
(33) Huerta-Fontela, M.; Galceran, M. T.; Ventura, F.; Occurrence and removal of pharmaceuticals and hormones through drinking water treatment. *Water Res.* **2011**, 45(3), 1432-1442.

(34) Loraine, G. A.; Pettigrove, M. E.; Seasonal variations in concentrations of pharmaceuticals and personal care products in drinking water and reclaimed wastewater in southern California. *Environ. Sci. Technol.* **2006**, 40(3), 687-695.
(35) Jin, X.; Peldszus, S.; Selection of representative emerging micropollutants for drinking water treatment studies: A systematic approach. *Sci. Total Environ.* **2012**, 414, 653-663.
(36) Padhye, L. P.; Yao, H.; Kung'u, F. T.; Huang, C.-H.; Year-long evaluation on the occurrence and fate of pharmaceuticals, personal care products, and endocrine disrupting chemicals in an urban drinking water treatment plant. *Water Res.* **2014**, 51, 266-276.
(37) Legrini, O.; Oliveros, E.; Braun, A. M.; Photochemical processes for water treatment. *Chem. Rev.* **1993**, 93(2), 671-698.
(38) Pignatello, J. J.; Oliveros, E.; Mackay, A.; Advanced oxidation processes for organic contaminant destruction based on the Fenton reaction and related chemistry. *Crit. Rev. Environ. Sci. Technol.* **2006**, 36, 1-84.
(39) Watts, M. J.; Linden, K. G.; Chlorine photolysis and subsequent •OH radical production during UV treatment of chlorinated water. *Water Res.* **2007**, 41(13), 2871-2878.
(40) Jin, J.; El-Din, M. G.; Bolton, J. R.; Assessment of the UV/chlorine process as an advanced oxidation process. *Water Res.* **2011**, 45(4), 1890-1896.
(41) Wang, D.; Bolton, J. R.; Hofmann, R.; Medium pressure UV combined with chlorine advanced oxidation for trichloroethylene destruction in a model water. *Water Res.* **2012**, 46(15), 4677-4686.
(42) Sichel, C.; Garcia, C.; Andre, K.; Feasibility studies: UV/chlorine advanced oxidation treatment for the removal of emerging contaminants. *Water Res.* **2011**, 45(19), 6371-6380.
(43) Bossmann, S. H.; Oliveros, E.; Gob, S.; Siegwart, S.; Dahlen, E. P.; Payawan, L.; Straub, M.; Worner, M.; Braun, A. M.; New evidence against hydroxyl radicals as reactive intermediates in the thermal and photochemically enhanced Fenton reactions. *J. Phys. Chem. A* **1998**, 102, 5542-5550.
(44) Buxton, G. V.; Greenstock, C. L.; Helman, W. P.; Ross, A. B.; Critical review of rate constants for reactions of hydrated electrons, hydrogen atoms and hydroxyl radicals in aqueous solution. *J. Phys. Chem. Ref. Data* **1988**, 17, 513-886.
(45) Buxton, G. V.; Subhani, M. S.; Radiation chemistry and photochemistry of oxychlorine ions. Part 2. Photodecomposition of aqueous solutions of hypochlorite ions. *J. Chem. Soc. Faraday Trans.* **1972**, 68(0), 958-969.
(46) Kläning, U. K.; Sehested, K.; Wolff, T.; Ozone formation in laser flash photolysis of oxoacids and oxoanions of chlorine and bromine. *J. Chem. Soc. Faraday Trans.* **1984**, 80(11), 2969-2979.
(47) Vogt, R.; Schindler, R. N.; Product channels in the photolysis of HOCl. *J. Photochem. Photobiol. A: Chem.* **1992**, 66(2), 133-140.
(48) Nakamura, M.; Ogata, Y.; Photolytic oxidation of alkylbenzenesulfonic acids by aqueous sodium hypochlorite. *Bull. Chem. Soc. Jpn.* **1977**, 50(9), 2396-2399.
(49) Oliver, B. G.; Carey, J. H.; Photochemical production of chlorinated organics in aqueous solutions containing chlorine. *Environ. Sci. Technol.* **1977**, 11(9), 893-895.
(50) Nowell, L. H.; Hoigné, J.; Photolysis of aqueous chlorine at sunlight and ultraviolet wavelengths. 2. Hydroxyl radical production. *Water Res.* **1992**, 26(5), 599-605.
(51) Chan, P. Y.; El-Din, M. G.; Bolton, J. R.; A solar-driven UV/chlorine advanced oxidation process. *Water Res.* **2012**, 46(17), 5672-5682.

(52) Forsyth, J. E.; Zhou, P.; Mao, Q.; Asato, S. S.; Meschke, J. S.; Dodd, M. C.; Enhanced inactivation of *Bacillus subtilis* spores during solar photolysis of free available chlorine. *Environ. Sci. Technol.* **2013**, 47(22), 12976-12984.

(53) Fang, J.; Fu, Y.; Shang, C.; The roles of reactive species in micropollutant degradation in the UV/free chlorine system. *Environ. Sci. Technol.* **2014**, 48(3), 1859-1868.

(54) Ben, W.; Sun, P.; Huang, C.-H.; Effects of combined UV and chlorine treatment on chloroform formation from triclosan. *Chemosphere* **2015**, 150, 715-722.

(55) Zhou, P.; Di Giovanni, G. D.; Meschke, J. S.; Dodd, M. C.; Enhanced inactivation of *Cryptosporidium parvum* oocysts during solar photolysis of free available chlorine. *Environ. Sci. Technol. Lett.* **2014**, 1(11), 453-458.

(56) Boal, A. K.; Rhodes, C.; Garcia, S.; Pump-and-treat groundwater remediation using chlorine/ultraviolet advanced oxidation processes. *Groundwater Monitor. Remed.* **2015**, 35(2), 93-100.

(57) Cooper, W. J.; Jones, A. C.; Whitehead, R. F.; Zika, R. G.; Sunlight-induced photochemical decay of oxidants in natural waters: implications in ballast water treatment. *Environ. Sci. Technol.* **2007**, 41(10), 3728-3733.

(58) Qian, Y.; Wang, W.; Li, X.-F.; Hrudey, S. E.; Evaluation of approaches for consumers to eliminate chlorine off-flavors from drinking water at point-of-use. *Wat. Sci. Technol. Wat. Supply* **2015**, 15(1), 84-93.

(59) Nowell, L. H.; Hoigné, J.; Photolysis of aqueous chlorine at sunlight and ultraviolet wavelengths—I. Degradation rates. *Water Res.* **1992**, 26(5), 593-598.

(60) Gu, A. Z.; Neethling, J. B.; Investigation and modeling of solar UV-induced chlorine decay in disinfection contact basins at full-scale wastewater treatment plants. *Wat. Environ. Res.* **2008**, 80(2), 179-185.

(61) Spiliotopoulou, A.; Hansen, K. M. S.; Andersen, H. R.; Secondary formation of disinfection by-products by UV treatment of swimming pool water. *Sci. Total Environ.* **2015**, 520(C), 96-105.

(62) Zhang, X.; Li, W.; Blatchley, I. I. I., Ernest R; Wang, X.; Ren, P.; UV/chlorine process for ammonia removal and disinfection by-product reduction: Comparison with chlorination. *Water Res.* **2015**, 68(C), 804-811.

(63) Feng, Y.; Smith, D. W.; Bolton, J. R.; Photolysis of aqueous free chlorine species (HOCl and OCl^-) with 254 nm ultraviolet light. *J. Environ. Eng. Sci.* **2007**, 6(3), 277-284.

(64) Zhao, Q.; Shang, C.; Zhang, X.; Effects of bromide on UV/chlorine advanced oxidation process. *Water Sci. Tech.* **2009**, 9(6), 627-634.

(65) Molina, M. J.; Ishiwata, T.; Molina, L. T.; Production of hydroxyl from photolysis of hypochlorous acid at 307-309 nm. *J. Phys. Chem.* **1980**, 84(8), 821-826.

(66) McGrath, W. D.; McGarvey, J. J.; The production, deactivation and chemical reactions of $O(^1D)$ atoms. *Planet. Space Sci.* **1967**, 15(3), 427-455.

(67) Deborde, M.; von Gunten, U.; Reactions of chlorine with inorganic and organic compounds during water treatment - kinetics and mechanisms: A critical review. *Water Res.* **2008**, 42(1-2), 13-51.

(68) Schindler, R. N.; Liesner, M.; Schmidt, S.; Kirchner, U.; Identification of nascent products formed in the laser photolysis of CH_3OCl and HOCl at 308 nm and around 235 nm. Total Cl-atom quantum yields and the state and velocity distributions of Cl(2PJ). *J. Photochem. Photobiol. A: Chem.* **1997**, 107, 9-19.

(69) Kläning, U. K.; Wolff, T.; Laser flash photolysis of HClO, ClO^-, HBrO, and BrO^- in aqueous solution. Reactions of Cl- and Br-atoms. *Ber. Bunsenges. Phys. Chem.* **1985**, 89(3), 243-245.

(70) Buxton, G. V.; Subhani, M. S.; Radiation chemistry and photochemistry of oxychlorine ions. Part 3. Photodecomposition of aqueous solutions of chlorite ions. *J. Chem. Soc. Faraday T.* **1972**, 68(0), 970-977.

(71) Treinin, A.; The photochemistry of oxyanions. *Isr. J. Chem.* **1970**, 8(2), 103-113.

(72) Buxton, G. V.; Subhani, M. S.; Radiation chemistry and photochemistry of oxychlorine ions. Part 1. Radiolysis of aqueous solutions of hypochlorite and chlorite ions. *J. Chem. Soc. Faraday T.* **1972**, 68(0), 947-957.

(73) Buxton, G. V.; Bydder, M.; Salmon, G. A.; Williams, J. E.; The reactivity of chlorine atoms in aqueous solution. Part III. The reactions of $Cl^•$ with solutes. *Phys. Chem. Chem. Phys.* **2000**, 2(2), 237-245.

(74) Kumar, K.; Margerum, D. W.; Kinetics and mechanism of general-acid-assisted oxidation of bromide by hypochlorite and hypochlorous acid. *Inorg. Chem.* **1987**, 26(16), 2706-2711.

(75) Connick, R. E.; The interaction of hydrogen peroxide and hypochlorous acid in acidic solutions containing chloride ion. *J. Am. Chem. Soc.* **1947**, 69, 1509-1514.

(76) Matthew, B. M.; Anastasio, C.; A chemical probe technique for the determination of reactive halogen species in aqueous solution: Part 1–bromide solutions. *Atmos. Chem. Phys* **2006**, 6, 2423-2437.

(77) Zuo, Z.; Katsumura, Y.; Ueda, K.; Ishigure, K.; Reactions between some inorganic radicals and oxychlorides studied by pulse radiolysis and laser photolysis. *J. Chem. Soc. Faraday T.* **1997**, 93(10), 1885-1891.

(78) Jayson, G. G.; Parsons, B. J.; Swallow, A. J.; Some simple, highly reactive, inorganic chlorine derivatives in aqueous solution. Their formation using pulses of radiation and their role in the mechanism of the fricke dosimeter. *J. Chem. Soc. Faraday T.* **1973**, 69(0), 1597-1607.

(79) Buxton, G. V.; Bydder, M.; Arthur Salmon, G.; Reactivity of chlorine atoms in aqueous solution part. 1 The equilibrium $Cl^• + Cl^- = Cl_2^{•-}$. *J. Chem. Soc. Faraday Trans.* **1998**, 94(5), 653-657.

(80) Gilbert, B. C.; Stell, J. K.; Peet, W. J.; Radford, K. J.; Generation and reactions of the chlorine atom in aqueous solution. *J. Chem. Soc. Faraday Trans.* **1988**, 84(10), 3319-3330.

(81) Nagarajan, V.; Fessenden, R. W.; Flash photolysis of transient radicals. 1. $X_2^{•-}$ with X= Cl, Br, I, and SCN. *J. Phys. Chem.* **1985**, 89, 2330-2335.

(82) Hasegawa, K.; Neta, P.; Rate constants and mechanisms of reaction of chloride ($Cl_2^{•-}$) radicals. *J. Phys. Chem.* **1978**, 82(8), 854-857.

(83) Grigorev, A. E.; Makarov, I. E.; Pikaev, A. K.; Formation of $Cl_2^{•-}$ in the bulk solution during the radiolysis of concentrated aqueous solutions of chloride. *High Energy Chem.* **1987**, 21, 99-102.

(84) von Gunten, U.; Ozonation of drinking water: Part 1. Oxidation kinetics and products formation. *Water Res.* **2003**, 37, 1443-1467.

(85) Deborde, M.; Rabouan, S.; Duguet, J.-P.; Legube, B.; Kinetics of aqueous ozone-induced oxidation of some endocrine disruptors. *Environ. Sci. Technol.* **2005**, 39(16), 6086-6092.

(86) von Gunten, U.; Hoigne, J.; Bromate formation during ozonization of bromide-containing waters: Interaction of ozone and hydroxyl radical reactions. *Environ. Sci. Technol.* **1994**, 28(7), 1234-1242.

(87) von Gunten, U.; Ozonation of drinking water: Part 2. Disinfection and by-product formation in presence of bromide, iodide, or chlorine. *Water Res.* **2003**, 37, 1469-1487.
(88) Lyon, B. A.; Dotson, A. D.; Linden, K. G.; Weinberg, H. S.; The effect of inorganic precursors on disinfection byproduct formation during UV-chlorine/chloramine drinking water treatment. *Water Res.* **2012**, 46(15), 4653-4664.
(89) Amichai, O.; Treinin, A.; Chemical reactivity of $O(^3P)$ atoms in aqueous solution. *Chem. Phys. Lett.* **1969**, 3(8), 611-613.
(90) Fischbacher, A.; Löppenberg, K.; von Sonntag, C.; Schmidt, T. C.; A new reaction pathway for bromite to bromate in the ozonation of bromide. *Environ. Sci. Technol.* **2015**, 49(19), 11714-11720.
(91) Buxton, G. V.; Dainton, F. S.; The radiolysis of aqueous solutions of oxybromine compounds; the spectra and reactions of BrO and BrO_2. *Proc. Roy. Soc. A* **1968**, 304, 427-439.
(92) Pisarenko, A. N.; Stanford, B. D.; Snyder, S. A.; Rivera, S. B.; Boal, A. K.; Investigation of the use of chlorine based advanced oxidation in surface water: Oxidation of natural organic matter and formation of disinfection byproducts. *J. Adv. Oxid. Technol.* **2013**, 16(1), 137-150.
(93) Ashton, L.; Buxton, G. V.; Stuart, C. R.; Temperature dependence of the rate of reaction of oh with some aromatic compounds in aqueous solution. *J. Chem. Soc. Faraday Trans.* **1995**, 91(11), 1631-1633.
(94) Mártire, D. O.; Rosso, J. A.; Bertolotti, S.; Le Roux, G. C.; Braun, A. M.; Gonzalez, M. C.; Kinetic study of the reactions of chlorine atoms and $Cl_2^{\bullet-}$ radical anions in aqueous solutions. II. Toluene, benzoic acid, and chlorobenzene. *J. Phys. Chem. A* **2001**, 105(22), 5385-5392.
(95) Horvath, O.; Geminate-pair scavenging mechanism in photochemical reactions of chlorocuprate (II) complexes in acetonitrile solutions containing alcohols. *J. Photochem. Photobiol. A: Chem.* **1989**, 48, 243-248.
(96) Mertens, R.; Von Sonntag, C.; Photolysis (λ= 254 nm) of tetrachloroethene in aqueous solutions. *J. Photochem. Photobiol. A: Chem.* **1995**, 85, 1-9.
(97) Neta, P.; Dorfman, L. M.; Pulse radiolysis studies. 13. Rate constants for reaction of hydroxyl radicals with aromatic compounds in aqueous solutions. *Adv. Chem. Ser.* **1968**, 81, 222-230.
(98) Zhao, Q.; Shang, C.; Zhang, X.; Ding, G.; Yang, X.; Formation of halogenated organic byproducts during medium-pressure UV and chlorine co-exposure of model compounds, NOM and bromide. *Water Res.* **2011**, 45(19), 6545-6554.
(99) Getoff, N.; Radiation-and photoinduced degradation of pollutants in water. A comparative study. *Radiat. Phys. Chem.* **1991**, 37(5/6), 673-680.
(100) Chateauneuf, J. E.; Direct measurement of the absolute kinetics of chlorine atom in carbon tetrachloride. *J. Am. Chem. Soc.* **1990**, 112, 442-444.
(101) Klein, G. W.; Bhatia, K.; Madhavan, V.; Schuler, R. H.; Reaction of hydroxyl radicals with benzoic acid. Isomer distribution in the radical intermediates. *J. Phys. Chem.* **1975**, 79, 1767-1774.
(102) Keenan, C. R.; Sedlak, D. L.; Factors affecting the yield of oxidants from the reaction of nanoparticulate zero-valent iron and oxygen. *Environ. Sci. Technol.* **2008**, 42, 1262-1267.
(103) Ogata, Y.; Suzuki, T.; Takagi, K.; Photolytic oxidation of aliphatic acids by aqueous sodium hypochlorite. *J. Chem. Soc. Perk. Trans. 2* **1979**, 2(12), 1715-1719.

(104) Kimura, M.; Ogata, Y.; Photooxidation of some aromatic sulfonic acids with alkaline hypochlorite. *Bull. Chem. Soc. Jpn.* **1983**, 56, 471-473.
(105) Tucker, M. D.; Barton, L. L.; Thomson, B. M.; Wagener, B. M.; Treatment of waste containing EDTA by chemical oxidation. *Waste Manage.* **1999**, 19, 477-482.
(106) Shu, Z.; Li, C.; Belosevic, M.; Bolton, J. R.; El-Din, M. G.; Application of a solar UV/chlorine advanced oxidation process to oil sands process-affected water remediation. *Environ. Sci. Technol.* **2014**, 48(16), 9692-9701.
(107) Guo, Z.-B.; Lin, Y.-L.; Xu, B.; Huang, H.; Zhang, T.-Y.; Tian, F.-X.; Gao, N.-Y.; Degradation of chlortoluron during UV irradiation and UV/chlorine processes and formation of disinfection by-products in sequential chlorination. *Chem. Eng. J.* **2016**, 283(C), 412-419.
(108) Wang, D.; Bolton, J. R.; Andrews, S. A.; Hofmann, R.; UV/chlorine control of drinking water taste and odour at pilot and full-scale. *Chemosphere* **2015**, 136(C), 239-244.
(109) Yoon, Y.; Choi, D.-J.; Zoh, K.-D.; Degradation characteristics of metoprolol during UV/chlorination reaction and a factorial design optimization. *J. Haz. Mat.* **2015**, 285, 453-463.
(110) Qin, L.; Lin, Y.-L.; Xu, B.; Hu, C.-Y.; Tian, F.-X.; Zhang, T.-Y.; Zhu, W.-Q.; Huang, H.; Gao, N.-Y.; Kinetic models and pathways of ronidazole degradation by chlorination, UV irradiation and UV/chlorine processes. *Water Res.* **2014**, 65(C), 271-281.
(111) Kishimoto, N.; Nishimura, H.; Effect of pH and molar ratio of pollutant to oxidant on a photochemical advanced oxidation process using hypochlorite. *Environ. Technol.* **2015**, 36(19), 2436-2442.
(112) Ogata, Y.; Takagi, K.; Suzuki, T.; Photolytic oxidation of ethylene glycol dimethyl ether and related compounds by aqueous hypochlorite. *J. Chem. Soc. Perk. Trans. 2* **1978**, (6), 562-567.
(113) Watts, M. J.; Hofmann, R.; Rosenfeldt, E. J.; Low-pressure UV/Cl_2 for advanced oxidation of taste and odor. *J. Am. Water Works Assoc.* **2012**, 104(1), 47-48.
(114) Rosenfeldt, E.; Boal, A. K.; Springer, J.; Stanford, B.; Comparison of UV-mediated advanced oxidation. *J. Am. Water Works Assoc.* **2013**, 105(7), 29-33.
(115) Wang, Z.; Lin, Y.-L.; Xu, B.; Xia, S.-J.; Zhang, T.-Y.; Gao, N.-Y.; Degradation of iohexol by UV/chlroine process and formation of iodinated trihalomethanes during post-chlorination. *Chem. Eng. J.* **2016**, 283(C), 1090-1096.
(116) Wang, D.; Bolton, J. R.; Andrews, S. A.; Hofmann, R.; Formation of disinfection by-products in the ultraviolet/chlorine advanced oxidation process. *Sci. Total Environ.* **2015**, 518-519(C), 49-57.
(117) Hancil, V.; Smith, J. M.; Chlorine-sensitized photochemical oxidation of soluble organics in municipal wastewater. *Ind. Eng. Chem. Process Des. Develop.* **1971**, 10(4), 515-523.
(118) Zhang, X. R.; Li, W. G.; Ren, P. F.; Natural organic matter removal by uv/chlorine process: Modeling and optimization. *Adv. Mater. Res.* **2013**, 807-809, 466-471.
(119) Gonenc, D.; Bekbolet, M.; Interactions of hypochlorite ion and humic acid: Photolytic and photocatalytic pathways. *Wat. Sci. Tech.* **2001**, 44(5), 205-210.
(120) Lamsal, R.; Walsh, M. E.; Gagnon, G. A.; Comparison of advanced oxidation processes for the removal of natural organic matter. *Water Res.* **2011**, 45(10), 3263-3269.
(121) Feng, Y.; Smith, D. W.; Bolton, J. R.; A potential new method for determination of the fluence (UV dose) delivered in UV reactors involving the photodegradation of free chlorine. *Wat. Environ. Res.* **2010**, 82(4), 328-334.

(122) National Primary Drinking Water Regulations: Disinfectants and Disinfection Byproducts Rule; U.S. Environmental Protection Agency: Washington DC, **1998**.
(123) National Primary Drinking Water Regulations: Stage 2 Disinfectants and Disinfection Byproducts Rule; U.S. Environmental Protection Agency: Washington DC, **2006**.
(124) Plewa, M. J.; Wagner, E. D.; Metz, D. H.; Kashinkunti, R.; Jamriska, K. J.; Meyer, M.; Differential toxicity of drinking water disinfected with combinations of ultraviolet radiation and chlorine. *Environ. Sci. Technol.* **2012**, 46(14), 7811-7817.
(125) Weng, S.; Li, J.; Blatchley, I. I. I., Ernest R; Effects of UV_{254} irradiation on residual chlorine and DBPs in chlorination of model organic-N precursors in swimming pools. *Water Res.* **2012**, 46(8), 2674-2682.
(126) Weng, S.; Blatchley, I. I. I., Ernest R; Ultraviolet-induced effects on chloramine and cyanogen chloride formation from chlorination of amino acids. *Environ. Sci. Technol.* **2013**, 47(9), 4269-4276.
(127) Deng, L.; Huang, C.-H.; Wang, Y.-L.; Effects of combined UV and chlorine treatment on the formation of trichloronitromethane from amine precursors. *Environ. Sci. Technol.* **2014**, 48(5), 2697-2705.
(128) Hansen, K. M. S.; Zortea, R.; Piketty, A.; Vega, S. R.; Andersen, H. R.; Photolytic removal of DBPs by medium pressure UV in swimming pool water. *Sci. Total Environ.* **2013**, 443(C), 850-856.
(129) Fiz, N.; Usero, J. L.; Casado, J.; Photolysis of N-nitrosamines in neutral media. *Int. J. Chem. Kinet.* **1993**, 25, 341-351.
(130) Fang, J.-Y.; Ling, L.; Shang, C.; Kinetics and mechanisms of pH-dependent degradation of halonitromethanes by UV photolysis. *Water Res.* **2013**, 47(3), 1257-1266.
(131) Dai, N.; Mitch, W. A.; Controlling nitrosamines, nitramines, and amines in amine-based CO_2 capture systems with continuous ultraviolet and ozone treatment of washwater. *Environ. Sci. Technol.* **2015**, 49(14), 8878-8886.
(132) Hoigné, J.; Bader, H.; Kinetics of reactions of chlorine dioxide (OClO) in water—I. Rate constants for inorganic and organic compounds. *Water Res.* **1994**, 28(1), 45-55.
(133) Haag, W. R.; Hoigné, J.; Ozonation of water containing chlorine or chloramines. Reaction products and kinetics. *Water Res.* **1983**, 17(10), 1397-1402.
(134) U.S. Environmental Protection Agency, Contaminant Candidate List 3, 2009. Retrieved from http://www2.epa.gov/ccl/contaminant-candidate-list-3-ccl-3 (accessed December 1, 2015).
(135) Kang, N.; Anderson, T. A.; Andrew Jackson, W.; Photochemical formation of perchlorate from aqueous oxychlorine anions. *Anal. Chim. Acta* **2006**, 567(1), 48-56.
(136) Rao, B.; Estrada, N.; Mcgee, S.; Mangold, J.; Gu, B.; Jackson, W. A.; Perchlorate production by photodecomposition of aqueous chlorine solutions. *Environ. Sci. Technol.* **2012**, 46(21), 11635-11643.
(137) Kang, N.; Anderson, T. A.; Rao, B.; Jackson, W. A.; Characteristics of perchlorate formation via photodissociation of aqueous chlorite. *Environ. Chem.* **2009**, 6, 53-59.
(138) Zhang, H.; Zhang, Y.; Shi, Q.; Hu, J.; Chu, M.; Yu, J.; Yang, M.; Study on transformation of natural organic matter in source water during chlorination and its chlorinated products using ultrahigh resolution mass spectrometry. *Environ. Sci. Technol.* **2012**, 46(8), 4396-4402.
(139) Zhang, H.; Zhang, Y.; Shi, Q.; Ren, S.; Yu, J.; Ji, F.; Luo, W.; Yang, M.; Characterization of low molecular weight dissolved natural organic matter along the treatment train of a

waterworks using Fourier transform ion cyclotron resonance mass spectrometry. *Water Res.* **2012**, 46(16), 5197-5204.

(140) Zhang, H.; Zhang, Y.; Shi, Q.; Zheng, H.; Yang, M.; Characterization of unknown brominated disinfection byproducts during chlorination using ultrahigh resolution mass spectrometry. *Environ. Sci. Technol.* **2014**, 48(6), 3112-3119.

(141) Lavonen, E. E.; Gonsior, M.; Tranvik, L. J.; Schmitt-Kopplin, P.; Köhler, S. J.; Selective chlorination of natural organic matter: Identification of previously unknown disinfection byproducts. *Environmental Science & Technology* **2013**, 47(5), 2264-2271.

(142) Gonsior, M.; Schmitt-Kopplin, P.; Stavklint, H.; Richardson, S. D.; Hertkorn, N.; Bastviken, D.; Changes in dissolved organic matter during the treatment processes of a drinking water plant in Sweden and formation of previously unknown disinfection byproducts. *Environ. Sci. Technol.* **2014**, 48(21), 12714-12722.

Chapter 3

The impact of pH and wavelength on the formation of reactive oxidants during chlorine photolysis[2]

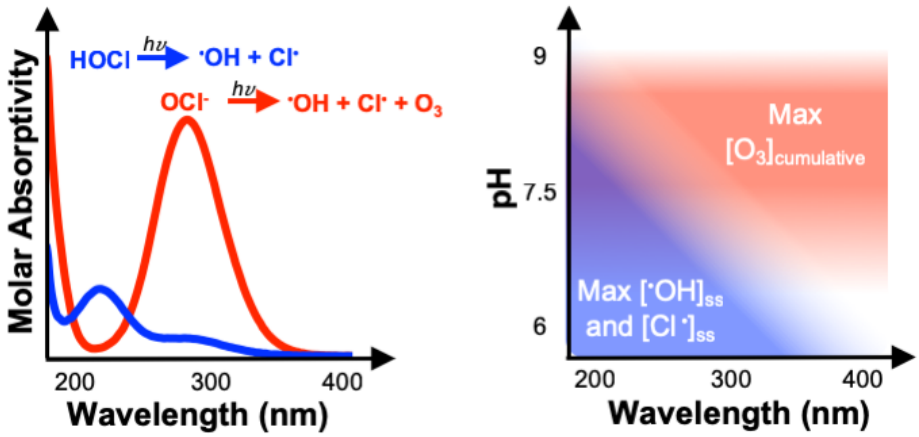

3.1 Abstract

Chlorine photolysis is an advanced oxidation process which relies on photolytic cleavage of free available chlorine (i.e., hypochlorous acid and hypochlorite) to generate hydroxyl radical, along with ozone and a suite of halogen radicals. Little is known about the impact of wavelength on reactive oxidant generation even though chlorine absorbs light within the solar spectrum. This study investigates the formation of reactive oxidants during chlorine photolysis as a function of pH (6 – 10) and irradiation wavelength (254, 311, and 365 nm) using a combination of reactive oxidant quantification with validated probe compounds and kinetic modeling. Observed chlorine loss rate constants increase with pH during irradiation at high wavelengths due to the higher molar

[2] Reproduced with permission from *Environmental Science and Technology.* Bulman, D. M.; Mezyk, S. P.; Remucal, C. K. 2019, 53(8), 4450-4459. Copyright 2019, American Chemical Society.

Stephen P. Mezyk provided technical assistance and oversight that allowed the collection of rate constants using electron pulse radiolysis and transient absorption spectroscopy using the LINAC at Notre Dame.

absorptivity of hypochlorite (pK_a = 7.5), while there is no change at 254 nm. Hydroxyl radical and chlorine radical steady-state concentrations are greatest under acidic conditions for all tested wavelengths and are highest using 254 and 311 nm irradiation. Ozone generation is observed under all conditions, with maximum cumulative concentrations at pH 8 for 311 and 365 nm. A comprehensive kinetic model generally predicts the trends in chlorine loss and oxidant concentrations, but a comparison of previously published kinetic models reveals the challenges of modeling this complex system.

3.2 Introduction

The presence of organic contaminants, such as pesticides and pharmaceuticals, in drinking water sources poses a challenge to water utilities. These chemicals are released into the environment through municipal wastewater, agricultural runoff, and landfill leachate[1–8] and are often poorly removed by conventional water treatment processes.[9] In contrast, advanced oxidation processes (AOPs) can degrade a wide range of organic contaminants by producing hydroxyl radical ($^{\bullet}$OH), a highly reactive, non-selective oxidant that reacts with nearly all organic compounds at diffusion-controlled rate constants.[10–19] Traditional AOPs, such as hydrogen peroxide photolysis, require costly retrofits to existing plants and can be expensive to maintain due to the necessary quenching of hydrogen peroxide, among other factors.[18,20–25]

Chlorine photolysis is emerging as an attractive alternative to traditional AOPs. This system relies on the irradiation of free available chlorine (FAC), a combination of hypochlorous acid (HOCl) and hypochlorite (OCl^-), to generate reactive oxidants. While hydrogen peroxide and persulfate-based AOPs can only use light in the UV-C range due to limits in molar absorptivity,[26,27] solar treatment applications of chlorine photolysis are possible because HOCl and OCl^- absorb

light at higher wavelengths.[14,28–30] Furthermore, chlorine photolysis utilizes a common disinfectant that is easily transported and the AOP is more cost effective under many conditions compared to hydrogen peroxide and persulfate-based AOPs.[18,31]

The chemistry of chlorine photolysis is complex due to the wavelength dependent photolysis of chlorine and its subsequent oxidant formation mechanisms. The acid dissociation constant (pK_a) of hypochlorous acid is 7.5, making the photochemistry of both species important under environmentally relevant pH values.[32] Hypochlorous acid photolyzes to form $^{\bullet}OH$ and chlorine radical ($Cl^{\bullet}$; Reaction 1 in Schematic 3.1).[33] Hypochlorite photolysis is more complex because it forms $O^{\bullet-}$, the conjugate base of $^{\bullet}OH$, as well as two excited states of oxygen, $O(^1D)$ and $O(^3P)$ (Reactions 2 – 4).[34] Additional reactive chlorine species (RCS) form during chlorine photolysis. For example, $Cl_2^{\bullet-}$ forms by reaction of $Cl^{\bullet}$ with Cl^-, while $ClO^{\bullet}$ forms by reaction of $Cl^{\bullet}$ or $^{\bullet}OH$ with chlorine. $Cl^{\bullet}$ is more selective than $^{\bullet}OH$, but reacts at near-diffusion controlled rates with electron-rich compounds.[35,36] $Cl_2^{\bullet-}$ and $ClO^{\bullet}$ are generally less reactive compared to $^{\bullet}OH$ and $Cl^{\bullet}$, but they react selectively with some organic compounds (e.g., phenolates and methoxybenzenes).[37–41] $Cl^{\bullet}$ and $Cl_2^{\bullet-}$ may be considered problematic because these species could potentially form chlorinated disinfection byproducts via chlorine addition or substitution.[37,40–42]

While the presence of multiple potential oxidants makes chlorine photolysis effective at oxidizing a wide range of organic contaminants, it also makes the system challenging to study. Experimental studies rely on the use of probe compounds to quantify oxidant species. Nitrobenzene is frequently used as a selective $^{\bullet}OH$ probe due to its photostability and low reactivity with other oxidants (i.e., HOCl and RCS).[22–24,33,40,44,45] Measurements of $Cl^{\bullet}$ and $Cl_2^{\bullet-}$ are infrequent, but typically use benzoate in combination with nitrobenzene. Benzoate has literature

rate constants with all three species, although there is debate about which reaction mechanisms (i.e., with $^{\bullet}OH$, $Cl^{\bullet}$, and/or $Cl_2^{\bullet-}$) are dominant.[22,33,46]

Organic compound degradation during chlorine photolysis provides additional insight into the formation of reactive oxidants under 254 nm irradiation, which is the most studied wavelength. The fraction of contaminant lost to reaction with $^{\bullet}OH$ is typically estimated by combining measured $^{\bullet}OH$ steady-state concentrations with literature bimolecular rate constants after correcting for loss due to dark chlorination or direct UV photolysis,[23,37] and any remaining degradation is attributed to RCS. The relative impacts of multiple quenchers are used to assess the contribution of RCS to contaminant degradation, although this approach does not always generate meaningful results.[24] For example, the impact of *t*-butanol (i.e., a quencher of $^{\bullet}OH$, $Cl^{\bullet}$, and $ClO^{\bullet}$) may be compared to the impact of bicarbonate (i.e., a quencher of $^{\bullet}OH$, $Cl^{\bullet}$, and $Cl_2^{\bullet-}$).[14,23] As a result, $ClO^{\bullet}$ is increasingly evoked as an important oxidant for organic compound degradation (e.g., naproxen, caffeine, trimethoprim, and microcystin-LR).[14,23,37,47] However, many of these compounds react with ozone,[48,49] which is overlooked in studies conducted at 254 nm and whose precursor (i.e., $O(^3P)$) is quenched by *t*-butanol.[28]

Understanding the formation of reactive oxidants is critical to the application of chlorine photolysis for water treatment. Importantly, results generated at 254 nm provide a limited view of chlorine photolysis and cannot be extrapolated to potential solar applications because quantum yields and reaction mechanisms change with irradiation wavelength (Scheme 3.1). Thus, we aim to determine how reactive oxidant generation varies with treatment conditions by quantifying the steady-state concentrations of $^{\bullet}OH$ and $Cl^{\bullet}$ and the cumulative concentration of O_3 as a function of pH and wavelength using a series of validated probes. We also develop a comprehensive kinetic

model that we compare to five previously published models[22,29,33,40,46] to highlight the limitations of relying on kinetic models in the absence of experimental measurements.

3.3 Materials and Methods

3.3.1 Materials

Sodium hypochlorite stock solutions were standardized using a Shimadzu UV-visible spectrometer.[32] All other compounds were used as received (Section B1 in Appendix B).

3.3.2 Irradiation Experiments

Photolysis experiments were conducted in Rayonet merry-go-round photoreactor with either four 254-nm bulbs, sixteen 311-nm bulbs, or sixteen 365-nm bulbs (Figure B1). These bulbs were selected because they represent different regions in the ultraviolet light spectrum and are not monochromatic light sources. Bulbs are identified by the λ_{max}. All experiments were conducted in triplicate alongside a chemical actinometer (*p*-nitroanisole/pyridine at 365 nm,[50–52] 2-nitrobenzaldehyde at 311 nm,[53] and sulfamethoxazole and diclofenac at 254 nm).[54] Bulb specifications and actinometer conditions are provided in Section B2. Error bars in all figures represent the standard deviation of triplicate analyses.

Irradiation experiments were conducted using 10 mM phosphate (pH 6 – 7) or borate (pH 8 – 10) buffer. The experimental duration varied with wavelength due to variance in bulb intensity (i.e., 2 min at 254 nm, 100 sec at 311 nm, and 10 min at 365 nm). The pseudo-first-order rate constants of chlorine degradation were measured by photolyzing buffered solutions of chlorine (initial concentration = 4 mg-Cl_2/L) at pH 6 – 10 and 254, 311, and 365 nm.

Nitrobenzene, benzoate (pK_a = 4.19),[55] and cinnamic acid were selected as probe compounds for hydroxyl radical, RCS, and ozone, respectively, due to their specific reactivity and photostability at the irradiation wavelengths (Figure B2). Oxidant measurements were conducted at each pH and wavelength with 10 mM phosphate or borate buffer, 4 mg-Cl_2/L, and 10 μM probe.

3.3.3 Probe Validation

A series of experiments were conducted to assess the reactivity of nitrobenzene and benzoate with O_3, $^{\bullet}OH$, $Cl^{\bullet}$, $Cl_2^{\bullet-}$, and $ClO^{\bullet}$ under experimental conditions. First, solutions were purged with nitrogen to limit ozone formation[30,34] to confirm that reaction between the probes and O_3 is minimal. Second, chlorine photolysis experiments were conducted at low pH (i.e., pH 0.25), which is considered to be a clean source of $Cl^{\bullet}/Cl_2^{\bullet-}$,[32,44] to validate the selectivity of nitrobenzene for $^{\bullet}OH$.[56] Third, the reactivity of benzoate with reactive halogen species was verified using competition kinetics with nitrobenzene. Finally, experiments were conducted with elevated chloride (0 – 500 mM) and chlorine (0.4 – 100 mg-Cl_2/L) to shift the RCS toward $Cl_2^{\bullet-}$ and $ClO^{\bullet}$, respectively, in order to identify which RCS react with benzoate. Details are provided in Section B3.

3.3.4 Analytical Methods

Chlorine concentrations were measured immediately using the *N,N*-diethyl-*p*-phenylenediamine colorimetric method.[57] Chloride and sulfate concentrations were measured using anion chromatography after quenching chlorine samples using 0.5 M sodium thiosulfate to determine the initial chloride concentration, where the initial concentration of chloride is the difference between sulfate and chloride after quenching.[58] The initial chloride concentration in 4

mg-Cl_2/L was 1.25 x 10^{-4} M. The loss of nitrobenzene and benzoate and formation of benzaldehyde were quantified by high-performance liquid chromatography (Section B4).

3.3.5 Kinetic Modeling

A kinetic model containing 199 elementary reactions was built using Kintecus 4.55.[59] The model was based on previous literature models[22,29,33,40,46] and was amended with additional rate constants from the literature (Table B2), including the formation and reaction of ozone. The model was compared with the results of previously published models that were re-built in Kintecus and run with the same input rates (Section B5).[22,29,33,40,46,59]

3.3.6 Rate Constant Measurements

The second-order rate constants of $^{\bullet}OH$ with HOCl and OCl^- were measured using electron pulse radiolysis and transient absorption spectroscopy (Section B6).

3.4 Results and Discussion

3.4.1 Direct and Indirect Photolysis of Chlorine

Both the direct photolysis of chlorine and the subsequent formation of reactive oxidants are dependent on pH and wavelength. Therefore, identifying how chlorine loss rate constants respond to these parameters will improve our understanding of oxidant production. To determine the effect of pH and wavelength on chlorine degradation, the observed loss rate constant was quantified at pH 6 – 10 with 254, 311, and 365 nm irradiation. Chlorine degradation followed pseudo-first order kinetics, with observed rate constants ranging from 3.79 x 10^{-4} s^{-1} (365 nm, pH 6) to 2.53 x 10^{-2} s^{-1} (311 nm, pH 10).

Chlorine degradation was independent of pH at 254 nm (Figure 3.1a). This observation agrees with past work in which the observed chlorine loss rate constant does not change with pH under UV-C irradiation.[29,33,60,61] This effect may partially be explained by the relative molar absorptivities of the two chlorine species,[60,62] which are nearly equal at 254 nm (Figure B1). For example, the ratio of molar absorptivities is on the same order of magnitude as the ratio of $k_{obs,FAC}$ (A_{254,OCl^-}:$A_{254,HOCl}$ = 0.96; k_{obs,OCl^-}:$k_{obs,HOCl}$ = 1.32; Table B3). However, it is important to note that $k_{obs,FAC}$ includes both direct and indirect photolysis reactions (i.e., additional chlorine loss via reaction with $^{\bullet}$OH or RCS). Since the quantum yields of $^{\bullet}$OH formation from HOCl and OCl^- at 254 nm are similar (Scheme 3.1), k_{obs,OCl^-}:$k_{obs,HOCl}$ is greater than predicted based on molar absorptivities because $^{\bullet}$OH reacts more quickly with OCl^- than with HOCl ($(6.37 \pm 0.06) \times 10^9$ and $(1.21 \pm 0.17) \times 10^9$ $M^{-1}s^{-1}$, respectively; Section B6). Relying on measured $k_{obs,FAC}$ to calculate quantum yields for Reactions 1 – 4 results in values > 1 due to indirect photolysis reactions,[32,46,62-64] which are sometimes erroneously used in kinetic models in place of quantum yields of radical formation.[29,46]

The chlorine loss rate constant increased with pH at higher irradiation wavelengths (Figure 3.1a), which agrees with the trend observed under simulated sunlight and using UV-C and near UV-C irradiation.[29,60,61] OCl^- absorbs more light compared to HOCl at 311 and 365 nm (Table B3; Figure B1), yet the $^{\bullet}$OH quantum yields from OCl^- are much lower than HOCl at these wavelengths (Scheme 3.1). Therefore, the difference in molar absorptivity (i.e., direct photolysis) is the dominant driver of the observed pH dependence of chlorine loss. Deviations from this trend are attributable to indirect photolysis of HOCl due to elevated steady-state concentrations $^{\bullet}$OH at lower pH values.

Comparison of absolute chlorine loss rate constants and oxidant steady-state concentrations provides insight across pH values. When the data are fluence-normalized, comparison across wavelengths is possible. Both 254 and 311 nm irradiation wavelengths are more efficient in producing oxidants than 365 nm. Chlorine loss rate constants are faster at 254 and 311 nm than at 365 nm. The primary difference between the unnormalized data and the fluence-normalized data is that 365 nm chlorine loss rate constants and oxidant concentrations are on the same order of magnitude at the other wavelengths when normalized.

3.4.2 Validation of Probe Compounds

Nitrobenzene and benzoate are ideal reactive oxidant probes in chlorine photolysis systems because they are unreactive with chlorine[44] and do not undergo direct photolysis between 254 and 365 nm (Figure B2).[32,33,44] Furthermore, the reaction of both compounds with O_3 is negligible under these experimental conditions,[65] which was confirmed by conducting experiments in N_2-purged solutions to limit O_3 formation (Figure B3). Nitrobenzene is considered to be highly selective for $^{\bullet}OH$ compared to RCS,[22,32,33,44] although there are no published rate constants for its reaction with $Cl^{\bullet}$ or $Cl_2^{\bullet-}$.[20,32,44] In contrast, benzoate reacts with $^{\bullet}OH$, $Cl^{\bullet}$, and $Cl_2^{\bullet-}$,[33] and has been used in multiple kinetic modeling studies.[22,29,33,40,46] There is debate about whether its RCS-mediated degradation is dominated by $Cl^{\bullet}$ or $Cl_2^{\bullet-}$,[22,29,33,46] with one kinetic modeling study suggesting reaction with RCS is negligible.[33] We conducted a series of experiments to validate the selectivity of nitrobenzene and to identify which reactive species are responsible for benzoate degradation under our experimental conditions. These experiments are described in detail in Section B3 and summarized here.

In order to test the selectivity of nitrobenzene for $^{\bullet}OH$, we conducted experiments under highly acidic conditions where Cl_2 is the primary chlorine species (Figure 3.2a). This approach has been used to assess the reactivity of organic compounds with RCS since photolysis of Cl_2 is considered to be a clean source of $Cl^{\bullet}/Cl_2^{\bullet-}$.[44] Contrary to previous studies that observed no nitrobenzene degradation at pH 1 (254 nm; 4-16 mg-Cl_2/L),[32,44] nitrobenzene loss was observed when 4 mg-Cl_2/L was irradiated at 254 nm at pH 0.25 (Figure B4), suggesting that nitrobenzene reacts with $Cl^{\bullet}$ or $Cl_2^{\bullet-}$. However, further investigation of chlorine speciation shows that 0.71 mg-Cl_2/L HOCl is present in 4 mg-Cl_2/L total chlorine at pH 0.25 (Figure 3.2a) and additional experiments demonstrate that this concentration is capable of producing $^{\bullet}OH$ responsible for ~90% of the observed nitrobenzene loss (Figure B5). The remaining $^{\bullet}OH$ production may be attributable to $^{\bullet}OH$ formed via reaction of $Cl^{\bullet}$ with H_2O (Reactions 57 and 146). Thus, these results confirm the selectivity of nitrobenzene for $^{\bullet}OH$ and demonstrate that low pH conditions are not appropriate for generating $Cl^{\bullet}/Cl_2^{\bullet-}$ in the absence of $^{\bullet}OH$.

A series of experiments were used to identify which species are responsible for benzoate degradation under our experimental conditions. First, competition kinetics with nitrobenzene was used to evaluate the reactivity of benzoate towards RCS at pH 6 under 365 nm irradiation. The degradation of benzoate could not be explained by measured $[^{\bullet}OH]_{ss}$ alone (Figure B7), indicating that RCS also contribute to benzoate degradation. The effect of carbon-centered radicals on benzoate degradation is beyond the scope of this study and was not considered. In order to identify whether $Cl^{\bullet}$, $Cl_2^{\bullet-}$, or $ClO^{\bullet}$ contribute to benzoate loss, experiments with varied chloride and chlorine concentrations were conducted to produce conditions that favor $Cl_2^{\bullet-}$ and $ClO^{\bullet}$, respectively.[22,29,37,40,44,46] Elevated chloride shifts the $Cl^{\bullet}/Cl_2^{\bullet-}$ equilibria toward $Cl_2^{\bullet-}$, while increased chlorine concentrations result in higher production of $ClO^{\bullet}$ due to quenching of $^{\bullet}OH$ and

$Cl^{\bullet}$ by both chlorine species (Reactions 29, 37, 54,[67,68] and 55[67,69]). Benzoate reactivity decreased under conditions that favor $ClO^{\bullet}$ during chlorine variation experiments (Figure B8), demonstrating that reaction with $ClO^{\bullet}$ is negligible, as expected based on the slow reaction rate (3.0×10^6 M^{-1} s^{-1}).[38] Similarly, the degradation rate of benzoate decreased with $[Cl^-]$ (Figure 3.2b; Figure B9), suggesting that reaction with $Cl_2^{\bullet-}$ is less important than $Cl^{\bullet}$.

The limited contribution of $Cl_2^{\bullet-}$ in the absence of added chloride was further confirmed by calculating $Cl^{\bullet}$ and $Cl_2^{-\bullet}$ steady-state concentrations using a systems of equations that combines measured $[Cl^-]$ and experimentally determined $[^{\bullet}OH]_{ss}$ with $Cl^{\bullet}/Cl_2^{\bullet-}$ equilibria (Section B3). For example, $Cl_2^{\bullet-}$ is responsible for 0.1% of benzoate loss with no added chloride and 30.8% with 125 mM added chloride at pH 6 (Figure 3.2b). Collectively, the results indicate that benzoate can be used to quantify $Cl^{\bullet}$ after considering oxidation by $^{\bullet}OH$ in conditions with low $[Cl^-]$. Furthermore, the systems of equations approach can be used to quantitatively distinguish between $^{\bullet}OH$, $Cl^{\bullet}$, and $Cl_2^{\bullet-}$ under other experimental conditions.

3.4.3 Trends in Reactive Oxidant Production

In order to identify optimum conditions for chlorine photolysis as an AOP and to consider its application using light within the solar spectrum, it is critical to quantify the effect of solution conditions on reactive oxidant production. Using the probes validated in this study, we quantified steady-state concentrations of $^{\bullet}OH$ and $Cl^{\bullet}$ and cumulative ozone concentrations as a function of pH and wavelength because these parameters influence chlorine speciation, molar absorptivity, and quantum yields (Scheme 3.1).[33,34,70] Experimentally determined concentrations are presented in Figure 3.1, while fluence- and chlorine loss-normalized data are shown in Figures B12 and B13.

Experimental •OH steady-state concentrations decreased with increasing pH under all three irradiation wavelengths (Figure 3.1b). The observation of elevated $[^{\bullet}OH]_{ss}$ under acidic conditions agrees with previous measurements under UV-C irradiation,[32,33,40,60] while pH trends using UV-B and UV-A light have not been previously reported. $[^{\bullet}OH]_{ss}$ ranged from 6.2 x 10^{-13} – 2.1 x 10^{-12} M at 254 nm and 311 nm (Figure 3.1b), which is within the literature range of 10^{-14} – 10^{-12} M quantified using similar nitrobenzene concentrations (254 nm, 4 – 10 mg-Cl_2/L).[33,71] While $[^{\bullet}OH]_{ss}$ was higher under acidic conditions using 254 nm irradiation compared to 311 nm, this effect is reversed when the data is normalized by fluence or chlorine loss (Figures B12 and B13). $[^{\bullet}OH]_{ss}$ was a factor of 4 – 10 lower at 365 nm compared to 254 and 311 nm irradiation on an absolute basis (i.e., 6.0 x 10^{-14} – 1.9 x 10^{-13} M) and 20 – 200 times lower on a fluence-normalized basis. $[^{\bullet}OH]_{ss}$ at 365 nm are similar to a steady-state concentration of 3 x 10^{-14} M measured under simulated sunlight.[28] Note that the $[^{\bullet}OH]_{ss}$ experienced by contaminants in a chlorine photolysis system may be up to 10 – 20% higher than the values reported here due to scavenging by nitrobenzene depending on the presence of other constituents.

The impact of pH on $[^{\bullet}OH]_{ss}$ is partially attributable to differences in the quantum yields and reaction mechanisms of HOCl and OCl^- (Scheme 3.1). Although the OCl^- molar absorptivity is higher than that of HOCl at wavelengths >254 nm (Figure B1), the HOCl quantum yield is higher than that of OCl^- at each wavelength in this study (Scheme 3.1). While the decrease in •OH production with increasing pH at 254 nm is often solely attributed to the lower quantum yield of OCl^-,[33,46] it is important to note that the reaction mechanisms of HOCl and OCl^- are also different. HOCl undergoes homolytic cleavage to form •OH and Cl• with reported quantum yields ranging from 0.6 – 1.4.[32,33] The quantum yield of HOCl at 365 nm is unknown, but is hypothesized to be similar to 311 nm. In contrast, OCl^- undergoes photolysis via three separate reactions that each

generate different reactive species: $O^{\bullet-}$ reacts with water to form $^{\bullet}OH$, $O(^1D)$ reacts with water to form two $^{\bullet}OH$, and $O(^3P)$ reacts with oxygen to form O_3.[34] There is less variability in the reported quantum yields of OCl^- photolysis. For example, the recently reported quantum yield of 0.55 for $^{\bullet}OH$ production by OCl^- at 254 nm[33] is nearly identical to the quantum yield of 0.544 calculated from the earlier reported quantum yields of two OCl^- photolysis pathways (Reaction 2 + 2 x Reaction 3).[34] Thus, the quantum yield of HOCl is 1.1 – 2.6 times higher than the quantum yield of OCl^- at 254 nm, which does not fully explain the 5.2 times higher $[^{\bullet}OH]_{ss}$ quantified at pH 6 compared to pH 10.

Preferential scavenging of $^{\bullet}OH$ by OCl^- compared to HOCl also contributes to the decrease in $[^{\bullet}OH]_{ss}$ at high pH, regardless of irradiation wavelength. The reaction of $^{\bullet}OH$ with HOCl and OCl^- is critical because, in addition serving as a major sink of $^{\bullet}OH$, the product of the reaction (i.e., $ClO^{\bullet}$; Reactions 29 and 37 in Table B2) may be responsible for the degradation of organic compounds at high pH.[22,33,47,72] However, there is uncertainty in the rate constants; literature values vary from $8.5 \times 10^4 – 2.0 \times 10^9$ $M^{-1} s^{-1}$ for the reaction of $^{\bullet}OH$ and HOCl, and $8.8 \times 10^8 – 9.8 \times 10^9$ $M^{-1} s^{-1}$ for the reaction of $^{\bullet}OH$ and OCl^-.[10,32,33,44,73–76] We used pulse radiolysis to directly determine the absolute second-order rate constants between these chlorine species and $^{\bullet}OH$, and found values of $(1.21 \pm 0.17) \times 10^9$ and $(6.37 \pm 0.06) \times 10^9$ $M^{-1} s^{-1}$ for HOCl and OCl^-, respectively. These rate constants are faster than those measured by gamma radiolysis[33] and those calculated using quantum mechanical models,[77] but confirm the higher reactivity of $^{\bullet}OH$ with OCl^- reported previously. Pulse radiolysis measures the rate constant directly while gamma radiolysis measures the product of a reaction sequence, adding additional error to the measurement. Quantum mechanical modeling relies on assumptions (e.g., the number of hydrating water molecules) that can alter the analysis.[77]

3.4.5 Production and Reactivity of $Cl^{\bullet}$

The trends in experimental $Cl^{\bullet}$ steady-state concentrations with pH and wavelength were similar to the trends observed with $^{\bullet}OH$. $[Cl^{\bullet}]_{ss}$ was generally an order of magnitude lower than $[^{\bullet}OH]_{ss}$, ranging from 3.1 x 10^{-14} – 4.5 x 10^{-13} M at 254 and 311 nm and from 2.9 x 10^{-15} – 1.3 x 10^{-13} M at 365 nm (Figure 3.1c). Similar $[Cl^{\bullet}]_{ss}$ of (0.4 - 6.3) x 10^{-14} M were reported at 254 nm (pH 7).[29,78] There is some scatter with the pH trends due to error introduced by subtracting $k_{obs,NB}$ from $k_{BA,obs}$ as this two probe method for $^{\bullet}OH$, $Cl^{\bullet}$, and $Cl_2^{\bullet-}$ is most accurate at relatively high $[Cl^{\bullet}]_{ss}$ and/or $[Cl_2^{\bullet-}]_{ss}$ (Section B3). Despite this limitation, $[Cl^{\bullet}]_{ss}$ decreases with pH at all three irradiation wavelengths. Experimental steady-state concentrations of $Cl^{\bullet}$ have not been previously reported as a function of pH at any wavelength, but kinetic models predict that $Cl^{\bullet}$ will decrease with increasing pH at 254 nm.[33,46] As with $^{\bullet}OH$, $[Cl^{\bullet}]_{ss}$ is higher at both 254 and 311 nm than 365 nm when normalized by fluence or chlorine loss across all pH values (Figures B12 and B13).

The quantum yields of HOCl and OCl^- photolysis, as well as their relative reaction rates with $Cl^{\bullet}$, result in the observed trends in $[Cl^{\bullet}]_{ss}$. The quantum yield of $Cl^{\bullet}$ from HOCl is identical to the $^{\bullet}OH$ quantum yield because HOCl undergoes homolytic cleavage to form the two radicals.[34] However, only one of the three OCl^- photolysis pathways produces $Cl^{\bullet}$ (Reaction 2), which emphasizes the importance of considering the three pathways of OCl^- photolysis separately. Thus, the quantum yield of $Cl^{\bullet}$ from OCl^- is 1.95 and 1.31 times lower than the quantum yield of $^{\bullet}OH$ at 254 and 311 nm, respectively, while the quantum yields of $^{\bullet}OH$ and $Cl^{\bullet}$ are identical at 365 nm because Reaction 3 is negligible (Scheme 3.1). In addition, OCl^- reacts with $Cl^{\bullet}$ 2.75 times more quickly than HOCl (Reactions 54 and 55). Collectively, these factors result in the observed decrease in $[Cl^{\bullet}]_{ss}$ with increasing pH for both 254 and 365 nm (Figure 3.1c). There is no pH trend

for $[Cl^{\bullet}]_{ss}$ at 311 nm, likely because OCl^- absorbs more light than HOCl so the difference in quantum yield is matched by the difference in molar absorptivity (Scheme 3.1; Figure B2).

3.4.6 Ozone Generation

Although O_3 has not previously been measured at wavelengths less than 320 nm,[20,22,33,47,72,74] we observe the formation of O_3 at all three irradiation wavelengths (Figure 3.1d). Cumulative O_3 concentrations were determined by the maximum production of benzaldehyde over the course of the experiment and were greatest at 254 nm (0.9 – 2.2 μM), followed by 365 nm (0.8 – 1.3 μM) and 311 nm (0.4 – 1.1 μM). These concentrations are similar to the 1.8 μM cumulative O_3 measured during sunlight irradiation of 8 mg-Cl_2/L.[28] These concentrations are low relative to the concentration of O_3 used as a primary oxidant (e.g., ~1 mg/L)[48] in drinking water treatment, but O_3 is still an important oxidant. Previous studies at sunlight wavelengths demonstrate that O_3 generated during chlorine photolysis contributes to organic compound degradation[79] and pathogen inactivation.[28]

The cumulative concentration of ozone generally increases with increasing pH because $O(^3P)$, the precursor to ozone generation, is only formed during the photolysis of OCl^- (Reaction 4). This trend is observed until pH 8 where O_3 concentration peaks at all three wavelengths (Figure 3.1d), suggesting an optimum condition for the formation of ozone. The final decrease at high pH may be attributable to scavenging of O_3 by OCl^- (Reactions 84 and 85). The concentration of O_3 was highest at 254 nm due to the higher molar absorptivity of OCl^- relative to 365 nm. The difference between cumulative O_3 at 254 and 311 nm cannot be explained by molar absorptivity or quantum yield. However, the difference between ozone concentration at each wavelength is less

than an order of magnitude in absolute terms (Figure 3.1d) and equivalent when fluence-normalized (Figure B12d).

Demonstration of O_3 formation during chlorine photolysis at 254 nm is a novel finding that changes the analysis of previous research. The increased degradation of organic compounds at high pH is typically attributed to reaction with $ClO^{\bullet}$ based on quenching by *t*-butanol and the high $[ClO^{\bullet}]_{ss}$ predicted by kinetic models (~10^{-9} M).[14,22,23,33,37,47,72] For example, the degradation of trimethoprim, carbamazepine, and microcystin-LR at high pH was attributed to reaction with $ClO^{\bullet}$.[14,40,47] However, these compounds also react relatively quickly with O_3 (k = (0.5 – 7.4) x 10^4, 3 x 10^5, and 3.8 x 10^4 M^{-1} s^{-1}, respectively) and O_3 has not been included in kinetic models.[48,49,80,81] Furthermore, it is important to note that *t*-butanol is also a quencher for $O(^3P)$ (i.e., the O_3 precursor; Reaction 9).[80,82] Thus, we propose that enhanced oxidation of compounds at high pH may be partially attributable to reaction with O_3 due to the direct evidence of O_3 formation over a wide range of irradiation conditions.

3.4.7 Comparison of Kinetic Models

Kinetic modeling is an important component of studying chlorine photolysis because the number of reactive species makes quenching and probe studies incomplete. Kinetic models that describe chlorine photolysis under UV-C irradiation range in complexity (25 – 78 reactions; Table B4) and are used to predict chlorine loss rates and reactive oxidant steady-state concentrations, as well as to optimize treatment systems.[22,29,33,40,46] While some models are validated against a limited number of experimental results,[22,33] models are frequently extrapolated to other conditions or contaminants without further validation and some are not compared directly to experimental measurements made in the same study (e.g., measured $[^{\bullet}OH]_{ss}$ or estimated contaminant loss due

to $ClO^{\bullet}$).[22,37,40] Furthermore, it is impossible to validate steady-state concentrations of reactive species for which there are no selective probes (e.g., $ClO^{\bullet}$). Finally, existing models do not incorporate the formation of O_3 as one of the relevant oxidant species. To address these gaps, we built a kinetic model containing 199 reactions by expanding the previous models to include the reactions of O_3 and additional radical-radical reactions that were discovered during a comprehensive literature search (Table B2).

The five previously published models were reconstructed in Kintecus and compared to the expanded model built in this study, along with the experimental data. Comparison between models is limited to 254 nm irradiation because all past work focused on this wavelength, while discussion of modeling efforts at 311 and 365 nm is below. The literature models were all run using the same chlorine photolysis rates, which were calculated based on the measured sample absorbance at each pH value and literature quantum yields (Section B5), in order to compare the accuracy of models based on their elementary reactions. The modeled results were compared to the experimental measurements of chlorine loss, $[^{\bullet}OH]_{ss}$, $[Cl^{\bullet}]_{ss}$, and cumulative O_3 concentrations by calculating root-mean-square error (Table B6).

The side-by-side comparison of existing models that were constructed to model highly similar conditions reveals that there is little agreement across the models for chlorine loss and the considered oxidants. There is wide variability in the predicted trends of chlorine loss, with some models (e.g., Sun et al. 2017 and Guo et al. 2017) showing a strong pH dependence that does not match the experimental results or the trends observed by the other four models (Figure 3.3a). It is worth noting that the model that most accurately describes chlorine loss (Chuang et al. 2017) was developed for this specific parameter.[33] All six considered models report that $[^{\bullet}OH]_{ss}$ decreases with increasing pH, in agreement with experimental observations (Figure 3.3b). However, the

magnitude of predicted $[^{\bullet}OH]_{ss}$ ranges widely (e.g., from 1.0 x 10^{-14} to 2.6 x 10^{-12} M at pH 6). Similar results are observed for $Cl^{\bullet}$ (Figure B14a), although both Chuang et al. 2017 and Li et al. 2017 models predict $[Cl^{\bullet}]_{ss}$ that is 1 – 2 orders of magnitude lower than the other models and the experimental data. This could explain why Chuang et al. 2017 estimated that 80% of benzoate reactivity was due to $^{\bullet}OH$, while experimental observations show that $Cl^{\bullet}$ is responsible for ~40% of benzoate loss (Figure 3.2b). As expected, the five previously published models did not predict any ozone formation, while our model underpredicted cumulative ozone generation by 0 to 4 orders of magnitude (Figure B14b).

There is no single model that predicts all four parameters considered in our comparison. For example, the model that most accurately predicts chlorine loss rate constant (Chuang et al. 2017) overpredicts $[^{\bullet}OH]_{ss}$ and underpredicts $[Cl^{\bullet}]_{ss}$ (Figures 3.3b and B14a). Similarly, the model that accurately predicts both $[^{\bullet}OH]_{ss}$ and $[Cl^{\bullet}]_{ss}$ (Fang et al. 2014) is one of the least accurate in predicting chlorine loss. The model developed in this study generally predicts the order of magnitude and trends in chlorine loss, $[^{\bullet}OH]_{ss}$, and $[Cl^{\bullet}]_{ss}$, but is never the most, or least, accurate predictor.

The differences in model output result from the sets of reactions included in each model. For example, modeled $[^{\bullet}OH]_{ss}$ varies by two orders of magnitude when the models are run with the same direct photolysis rates and quantum yields (Table B5). Surprisingly, the Fang et al. 2014 model[46] is the most accurate at predicting $[^{\bullet}OH]_{ss}$ even though it is the most simplistic model (Table B4), with very few reactions describing $^{\bullet}OH$ reactivity. In contrast, the two models with the most reactions, this study and Chuang et al. 2017, are the worst predictors of $[^{\bullet}OH]_{ss}$ (Table B6).[33] These discrepancies are representative across parameters, where changes in the number of reactions describing a compound impact its formation and loss. While there are many missing rate

constants that need to be filled in for all reactive oxidants (e.g., reactions between oxidants and buffers), the side-by-side model comparison suggests that simply adding additional reactions does not improve model accuracy. There are also differences in the rate constants used for some reactions, but these values generally differ by less than an order of magnitude and are for minor reactions that are unlikely to impact the model.

The loss of chlorine and production of oxidants was also modeled at 311 and 365 nm using measured absorbance, literature quantum yields (Scheme 3.1), and known kinetic reactions (Table B2). The 311 nm model results in the most accurate predictions of O_3 production and accurately predicts the observed loss rate of chlorine and $[Cl^{\bullet}]_{ss}$ (Figure B15). However, the model overpredicts $[^{\bullet}OH]_{ss}$ by more than an order of magnitude at high pH, which may be the result of the high molar absorptivity of OCl^- and correspondingly high expected production of $^{\bullet}OH$. While the 311 nm model was successful for three of the considered parameters, the 365 nm kinetic model was less accurate for all parameters (Figure B16). For example, the 365 nm model overpredicts chlorine loss rate constants and $[^{\bullet}OH]_{ss}$, while underpredicting O_3 formation. This model is based on an assumed quantum yield of 1.0 for HOCl because a literature value is not available, which likely introduces uncertainty to the model. Although there are no existing kinetic models available for comparison at the higher wavelengths, the overall accuracy of these models is similar to that of the revised 254 nm model.

The wide variety of model results suggests that a comprehensive model for chlorine photolysis based on a first principles approach is not yet possible. The addition of >100 reactions to previously published models resulted in a model that is moderately good at predicting the formation of oxidants by chlorine photolysis relative to others. However, it is still not the best model for any of the parameters. It is possible that additional elementary reactions could further

improve this model, but we may never have all of the necessary rate constants to accurately determine the formation of oxidants in this system due to the number of radicals and subsequent chain reactions. Due to the challenges in predicting the production of reactive oxidants that can be compared to experimental data, it is unlikely that models can accurately determine the formation of other oxidant species that cannot yet be validated experimentally, such as $ClO^{\bullet}$. Additionally, the variability between models suggests that using models to attribute reactivity towards a given organic compound may not be accurate, as seen with the modeled difference in benzoate reactivity towards $Cl^{\bullet}$ and $^{\bullet}OH$.[33,46]

3.5 Implications for Water Treatment

Understanding the formation of reactive oxidants during chlorine photolysis is essential to future applications of advanced oxidation or disinfection.[72,83–86] Chlorine photolysis produces a suite of reactive oxidants, including $^{\bullet}OH$, $Cl^{\bullet}$, and O_3, that are capable of degrading organic contaminants. $^{\bullet}OH$ and $Cl^{\bullet}$ steady-state concentrations are greater under acidic conditions using 254 or 311 nm irradiation, while O_3 is generally greatest at high pH using 254 nm irradiation (**Figure 3.1**). $Cl^{\bullet}$ and $Cl_2^{\bullet-}$ may be problematic because they can react via chlorine addition to form chlorinated disinfection byproducts.[37,40–42] Both O_3 and $^{\bullet}OH$ are optimized during treatment at 254 nm, though at opposite ends of the pH spectrum. The fluence- and chlorine loss-normalized oxidant concentrations provide additional insight into this system. If treatment is chlorine limited, 254 nm is the optimum irradiation wavelength because it produces the most $^{\bullet}OH$ per chlorine molecule degraded (**Figure B13**). If energy consumption is the primary concern, 311 nm will optimize the production of $^{\bullet}OH$ for each photon produced (**Figure B12**). These results agree with previous observations of chlorine loss rates and $[^{\bullet}OH]_{ss}$ at $\lambda < 301$ nm.[60]

O_3 is a powerful oxidant that has been largely overlooked in previous studies. Experimentally determined cumulative ozone concentrations demonstrate that this oxidant is present under all studied conditions, albeit at lower concentrations than O_3 is typically used in drinking water treatment. As O_3 reacts with many organic compounds,[48,83,86,87] further investigation into its role in contaminant degradation during chlorine photolysis is needed. The formation of O_3 is also crucial because it results in bromate formation in bromine-containing waters.[48,88–90]

Finally, this study suggests that chlorine photolysis has potential in solar treatment applications. Although 254 nm is the most effective wavelength at producing $^{\bullet}OH$, both 311 and 365 nm irradiation result in oxidant generation. Thus, chlorine photolysis is unique among light-based AOPs as it could be applied in regions without access to conventional drinking water treatment for point-of-use solar water disinfection.[20,30,72,83–86] For example, degradation of DEET, caffeine, and carbamazepine and enhanced inactivation of *Cryptosporidium parvum* have been observed when chlorine undergoes photolysis by solar light.[29,30,80,82] Our work provides insight into the mechanism of oxidant production under these conditions and suggests that $^{\bullet}OH$ and O_3 may contribute to previously observed contaminant removal.

3.6 Acknowledgements

This work was supported by an NSF CAREER award (CBET-1451932) and a National Water Research Institute Graduate Research Fellowship (awarded to D.M.B.)

3.7 Supporting Information

Additional details pertaining to analytical methods, probe validation, comprehensive kinetic model comparison, rate constant measurements, and fluence- and chlorine loss-normalized reactive oxidant production can be found in Appendix B.

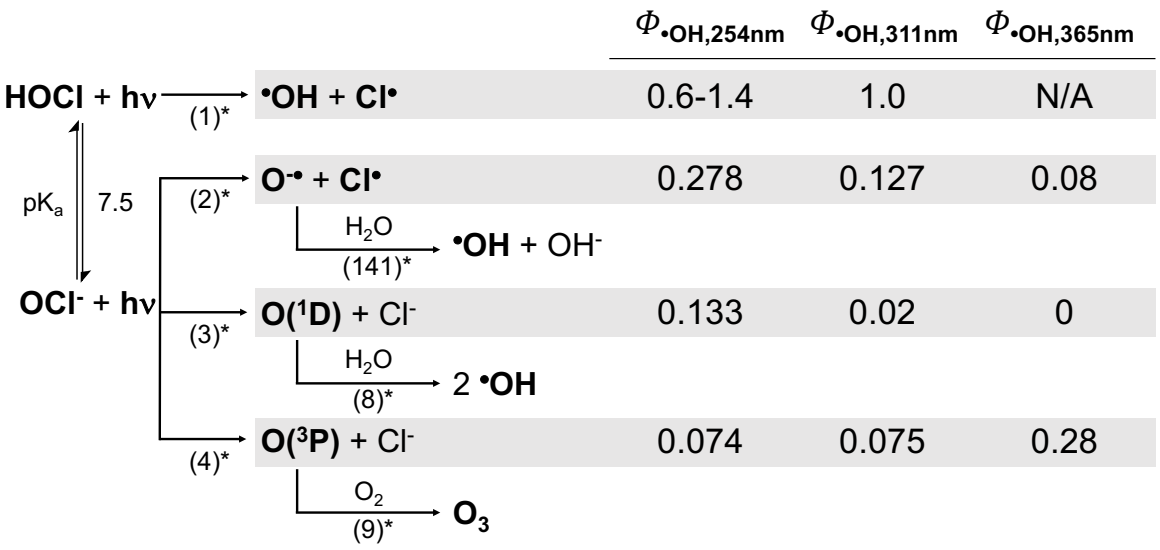

	$\Phi_{\bullet OH,254nm}$	$\Phi_{\bullet OH,311nm}$	$\Phi_{\bullet OH,365nm}$
•OH + Cl•	0.6-1.4	1.0	N/A
$O^{-\bullet}$ + Cl•	0.278	0.127	0.08
$O(^1D)$ + Cl^-	0.133	0.02	0
$O(^3P)$ + Cl^-	0.074	0.075	0.28

Scheme 3.1. Literature quantum yields of photolysis for both HOCl and OCl^- at 254, 311, and 365 nm.[20,32–34,43] *Reaction numbers correspond to reactions in Table B2.

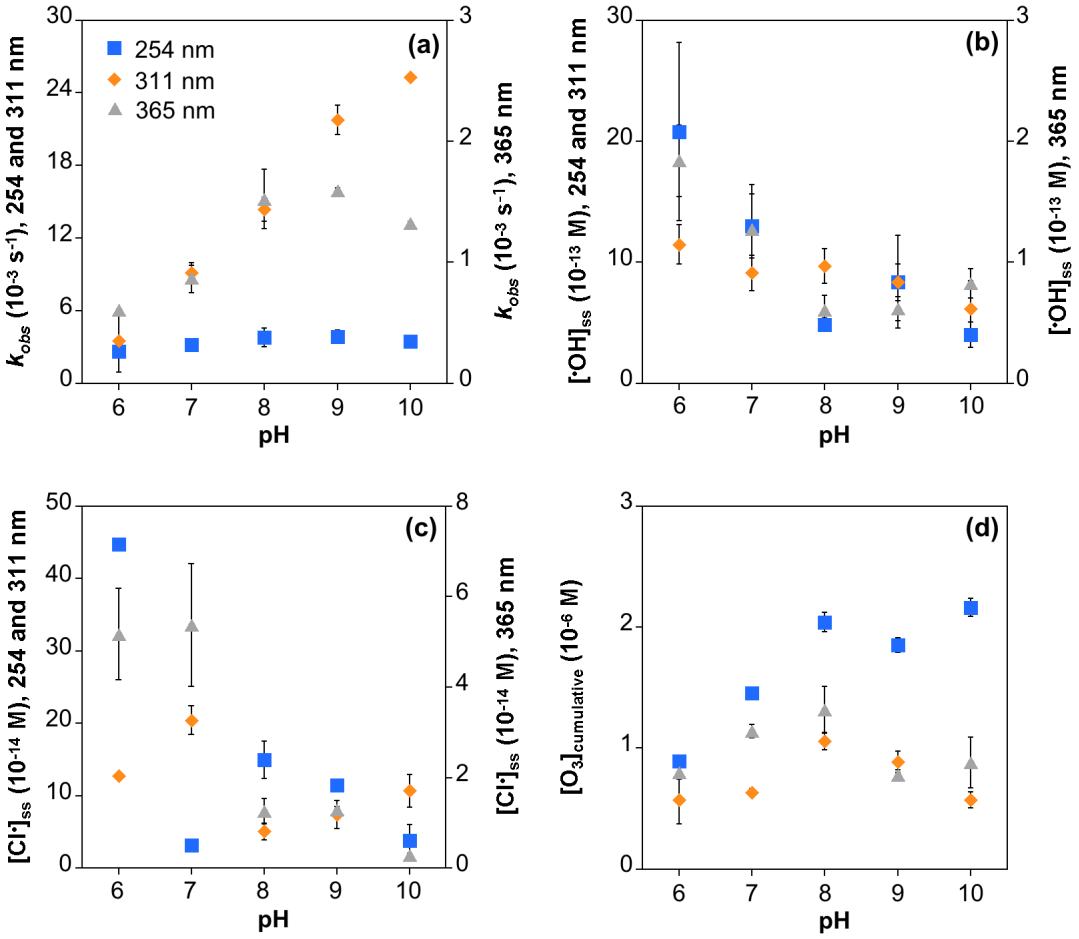

Figure 3.1. (a) Observed free chlorine loss rate constant, (b) hydroxyl radical steady-state concentration, (c) chlorine radical steady-state concentration, and (d) cumulative ozone formation as a function of pH during irradiation at 254, 311, and 365 nm (secondary axis).

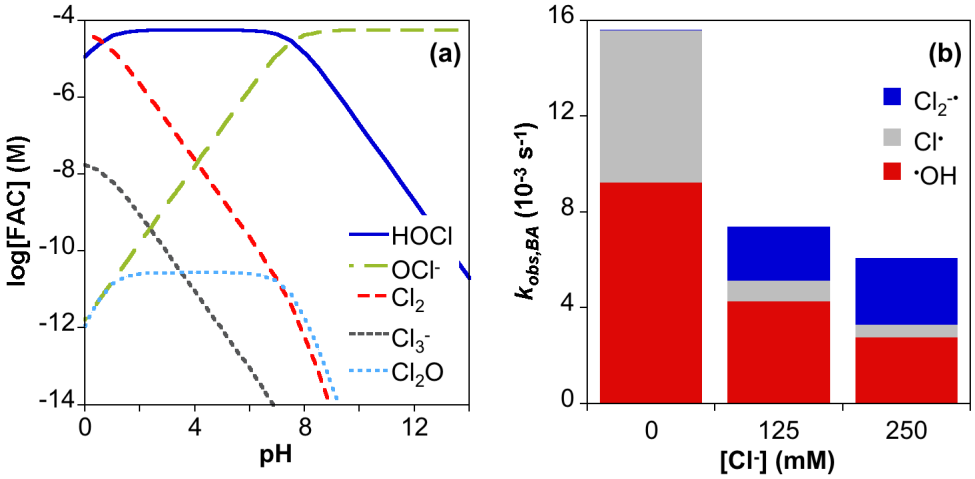

Figure 3.2. (a) Chlorine speciation as a function of pH for 4 mg-Cl_2/L total chlorine and 75 mg/L chloride calculated using equilibrium constants from Ref. 66. (b) Contribution of $^{\bullet}OH$, $Cl^{\bullet}$, and $Cl_2^{-\bullet}$ to benzoate loss as a function of chloride concentration at 254 nm (4 mg-Cl_2/L, pH 6).

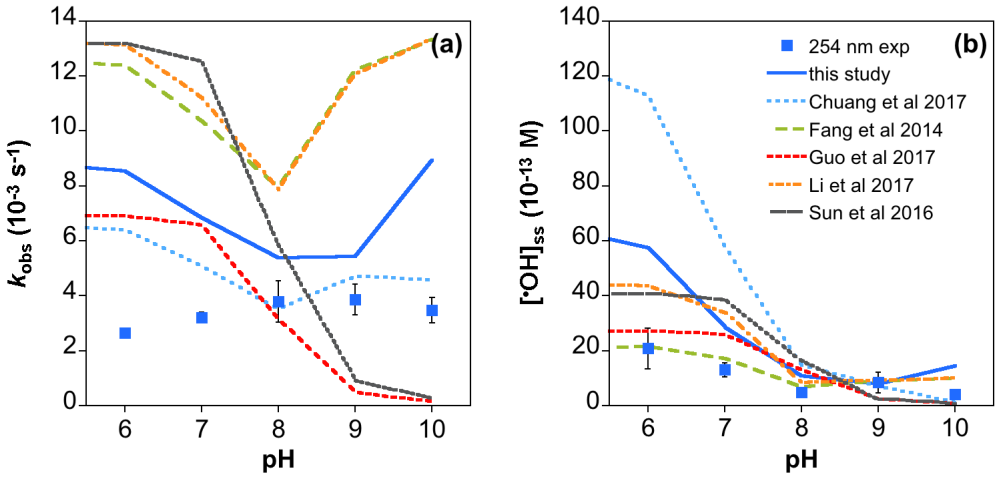

Figure 3.3. Comparison of experimental data with model output from the model developed in this study along with literature models[22,29,33,40,46] for the (a) observed free chlorine loss rate constants and (b) hydroxyl radical steady-state concentrations as a function of pH during irradiation of 4 mg-Cl_2/L at 254 nm.

3.8 References

(1) Benotti, M. J.; Trenholm, R. A.; Vanderford, B. J.; Holady, J. C.; Stanford, B. D.; Snyder, S. A.; Pharmaceuticals and endocrine disrupting compounds in U.S. drinking water. *Environ. Sci. Technol.* **2009**, 43(3), 597-603.

(2) Fairbairn, D. J.; Arnold, W. A.; Barber, B. L.; Kaufenberg, E. F.; Koskinen, W. C.; Novak, P. J.; Rice, P. J.; Swackhamer, D. L.; Contaminants of emerging concern: Mass balance and comparison of wastewater effluent and upstream sources in a mixed-use watershed. *Environ. Sci. Technol.* **2016**, 50(1), 36-45.

(3) Kolpin, D. W.; Furlong, E. T.; Meyer, M. T.; Thurman, E. M.; Zaugg, S. D.; Barber, L. B.; Buxton, H. T.; Pharmaceuticals, hormones, and other organic wastewater contaminants in U.S. streams, 1999−2000: A national reconnaissance. *Environ. Sci. Technol.* **2002**, 36(6), 1202-1211.

(4) Kostich, M. S.; Batt, A. L.; Lazorchak, J. M.; Concentrations of prioritized pharmaceuticals in effluents from 50 large wastewater treatment plants in the U.S. and implications for risk estimation. *Environ. Pollut.* **2014**, 184, 354-359.

(5) Stackelberg, P. E.; Furlong, E. T.; Meyer, M. T.; Zaugg, S. D.; Henderson, A. K.; Reissman, D. B.; Persistence of pharmaceutical compounds and other organic wastewater contaminants in a conventional drinking-water-treatment plant. *Sci. Total Environ.* **2004**, 329(1-3), 99-113.

(6) Mompelat, S.; Le Bot, B.; Thomas, O.; Occurrence and fate of pharmaceutical products and by-products, from resource to drinking water. *Environ. Int.* **2009**, 35(5), 803-814.

(7) Masoner, J. R.; Kolpin, D. W.; Furlong, E. T.; Cozzarelli, I. M.; Gray, J. L.; Landfill leachate as a mirror of today's disposable society: Pharmaceuticals and other contaminants of emerging concern in final leachate from landfills in the conterminous united states. *Environ. Toxicol. Chem.* **2016**, 35(4), 906-918.

(8) Gray, J. L.; Borch, T.; Furlong, E. T.; Davis, J. G.; Yager, T. J.; Yang, Y. Y.; Kolpin, D. W.; Rainfall-runoff of anthropogenic waste indicators from agricultural fields applied with municipal biosolids. *Sci. Total Environ.* **2017**, 580, 83-89.

(9) Richardson, S. D.; Ternes, T. A.; Water analysis: Emerging contaminants and current issues. *Anal. Chem.* **2011**, 83(12), 4614-4648.

(10) Buxton, G. V.; Greenstock, C. L.; Helman, W. P.; Ross, A. B.; Critical review of rate constants for reactions of hydrated electrons, hydrogen atoms and hydroxyl radicals (OH/O^- in aqueous solution. *J. Phys. Chem. Ref. Data* **1988**, 17(2), 513-886.

(11) Buxton, G. V.; Bydder, M.; Salmon, G. A.; Williams, J. E.; The reactivity of chlorine atoms in aqueous solution part III. The reactions of Cl with solutes. *Phys. Chem. Chem. Phys.* **2000**, 2, 237-245.

(12) An, T.; Yang, H.; Li, G.; Song, W.; Cooper, W. J.; Nie, X.; Kinetics and mechanism of advanced oxidation processes (AOPs) in degradation of ciprofloxacin in water. *Appl. Catal. B-Environ.* **2010**, 94(3-4), 288-294.

(13) Cai, M.; Sun, P.; Zhang, L.; Huang, C. H.; UV/peracetic acid for degradation of pharmaceuticals and reactive species evaluation. *Environ. Sci. Technol.* **2017**, 51(24), 14217-14224.

(14) Duan, X.; Sanan, T.; De La Cruz, A.; He, X.; Kong, M.; Dionysiou, D. D.; Susceptibility of the algal toxin microcystin-LR to UV/chlorine process: Comparison with chlorination. *Environ. Sci. Technol.* **2018**, 52(15), 8252-8262.

(15) García Einschlag, F. S.; Carlos, L.; Capparelli, A. L.; Competition kinetics using the UV/H_2O_2 process: A structure reactivity correlation for the rate constants of hydroxyl radicals toward nitroaromatic compounds. *Chemosphere* **2003**, 53(1), 1-7.
(16) Huang, Y.; Liu, Y.; Kong, M.; Xu, E. G.; Coffin, S.; Schlenk, D.; Dionysiou, D. D.; Efficient degradation of cytotoxic contaminants of emerging concern by UV/H_2O_2. *Environ. Sci.: Water Res. Technol.* **2018**, 4(9), 1272-1281.
(17) Khan, S. J.; Gagnon, G. A.; Templeton, M. R.; Dionysiou, D. D.; The rapidly growing role of UV-AOPs in the production of safe drinking water. *Environ. Sci.: Water Res. Technol.* **2018**, 4(9), 1211-1212.
(18) Lee, Y.; Gerrity, D.; Lee, M.; Gamage, S.; Pisarenko, A.; Trenholm, R. A.; Canonica, S.; Snyder, S. A.; Von Gunten, U.; Organic contaminant abatement in reclaimed water by UV/H_2O_2 and a combined process consisting of O_3/H_2O_2 followed by UV/H_2O_2: Prediction of abatement efficiency, energy consumption, and byproduct formation. *Environ. Sci. Technol.* **2016**, 50(7), 3809-3819.
(19) Bossmann, S. H.; Oliveros, E.; Göb, S.; Siegwart, S.; Dahlen, E. P.; Payawan, L.; Straub, M.; Wörner, M.; Braun, A. M.; New evidence against hydroxyl radicals as reactive intermediates in the thermal and photochemically enhanced Fenton reactions. *J. Phys. Chem. A* **1998**, 102(28), 5542-5550.
(20) Remucal, C. K.; Manley, D.; Emerging investigators series: The efficacy of chlorine photolysis as an advanced oxidation process for drinking water treatment. *Environ. Sci.: Water Res. Technol.* **2016**, 2(4), 565-579.
(21) Huang, W.; Bianco, A.; Brigante, M.; Mailhot, G.; UVA-UVB activation of hydrogen peroxide and persulfate for advanced oxidation processes: Efficiency, mechanism and effect of various water constituents. *J. Hazard. Mater.* **2018**, 347, 279-287.
(22) Li, W.; Jain, T.; Ishida, K.; Remucal, C. K.; Liu, H.; A mechanistic understanding of the degradation of trace organic contaminants by UV/hydrogen peroxide, UV/persulfate and UV/free chlorine for water reuse. *Environ. Sci.: Water Res. Technol.* **2017**, 3(1), 128-138.
(23) Pan, M.; Wu, Z.; Tang, C.; Guo, K.; Cao, Y.; Fang, J.; Emerging investigators series: Comparative study of naproxen degradation by the UV/chlorine and the UV/H_2O_2 advanced oxidation processes. *Environ. Sci.: Water Res. Technol.* **2018**, 4(9), 1219-1230.
(24) Pati, S. G.; Arnold, W. A.; Reaction rates and product formation during advanced oxidation of ionic liquid cations by UV/peroxide, UV/persulfate, and UV/chlorine. *Environ. Sci.: Water Res. Technol.* **2018**, 4(9), 1310-1320.
(25) Chu, W.; Gao, N.; Yin, D.; Krasner, S. W.; Mitch, W. A.; Impact of UV/H_2O_2 pre-oxidation on the formation of haloacetamides and other nitrogenous disinfection byproducts during chlorination. *Environ. Sci. Technol.***2014**, 48(20), 12190-12198.
(26) Morgan, M. S.; Van Trieste, P. F.; Garlick, S. M.; Mahon, M. J.; Smith, A. L.; Ultraviolet molar absorptivities of aqueous hydrogen peroxide and hydroperoxyl ion. *Anal. Chim. Acta* **1988**, 215, 325-329.
(27) Buck, R. P.; Singhadeja, S.; Rogers, L. B.; Ultraviolet absorption spectra of some inorganic ions in aqueous solutions. *Anal. Chem.* **1954**, 26 (7), 1240-1242.
(28) Forsyth, J. E.; Zhou, P.; Mao, Q.; Asato, S. S.; Meschke, J. S.; Dodd, M. C.; Enhanced inactivation of bacillus subtilis spores during solar photolysis of free available chlorine. *Environ. Sci. Technol.* **2013**, 47(22), 12976-12984.

(29) Sun, P.; Lee, W. N.; Zhang, R.; Huang, C. H.; Degradation of DEET and caffeine under UV/chlorine and simulated sunlight/chlorine conditions. *Environ. Sci. Technol.* **2016**, 50(24), 13265-13273.
(30) Young, T. R.; Li, W.; Guo, A.; Korshin, G. V.; Dodd, M. C.; Characterization of disinfection byproduct formation and associated changes to dissolved organic matter during solar photolysis of free available chlorine. *Water Res.* **2018**, 146, 318-327.
(31) Yin, R.; Zhong, Z.; Ling, L.; Shang, C.; The fate of dichloroacetonitrile in UV/Cl_2 and UV/H_2O_2 processes: Implications on potable water reuse. *Environ. Sci.: Water Res. Technol.* **2018**, 4(9), 1295-1302.
(32) Watts, M. J.; Linden, K. G.; Chlorine photolysis and subsequent OH radical production during UV treatment of chlorinated water. *Water Res.* **2007**, 41(13), 2871-2878.
(33) Chuang, Y. H.; Chen, S.; Chinn, C. J.; Mitch, W. A.; Comparing the UV/monochloramine and UV/free chlorine advanced oxidation processes (AOPs) to the UV/hydrogen peroxide AOP under scenarios relevant to potable reuse. *Environ. Sci. Technol.* **2017**, 51(23), 13859-13868.
(34) Buxton, G. V.; Subhani, M. S.; Radiation chemistry and photochemistry of oxychlorine ions Part 2. Photodecomposition of aqueous solutions of hypochlorite ions. *J. Chem. Soc., Faraday Trans. 1* **1972**, 68, 958-969.
(35) Gilbert, B. C.; Stell, J. K.; Peet, W. J.; Radford, K. J.; Generation and reactions of the chlorine atom in aqueous solution. *J. Chem. Soc., Faraday Trans. 1* **1988**, 84 (10), 3319-3330.
(36) Zhang, K.; Parker, K. M.; Halogen radical oxidants in natural and engineered aquatic systems. *Environ. Sci. Technol.* **2018**, 52(17), 9579-9594.
(37) Wu, Z.; Guo, K.; Fang, J.; Yang, X.; Xiao, H.; Hou, S.; Kong, X.; Shang, C.; Yang, X.; Meng, F.; Chen, L.; Factors affecting the roles of reactive species in the degradation of micropollutants by the UV/chlorine process. *Water Res.* **2017**, 126, 351-360.
(38) Alfassi, Z. B.; Huie, R. E.; Mosseri, S.; Neta, P.; Kinetics of one-electron oxidation by the ClO radical. *Radiat. Phys. Chem.* **1988**, 32 (1), 85-88.
(39) Hasegawa, K.; Neta, P.; Rate constants and mechanisms of reaction of chloride (Cl_2^-) radicals. *J. Phys. Chem.* **1978**, 82(8), 854-857.
(40) Guo, K.; Wu, Z.; Shang, C.; Yao, B.; Hou, S.; Yang, X.; Song, W.; Fang, J.; Radical chemistry and structural relationships of PPCP degradation by UV/chlorine treatment in simulated drinking water. *Environ. Sci. Technol.* **2017**, 51(18), 10431-10439.
(41) Yang, Y.; Pignatello, J. J.; Participation of the halogens in photochemical reactions in natural and treated waters. *Molecules* **2017**, 22(10).
(42) Liu, W.; Cheung, L.-M.; Yang, X.; Shang, C.; THM, HAA and CNCl formation from UV irradiation and chlor(am)ination of selected organic waters. *Water Res.* **2006**, 40(10), 2033-2043.
(43) Molina, M. J.; Ishiwata, T.; Molina, L. T.; Production of hydroxyl from photolysis of hypochlorous acid at 307-309 nm. *J. Phys. Chem.* **1980**, 84(8), 821-826.
(44) Nowell, L. H.; Hoigné, J.; Photolysis of aqueous chlorine at sunlight and ultraviolet wavelengths - II. Hydroxyl radical production. *Water Res.* **1992**, 5, 599-605.
(45) Cheng, S.; Zhang, X.; Yang, X.; Shang, C.; Song, W.; Fang, J.; Pan, Y.; The multiple role of bromide ion in PPCPs degradation under UV/chlorine treatment. *Environ. Sci. Technol.* **2018**, 52(4), 1806-1816.
(46) Fang, J.; Fu, Y.; Shang, C.; The roles of reactive species in micropollutant degradation in the UV/free chlorine system. *Environ. Sci. Technol.* **2014**, 48(3), 1859-1868.

(47) Wu, Z.; Fang, J.; Xiang, Y.; Shang, C.; Li, X.; Meng, F.; Yang, X.; Roles of reactive chlorine species in trimethoprim degradation in the UV/chlorine process: Kinetics and transformation pathways. *Water Res.* **2016**, 104, 272-282.
(48) von Gunten, U.; Ozonation of drinking water: Part I. Oxidation kinetics and product formation. *Water Res.* **2003**, 37, 1443-1467.
(49) Kuang, J.; Huang, J.; Wang, B.; Cao, Q.; Deng, S.; Yu, G.; Ozonation of trimethoprim in aqueous solution: Identification of reaction products and their toxicity. *Water Res.* **2013**, 47(8), 2863-2872.
(50) Laszakovits, J. R.; Berg, S. M.; Anderson, B. G.; O'Brien, J. E.; Wammer, K. H.; Sharpless, C. M.; *p*-Nitroanisole/pyridine and *p*-nitroacetophenone/pyridine actinometers revisited: Quantum yield in comparison to ferrioxalate. *Environ. Sci. Tech. Lett.* **2017**, 4(1), 11-14.
(51) McConville, M. B.; Hubert, T. D.; Remucal, C. K.; Direct photolysis rates and transformation pathways of the lampricides TFM and niclosamide in simulated sunlight. *Environ. Sci. Technol.* **2016**, 50(18), 9998-10006.
(52) Maizel, A. C.; Li, J.; Remucal, C. K.; Relationships between dissolved organic matter composition and photochemistry in lakes of diverse trophic status. *Environ. Sci. Technol.* **2017**, 51(17), 9624-9632.
(53) Galbavy, E. S.; Ram, K.; Anastasio, C.; 2-Nitrobenzaldehyde as a chemical actinometer for solution and ice photochemistry. *Photochem. Photobio. A* **2010**, 209(2-3), 186-192.
(54) Baeza, C.; Knappe, D. R. U.; Transformation kinetics of biochemically active compounds in low-pressure UV photolysis and UV/H_2O_2 advanced oxidation processes. *Water Res.* **2011**, 45(15), 4531-4543.
(55) Hollingsworth, C. A.; Seybold, P. G.; Hadad, C. M.; Substituent effects on the electronic structure and pK_a of benzoic acid. *Int. J. Quantum Chem.* **2002**, 90(4-5), 1396-1403.
(56) Neta, P.; Madhavan, V.; Zemel, H.; Fessenden, R. W.; Rate constants and mechanism of reaction of SO_4^- with aromatic compounds. *J. Am. Chem. Soc.* **1977**, 99(1), 163-164.
(57) Eaton, A. D.; Clesceri, L. S.; Greenberg, A. E., Eds. *Standard Methods for the Examination of Water and Wastewater*, ed.; United Book Press, Inc., Baltimore, 1995.
(58) Willson, V. A.; Determination of available chlorine in hypochlorite solutions by direct titration with sodium thiosulfate. *Indus. Eng. Chem. Anal. Ed.* **1935**, 7 (1), 44-45.
(59) Ianni, J. C. , "A Comparison of the Bader-Deuflhard and the Cash-Karp Runge-Kutta Integrators for the GRI-MECH 3.0 Model Based on the Chemical Kinetics Code Kintecus", pg.1368-1372, Computational Fluid and Solid Mechanics 2003, K.J. Bathe editor, Elsevier Science Ltd., Oxford, UK., 2003.
(60) Yin, R.; Ling, L.; Shang, C.; Wavelength-dependent chlorine photolysis and subsequent radical production using UV-LEDs as light sources. *Water Res.* **2018**, 142, 452-458.
(61) Kwon, M.; Yoon, Y.; Kim, S.; Jung, Y.; Hwang, T.-M.; Kang, J.-W.; Removal of sulfamethoxazole, ibuprofen and nitrobenzene by UV and UV/chlorine processes: A comparative evaluation of 275 nm LED-UV and 254 nm LP-UV. *Sci. Total Environ.* **2018**, 637-638, 1351-1357.
(62) Feng, Y.; Smith, D. W.; Bolton, J. R.; Photolysis of aqueous free chlorine species (HOCl and OCl^-) with 254 nm ultraviolet light. *Environ. Eng. Sci.* **2007**, 6(3), 277-284.
(63) Jin, J.; El-Din, M. G.; Bolton, J. R.; Assessment of the UV/chlorine process as an advanced oxidation process. *Water Res.* **2011**, 45(4), 1890-1896.
(64) Zhao, Q.; Shang, C.; Zhang, X.; Effects of bromide on UV/chlorine advanced oxidation process. *Water Sci. Technol. Water Supply* **2009**, 9(6), 627.

(65) Hoigné, J.; Bader, H.; Rate constants of reactions of ozone with organic and inorganic compounds in water-I: Non-dissociating organic compounds. *Water Res.* **1983**, 17, 173-183.
(66) G. V. Korshin, in Aquatic Redox Chemistry, ed. P. G. Tratnyek, T. J. Grundl and S. B. Haderlein, American Chemical Society, Washington, DC, 2011, ch. 11, vol. 1071, pp. 223–245
(67) Zehavi, D.; Rabani, J.; Pulse radiolytic investigation of O_{aq}^- radical ions. *J. Phys. Chem.* **1971**, 75 (11), 1738-1744.
(68) Zehavi, D.; Rabani, J.; Pulse radiolytic investigation of oaq- radical ions. *The Journal of Physical Chemistry* **1971**, 75 (11), 1738-1744.
(69) Jayson, G. G.; Parsons, B. J.; Swallow, A. J.; Some simple, highly reactive, inorganic chlorine derivatives in aqueous solution. *J. Chem. Soc., Faraday Trans. 1* **1973**, 69, 1597-1607.
(70) Buxton, G. V.; Subhani, M. S.; Radiation chemistry and photochemistry of oxychlorine ions Part 1. Radiolysis of aqueous solutions of hypochlorite and chlorite ions. *J. Chem. Soc., Faraday Trans. 1* **1972**, 68 (0), 947-957.
(71) Wang, D.; Bolton, J. R.; Hofmann, R.; Medium pressure UV combined with chlorine advanced oxidation for trichloroethylene destruction in a model water. *Water Res* **2012**, 46(15), 4677-4686.
(72) Dodd, M. C.; Huang, C. H.; Aqueous chlorination of the antibacterial agent trimethoprim: Reaction kinetics and pathways. *Water Res.* **2007**, 41(3), 647-655.
(73) Connick, R. E.; The interaction of hydrogen peroxide and hypochlorous acid in acidic solutions containing chloride ion. *J. Am. Chem. Soc.* **1947**, 69 (6), 1509-1514.
(74) Buxton, G. V.; Subhani, M. S.; Radiation chemistry and photochemistry of oxychlorine ions Part 3. Photodecomposition of aqueous solutions of chloride ions. *J. Chem. Soc., Faraday Trans.* **1972**, 68, 970-977.
(75) Anastasio, C.; B.M., M.; A chemical probe technique for the determination of reactive halogen species in aqueous solution: Part 2 Chloride solutions and mixed bromide/chloride solutions. *Atmos. Chem. Phys.* **2006**, 6, 2439-2451.
(76) Zuo, Z.; Katsumura, Y.; Ueda, K.; Ishigure, K.; Reactions between some inorganic radicals and oxychlorides studied by pulse radiolysis and laser photolysis. *J. Chem. Soc., Faraday Trans.* **1997**, 93 (10), 1885-1891.
(77) Minakata, D.; Kamath, D.; Maetzold, S.; Mechanistic insight into the reactivity of chlorine-derived radicals in the aqueous-phase UV-chlorine advanced oxidation process: Quantum mechanical calculations. *Environ. Sci. Technol.* **2017**, 51(12), 6918-6926.
(78) Varanasi, L.; Coscarelli, E.; Khaksari, M.; Mazzoleni, L. R.; Minakata, D.; Transformations of dissolved organic matter induced by UV photolysis, hydroxyl radicals, chlorine radicals, and sulfate radicals in aqueous-phase UV-based advanced oxidation processes. *Water Res.* **2018**, 135, 22-30.
(79) Hua, Z.; Guo, K.; Kong, X.; Lin, S.; Wu, Z.; Wang, L.; Huang, H.; Fang, J.; PPCP degradation and DBP formation in the solar/free chlorine system: Effects of pH and dissolved oxygen. *Water Res.* **2019**, 150, 77-85.
(80) Yang, B.; Kookana, R. S.; Williams, M.; Du, J.; Doan, H.; Kumar, A.; Removal of carbamazepine in aqueous solutions through solar photolysis of free available chlorine. *Water Res.* **2016**, 100, 413-420.
(81) Shawwa, A. R.; Smith, D. W.; Sego, D. C.; Color and chlorinated organics removal from pulp mills wastewater using activated petroleum coke. *Water Res.* **2001**, 35(3), 745-749.

(82) Zhou, P.; Di Giovanni, G. D.; Meschke, J. S.; Dodd, M. C.; Enhanced inactivation of cryptosporidium parvum oocysts during solar photolysis of free available chlorine. *Environ. Sci. Tech. Lett.* **2014**, 1(11), 453-458.
(83) Dodd, M. C.; Kohler, H.-P. E.; Von Gunten, U.; Oxidation of antibacterial compounds by ozone and hydroxyl radical: Elimination of biological activity during aqueous ozonation processes. *Environ. Sci. Technol.* **2009**, 43(7), 2498-2504.
(84) Dodd, M. C.; Potential impacts of disinfection processes on elimination and deactivation of antibiotic resistance genes during water and wastewater treatment. *J. Environ. Monitor.* **2012**, 14(7), 1754-1771.
(85) Dodd, M. C.; Vu, N. D.; Ammann, A.; Le, V. C.; Kissner, R.; Pham, H. V.; Cao, T. H.; Berg, M.; Von Gunten, U.; Kinetics and mechanistic aspects of As(III) oxidation by aqueous chlorine, chloramines, and ozone: Relevance to drinking water treatment. *Environ. Sci. Technol.* **2006**, 40(10), 3285-3292.
(86) Dodd, M. C.; Buffle, M.-O.; Von Gunten, U.; Oxidation of antibacterial molecules by aqueous ozone: moiety-specific reaction kinetics and application to ozone-based wastewater treatment. *Environ. Sci. Technol.* **2006**, 40(6), 1969-1977.
(87) Dai, N.; Mitch, W. A.; Controlling nitrosamines, nitramines, and amines in amine-based co_2 capture systems with continuous ultraviolet and ozone treatment of washwater. *Environ. Sci. Technol.* **2015**, 49(14), 8878-8886.
(88) von Gunten, U.; Ozonation of drinking water: Part II. Disinfection and by-product formation in presence of bromide, iodide, or chlorine. *Water Res.* **2003**, 37, 1469-1487.
(89) Ed. *Chemistry of aqueous ozone and transformation of pollutants by ozonation and advanced oxidation processes*, ed.; Springer-Verlag, Berlin Heidelberg, 1998.
(90) Liu, C.; Croué, J. P.; Formation of bromate and halogenated disinfection byproducts during chlorination of bromide-containing waters in the presence of dissolved organic matter and CuO. *Environ. Sci. Technol.* **2016**, 50(1), 135-144.

Chapter 4

The role of reactive halogen species in disinfection by-product formation during chlorine photolysis[3]

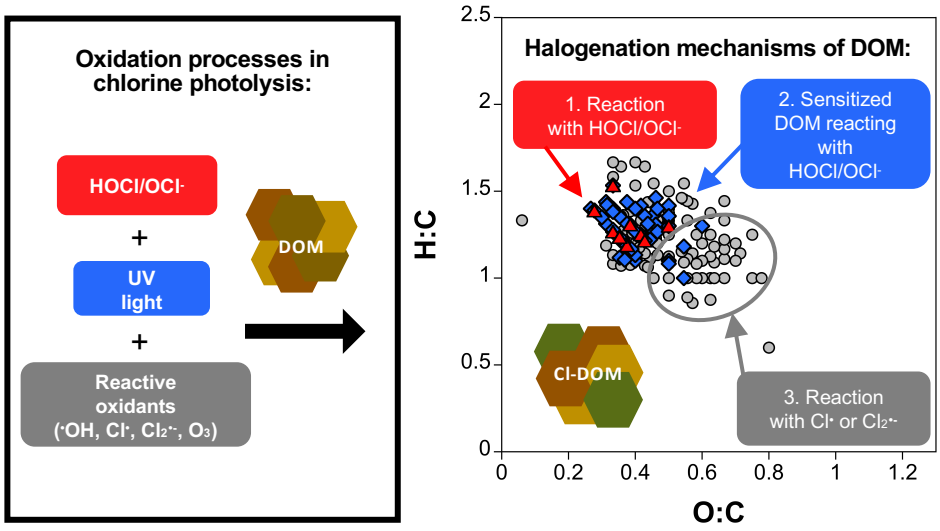

4.1 Abstract

The multiple reactive oxidants produced during chlorine photolysis effectively degrade organic contaminants during water treatment, but their role in disinfection by-product (DBP) formation is unclear. The impact of chlorine photolysis on dissolved organic matter (DOM) composition and DBP formation is investigated using lake water collected after coagulation, flocculation, and filtration at pH 6.5 and pH 8.5 with irradiation at three wavelengths (254, 311, and 365 nm). The steady-state concentrations of hydroxyl radical and chlorine radical decrease by 38 - 100% in drinking water compared to ultrapure water, which is primarily attributed to radical scavenging by natural water constituents. Chlorine photolysis transforms DOM through multiple mechanisms to produce DOM that is more aliphatic in nature and contains novel high molecular

[3] Reproduced with permission from *Environmental Science and Technology.* Bulman, D. M.; Remucal, C. K. 2020, https://doi.org/10.1021/acs.est.0c02039. Copyright 2020, American Chemical Society.

weight chlorinated DBPs that are detected via high-resolution mass spectrometry. Quenching experiments demonstrate that reactive chlorine species are partially responsible for the formation of halogenated DOM, haloacetic acids, and haloacetonitriles, whereas trihalomethane formation decreases during chlorine photolysis. Furthermore, DOM transformation primarily due to direct photolysis alters DOM such that it is more reactive with chlorine, which also contributes to enhanced formation of novel DBPs during chlorine photolysis.

4.2 Introductions

Organic contaminants including pharmaceuticals and pesticides are found in drinking water sources[1–5] and present an unknown risk to human health.[4–6] Many of these compounds are not removed by traditional drinking water[7] or wastewater[8–10] treatment processes. As the impact of climate change becomes more profound, water scarcity will continue to increase, resulting in greater reliance on alternative water sources such as potable reuse options.[11]

Advanced oxidation processes (AOPs) such as chlorine[12–15] or hydrogen peroxide[14,16,17] photolysis are effective for oxidizing organic contaminants. These AOPs generate hydroxyl radical ($^{\bullet}OH$), a highly reactive and nonselective oxidant that reacts with most organic compounds.[12-15,18,19] Additionally, chlorine photolysis generates other reactive oxidants, including chlorine radical ($Cl^{\bullet}$), dichloride radical anion ($Cl_2^{\bullet-}$), and ozone (O_3), via homolytic cleavage of free available chlorine (i.e., the mixture of hypochlorous acid and hypochlorite, referred to here as chlorine; Schematic C1 in Appendix C).[20–24] These reactive oxidants are scavenged by naturally occurring constituents in water such as organic and inorganic carbon,[14,21,25–27] resulting in lower oxidant steady-state concentrations. The effect of scavenging is thought to be greater for $^{\bullet}OH$ than for other oxidants[25,28,29] due to the greater reactivity of $^{\bullet}OH$ with organic and inorganic carbon.[27,30]

Decreasing the reactive oxidant concentration will limit the efficacy of contaminant removal during chlorine photolysis, highlighting the need for insight into radical scavenging during chlorine photolysis.

Halogenated disinfection by-products (DBPs) form during the reaction of dissolved organic matter (DOM) with chlorine-based disinfectants[31–35] and are of concern due to potential carcinogenicity and other human health risks.[36–40] However, only nine organic DBPs are regulated in drinking water in the United States despite the identification of over 600 different halogenated organic compounds in drinking water treated with chlorine.[35–38,40–42] During DBP formation, chlorine, a strong electrophile,[43] preferentially reacts with electron-rich moieties within DOM.[34,44] These same electron-rich moieties may also be highly susceptible to reaction with reactive chlorine species, including $Cl^{\bullet}$ and $Cl_2^{\bullet-}$. Because $Cl^{\bullet}$ and $Cl_2^{\bullet-}$ can react by either electron transfer or chlorine addition,[45] it is possible that halogen radical reactions could lead to elevated DBP production during chlorine photolysis.

Targeted DBP formation during chlorine photolysis compared to chlorine alone ranges widely in past studies.[46] Generally, trihalomethanes (THMs) do not change or increase slightly during chlorine photolysis with low pressure UV light (LP UV; single-wavelength 254 nm light) compared to dark chlorination,[47–50] but increase with medium pressure UV light (MP UV; broad spectrum light ranging 200-400 nm)[47,51] and UV-A light.[48] Haloacetic acids (HAAs) decrease during chlorine photolysis with LP UV light,[47–49] but increase with MP UV and UV-A light.[47,48,51] Haloacetonitriles (HANs) increase during chlorine photolysis with both MP and LP UV light.[49,51,52] Despite these common trends, past studies do not yield a conclusive understanding of how the unique combination of chlorine, UV light, and reactive oxidants present in chlorine photolysis affect DBP formation.

High-resolution mass spectrometry methods such as Fourier transform-ion cyclotron resonance mass spectrometry (FT-ICR MS) can be used to investigate molecular-level changes in DOM and to identify high molecular weight halogenated organic compounds. Changes in DOM composition provide insight into how DOM may react in subsequent treatments (e.g., with residual disinfectant in the distribution system).[34,53] For example, previous investigation into DOM composition during conventional water treatment with FT-ICR MS found ~800 halogenated formulas post-chlorination.[42] The formation of novel high molecular weight chlorinated formulas during chlorine photolysis has not yet been investigated.

All waters that might be treated by chlorine photolysis contain DOM, which may scavenge reactive oxidants and form DBPs. Therefore, understanding the impact of natural water constituents on oxidant production during chlorine photolysis, as well as the formation of both novel and known DBPs, is critical to applying the AOP in water treatment. Furthermore, the ability of reactive halogen species to form DBPs through halogen addition is a concern for chlorine photolysis, but this mechanism has not yet been shown experimentally in DOM. We combine bulk and molecular-level techniques to quantify oxidant scavenging and to investigate the transformation of dissolved organic matter during chlorine photolysis with UV-C light used in engineered applications and UV-B and UV-A light that is found in the solar spectrum. Additionally, we evaluate the role of multiple oxidative processes to provide mechanistic insight into halogenated disinfection by-product formation during chlorine photolysis.

4.3 Materials and Methods

4.3.1 Materials

Sodium hypochlorite was standardized using a Shimadzu UV-visible spectrometer (ε_{292} = 365 M^{-1} cm^{-1}).[22] All other compounds were used as received (Section C1). Water samples (treated Mendota water, TMW) were collected from a pilot-scale drinking water treatment plant in the Water Science and Engineering Laboratory (University of Wisconsin-Madison) in which water from eutrophic Lake Mendota undergoes alum coagulation/flocculation, sedimentation, and dual-media filtration.[54] Samples were further filtered through a 0.2 μm filter before storing at 4°C. This sample was selected because it is representative of a treated surface water (Table C1). The first TMW sample (March 8, 2019) was used for all experiments except the sequential treatment experiments, in which a second TMW sample (TMW2, October 31, 2019) was used due to sample volume limitations.

4.3.2 Sample Treatments

All experiments were conducted with 10 mM phosphate (pH 6.5) or borate (pH 8.5) buffer. The pH values were selected to fall above and below the acid dissociation constant of chlorine (pK_a = 7.5).[22] All solutions were brought to room temperature and were in equilibrium with the atmosphere. The initial chlorine concentration in chlorinated samples was 4 mg-Cl_2/L. The chlorine demand of TMW was < 0.5 mg-Cl_2/L over the experimental duration (Figure C2). Photolysis experiments were conducted in a Rayonet merry-go-round photoreactor with either four 254 ± 1 nm bulbs, sixteen 311 ± 22 nm bulbs, or sixteen 365 ± 10 nm bulbs (Section C2).[20] 254 nm is representative of LP UV irradiation used during water treatment. The longer wavelengths are emitted by medium pressure UV lamps (200 - 400 nm)[20] and are found in the solar spectrum,

making them relevant for solar applications.[20,21,55] Sample treatment times of six (254 nm), five (311 nm), and thirty minutes (365 nm) were selected to normalize total chlorine loss.

TMW samples were treated with dark chlorination, direct photolysis, chlorine photolysis, or quenched chlorine photolysis. Quenched chlorine photolysis samples contained 6 mM *tert*-butanol (*t*-BuOH), which scavenges > 98% $^{\bullet}OH$ and $Cl^{\bullet}$ and decreases [O_3] by 20 - 30% by scavenging $O(^3P)$.[21] Residual chlorine was quenched with sodium thiosulfate.[20,56]

4.3.3 Analytical Methods

Dissolved organic carbon concentrations ([DOC]) were measured using a total organic carbon analyzer (Section C4). Anions were quantified using ion chromatography. Specific UV absorbance at 254 nm ($SUVA_{254}$) was calculated as the ratio of the absorbance at 254 nm to [DOC].[57]

Reactive oxidants were quantified using nitrobenzene ($^{\bullet}OH$), benzoate ($^{\bullet}OH$, $Cl^{\bullet}$, and $Cl_2^{\bullet-}$), and cinnamic acid (O_3) as probe compounds as described previously.[20] Free available chlorine was quantified using 1,3,5-trimethoxybenzene.[58] All probe compounds were quantified using high-performance liquid chromatography (Section C4).

Targeted DBPs including THMs (chloroform, bromoform, bromodichloromethane, and dibromochloromethane), HAAs (bromochloroacetic acid, bromodichloroacetic acid, chlorodibromoacetic acid, dibromoacetic acid, dichloroacetic acid, monobromoacetic acid, monochloroacetic acid, tribromoacetic acid, and trichloroacetic acid), and HANs (bromochloroacetonitrile, dibromoacetonitrile, dichloroacetonitrile, and trichloroacetonitrile) were quantified using EPA methods 551.1 (THMs and HANs)[59] and 552.2 (HAAs; Section C6).[60]

4.3.4 High-Resolution Mass Spectrometry

Samples were prepared using solid-phase extraction after adjusting to pH < 2.5 with formic acid[61–63] and analyzed by FT-ICR MS (SolariX XR 12T) using negative mode electrospray ionization. Molecular formulas with $C_{0\text{-}80}H_{0\text{-}140}O_{0\text{-}80}N_{0\text{-}1}S_{0\text{-}1}P_{0\text{-}1}Cl_{0\text{-}3}{}^{13}C_{0\text{-}1}$ and a mass error < 0.5 ppm were allowed after internal calibration.[64–66] All masses matched to chlorine-containing formulas were required to have a ^{37}Cl isotopologue. Bulk DOM properties including $H{:}C_w$, $O{:}C_w$, and carbon-normalized double bond equivalents (DBE/C_w) were calculated as relative intensity-weighted averages from the assigned molecular formulas in each sample. Details on instrumental settings and data processing are provided in Sections C7 and C8.

4.3.5 Sequential Treatment

Sequential treatment experiments to investigate the impact of direct photolysis and reaction with $^{\bullet}OH$ on DOM reactivity were conducted with the TMW2 sample (Section C9). Hydroxyl radical control samples were generated using UV/H_2O_2 at 254 nm.[14] $[H_2O_2]_{initial}$ was 40 μM in order to achieve the same hydroxyl radical steady-state concentration as the chlorine photolysis treatment (Figure C15) and excess H_2O_2 was quenched with sodium thiosulfate.[67] Sequential treatment samples at pH 6.5 were treated with irradiation or UV/H_2O_2 for 6 minutes followed by 6 minutes of dark chlorination (4 mg-Cl_2/L), which was analogous to the chlorine photolysis treatment time. Samples were extracted and analyzed by FT-ICR MS.

4.4 Results and Discussion

4.4.1 Effect of Natural Water Constituents on Reactive Oxidants

DOM and inorganic constituents can decrease contaminant removal during chlorine photolysis by consuming chlorine, scavenging reactive oxidants, or limiting oxidant production through light screening. The importance of these processes is investigated by quantifying the observed chlorine loss rate constant ($k_{obs,chlorine}$) and oxidant concentrations at pH 6.5 and 8.5 with 254, 311, and 365 nm irradiation in buffered Milli-Q water and in treated Lake Mendota water (Table C1). The chlorine loss rate constant is higher in TMW than in Milli-Q water under nearly all conditions (Figures 4.1a and C1a), with the exception of one sample due to the high molar absorptivity of OCl^- at pH 8.5 and 311 nm.[20] The increase in $k_{obs,chlorine}$ is not attributable to chlorine demand during the short experimental timescales (Figure C2a). Additionally, light screening is minimal as the same trends are observed when the data is corrected for light screening (Figure C1f; Table C2). Therefore, the increase in $k_{obs,chlorine}$ in natural water is attributed to radical chain reactions involving carbon-centered radicals, which is similarly responsible for increases in $k_{obs,chlorine}$ in the presence of model compounds (e.g., methanol).[68] This conclusion is supported by the greater relative increase in $k_{obs,chlorine}$ at shorter wavelengths where radical steady-state concentrations are higher (Figures 4.1 and C1), allowing for more radical-induced chlorine loss.

$^{\bullet}OH$ is a desirable oxidant in AOPs because it reacts with most organic contaminants of interest.[29,69,70] However, the non-selectivity of $^{\bullet}OH$ means that it is scavenged by natural water constituents. $^{\bullet}OH$ steady-state concentrations ($[^{\bullet}OH]_{ss}$) are 38.4 to 80.3% lower in TMW compared to Milli-Q water under all conditions tested (Figures 4.1b and C1b; Table C4). Higher $[^{\bullet}OH]_{ss}$ is observed at low pH and shorter wavelengths in agreement with past work in the absence of DOM.[13,14,20,22,71] $^{\bullet}OH$ scavenging in natural waters is primarily due to organic and inorganic

carbon,[13,27,72] and branching ratio calculations demonstrate that > 93% of carbon-scavenged $^{\bullet}OH$ reacts with DOM (Table C5). Chloride reacts rapidly with $^{\bullet}OH$ (~10^9 M^{-1} s^{-1}) to form $HOCl^{\bullet-}$,[73-77] but the rapid reverse reaction ensures that there is no net scavenging by Cl^-.[78-80] Note that $[^{\bullet}OH]_{ss}$ during photolysis of natural water constituents (e.g., DOM, NO_2^-) is an order of magnitude lower than $[^{\bullet}OH]_{ss}$ during chlorine photolysis (Figure C2d).

Reactive chlorine species (RCS) can degrade organic contaminants during chlorine photolysis (Schematic C1) and are scavenged by natural water constituents.[13,45] $[Cl^{\bullet}]_{ss}$ decreases 48 to 100% in TMW compared to Milli-Q water (Figures 4.1c and C1c; Table C4), with 72 - 77% of the carbon-scavenged $Cl^{\bullet}$ attributable to HCO_3^-. Furthermore, the forward rate constant for the reaction of $Cl^{\bullet}$ with Cl^- is faster than the reverse reaction, suggesting that additional scavenging by Cl^- is possible.[27,30,73-77,81]

The reaction of $Cl^{\bullet}$ with Cl^- produces $Cl_2^{\bullet-}$ (Schematic C1). $[Cl_2^{\bullet-}]_{ss}$ is three orders of magnitude higher than $[Cl^{\bullet}]_{ss}$ at low pH for all wavelengths in TMW but is below the detection limit in Milli-Q water (Figure C1e). $Cl_2^{\bullet-}$ is a selective oxidant and typically reacts with organic contaminants at a lower rate constant than $Cl^{\bullet}$.[13,27,45] Conversion of $Cl^{\bullet}$ to $Cl_2^{\bullet-}$ is proportional to $[Cl^-]$; therefore, contaminant removal during chlorine photolysis will be more efficient at lower $[Cl^-]$ for compounds that do not react with $Cl_2^{\bullet-}$.[20,45,76,77,82]

Ozone is produced during chlorine photolysis under the three irradiation conditions considered here,[20,55] but the impact of natural water constituents on its production has not been considered. The cumulative concentration of ozone is greater in Milli-Q water (i.e., (8.9 – 21.7) x 10^{-7} M vs. (4.0 – 14.2) x 10^{-7} M in TMW; Figures 4.1d and C1d). $[O_3]$ decreases with wavelength at low pH, while the opposite is true at high pH due to the higher molar absorptivity of OCl^- than HOCl at high wavelengths and the more efficient formation of $O(^3P)$, the O_3 precursor, from

OCl^-.[20,21] Literature measurements similarly range from 4.0 x 10^{-7} M to 2.2 x 10^{-6} M in Milli-Q water,[20,21] with higher O_3 concentrations observed at high pH (Schematic C1).[20,23] The cumulative O_3 concentration decreases by 20.6 to 54.7% in TMW compared to Milli-Q water (Figures 4.1d and C1d; Table C4). Reported rate constants for O_3 and DOM are ~10^3 L mg-C^{-1} s^{-1},[83,84] while reaction rate constants between O_3 and inorganic water constituents are low (Table C8).[83–86] Therefore, we attribute the decrease in cumulative [O_3] to scavenging by DOM (Table C7), which likely occurs through highly reactive phenolic moieties.[83,84,87]

4.4.2 Transformation of Dissolved Organic Matter

Understanding DOM transformation during chlorine photolysis provides insight into mechanisms of reaction during water treatment.[28,88] For example, the composition of DOM determines its DBP formation potential.[34,89–91] Therefore, changes in DOM composition during chlorine photolysis through a combination of direct photolysis, dark chlorination, or reaction with reactive oxidants might alter its reactivity with chlorine in distribution systems.[88,91,92] DOM composition following dark chlorination, direct photolysis, chlorine photolysis, and chlorine photolysis with a radical scavenger is investigated using UV-visible spectroscopy and high-resolution mass spectrometry to identify how chlorine, light, and reactive oxidants contribute to DOM alteration.

The dissolved organic carbon concentration reflects the total amount of carbon, whereas optical properties provide insight into DOM composition. For example, $SUVA_{254}$ is proportional to aromaticity.[57] The initial TMW sample has a low [DOC] (i.e., 1.71 mg-C/L) as a result of the treatment plant processing. There is no evidence of mineralization during chlorine photolysis (Table C14), consistent with previous observations at pH 6.2 and 254 nm.[28] The initial TMW

sample has a $SUVA_{254}$ value of 2.01 L mg-C^{-1} m^{-1}, indicating that the DOM is relatively aliphatic, as expected due to high microbial productivity in eutrophic lakes (Figure 4.2a).[65,66]

Dark chlorination and chlorine photolysis result in consistent decreases in $SUVA_{254}$ under all tested conditions, while direct photolysis results in a small increase or no change in $SUVA_{254}$ (Figure 4.2a; Table C14). A decrease in $SUVA_{254}$ during dark chlorination is expected because chlorine reacts preferentially with electron-rich compounds (e.g., aromatic moieties).[43] The largest decreases in $SUVA_{254}$ (i.e., 11.4 - 28.4%) are observed during chlorine photolysis which may be attributable to reaction of $^{\bullet}OH$ and RCS with aromatic DOM moieties.[45,46] The addition of *t*-BuOH during chlorine photolysis limits the effect on $SUVA_{254}$, with values decreasing 16.4% on average during quenched chlorine photolysis compared to 22.0% during chlorine photolysis. These observations suggest that reactive oxidants and direct reaction with $HOCl/OCl^-$ contribute to the degradation of aromatic DOM, with minimal changes due to direct photolysis.

FT-ICR MS analysis is used to investigate molecular changes in DOM. An average of 2,722 formulas are assigned to the initial and treated TMW samples (Table C13). Bray-Curtis dissimilarity and principal component analysis (PCA) compare similarity of DOM composition in all samples. Bray-Curtis dissimilarity analysis shows that treated samples group together (Figure C7). Similarly, PCA shows all treated samples clustering separately from initial samples. Additionally, PCA reveals that chlorine photolysis-treated samples group separately from the other treatments at 254 and 311 nm, while quenched chlorine photolysis samples fall in between chlorine photolysis and dark chlorination samples (Figure 4.2f). It is noteworthy that quenching radical species results in DOM transformation that is different than either dark chlorination or direct photolysis alone.

As with $SUVA_{254}$, FT-ICR MS results demonstrate the loss of aromaticity with all treatments. Carbon-normalized double bond equivalents increase proportionally to aromaticity, while $H:C_w$ increases as the DOM becomes more aliphatic. DBE/C_w decreases and $H:C_w$ increases in all treated conditions relative to the initial sample (Figures 4.2b and C5a). Decreases in aromaticity are expected for all treatments because electron-rich aromatic systems are more reactive with chlorine and with radical species, resulting in possible ring cleavage products, and light is more readily absorbed by aromatic pi systems.[28,93–95] Interestingly, the decrease in aromaticity does not vary with treatment type at the molecular level, but does vary with pH. For all treatments and wavelengths, DBE/C_w decreases more at pH 6.5 compared to pH 8.5. For dark chlorination, this change is attributable to the higher reactivity of HOCl than OCl^- and is most pronounced with longer reaction times (365 nm; Figure 4.2b).[43] During chlorine photolysis, the change in DBE/C_w is attributable to the higher production of radicals at low pH (Figure 4.1), along with the combined effects of direct photolysis and reaction with HOCl.

The decrease in aromaticity during chlorine photolysis is further demonstrated by evaluating the change in intensity of molecular formulas found in both the initial and treated samples. Formulas that decrease in intensity during chlorine photolysis are aromatic (low H:C) and reduced (low O:C) and are tightly clustered in the lignin- and tannin-like regions of the van Krevelen diagram (Figure 4.2c).[96–98] These reactive formulas are similar across all considered treatments (Figure C9), highlighting the selective nature of light, chlorine, and reactive oxidants for aromatic, electron-rich compounds. In contrast, formulas that increase in intensity and are possible reaction products are widely distributed across the van Krevelen diagram with clear differences between treatments (Figure C10). In particular, formulas in the high O:C region only increase in relative intensity during chlorine photolysis (Figure 4.2d), which may be attributable

to oxygen addition due to radical reactions with phenolic moietes.[13,27,30,45,68] Quenching the radical species during chlorine photolysis prevents the increase in intensity in this region (Figure C10d).

$O:C_w$ is a proxy for DOM oxidation state and is expected to increase with treatment because dark chlorination, direct photolysis, and chlorine photolysis are all oxidative processes. However, $O:C_w$ only increases during chlorine photolysis at low pH and wavelength when enough radical species are generated to sufficiently oxidize DOM (Figure C5b). Under all other conditions, $O:C_w$ decreases with treatment. Reaction with light, chlorine, and reactive oxidant species occurs in lower H:C (i.e., aromatic) formulas with a wide range of O:C values (Figure C9), producing formulas that are generally more aliphatic in nature (Figure C10). With the exception of chlorine photolysis (i.e., when high O:C formulas could be produced by O-addition due to $^{\bullet}OH$ reactions;[88,99] Figure 4.2d), the product formulas are generally lower in O:C and may be attributable to double-bond attack/ring cleavage reactions characteristic of reaction with $^{\bullet}OH$ and RCS (Figure C10).[45,46,100,101]

Oxidation is further investigated at the molecular level by considering the addition of 1 or 2 oxygen atoms to molecular formulas found in the initial sample. This analysis requires that oxygen addition products are only found after treatment and it is possible that a single product may be attributable to a +1O or +2O reaction (Section C8). Chlorine photolysis results in the formation of >210 oxygen addition products localized in the high O:C region of the van Krevelen diagram (Figures 4.2e and C14; Table C16). Fewer oxygen-addition products are formed in quenched samples (130 on average), suggesting that reactive oxidants such as $^{\bullet}OH$ and O_3 contribute to oxygen-addition as expected based on their known reactivity with model compounds.[29,86] Therefore, there is evidence of oxidation at the molecular level during chlorine photolysis despite the decrease in $O:C_w$ at high pH and wavelengths (Figure C5b).

4.4.3 Formation of Halogenated Dissolved Organic Matter

FT-ICR MS enables the identification of chlorinated formulas, which can be considered as novel, high molecular weight disinfection by-products.[42,44,102] CHOCl formulas are absent in initial samples and in samples exposed only to light but are found in all samples treated with chlorine (Figure C11; Table C13). Dark chlorination results in up to 9 CHOCl formulas, with more CHOCl formulas formed at low pH because HOCl is a stronger electrophile than OCl^-.[43] Fewer CHOCl formulas are identified than in previous dark chlorination studies that had a longer disinfectant contact time, higher [DOC], acidification with hydrochloric acid rather than formic acid, and a less conservative approach to matching CHOCl formulas.[42,102] CHOCl formulas formed during dark chlorination are primarily in the lignin- and tannin-like regions of the van Krevelen diagram (Figures 4.3a and C11), which is consistent with previous observations of preferential chlorine reactivity with low H:C formulas in the same regions.[44,98] These CHOCl formulas are formed in the same region as formulas shown to be reactive during chlorination (Figure C9).

More CHOCl formulas are formed during chlorine photolysis than dark chlorination, with an average of 84 CHOCl formulas across the six chlorine photolysis treatment conditions (Table C13). The addition of *t*-BuOH as a quencher decreases the average number of CHOCl formulas under most chlorine photolysis conditions (i.e., low pH and wavelength; Figures C11a-C11c) to an average of 57, which is higher than the number observed during dark chlorination. However, quenching does not affect the formation of CHOCl formulas at pH 8.5 and 311 or 365 nm irradiation where radical concentrations are lower (Figures C11d and C11f; Table C13). The CHOCl formulas that are prevented by quenching are attributable to reaction of reactive chlorine species (i.e., $Cl^{\bullet}$ and/or $Cl_2^{\bullet-}$) with DOM directly via chlorine addition,[45] demonstrating that RCS partially contribute to the formation of chlorinated DOM. The chlorinated formulas attributed to

RCS halogenation are in the high O:C, low H:C region of the van Krevelen diagram (Figure C11a) where aromatic rings with hydroxy and methoxy substitution, along with other electron rich moieties, fall. These types of compounds are known to have high reactivity with $Cl^{\bullet}$ and $Cl_2^{\bullet-}$.[13,45] However, the inability of *t*-BuOH to prevent enhanced halogenation of DOM indicates that other processes, such as DOM transformation and subsequent changes in reactivity, may also impact elevated DOM chlorination during chlorine photolysis.

It is noteworthy that some of the novel DBPs contain nitrogen due to the increased toxicity of nitrogen-containing DBPs.[103,104] Fifteen distinct CHON formulas are formed during chlorine photolysis or quenched chlorine photolysis that contain either 1 or 2 chlorine atoms (Table C15), but are absent in control samples as well as samples treated by dark chlorination or UV irradiation. These formulas are found primarily at low pH and in greater abundance during chlorine photolysis in the absence of *t*-BuOH, suggesting that reactive chlorine species contribute to the formation of high molecular weight N-DBPs.

4.4.4 Impact of DOM Transformation on Organohalogenation

Chlorine photolysis involves a combination of light, chlorine, and multiple reactive oxidants that alter DOM composition. While the quenching experiments demonstrate that RCS contribute to direct halogenation of DOM, we hypothesized that alteration of DOM (e.g., via direct photolysis or reaction with non-halogenating oxidants) could make DOM more susceptible to dark chlorination. For example, phenolic products produced by $^{\bullet}OH$ attack could make DOM more reactive; this mechanism has been proposed for model compounds (e.g., nitrobenzene and benzoate), but has not been considered in DOM.[22,68,105] Thus, we conducted a series of sequential experiments that exposed treated Mendota water to oxidation via UV/H_2O_2 (i.e., a source of $^{\bullet}OH$)

or direct photolysis followed by dark chlorination (Section C9). $[^{\bullet}OH]_{ss}$ in the UV/H_2O_2 experiment was equivalent to the value measured during chlorine photolysis (Figure C15). These experiments used a second Mendota water sample (TMW2) so small differences are observed in the initial water chemistry (Table C1). These experiments were conducted at pH 6.5 with 254 nm irradiation because these conditions generate the highest $[^{\bullet}OH]_{ss}$ and $[Cl^{\bullet}]_{ss}$ (Figure 4.1).

DOM transformation from direct photolysis and reaction with $^{\bullet}OH$ causes DOM to be more reactive towards chlorine, resulting in increased formation of CHOCl formulas (Figure 4.3a). A similar number of CHOCl formulas are found in both sequential samples (i.e., 32 CHOCl formulas in the direct photolysis-transformed sample and 27 in the UV/H_2O_2-transformed sample; Table C17), suggesting that UV photolysis is a major factor. The decrease in DBE/C_w indicates that direct photolysis produces DOM that is, on average, more aliphatic. However, DOM photolysis also produces reactive intermediates that oxidize DOM moieties, as evidenced by the large number of oxygen addition formulas, making them more reactive with chlorine (Tables C16 and C17).[66,106,107] DOM sensitization by direct photolysis is further supported by the higher O:C ratio of CHOCl formulas compared to all matched formulas (Figure 4.6), which indicates preferential reactivity of chlorine with oxidized DOM. In contrast, only 4 CHOCl formulas are formed during dark chlorination for the same amount of time with no prior oxidation. As observed in the experiments conducted with TMW at two different pH values and three different wavelengths (Table C13), the most extensive halogenation (i.e., 124 formulas) is observed during chlorine photolysis. The increase in CHOCl formation in sequential treatment demonstrates that DOM is transformed via UV-mediated sensitization, making it more susceptible to direct reaction with chlorine. This mechanism accounts for CHOCl formulas formed during chlorine photolysis when RCS are quenched with *t*-BuOH. These results demonstrate that the combination of processes

present during chlorine photolysis collectively contribute to enhanced halogenation, rather than simply direct reaction of RCS or chlorine.

4.4.5 Formation of Targeted Disinfection By-Products

Halogenated DBPs present a known risk to human health and a subset of aliphatic DBPs (i.e., THMs and HAAs) are regulated in drinking water in the U.S.[36,37,41,42] Additionally, unregulated DBPs, such as halogenated aromatics, can have greater toxicity than regulated compounds.[35,38,40,108] This study focuses on the formation of THMs, HAAS, and HANs during chlorine photolysis to enable comparison with the conflicting literature on these DBPs. Previous investigations into the formation of these DBPs during chlorine photolysis are inconsistent, with some studies observing increased DBP formation compared to dark chlorination and other studies observing opposite trends.[47–52] These studies vary in water source, chlorine concentration, light source, and reaction time, making it challenging to draw clear conclusions.[46] We quantified the formation of four THMs, nine HAAs, and four HANs at two pH values and three wavelengths to investigate how pH and wavelength alter DBP formation in the same water sample with the same initial chlorine concentration.

The TMW sample did not contain any DBPs prior to treatment and DBPs are formed in all treatment conditions except direct photolysis (Tables C10-C12). Total THMs and HAAs (average of 12.5 μg/L and 12.6 μg/L, respectively) are formed during dark chlorination, whereas HANs are generally below the detection limit (Figures 4.3b and C4). There is no effect of sample pH on DBP formation despite the greater reactivity of HOCl.[44] Treatment time is important, with more formation of all DBP classes at 30 min (i.e., used for comparison with 365 nm irradiation) than 5

min (i.e., used for comparison with 254 and 311 nm). This result is expected because DBP concentrations generally increase with contact time.[109]

THM formation decreases during chlorine photolysis compared to dark chlorination under most conditions. This trend is seen at both low and high pH, although the relative decrease in total THM concentration ([TTHM]) compared to dark chlorination is greater at high pH (Figures 4.3b and C4; Table C10). The decrease in [TTHM] during chlorine photolysis shows that the reactive oxidants produced during chlorine photolysis are less efficient at forming THMs than chlorine alone. It is likely that decreased chlorine contact time from chlorine degradation via photolysis and radical chain reactions,[50,55] along with the removal of aromatic precursors,[31,110,111] limits THM formation. Quenching $^{\bullet}$OH and Cl$^{\bullet}$ with *t*-BuOH during chlorine photolysis has minimal effect on THM formation, further suggesting RCS are not involved in generating THMs (Table C10). These results are contrary to previous studies with higher initial chlorine concentrations and longer reaction times that showed an increase in THM formation during chlorine photolysis compared to dark chlorination.[47,51]

HAAs show the opposite trend as THMs and increase in concentration during chlorine photolysis relative to dark chlorination (Figures 4.3b and C4), which is consistent with previous studies at longer wavelengths.[47,48,51] Quenching radical species decreases HAA formation under most pH and wavelength combinations, though not down to the level of dark chlorination (Table C11). These data suggest that reactive chlorine species may contribute to the formation of HAAs. However, the increased formation of HAAs during chlorine photolysis may also be attributable to formation of HAA precursors from DOM transformation (i.e., as observed in the sequential experiments for novel DBP formation; Figure 4.3a) because quenching does not completely prevent the increased formation of HAAs.

HAN formation is greatest during chlorine photolysis compared to dark chlorination and quenched chlorine photolysis (Figure 4.3b and C4), in agreement with previous studies.[49,49,52] Only one sample for all pH and wavelength conditions had measurable HANs during radical quenching (i.e., 365 nm, pH 6.5; Table C12). The near complete inhibition of HAN formation during quenched chlorine photolysis indicates that HAN precursors are degraded during chlorine photolysis and suggests that enhanced formation of HANs is mediated by radical reactions, as observed for novel N-DBPs (Table C15).

4.5 Implications for Water Treatment

This study investigates the effect of natural water constituents on reactive oxidant concentrations and the effect of those oxidants on DOM transformation. The observed chlorine loss rate constant increases in the presence of DOM due to radical chain reactions (Figure 4.1a). Water with higher [DOC] will have enhanced $k_{obs,chlorine}$ in practical applications of chlorine photolysis. This effect is less pronounced at high pH and wavelength and is therefore less important in solar chlorine photolysis applications.

Natural water constituents are major radical scavengers and can decrease the efficacy of chlorine photolysis as an advanced oxidation process. Organic and inorganic carbon are the primary sinks for reactive oxidants such as $^{\bullet}OH$ and $Cl^{\bullet}$, respectively, under our experimental conditions[13,27,30,72] and will lead to lower steady-state concentrations in natural waters. O_3 is more selective and less impacted by natural water constituents, suggesting that contaminants that react with ozone will be removed even in natural waters.

The alteration of DOM during chlorine photolysis has implications for DBP formation. DOM transformation during chlorine photolysis results in DOM that is more aliphatic and reduced

as reactive, electron-rich DOM moieties are transformed, with the formation of oxygen addition products demonstrating oxidation at the molecular level (Figure 4.2). Importantly, the combination of oxidants (e.g., UV light and $^{\bullet}OH$) present during chlorine photolysis transforms DOM so that it is more reactive with chlorine, as shown using the sequential treatment experiments (Figure 4.3a). As a result, treatment systems that use chlorine photolysis may see increased formation of disinfection by-products in the distribution system due to reaction of transformed DOM with residual disinfectant.

Furthermore, the analysis of DOM transformation by FT-ICR MS demonstrates that reactive chlorine species such as $Cl^{\bullet}$ and $Cl_2^{\bullet-}$ react with DOM via chlorine addition to form novel DBPs. This mechanism is demonstrated by the enhanced formation of CHOCl formulas during 254 and 311 nm chlorine photolysis and the ability of *t*-BuOH to limit the formation of some, but not all, of these formulas (Figures C11a-C11d). This is the first study to demonstrate the role of reactive chlorine species in forming high molecular weight halogenated DBPs, which could have implications for human health. The combination of RCS and DOM transformation also impacts the formation of targeted DBPs. THMs decrease during chlorine photolysis compared to dark chlorination due to consumption of chlorine. However, HAAs and HANs increase in concentration due to the formation of precursors from DOM transformation and from radical reactions. This study demonstrates that an understanding of multiple reaction pathways is necessary to mitigate DBP formation in this complex AOP.

4.6 Acknowledgements

This work was supported by an NSF CAREER award (CBET-1451932). The authors would like to thank Professor Greg Harrington for his assistance in collecting the treated surface water samples. The authors acknowledge the UW-Madison Human Proteomics Program Mass Spectrometry Facility (initially funded by Wisconsin partnership funds) for support in obtaining mass spectrometry data and NIH S10OD018475 for the acquisition of an ultrahigh-resolution mass spectrometer.

4.7 Supporting Information

Additional details pertaining to materials, analytical methods, water chemistry data, reactive oxidant quantification, FT-ICR MS data analysis, targeted DBP measurements, and sequential experimental design can be found in Appendix C.

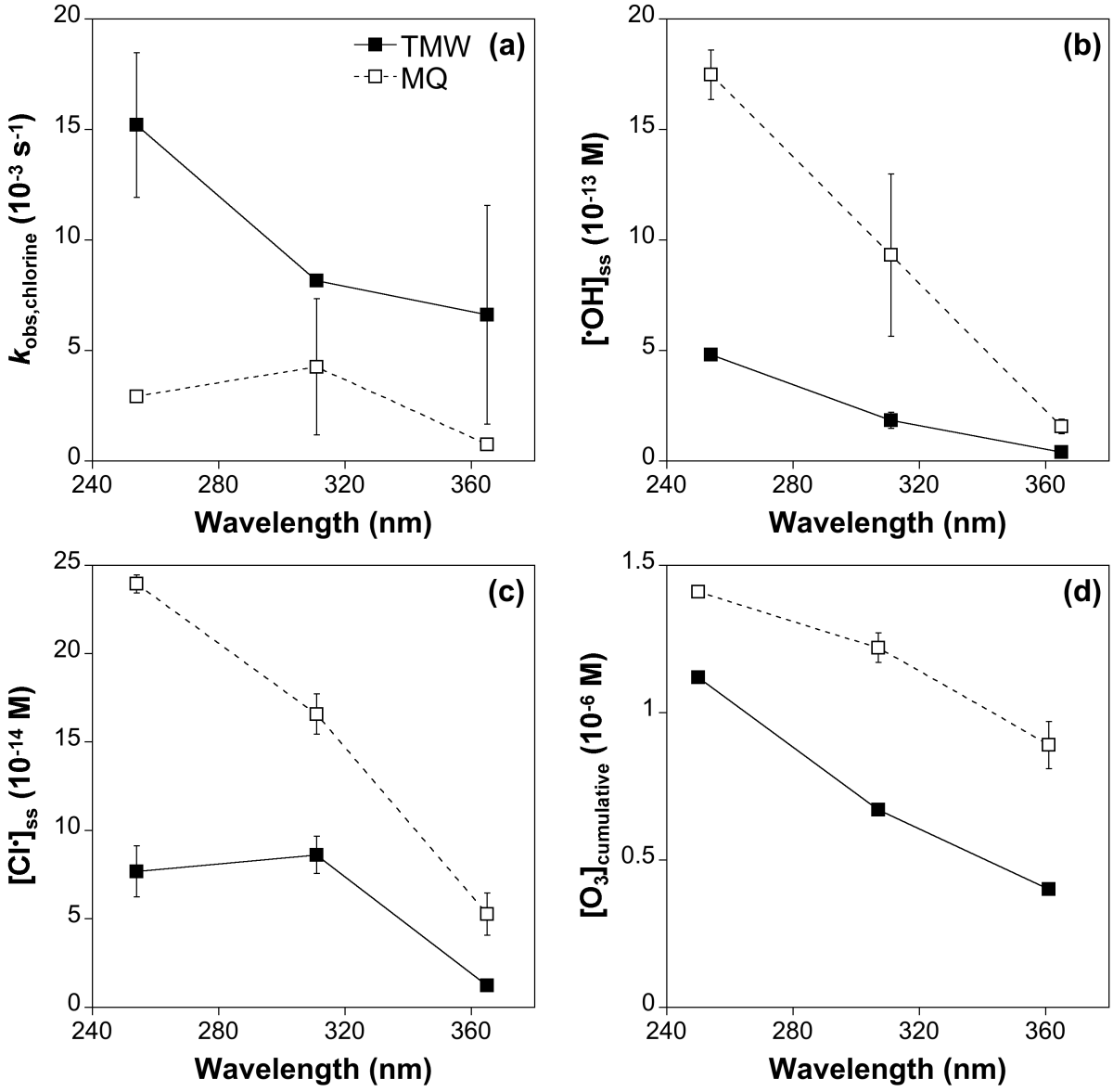

Figure 4.1. (a) Observed chlorine loss rate constant, (b) hydroxyl radical steady-state concentration, (c) chlorine radical steady-state concentration, and (d) cumulative ozone concentration as a function of wavelength at pH 6.5 in Milli-Q water (MQ) and treated Mendota water (TMW) during chlorine photolysis.

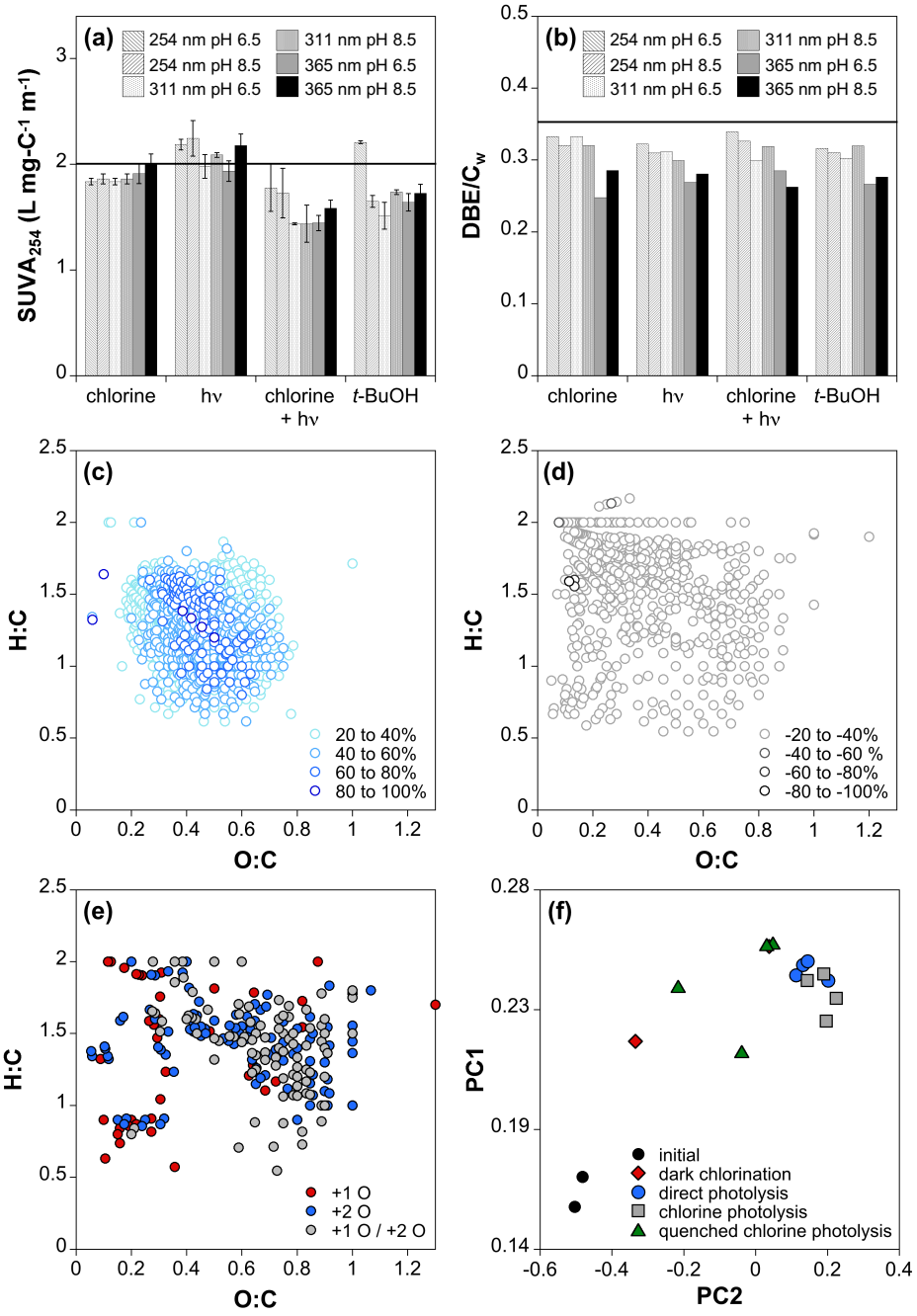

Figure 4.2. (a) $SUVA_{254}$ and (b) intensity weighted double bond equivalents per carbon (DBE/C_w) grouped by treatment at pH 6.5 and 8.5 and 254, 311, and 365 nm. Solid lines represent the initial values of $SUVA_{254}$ and DBE/C_w, respectively. van Krevelen diagrams of formulas common to the initial and all treated samples (pH 6.5 and 254, 311, and 365 nm) that (c) decrease or (d) increase in relative intensity during chlorine photolysis. Color corresponds to the percent change. Note that nearly all points in panel (d) fall within the -20 to -40% range. (e) van Krevelen diagram of oxygen addition formulas found after chlorine photolysis that are +1O (red), +2O (blue), or either +1O or +2O (grey) from a formula in the initial sample. (f) Principal component analysis of the initial and treated samples at 254 and 311 nm, pH 6.5 and 8.5.

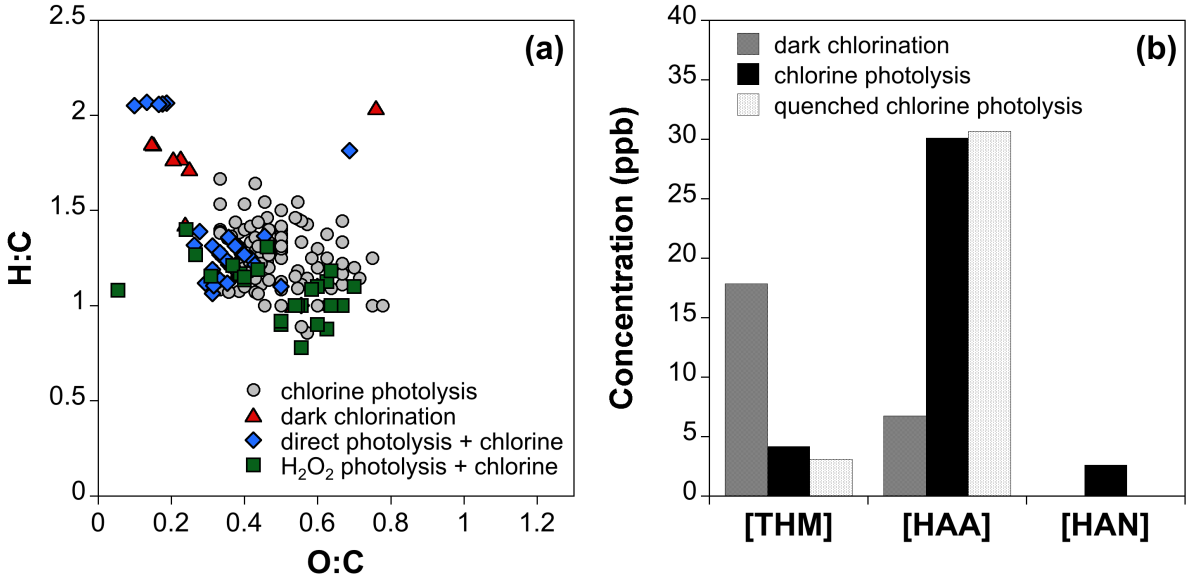

Figure 4.3. (a) CHOCl formulas formed during dark chlorination, chlorine photolysis, and sequential treatments in the second treated Mendota water sample (254 nm, pH 6.5). (b) Concentration of THMs, HAAs, and HANs during dark chlorination, chlorine photolysis, and quenched chlorine photolysis at 254 nm, pH 6.5.

4.8 References

(1) Kolpin, D. W.; Furlong, E. T.; Meyer, M. T.; Thurman, E. M.; Zaugg, S. D.; Barber, L. B.; Buxton, H. T.; Pharmaceuticals, hormones, and other organic wastewater contaminants in U.S. Streams, 1999−2000: A national reconnaissance. *Environ. Sci. Technol.* **2002**, 36(6), 1202-1211.

(2) Schwarzenbach, R. P.; Escher, B. I.; Fenner, K.; Hofstetter, T. B.; Johnson, C. A.; von Gunten, U.; Wehrli, B.; The challenge of micropollutants in aquatic systems. *Science* **2006**, 313(5790), 1072-1077.

(3) Mompelat, S.; Thomas, O.; Le Bot, B.; Contamination levels of human pharmaceutical compounds in french surface and drinking water. *J. Environ. Monit.* **2011**, 13(10), 2929-2939.

(4) Valcárcel, Y.; González Alonso, S.; Rodríguez-Gil, J. L.; Gil, A.; Catalá, M.; Detection of pharmaceutically active compounds in the rivers and tap water of the Madrid region (Spain) and potential ecotoxicological risk. *Chemosphere* **2011**, 84(10), 1336-1348.

(5) Kostich, M. S.; Batt, A. L.; Lazorchak, J. M.; Concentrations of prioritized pharmaceuticals in effluents from 50 large wastewater treatment plants in the U.S. and implications for risk estimation. *Environ. Pollut.* **2014**, 184, 354-359.

(6) Stalter, D.; O'Malley, E.; von Gunten, U.; Escher, B. I.; Fingerprinting the reactive toxicity pathways of 50 drinking water disinfection by-products. *Water Res.* **2016**, 91, 19-30.

(7) Westerhoff, P.; Yoon, Y.; Snyder, S.; Wert, E.; Fate of endocrine-disruptor, pharmaceutical, and personal care product chemicals during simulated drinking water treatment processes. *Environ. Sci. Technol.* **2005**, 39(17), 6649-6663.

(8) Fairbairn, D. J.; Arnold, W. A.; Barber, B. L.; Kaufenberg, E. F.; Koskinen, W. C.; Novak, P. J.; Rice, P. J.; Swackhamer, D. L.; Contaminants of emerging concern: Mass balance and comparison of wastewater effluent and upstream sources in a mixed-use watershed. *Environ. Sci. Technol.* **2016**, 50(1), 36-45.

(9) Li, Z.; Sobek, A.; Radke, M.; Fate of pharmaceuticals and their transformation products in four small European rivers receiving treated wastewater. *Environ. Sci. Technol.* **2016**, 50(11), 5614-5621.

(10) Stackelberg, P. E.; Furlong, E. T.; Meyer, M. T.; Zaugg, S. D.; Henderson, A. K.; Reissman, D. B.; Persistence of pharmaceutical compounds and other organic wastewater contaminants in a conventional drinking-water-treatment plant. *Sci. Total. Environ.* **2004**, 329(1-3), 99-113.

(11) Dong, S.; Page, M. A.; Massalha, N.; Hur, A.; Hur, K.; Bokenkamp, K.; Wagner, E. D.; Plewa, M. J.; Toxicological comparison of water, wastewaters, and processed wastewaters. *Environ. Sci. Technol.* **2019**, 53(15), 9139-9147.

(12) Kwon, M.; Yoon, Y.; Kim, S.; Jung, Y.; Hwang, T.-M.; Kang, J.-W.; Removal of sulfamethoxazole, ibuprofen and nitrobenzene by UV and UV/chlorine processes: A comparative evaluation of 275 nm LED-UV and 254 nm LP-UV. *Sci. Total Environ.* **2018**, 637-638, 1351-1357.

(13) Guo, K.; Wu, Z.; Shang, C.; Yao, B.; Hou, S.; Yang, X.; Song, W.; Fang, J.; Radical chemistry and structural relationships of PPCP degradation by UV/chlorine treatment in simulated drinking water. *Environ. Sci. Technol.* **2017**, 51(18), 10431-10439.

(14) Chuang, Y.-H.; Chen, S.; Chinn, C. J.; Mitch, W. A.; Comparing the UV/monochloramine and UV/free chlorine advanced oxidation processes (AOPs) to the UV/hydrogen peroxide AOP under scenarios relevant to potable reuse. *Environ. Sci. Technol.* **2017**, 51(23), 13859-13868.

(15) Hua, Z.; Guo, K.; Kong, X.; Lin, S.; Wu, Z.; Wang, L.; Huang, H.; Fang, J.; PPCP degradation and DBP formation in the solar/free chlorine system: Effects of pH and dissolved oxygen. *Water Res.* **2019**, 150, 77-85.

(16) Li, M.; Li, W.; Wen, D.; Bolton, J. R.; Blatchley, E. R.; Qiang, Z.; Micropollutant degradation by the UV/H_2O_2 process: Kinetic comparison among various radiation sources. *Environ. Sci. Technol.* **2019**, 53(9), 5241-5248.

(17) Miklos, D. B.; Hartl, R.; Michel, P.; Linden, K. G.; Drewes, J. E.; Hübner, U.; UV/H_2O_2 process stability and pilot-scale validation for trace organic chemical removal from wastewater treatment plant effluents. *Water Res.* **2018**, 136, 169-179.

(18) Yin, R.; Zhong, Z.; Ling, L.; Shang, C.; The fate of dichloroacetonitrile in UV/Cl_2 and UV/H_2O_2 processes: Implications on potable water reuse. *Environ. Sci. Water Res. Tech.* **2018**, 4(9), 1295-1302.

(19) Lu, X.; Shao, Y.; Gao, N.; Chen, J.; Deng, H.; Chu, W.; An, N.; Peng, F.; Investigation of clofibric acid removal by UV/persulfate and UV/chlorine processes: Kinetics and formation of disinfection byproducts during subsequent chlor(am)ination. *Chem. Eng. J.* **2018**, 331, 364-371.

(20) Bulman, D. M.; Mezyk, S. P.; Remucal, C. K.; The impact of pH and irradiation wavelength on the production of reactive oxidants during chlorine photolysis. *Environ. Sci. Technol.* **2019**, 53(8), 4450-4459.

(21) Forsyth, J. E.; Zhou, P.; Mao, Q.; Asato, S. S.; Meschke, J. S.; Dodd, M. C.; Enhanced inactivation of *Bacillus subtilis* spores during solar photolysis of free available chlorine. *Environ. Sci. Technol.* **2013**, 47(22), 12976-12984.

(22) Watts, M. J.; Linden, K. G.; Chlorine photolysis and subsequent $^{\bullet}OH$ radical production during UV treatment of chlorinated water. *Water Res.* **2007**, 41(13), 2871-2878.

(23) Buxton, G. V.; Subhani, M. S.; Radiation chemistry and photochemistry of oxychlorine ions. Part 1. Radiolysis of aqueous solutions of hypochlorite and chlorite ions. *J. Chem. Soc. Faraday Trans. 1* **1972**, 68, 947-957.

(24) Buxton, G. V.; Subhani, M. S.; Radiation chemistry and photochemistry of oxychlorine ions. Part 2. Photodecomposition of aqueous solutions of hypochlorite ions. *J. Chem. Soc. Faraday Trans. 1* **1972**, 68, 958-969.

(25) Nowell, L. H.; Hoigné, J.; Photolysis of aqueous chlorine at sunlight and ultraviolet wavelengths. 1. Degradation rates. *Water Res.* **1992**, 26(5), 593-598.

(26) Buxton, G. V.; Pulse radiolysis of aqueous solutions. Some rates of reaction of $^{\bullet}OH$ and $O^{\bullet-}$ and pH dependence of the yield of O_3^-. *Trans. Faraday Soc.* **1969**, 65, 2150-2158.

(27) Fang, J.; Fu, Y.; Shang, C.; The roles of reactive species in micropollutant degradation in the UV/free chlorine system. *Environ. Sci. Technol.* **2014**, 48(3), 1859-1868.

(28) Varanasi, L.; Coscarelli, E.; Khaksari, M.; Mazzoleni, L. R.; Minakata, D.; Transformations of dissolved organic matter induced by UV photolysis, hydroxyl radicals, chlorine radicals, and sulfate radicals in aqueous-phase UV-based advanced oxidation processes. *Water Res.* **2018**, 135, 22-30.

(29) Buxton, G. V.; Greenstock, C. L.; Helman, W. P.; Ross, A. B.; Critical review of rate constants for reactions of hydrated electrons, hydrogen atoms and hydroxyl radicals ($^{\bullet}OH$/ $O^{\bullet-}$) in aqueous solution. *J. Phys. Chem. Ref. Data* **1988**, 17(2), 513-886.

(30) Zhang, K.; Parker, K. M.; Halogen radical oxidants in natural and engineered aquatic systems. *Environ. Sci. Technol.* **2018**, 52(17), 9579-9594.

(31) Heller-Grossman, L.; Manka, J.; Limoni-Relis, B.; Rebhun, M.; THM, haloacetic acids and other organic DBPs formation in disinfection of bromide rich sea of Galilee (Lake Kinneret) water. *Water Sci. Technol. Water Supply* **2001**, 1(2), 259-266.

(32) Agus, E.; Voutchkov, N.; Sedlak, D. L.; Disinfection by-products and their potential impact on the quality of water produced by desalination systems: A literature review. *Desalination* **2009**, 237(1-3), 214-237.

(33) Shah, A. D.; Mitch, W. A.; Halonitroalkanes, halonitriles, haloamides, and *N*-nitrosamines: A critical review of nitrogenous disinfection byproduct formation pathways. *Environ. Sci. Technol.* **2012**, 46(1), 119-131.

(34) Pifer, A. D.; Fairey, J. L.; Suitability of organic matter surrogates to predict trihalomethane formation in drinking water sources. *Environ. Eng. Sci.* **2014**, 31(3), 117-126.

(35) Yang, M.; Zhang, X.; Liang, Q.; Yang, B.; Application of (LC/)MS/MS precursor ion scan for evaluating the occurrence, formation and control of polar halogenated DBPs in disinfected waters: A review. *Water Res.* **2019**, 158, 322-337.

(36) Richardson, S. D.; Ternes, T. A.; Water analysis: Emerging contaminants and current issues. *Anal. Chem.* **2011**, 83(12), 4614-4648.

(37) Muellner, M. G.; Wagner, E. D.; Mccalla, K.; Richardson, S. D.; Woo, Y.-T.; Plewa, M. J.; Haloacetonitriles vs. regulated haloacetic acids: Are nitrogen-containing DBPs more toxic? *Environ. Sci. Technol.* **2007**, 41(2), 645-651.

(38) Plewa, M. J.; Wagner, E. D.; Richardson, S. D.; Tic-tox: A preliminary discussion on identifying the forcing agents of DBP-mediated toxicity of disinfected water. *J. Environ. Sci.* **2017**, 58, 208-216.

(39) Han, J.; Zhang, X.; Evaluating the comparative toxicity of DBP mixtures from different disinfection scenarios: A new approach by combining freeze-drying or rotoevaporation with a marine polychaete bioassay. *Environ. Sci. Technol.* **2018**, 52(18), 10552-10561.

(40) Richardson, S. D.; Ternes, T. A.; Water analysis: Emerging contaminants and current issues. *Anal. Chem.* **2018**, 90(1), 398-428.

(41) Jeong, C. H.; Wagner, E. D.; Siebert, V. R.; Anduri, S.; Richardson, S. D.; Daiber, E. J.; Mckague, A. B.; Kogevinas, M.; Villanueva, C. M.; Goslan, E. H.; Luo, W.; Isabelle, L. M.; Pankow, J. F.; Grazuleviciene, R.; Cordier, S.; Edwards, S. C.; Righi, E.; Nieuwenhuijsen, M. J.; Plewa, M. J.; Occurrence and toxicity of disinfection byproducts in European drinking waters in relation with the HIWATE epidemiology study. *Environ. Sci. Technol.* **2012**, 46(21), 12120-12128.

(42) Gonsior, M.; Schmitt-Kopplin, P.; Stavklint, H.; Richardson, S. D.; Hertkorn, N.; Bastviken, D.; Changes in dissolved organic matter during the treatment processes of a drinking water plant in Sweden and formation of previously unknown disinfection byproducts. *Environ. Sci. Technol.* **2014**, 48(21), 12714-12722.

(43) Acero, J. L.; Benitez, F. J.; Real, F. J.; Roldan, G.; Kinetics of aqueous chlorination of some pharmaceuticals and their elimination from water matrices. *Water Res.* **2010**, 44(14), 4158-4170.

(44) Lavonen, E. E.; Kothawala, D. N.; Tranvik, L. J.; Gonsior, M.; Schmitt-Kopplin, P.; Köhler, S. J.; Tracking changes in the optical properties and molecular composition of dissolved organic matter during drinking water production. *Water Res.* **2015**, 85, 286-294.

(45) Lei, Y.; Cheng, S.; Luo, N.; Yang, X.; An, T.; Rate constants and mechanisms of the reactions of $Cl^{\bullet}$ and $Cl_2^{\bullet-}$ with trace organic contaminants. *Environ. Sci. Technol.* **2019**, 53(19), 11170-11182.

(46) Remucal, C. K.; Manley, D.; Emerging investigators series: The efficacy of chlorine photolysis as an advanced oxidation process for drinking water treatment. *Environ. Sci. Water Res. Tech.* **2016**, 2(4), 565-579.

(47) Liu, W.; Cheung, L. M.; Yang, X.; Shang, C.; THM, HAA and CNCl formation from UV irradiation and chlor(am)ination of selected organic waters. *Water Res.* **2006**, 40(10), 2033-2043.

(48) Pisarenko, A. N.; Stanford, B. D.; Snyder, S. A.; Rivera, S. B.; Boal, A. K.; Investigation of the use of chlorine based advanced oxidation in surface water: Oxidation of natural organic matter and formation of disinfection byproducts. *J. Adv. Oxid. Technol.* **2013**, 16(1), 137-150.

(49) Zhang, X.; Li, W.; Blatchley, E. R.; Wang, X.; Ren, P.; UV/chlorine process for ammonia removal and disinfection by-product reduction: Comparison with chlorination. *Water Res.* **2015**, 68, 804-811.

(50) Ben, W.; Sun, P.; Huang, C.-H.; Effects of combined UV and chlorine treatment on chloroform formation from triclosan. *Chemosphere* **2016**, 150, 715-722.

(51) Wang, D.; Bolton, J. R.; Andrews, S. A.; Hofmann, R.; Formation of disinfection by-products in the ultraviolet/chlorine advanced oxidation process. *Sci. Total Environ.* **2015**, 518-519, 49-57.

(52) Shah, A. D.; Dotson, A. D.; Linden, K. G.; Mitch, W. A.; Impact of UV disinfection combined with chlorination/chloramination on the formation of halonitromethanes and haloacetonitriles in drinking water. *Environ. Sci. Technol.* **2011**, 45(8), 3657-3664.

(53) Ding, S.; Deng, Y.; Bond, T.; Fang, C.; Cao, Z.; Chu, W.; Disinfection byproduct formation during drinking water treatment and distribution: A review of unintended effects of engineering agents and materials. *Water Res.* **2019**, 160, 313-329.

(54) Xagoraraki, I.; Harrington, G. W.; Assavasilavasukul, P.; Standridge, J. H.; Removal of emerging waterborne pathogens and pathogen indicators by pilot-scale conventional treatment. *J. Am. Water Works Assoc.* **2004**, 96(5), 102-113.

(55) Sun, P.; Lee, W.-N.; Zhang, R.; Huang, C.-H.; Degradation of DEET and caffeine under UV/chlorine and simulated sunlight/chlorine conditions. *Environ. Sci. Technol.* **2016**, 50(24), 13265-13273.

(56) Willson, V. A.; Determination of available chlorine in hypochlorite solutions by direct titration with sodium thiosulfate. *Ind. Eng. Chem. Anal. Ed.* **1935**, 7(1), 44-45.

(57) Weishaar, J. L.; Aiken, G. R.; Bergamaschi, B. A.; Fram, M. S.; Fujii, R.; Mopper, K.; Evaluation of specific ultraviolet absorbance as an indicator of the chemical composition and reactivity of dissolved organic carbon. *Environ. Sci. Technol.* **2003**, 37(20), 4702-4708.

(58) Lau, S. S.; Dias, R. P.; Martin-Culet, K. R.; Race, N. A.; Schammel, M. H.; Reber, K. P.; Roberts, A. L.; Sivey, J. D.; 1,3,5-Trimethoxybenzene (TMB) as a new quencher for preserving redox-labile disinfection byproducts and for quantifying free chlorine and free bromine. *Environ. Sci. Water Res. Tech.* **2018**, 4(7), 926-941.

(59) Hodgeson, J. W.; Cohen, A. L.; Munch, D. J.; Hautman, D. P.; Method 551.1. Determination of chlorination disinfection byproducts, chlorinated solvents, and halogenated pesticides/herbicides in drinking water by liquid-liquid extractions and gas chromatography with electron capture detection. *U.S. Environmental Protection Agency, Cincinnati* **1995**.

(60) Hodgeson, J. W.; Collins, J.; Barth, R. E.; Munch, D. J.; Munch, J. W.; Pawlecki, A. M.; Method 552.2 determination of haloacetic acids and dalapon in drinking water by liquid-liquid extraction, derivatization and gas chromatography with electron capture detection. *U.S. Environmental Protection Agency, Cincinnati* **1995**.

(61) Ziegler, G.; Gonsior, M.; Fisher, D. J.; Schmitt-Kopplin, P.; Tamburri, M. N.; Formation of brominated organic compounds and molecular transformations in dissolved organic matter (DOM) after ballast water treatment with sodium dichloroisocyanurate dihydrate (DICD). *Environ. Sci. Technol.* **2019**, 53(14), 8006-8016.

(62) Dittmar, T.; Koch, B.; Hertkorn, N.; Kattner, G.; A simple and efficient method for the solid-phase extraction of dissolved organic matter (SPE-DOM) from seawater. *Limnol. Oceanogr. Methods* **2008**, 6, 230-235.

(63) Maizel, A. C.; Remucal, C. K.; The effect of advanced secondary municipal wastewater treatment on the molecular composition of dissolved organic matter. *Water Res.* **2017**, 122, 42-52.

(64) Koch, B. P.; Dittmar, T.; Witt, M.; Kattner, G.; Fundamentals of molecular formula assignment to ultrahigh resolution mass data of natural organic matter. *Anal. Chem.* **2007**, 79(4), 1758-1763.

(65) Maizel, A. C.; Li, J.; Remucal, C. K.; Relationships between dissolved organic matter composition and photochemistry in lakes of diverse trophic status. *Environ. Sci. Technol.* **2017**, 51(17), 9624-9632.

(66) Berg, S. M.; Whiting, Q. T.; Herrli, J. A.; Winkels, R.; Wammer, K. H.; Remucal, C. K.; The role of dissolved organic matter composition in determining photochemical reactivity at the molecular level. *Environ. Sci. Technol.* **2019**, 53(20), 11725-11734.

(67) Chu, W.; Gao, N.; Yin, D.; Krasner, S. W.; Mitch, W. A.; Impact of UV/H_2O_2 pre-oxidation on the formation of haloacetamides and other nitrogenous disinfection byproducts during chlorination. *Environ. Sci. Technol.* **2014**, 48(20), 12190-12198.

(68) Oliver, B. G.; Carey, J. H.; Photochemical production of chlorinated organics in aqueous solutions containing chlorine. *Environ. Sci. Technol.* **1977**, 11(9), 893-895.

(69) Bossmann, S. H.; Oliveros, E.; Göb, S.; Siegwart, S.; Dahlen, E. P.; Payawan, L.; Straub, M.; Wörner, M.; Braun, A. M.; New evidence against hydroxyl radicals as reactive intermediates in the thermal and photochemically enhanced Fenton reactions. *J. Phys. Chem. A* **1998**, 102(28), 5542-5550.

(70) Nowell, L. H.; Hoigné, J.; Photolysis of aqueous chlorine at sunlight and ultraviolet wavelengths. 2. Hydroxyl radical production. *Water Res.* **1992**, 26(5), 599-605.

(71) Yin, R.; Ling, L.; Shang, C.; Wavelength-dependent chlorine photolysis and subsequent radical production using UV-LEDs as light sources. *Water Res.* **2018**, 142, 452-458.

(72) Wols, B. A.; Hofman-Caris, C. H. M.; Review of photochemical reaction constants of organic micropollutants required for UV advanced oxidation processes in water. *Water Res.* **2012**, 46(9), 2815-2827.

(73) Grigor'ev, A. E.; Makarov, I. E.; Pikaev, A. K.; Formation of $Cl_2^{\bullet-}$ in the bulk of solution during radiolysis of concentrated aqueous solutions of chlorides. *Khim. Vys. Energ.* **1987**, 21(2), 99-102.

(74) Jayson, G. G.; Parsons, B. J.; Swallow, A. J.; Some simple, highly reactive, inorganic chlorine derivatives in aqueous solution. *J. Chem. Soc. Faraday Trans. 1* **1973**, 69, 1597-1607.

(75) Kläning, U. K.; Wolff, T.; Laser flash photolysis of HClO, ClO^-, HBrO, and BrO^- in aqueous solution. Reactions of Cl^- and Br^- atoms. *Ber. Bunsen. Ges. Phys. Chem.* **1985**, 89, 243-245.

(76) Nagarajan, V.; Fessenden, R. W.; Flash photolysis of transient radicals. 1. X_2^- with X = Cl, Br, I, and SCN. *J. Phys. Chem.* **1985**, 89(11), 2330-2335.

(77) Yu, X.-Y.; Barker, J. R.; Hydrogen peroxide photolysis in acidic aqueous solutions containing chloride ions. I. Chemical mechanism. *J. Phys. Chem. A* **2003**, 107(9), 1313-1324.

(78) Wang, W.-L.; Wu, Q.-Y.; Huang, N.; Wang, T.; Hu, H.-Y.; Synergistic effect between UV and chlorine (UV/chlorine) on the degradation of carbamazepine: Influence factors and radical species. *Water Res.* **2016**, 98, 190-198.

(79) Gao, Y.-Q.; Gao, N.-Y.; Chen, J.-X.; Zhang, J.; Yin, D.-Q.; Oxidation of β-blocker atenolol by a combination of UV light and chlorine: Kinetics, degradation pathways and toxicity assessment. *Sep. Purif. Technol.* **2020**, 231, 115927.

(80) Dugan, H. A.; Summers, J. C.; Skaff, N. K.; Krivak-Tetley, F. E.; Doubek, J. P.; Burke, S. M.; Bartlett, S. L.; Arvola, L.; Jarjanazi, H.; Korponai, J.; Kleeberg, A.; Monet, G.; Monteith, D.; Moore, K.; Rogora, M.; Hanson, P. C.; Weathers, K. C.; Long-term chloride concentrations in North American and European freshwater lakes. *Nature: Scientific Data* **2017**, 4, 170101.

(81) Mertens, R.; Von Sonntag, C.; Photolysis (λ= 254 nm) of tetrachloroethene in aqueous solutions. *J. Photochem. Photobio. A* **1995**, 85, 1-9.

(82) Kläning, U. K.; Sehested, K.; Wolff, T.; Laser flash photolysis and pulse radiolysis of iodate and periodate in aqueous solution. Properties of iodine (VI). *J. Chem. Soc. Faraday Trans.* **1981**, 77, 1707-1718.

(83) Von Sonntag, C.; von Gunten, U. *Chemistry of ozone in water and wastewater treatment* (IWA publishing, **2012**).

(84) Elovitz, M. S.; von Gunten, U.; Kaiser, H.-P. The influence of dissolved organic matter character on ozone decomposition rates and R_{ct}. Barrett, Sylvia E.; Krasner, Stuart W.; Amy, Gary L.; eds.; ACS Publications: **2000**.

(85) Dodd, M. C.; Buffle, M.-O.; von Gunten, U.; Oxidation of antibacterial molecules by aqueous ozone: moiety-specific reaction kinetics and application to ozone-based wastewater treatment. *Environ. Sci. Technol.* **2006**, 40(6), 1969-1977.

(86) von Gunten, U.; Ozonation of drinking water: Part 1. Oxidation kinetics and products formation. *Water Res.* **2003**, 37, 1443-1467.

(87) Hammes, F.; Salhi, E.; Köster, O.; Kaiser, H.-P.; Egli, T.; von Gunten, U.; Mechanistic and kinetic evaluation of organic disinfection by-product and assimilable organic carbon (AOC) formation during the ozonation of drinking water. *Water Res.* **2006**, 40(12), 2275-2286.

(88) Phungsai, P.; Kurisu, F.; Kasuga, I.; Furumai, H.; Changes in dissolved organic matter composition and disinfection byproduct precursors in advanced drinking water treatment processes. *Environ. Sci. Technol.* **2018**, 52(6), 3392-3401.

(89) Gan, W.; Huang, S.; Ge, Y.; Bond, T.; Westerhoff, P.; Zhai, J.; Yang, X.; Chlorite formation during ClO_2 oxidation of model compounds having various functional groups and humic substances. *Water Res.* **2019**, 159, 348-357.

(90) Skibinski, B.; Uhlig, S.; Müller, P.; Slavik, I.; Uhl, W.; Impact of different combinations of water treatment processes on the concentration of disinfection byproducts and their precursors in swimming pool water. *Environ. Sci. Technol.* **2019**, 53(14), 8115-8126.

(91) Xu, J.; Kralles, Z. T.; Dai, N.; Effects of sunlight on the trichloronitromethane formation potential of wastewater effluents: Dependence on nitrite concentration. *Environ. Sci. Technol.* **2019**, 53(8), 4285-4294.

(92) Li, C.; Wang, D.; Xu, X.; Wang, Z.; Formation of known and unknown disinfection by-products from natural organic matter fractions during chlorination, chloramination, and ozonation. *Sci. Total Environ.* **2017**, 587-588, 177-184.

(93) Maizel, A. C.; Remucal, C. K.; Molecular composition and photochemical reactivity of size-fractionated dissolved organic matter. *Environ. Sci. Technol.* **2017**, 51(4), 2113-2123.

(94) Gligorovski, S.; Strekowski, R.; Barbati, S.; Vione, D.; Environmental implications of hydroxyl radicals ($^{\bullet}OH$). *Chem. Rev.* **2015**, 115(24), 13051-13092.

(95) Young, T. R.; Li, W.; Guo, A.; Korshin, G. V.; Dodd, M. C.; Characterization of disinfection byproduct formation and associated changes to dissolved organic matter during solar photolysis of free available chlorine. *Water Res.* **2018**, 146, 318-327.

(96) Chen, M.; Kim, S.; Park, J.-E.; Jung, H.-J.; Hur, J.; Structural and compositional changes of dissolved organic matter upon solid-phase extraction tracked by multiple analytical tools. *Anal. Bioanal. Chem.* **2016**, 408(23), 6249-6258.

(97) Ohno, T.; He, Z.; Sleighter, R. L.; Honeycutt, C. W.; Hatcher, P. G.; Ultrahigh resolution mass spectrometry and indicator species analysis to identify marker components of soil- and plant biomass- derived organic matter fractions. *Environ. Sci. Technol.* **2010**, 44(22), 8594-8600.

(98) Zhang, H.; Zhang, Y.; Shi, Q.; Ren, S.; Yu, J.; Ji, F.; Luo, W.; Yang, M.; Characterization of low molecular weight dissolved natural organic matter along the treatment train of a waterworks using Fourier transform ion cyclotron resonance mass spectrometry. *Water Res.* **2012**, 46(16), 5197-5204.

(99) Rosario-Ortiz, F. L.; Canonica, S.; Probe compounds to assess the photochemical activity of dissolved organic matter. *Environ. Sci. Technol.* **2016**, 50(23), 12532-12547.

(100) Du, Y.; Wu, Q.-Y.; Lv, X.-T.; Ye, B.; Zhan, X.-M.; Lu, Y.; Hu, H.-Y.; Electron donating capacity reduction of dissolved organic matter by solar irradiation reduces the cytotoxicity formation potential during wastewater chlorination. *Water Res.* **2018**, 145, 94-102.

(101) Wenk, J.; Aeschbacher, M.; Salhi, E.; Canonica, S.; von Gunten, U.; Sander, M.; Chemical oxidation of dissolved organic matter by chlorine dioxide, chlorine, and ozone: Effects on its optical and antioxidant properties. *Environ. Sci. Technol.* **2013**, 47(19), 11147-11156.

(102) Lavonen, E. E.; Gonsior, M.; Tranvik, L. J.; Schmitt-Kopplin, P.; Köhler, S. J.; Selective chlorination of natural organic matter: Identification of previously unknown disinfection byproducts. *Environ. Sci. Technol.* **2013**, 47(5), 2264-2271.

(103) Kundu, B.; Richardson, S. D.; Granville, C. A.; Shaughnessy, D. T.; Hanley, N. M.; Swartz, P. D.; Richard, A. M.; Demarini, D. M.; Comparative mutagenicity of halomethanes and halonitromethanes in Salmonella TA 100: Structure activity analysis and mutation spectra. *Mutat. Res.* **2004**, 554(1-2), 335-350.

(104) Plewa, M. J.; Wagner, E. D.; Mueller, M. G.; Hsu, K. M.; Richardson, S. Comparative mammalian cell toxicity of N-DBPs and C-DBPs; Occurrence, formation, health effects, and control of disinfection by-products in drinking water. In *Disinfection By-Products in Drinking Water*; Karanfil, T.; Krasner, S. W.; Westerhoff, P.; Xie, Y, Eds.; **2008**; pp 36.

(105) Zhao, Q.; Shang, C.; Zhang, X.; Ding, G.; Yang, X.; Formation of halogenated organic byproducts during medium-pressure UV and chlorine coexposure of model compounds, nom and bromide. *Water Res.* **2011**, 45(19), 6545-6554.

(106) Page, S. E.; Arnold, W. A.; McNeill, K.; Terephthalate as a probe for photochemically generated hydroxyl radical. *J. Environ. Monit.* **2010**, 12(9), 1658-1665.

(107) Sharpless, C. M.; Aeschbacher, M.; Page, S. E.; Wenk, J.; Sander, M.; McNeill, K.; Photooxidation-induced changes in optical, electrochemical, and photochemical properties of humic substances. *Environ. Sci. Technol.* **2014**, 48(5), 2688-2696.

(108) Yang, M.; Zhang, X.; Comparative developmental toxicity of new aromatic halogenated DBPs in a chlorinated saline sewage effluent to the marine polychaete *Platynereis dumerilii*. *Environ. Sci. Technol.* **2013**, 47(19), 10868-10876.

(109) Mercier Shanks, C.; Sérodes, J.-B.; Rodriguez, M. J.; Spatio-temporal variability of non-regulated disinfection by-products within a drinking water distribution network. *Water Res.* **2013**, 47(9), 3231-3243.

(110) Allard, S.; Tan, J.; Joll, C. A.; von Gunten, U.; Mechanistic study on the formation of $Cl^-/Br^-/I^-$ trihalomethanes during chlorination/chloramination combined with a theoretical cytotoxicity evaluation. *Environ Sci. Technol.* **2015**, 49(18), 11105-11114.

(111) Huang, K.; Shah, A. D.; Role of tertiary amines in enhancing trihalomethane and haloacetic acid formation during chlorination of aromatic compounds and a natural organic matter extract. *Environ. Sci. Water Res. Tech* **2018**, 4(5), 663-679.

Chapter 5

Proposed investigation of the impact of bromide on halogenated disinfection by-product formation during chlorine photolysis [4]

5.1 Project Summary

The prevalence of organic contaminants, such as pharmaceuticals, pesticides, and personal care products, in drinking water has resulted in increased interest into contaminant removal applications. Advanced oxidation processes (AOPs), such as chlorine photolysis, rely on the generation of hydroxyl radical to degrade these organic contaminants. The suite of reactive oxidants formed during chlorine photolysis, along with light and free available chlorine, can all act to degrade organic contaminants but will also react with dissolved organic matter and other naturally occurring water constituents such as inorganic carbon and bromide. Reaction of free available chlorine and reactive chlorine species with natural water constituents can result in the formation of halogenated disinfection by-products, some of which present a known risk to human health. The presence of bromide can further alter disinfection by-product generation by forming hypobromous acid, reacting with ozone to form bromate, or through bromine radical reactions. The proposed research seeks to explore the impact of bromide on the production of reactive oxidants during chlorine photolysis and evaluate the formation of halogenated disinfection by-products.

[4] The proposed experiments were planned for the Spring of 2020 but were delayed due to the COVID-19 pandemic.

The proposed research will use probe measurements of reactive oxidants, measurement of small aliphatic and inorganic disinfection by-products, and bulk and molecular measurements of dissolved organic matter to determine the impact of bromide on oxidant and disinfection by-product formation during chlorine photolysis. Some important questions that this research will try to answer are (1) is ozone generated from bromine photolysis under conditions relevant to water treatment, (2) will there be enhanced bromate formation during chlorine photolysis, (3) how does the presence of reactive bromine species affect the transformation of dissolved organic matter during chlorine photolysis, (4) do high molecular weight novel brominated disinfection by-products form during chlorine photolysis in the presence of bromide, and (5) does the presence of bromide affect the ratios of brominated and chlorinated disinfection by-products.

5.2 Introduction

Organic contamination has been found in surface and ground water sources for drinking water.[1–5] This contamination is not systematically regulated but presents a potential risk to human[4-6] and ecosystem health.[1,7] Advanced oxidation processes (AOPs) such as chlorine photolysis can degrade organic contaminants through generation of hydroxyl radical ($^{\bullet}OH$; Chapter 2.4.2).[8–10] In addition to $^{\bullet}OH$, chlorine photolysis generates a suite of reactive oxidants including ozone (O_3) and reactive chlorine species (RCS) such as chlorine radical ($Cl^{\bullet}$) and dichloride radical anion ($Cl_2^{\bullet-}$).[11–14] In surface waters containing bromide, reactive bromine species (RBS) can also form (Schematic 5.1).[15,16]

Bromide is found in natural waters with concentrations ranging from 1 ppb to over 65,000 ppm in seawater.[15,17–20] In source waters with elevated bromide concentrations (i.e., generally > 35 ppb),[17] hypobromous acid (HOBr) can form from the reaction of chlorine and bromide.[21,22] This

free available bromine (a mixture of hypobromous acid and hypobromite, pK_a = 8.8)[15] can undergo photolysis to form multiple reaction product including $^{\bullet}$OH and bromine radical (Br$^{\bullet}$; Schematic 5.1).[15,16,21]

The distribution of oxidants is different during bromine photolysis which results in lower $^{\bullet}$OH radical steady-state concentrations than chlorine photolysis. This lower steady-state concentration is due to differences in light absorption (Figure 5.1), a lower quantum yield (i.e., less efficient radical formation per photon absorbed; Table 5.1),[15,16] and more efficient radical scavenging by bromine and bromide (e.g., $k_{\bullet OH}^{Cl-}$ = 1.1 x 10^9 M^{-1} s^{-1} vs. $k_{\bullet OH}^{Br-}$ = 1.1 x 10^{10} M^{-1} s^{-1}).[23,24] Ozone formation during bromine photolysis is poorly understood. The ozone precursor, O(^{3}P) does form during photolysis of OBr^-,[25] but its quantum yield is unknown and ozone formation during bromine photolysis under conditions relevant to drinking water treatment studies has not been studied.[15,16]

The concentrations of RBS during bromine photolysis are higher than the concentrations of RCS during chlorine photolysis, which may result in faster degradation of some organic contaminants.[15] These RBS are analogous to the RCS formed during chlorine photolysis and include hypobromite radical ($BrO^{\bullet}$) and dibromide radical anion ($Br_2^{\bullet-}$; Schematic 5.1).[26] The reactivity of RBS towards organic compounds depends on compound class, but reactions are generally fast (e.g. $k_{phenols}$ = ~10^9 - 10^{10} M^{-1} s^{-1}, $k_{polyunsaturated\ fatty\ acids}$ = ~10^9 M^{-1} s^{-1}).[15] RBS are more reactive towards compounds with electron-donating functional groups.[15] In a recent study, RBS were found to react with ibuprofen primarily via hydroxylation, decarboxylation, and side-chain cleavage.[15]

Naturally occurring dissolved organic matter (DOM) can react with disinfectants such as chlorine to form potentially harmful disinfection by-products (DBPs).[27,28] During chlorine

photolysis, both chlorine and RCS can participate in the formation of these DBPs.[29] Understanding the formation of DBPs in source waters containing bromide is important as HOBr is more reactive than HOCl[27] and brominated DBPs are often more toxic than their chlorinated analogues.[30,31] As a result, the ratio of brominated to chlorinated DBPs increases with increasing bromide concentration,[27] which will affect water toxicity.

The ability of RBS to form Br-DBPs has not yet been investigated. Past research on RBS reactivity with model compounds suggests that the reactivity is similar to or exceeds that of RCS, so it is possible there will be greater DBP formation than during chlorine photolysis in the absence of bromide.[15,16] However, previous research also suggests that bromine substitution (i.e., direct bromination of model compounds) is possible but less common.[15]

There has been no research on the transformation of DOM or the formation of novel, high molecular weight DBPs during chlorine photolysis in the presence of bromide. Previous research has shown that DOM transformation during direct photolysis can result in DOM that is subsequently more reactive to FAC.[29,32] Additionally, RCS contribute to the formation of novel high molecular weight DBPs.[29] These DBPs can be more toxic than small aliphatic DBPs,[31,33] but are not regulated in drinking water. The transformation of DOM and formation of novel high molecular weight DBPs can be investigated using ultrahigh resolution mass spectrometry, a powerful technique which allows for the identification of thousands of molecular formulas present within DOM.[29,34–37]

Potentially harmful inorganic disinfection by-products can also form during drinking water treatment. Chlorite (ClO_2^-) has been linked to anemia and nervous system effects in infants and young children and is regulated in drinking water by the EPA with a maximum contaminant level (MCL) of 1.0 mg/L.[38] Bromate (BrO_3^-) is regulated in drinking water with a MCL of 0.01 mg/L

due to its carcinogenicity.[38] Chlorate (ClO_3^-) is not currently regulated in drinking water in the U.S., but is under consideration for regulation and is on the current candidate contaminant list.[39] Chlorite and chlorate form primarily through reaction of DOM with chlorine dioxide (ClO_2)[40] in conventional drinking water treatment, but can form during chlorine photolysis through a number of radical reactions (Table 5.3; Reaction 24 and 25).[24,25,41–47] Bromate is primarily thought to form from the reaction of bromide with ozone during ozonation,[48] but can also form via $^{\bullet}OH$ mediated pathways.[49]

Chlorine photolysis of waters containing bromide will result in the formation of RBS. Understanding the impact of bromide on the formation of reactive oxidants during chlorine photolysis, along with the formation of DBPs is important to applying chlorine photolysis in the treatment of bromide containing waters. The proposed work will investigate the formation of reactive oxidants using probe experiments. The formation of small aliphatic and inorganic DBPs will be measured. Additionally, we will combine bulk and molecular level techniques to evaluate DOM transformation and high molecular weight DBP formation.

5.3 Methods

5.3.1 Experimental Design

Experiments will be conducted using the DOM isolate Suwannee River fulvic acid (SRFA). An isolate will be used instead of a natural water sample to more carefully control the concentrations of inorganic species and to enable focus on the mechanism of DOM transformation. SRFA was selected because it is well characterized, highly reactive, and commonly used, which will allow for comparison across studies.[50–53] A sample water will be prepared at 4 mg-C/L with 5 mM phosphate and 1 mM bicarbonate and adjusted to pH 6.5. This pH was selected as it falls

below the pK_a of both chlorine and bromine (7.5 and 8.8, respectively).[8,15,21] Phosphate buffer was selected because it does not interfere with the radical reaction unlike organic buffers that work in the same pH range.[11] Bicarbonate will be added because it is present in mM concentrations in all natural waters. Radical scavenging by inorganic carbon is important in determining radical steady-state concentrations and results in the formation of carbonate radical.[15,26]

254 nm has been selected as the wavelength for photochemical treatment because it is commonly used in drinking water treatment.[54–56] Photolysis experiments will be performed in a Rayonet merry-go-round reactor.

Sixteen experimental conditions will be used to investigate the impact of bromide (0 – 2,000 ppb) and chlorine (0 - 10 mg-Cl_2/L) concentration variation. Free chlorine will be added to the bromide containing solution immediately prior to reaction. An additional condition will be used to investigate bromine photolysis (50 μM free bromine; Schematic 5.2). The free bromine stock solution will be prepared by reacting the free chlorine stock solution with potassium bromide at a 1:1.05 molar ratio overnight. The solution will then be standardized using ultraviolet-visible (UV-vis) spectroscopy (ε_{329} = 322 M^{-1} cm^{-1} at pH 11).[15] Free chlorine stock solutions contain chloride contamination, so chloride concentrations will be normalized to the concentration in the 10 mg-Cl_2/L sample in all experiments. Four treatments will be applied to each sample: dark treatment, irradiation, *tert*-butanol (*t*-BuOH)-scavenged irradiation, and *t*-BuOH-scavenged and N_2-quenched irradiation.

Chlorine photolysis is a complex system and SRFA can react with light, chlorine, and reactive oxidants so the treatments and conditions have been selected to allow for multiple controls. The dark control will allow us to verify the impact of chlorine alone on the transformation of dissolved organic matter and how the impact changes depending on the concentrations of

bromide and chlorine. Additionally, we will investigate the impact of dark bromination due to reaction with HOBr/OBr^- during dark treatment because there is some limited evidence that bromine is more likely to brominate organic compounds than RBS.[15] The photolysis condition will be used to evaluate both direct photolysis and chlorine photolysis (i.e., four samples contain no free chlorine and therefore represent the direct photolysis control; Schematic 5.2). In order to elucidate the importance of the reactive oxidants as compared with the concurrent presence of chlorine/bromine and light, two separate quenching conditions will be used. The first is the addition of *t*-BuOH which scavenges the radical species along with ~20 - 30% of the O_3.[57] The second is a combination of *t*-BuOH to scavenge the radicals and nitrogen sparging to remove oxygen and prevent the formation of O_3 (Reaction 13).[11,13,57]

5.3.2 Probe Measurements

Reactive oxidants, free chlorine, and free bromine will be quantified using probe compounds because the lifetime of most oxidants is too short to measure directly. 1,3,5-Trimethoxybenzene will be used to measure the concentration of free chlorine and free bromine as it reacts with each compound to form either 1-chloro-2,4,6-tromethoxybenzene or 1-bromo-2,4,6-trimethoxybenzene.[58] Nitrobenzene is a highly selective probe compound and reacts only with $^{\bullet}OH$ during chlorine photolysis.[11,14] Benzoate reacts with $^{\bullet}OH$ along with RCS and can be used to determine RCS reactivity.[11,59] Neither nitrobenzene or benzoate react with free chlorine or free bromine, nor do they undergo direct photodegradation.[11,15] In systems with no bromide, the benzoate loss rate constant can be used in combination with the $[^{\bullet}OH]_{ss}$ measured by nitrobenzene and $[Cl^-]$ to determine the steady-state concentrations of $Cl^{\bullet}$ and $Cl_2^{\bullet-}$ using a system of equations approach.[11] In solutions containing bromide, the formation of RBS prevents the determination of

exact radical steady-state concentrations, but can be used as a measure of overall RHS reactivity when compared across treatments and conditions.[15] Cinnamic acid reacts with ozone to form the selective product benzaldehyde, which can be used to determine the cumulative ozone production.[60] All probes will be quantified by high performance liquid chromatography.

5.3.3 Dissolved Organic Matter Analysis

Both bulk and molecular techniques will be used to characterize changes in DOM composition. Dissolved organic carbon concentration ([DOC]) will be measured using a total organic carbon analyzer. UV-vis spectroscopy can provide more information on the composition of the DOM. For example, $SUVA_{254}$ (i.e., the ratio of UV absorbance at 254 nm to [DOC]) is proportional to aromaticity,[61] while E_2:E_3 (i.e., the ratio of absorbance at 250 nm to 365 nm) is inversely proportional to molecular weight.[34,36,62] These bulk measurements can provide information on overall changes in the quantity and quality of DOM.

The composition of DOM will be investigated at the molecular level using Fourier-transform-ion cyclotron resonance mass spectrometry (FT-ICR MS). This high-resolution technique enables the identification of specific molecular formulas present within the DOM. Prior to FT-ICR MS analysis, samples will be prepared using solid-phase extraction on Agilent Bond Elut PPL cartridges to remove inorganic ions that lead to ion suppression.[35,63,63,64] Samples are acidified to pH <2.5 using formic acid, extracted on to the cartridges, and then eluted off into methanol.[29]

Formulas assignments will be made using a custom R script with $C_{0\text{-}80}H_{0\text{-}140}O_{0\text{-}80}N_{0\text{-}1}S_{0\text{-}1}P_{0\text{-}1}Cl_{0\text{-}3}Br_{0\text{-}3}{}^{13}C_{0\text{-}1}$ and a mass error < 0.5 ppm were allowed after internal calibration.[29,34,36,65] There will be no restriction on the number of heteroatoms (i.e., there may be CHOClBrN

formulas). Both brominated and chlorinated formulas will be verified with the ^{37}Cl or ^{81}Br isotopologue, respectively.[29] The matched formulas provide insight into DOM composition at the molecular level. The H:C ratio is a measure of aromaticity, while O:C is a measure of oxidation. By adding or removing functional groups from masses matched in the initial sample, we can determine reaction mechanism. For example, if a mass measured in a treated sample is a carboxyl group ($-CO_2$) less in mass than a mass in the initial sample that is evidence of decarboxylation reactions, a known mechanism of RBS.[15] Multiple reaction mechanisms will be considered including -H (H-abstraction), $-CO_2$ (decarboxylation), +O (hydroxyl addition), +2O (reaction with ozone), and halogen addition (+Cl and +Br).[29]

Additional analysis will be done to compare between treatment types including change in formula intensity, Spearman rank analysis, and principle component analysis. By comparing the variation in relative intensities, we can determine what molecular formulas are more reactive under different conditions, (e.g., if formulas degrade in the more aromatic or aliphatic regions of the van Krevelen diagram).[66,67] Spearman rank compares the change in formula intensity against an independent variable such as chlorine concentration, bromide concentration, or $[^{\bullet}OH]_{ss}$. The experimental design with varied chlorine and bromide concentrations was intentionally selected to enable this analysis. Principle component analysis compares the similarity of DOM composition across all samples.

5.3.4 Targeted Disinfection By-Products

We will measure targeted DBPs through three separate approaches in each experiment. First, we will quantify inorganic DBPs, including chlorite, chlorate, and bromate, using ion chromatography. Second, small aliphatic DBPs such as trihalomethanes, haloacetic acids, and haloacetonitriles will be measured by liquid-liquid extraction followed by gas-chromatography with electron-capture detection (GC-ECD).[68,69] Finally, the presence of halogenated aromatic DBPs will be investigated by comparing matched formulas and masses from the FT-ICR MS data to aromatic DBPs that have been identified in drinking water samples around the world.[70]

5.4 Expected Results and Discussion

5.4.1 Reactive Oxidant Formation

Formation of $^{\bullet}OH$ and other reactive oxidants is the critical component of any AOP. These oxidants, along with direct oxidation by chlorine and photolysis, are often responsible for the actual degradation of many organic contaminants during chlorine photolysis.[14,45,59,71] Understanding how the concentrations of these oxidants change is important to determining how bromide will impact the degradation of organic contaminants. Previous research has shown that the $^{\bullet}OH$ steady-state concentration is lower during chlorine photolysis in the presence of bromide than chlorine photolysis due to lower quantum yields (Reactions 1-8) and faster scavenging of $^{\bullet}OH$ by bromine than by chlorine (Reactions 22-23).[11,15,72] We will measure the $[^{\bullet}OH]_{ss}$ during chlorine photolysis in the presence of increasing concentrations of bromide and in the presence of DOM to determine how $[^{\bullet}OH]_{ss}$ changes. No previous studies have investigated radical formation during chlorine photolysis in the presence of both bromide and DOM.

Reactive halogen species are generated either through the direct photolysis of chlorine[8,13,14,73] and bromine[15,16,73] or through a series of reactions with other naturally occurring species (see Chapter 3). The presence of $Cl^{\bullet}$, $Br^{\bullet}$, $Cl_2^{\bullet-}$, and $Br_2^{\bullet-}$ has been verified in chlorine and bromine photolysis using the electron pulse spin resonance and laser flash photolysis.[15,16] The concentration of chlorine radical during free chlorine photolysis is reportedly lower than the concentration of bromine radical during free bromine photolysis, this could result in higher overall reactive halogen species reactivity as the concentration of bromide increases.[15] Additionally, the rate of degradation of some compounds will be increased if they are more reactive with RBS.

The remaining oxidant to be studied is ozone. Ozone is a more selective oxidant compared to $^{\bullet}OH$, but can react with many organic compounds and can inactivate some chlorine-resistant pathogens.[57,74,75] The formation of ozone is understudied in chlorine photolysis at 254 nm and is generally only considered for UV-A and UV-B light.[11,57,76] The formation of ozone during bromine photolysis in drinking water treatment studies has not been measured, but O_3 is known to form during bromine photolysis based on flash photolysis measurements.[22] It is possible that the ozone concentration will decrease as the concentration of free chlorine decreases with increasing bromide concentration (i.e., due to conversion to free bromine) because the known quantum yields of free bromine photolysis are lower than the quantum yields of free chlorine photolysis.

5.4.2 Dissolved Organic Matter Transformation

We will evaluate both bulk and molecular parameters to determine how DOM is transformed during chlorine photolysis as a function of bromide concentration. DOM concentrations will be assessed using [DOC] measurements, with limited mineralization expected during chlorine photolysis. However, reaction with light, chlorine/bromine, and reactive oxidants

can all change the composition of DOM by reacting primarily with aromatic and reduced moieties.[32,36,37,77,78] Understanding how the composition of DOM changes during treatment is important for assessing later DOM reactivity because DOM composition determines both photolytic and chemical reactivity.[34,36,78,79] For example, direct photolysis of DOM by 254 nm light and reaction with •OH can alter DOM so that is more susceptible to subsequent dark reaction with chlorine.[29] This DOM transformation then results in DOM that is likely to form DBPs during reaction with residual disinfectant in the distribution system.

A study on bromine photolysis has shown that organic compounds with electron-donating functional groups have enhanced degradation during reaction with RBS relative to RCS and that the primary mechanisms of reaction with RBS are hydroxylation and decarboxylation.[15] The primary mechanisms of RBS reactivity (i.e., hydroxylation and decarboxylation),[15] as measured with model organic compounds and not in DOM, differ from the primary mechanisms of RCS reactivity (i.e., H-abstraction and chlorine addition).[80] We will evaluate the formation of hydroxylation or decarboxylation products in the treated DOM by comparing masses in the treated sample to masses in the initial sample as was done in Chapter 4.2.2. In addition to +O and +2O reactions, we will also investigate H-abstraction (-H), decarboxylation ($-CO_2$), and halogen addition (+Cl or +Br).

DOM moieties react differently to various reactive oxidants. •OH reacts more quickly with phenolic and aromatic compounds, but it is non-selective and can react with many DOM functional groups.[45,59,79,81] Ozone is highly selective and only likely to react with compounds at double bonds (e.g., phenols and olefins).[74,75] Both free chlorine and free bromine can react with DOM, primarily by halogen addition. RCS and RBS both react by H-abstraction and double bond cleavage, but only RCS are likely to react by halogen addition based on model compound studies.[15,26,80] This

differential reactivity will result in different DOM fractions increasing or decreasing in relative intensity consistently with experimental changes. For example, as $[^{\bullet}OH]_{ss}$ increases with increasing chlorine dose, we expect that formula intensity will increase in the high O:C reaction due to hydroxyl addition reactions (Figure 5.2).

5.4.3 Formation of Brominated Dissolved Organic Matter

Brominated DOM can form during the reaction of bromine or reactive bromine species with DOM. Based on previous work with model organic compounds, we hypothesize that the formation of brominated DOM is more likely to be due to reaction with bromine directly as RBS are not likely to undergo bromine addition.[15] However, this mechanisms has not yet been assessed in DOM. Furthermore, sensitized DOM during chlorine photolysis can undergo reaction with chlorine directly to form CHOCl formulas in addition to direct halogenation by RCS.[29] Thus, there are four potential mechanisms for DOM halogenation: (1) direct reaction with free chlorine or free bromine, (2) direct reaction with RHS, or sequential reaction of DOM with (3) UV light or (4) $^{\bullet}OH$ followed by reaction with free chlorine or free bromine (Schematic 5.3). As RBS are likely less important than RCS in halogenation reactions, it is likely that we will see a large number of CHOBr formulas even in the scavenged condition as oxidized DOM reacts with bromine (Pathway 3 and 4, Schematic 5.3).[15]

The DOM fraction that is most reactive towards reaction with bromine and RBS can be identified by relating formulas that decrease in intensity to bromide concentration or RHS reactivity. The results of Spearman rank analysis can be presented as a heatmap to show where on the van Krevelen diagram the formulas that react most with bromine and RBS fall (Figure 5.2). We can also look at the ratio of halogenated DBPs relative to the ratio of free bromine and free

chlorine. Because free bromine is more reactive, we would expect that the ratio of Br-DBPs to Cl-DBPs would increase during dark treatment as the concentration of free bromine increases due to reaction of free chlorine with bromide.[27] The greater reactivity of RCS, relative to the reactivity of RBS, in halogenation reactions could result in less change to this ratio during chlorine photolysis as opposed to dark chlorination.

5.4.4 Formation of Halogenated Aromatics

Many halogenated aromatic disinfection by-products have been identified in drinking water samples from around the world.[31,82,83] These halogenated aromatic DBPs can be more toxic than aliphatic DBPs.[31,83–85] We will investigate if any of these compounds are found in our samples by comparing the masses and chemical formula of known halogenated organics against matched formulas found in our FT-ICR MS samples (Table 5.4). We previously investigated if a subset of these compounds were produced during chlorine photolysis in the absence of bromide but did not find evidence of them (Chapter 4). This is in large part due to the fact that many of the compounds are brominated or mixed chlorinated and brominated and we did not have any formulas that matched to CHOBr formulas in experiments conducted in the absence of Br^-.

5.4.5 Formation of Aliphatic Disinfection By-Products

The formation of small, halogenated DBPs (i.e., THMs, HAAs, and HANs) will also be investigated. THMs form from reaction with chlorine and decrease in concentration during chlorine photolysis.[29] HAAs increase during chlorine photolysis, likely due to reactions with RCS.[29] HANs increase during chlorine photolysis due to DOM transformation forming more HAN precursors.[29] Understanding how bromide will impact the formation of these compounds is

important because brominated DBPs form more readily.[19,27,28] Additionally, both THMs and HAAs are regulated in the U.S. based on their mass concentration which means that utilities can hit the U.S. Environmental Protection Agency's maximum contaminant level (MCL) very quickly as the ratio of DBPs shifts from chlorinated to brominated due to the higher molecular weight of bromine compared to chlorine.

5.4.6 Formation of Inorganic Disinfection By-Products

Inorganic disinfection by-products can also form during drinking water treatment. Chlorite and chlorate form in drinking water treated with ClO_2, but can also form during chlorine photolysis.[24,25,40–47] Bromide can react with ozone to form bromate, an inorganic DBP that is regulated in drinking water in the U.S. (MCL = 0.01 mg/L). Because chlorine and bromine photolysis are both known to produce ozone,[11,22,57] understanding what factors affect bromate formation is important.[48] Additionally, the reactive oxidants present during chlorine or bromine photolysis could contribute to the formation of bromate. Bromate has been detected at concentrations ranging from 0.1 to 2 μg/L during chlorine photolysis.[86]

5.5 Implications for Drinking Water Treatment

The presence of bromide has important implications for DBP formation during drinking water treatment. Bromide is present in drinking water sources at concentrations up to 65 ppm particularly in ground water sources with salt water intrusion and in post-reverse osmosis water after desalination.[15,20] If present in combination with chlorine, bromide will react to form bromine, which is a more reactive oxidant that can to react with DOM to form harmful DBPs.[21,22] As the concentration of bromide increases, so too does the concentration of brominated DBPs.

Brominated DBPs are more toxic than their chlorinated counterparts making this an undesirable outcome. Additionally, brominated DBPs are heavier in molecular weight and utilities are more likely to exceed MCLs in waters containing higher bromide. The formation of high MW brominated DBPs has not been previously investigated during chlorine or bromine photolysis leaving many unanswered questions about the formation of these toxic compounds during this AOP.

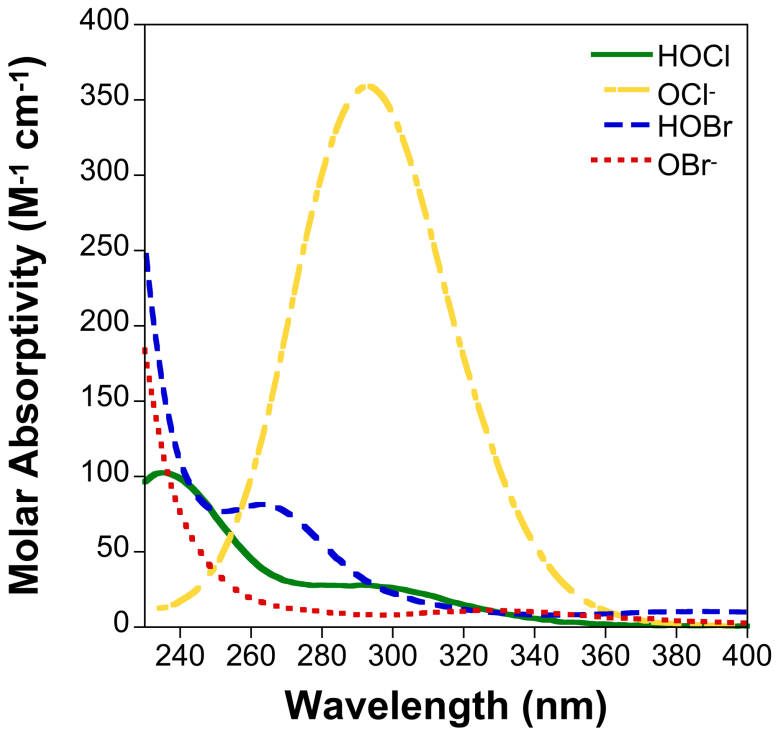

Figure 5.1. Molar absorptivity of HOCl, OCl^-, HOBr, and OBr^- as a function of wavelength.

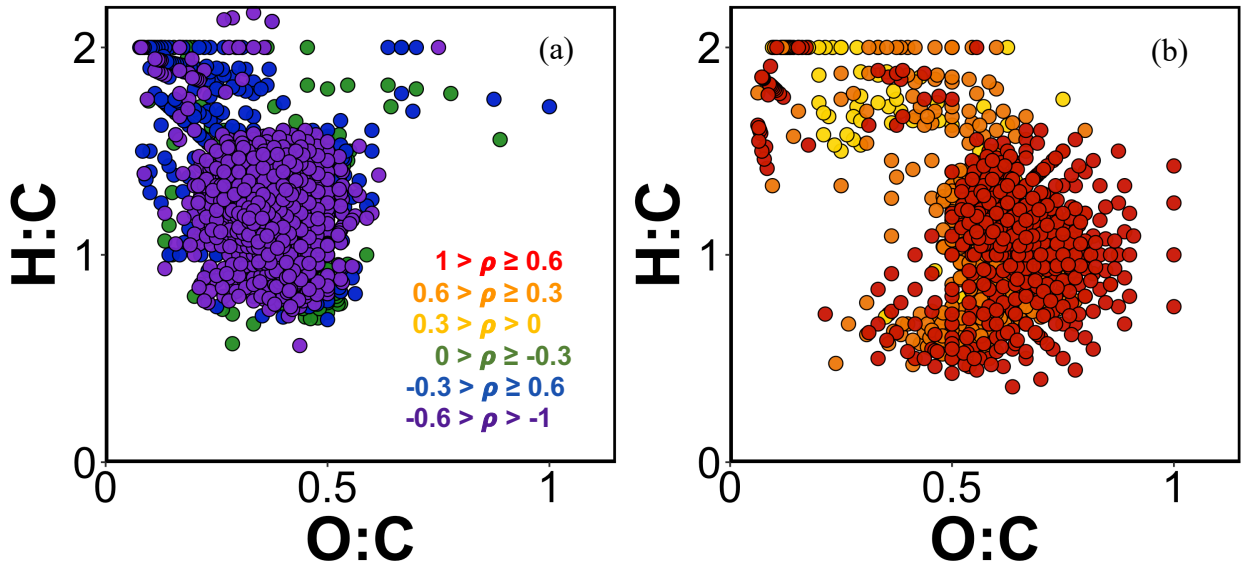

Figure 5.2. van Krevelen diagrams of Spearman rank correlations between formulas that (a) negatively or (b) positively correlate with $[^{\bullet}OH]_{ss}$. Figure made in collaboration with Michael C. Dodd and Tessora Young, University of Washington.

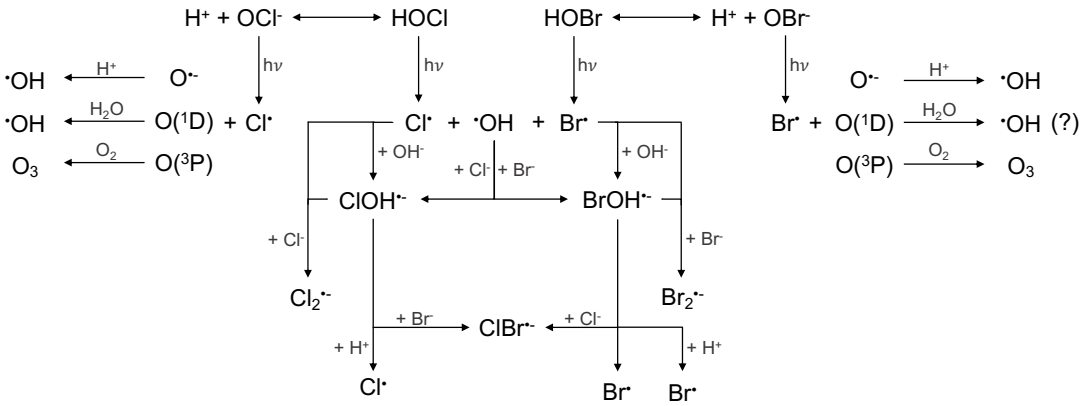

Schematic 5.1. Formation of reactive oxidants from chlorine and bromine photolysis. Reaction marked with a "?" has not been experimentally verified in bromine photolysis. Not all reactions are balanced.

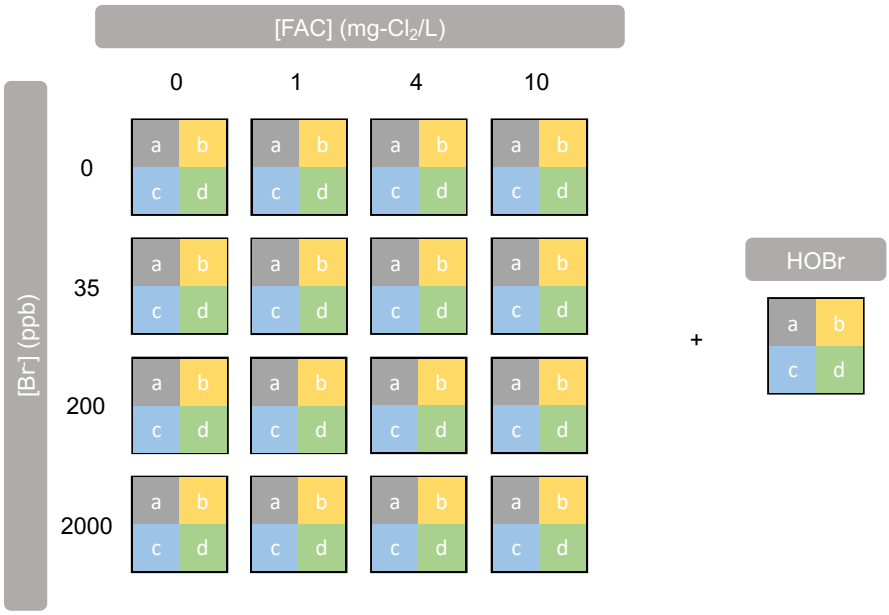

Schematic 5.2. Representation of experimental plan to investigate the formation of DBPs during chlorine photolysis in the presence of bromide. Each of the seventeen samples will undergo four different treatments. (a) dark reaction, (b) photolysis at 254 nm, (c) photolysis in the presence of *t*-BuOH, and (d) photolysis in the presence of *t*-BuOH and absence of O_2.

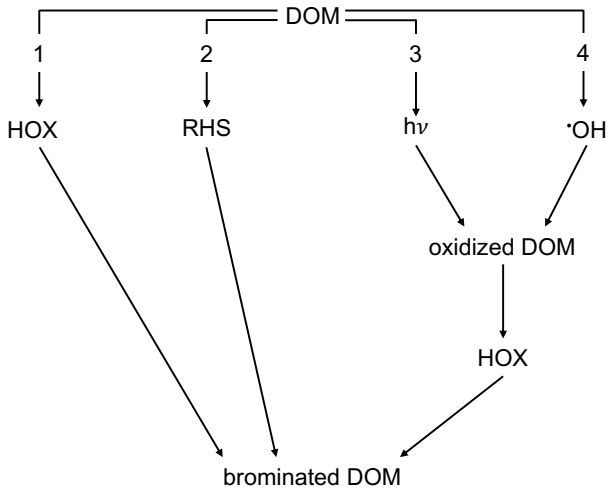

Schematic 5.3. DOM halogenation mechanisms during chlorine and bromine photolysis. (1) Direct reaction of DOM with free chlorine or free bromine. (2) Direct reaction of DOM with reactive halogen species. (3) Reaction of photolyzed DOM with free chlorine or free bromine. (4) Reaction of hydroxyl radical sensitized DOM with free chlorine or free bromine.

Table 5.1. Chlorine and bromine photolysis reactions.

Reaction #	Reaction	Quantum Yield
(1)	$HOCl + h\nu \rightarrow {}^{\bullet}OH + Cl^{\bullet}$	at 254 nm = 0.6 [9] at 311 nm = 1.0 [87] at 365 nm = unknown
(2)	$OCl^- + h\nu \rightarrow O^{\bullet-} + Cl^{\bullet}$	at 254 nm = 0.278 [13] at 311 nm = 0.127 [13] at 365 nm = 0.08 [13]
(3)	$OCl^- + h\nu \rightarrow O(^3P) + Cl^{\bullet}$	at 254 nm = 0.074 [13] at 311 nm = 0.075 [13] at 365 nm = 0.28[13]
(4)	$OCl^- + h\nu \rightarrow O(^1D) + Cl^{\bullet}$	at 254 nm = 0.133 [13] at 311 nm = 0.02 [13] at 365 nm = 0 [13]
(5)	$HOBr + h\nu \rightarrow {}^{\bullet}OH + Br^{\bullet}$	at 254 nm = 0.43 [15]
(6)	$OBr^- + h\nu \rightarrow O^{\bullet-} + Br^{\bullet}$	at 254 nm = 0.26 [15]
(7)	$OBr^- + h\nu \rightarrow O(^3P) + Br^{\bullet}$	unknown
(8)	$OBr^- + h\nu \rightarrow O(^1D) + Br^{\bullet}$	unknown

Table 5.2. Chlorine and bromine speciation reactions.

Reaction #	Reaction	pK_a
(9)	$HOCl \rightarrow OCl^- + H^+$	7.5 [8]
(10)	$HOBr \rightarrow OBr^- + H^+$	8.8 [15]
(11)	$HOCl + Br^- \rightarrow HOBr + Cl^-$	6.8×10^3 [88]
(12)	$OCl^- + Br^- \rightarrow OBr^- + Cl^-$	9.0×10^{-4} [88]

Table 5.3. Subsequent radical reactions during chlorine and bromine photolysis.

Reaction #	Reaction	Rate Constant (M^{-1} s^{-1})
(13)	$O(^3P) + O_2 \rightarrow O_3$	4.0×10^9 [13,25]
(14)	${}^{\bullet}OH + Br^- \rightarrow BrOH^{\bullet-}$	1.1×10^{10} [23]
(15)	$BrOH^{\bullet-} + Br^- \rightarrow Br_2^{\bullet-} + OH^-$	1.9×10^8 [23]
(16)	$BrOH^{\bullet-} + H^+ \rightarrow Br^{\bullet} + H_2O$	4.4×10^{10} [23]
(17)	$Br^{\bullet} + Br^- \rightarrow Br_2^{\bullet-}$	1.2×10^{10} [89]
(18)	$BrOH^{\bullet-} + Cl^- \rightarrow ClBr^{\bullet-}$	1.9×10^8 [90]
(19)	$ClOH^{\bullet-} + Br^- \rightarrow ClBr^{\bullet-}$	1.0×10^9 [90]
(20)	$Br^{\bullet} + Cl^- \rightarrow ClBr^{\bullet-}$	2.3×10^8 [91]
(21)	$Cl^{\bullet} + Br^- \rightarrow ClBr^{\bullet-}$	1.2×10^{10} [91]
(22)	${}^{\bullet}OH + HOBr \rightarrow BrO^{\bullet} + H_2O$	2.0×10^9 [41]
(23)	${}^{\bullet}OH + HOCl \rightarrow ClO^{\bullet} + H_2O$	1.21×10^9 [11]
(24)	$O(^3P) + OCl^- \rightarrow ClO_2^-$	9.4×10^9 [25,47]
(25)	${}^{\bullet}OH + ClO_2^{\bullet} \rightarrow ClO_3^- + H^+$	4.0×10^9 [24,41]

Table 5.4. Identified halogenated aromatic disinfection by-products.

Halogenated Aromatic DBP	**Reference**
2,5-dibromohydroquinone	85
4-bromo-2-chlorophenol	85
4-bromophenol	85
2,4-dibromophenol	85
2,6-dibromo-4-nitrophenol	85
2-bromo-4-chlorophenol	85
2,6-dichloro-4-nitrophenol	85
2,4-dichlorophenol	85
2,4,6-tribromophenol	85
3,5-dibromo-4-hydroxybenzaldehyde	85
2,4,6-trichlorophenol	85,92
2,6-dibromophenol	85
2,6-dichlorophenol	85
3,5-dichloro-4-hydroxybenzaldehyde	92,93
3,5-dichloro-4-hydroxybenzoic acid	92,93
3,5-dichlorosalicylic acid	92,93
3-bromo-5-chloro-4-hydroxybenzaldehyde	92,93
3,5-dibromo-salicylic acid	93
3,5-dibromo-4-hydroxybenzaldehyde	93
3,5-dibromo-4-hydroxybenzoic acid	93
2,6-dibromo-1,4-hydrobenzoquinone	93
2,4,6-tribromophenol	93
2,6-dichloro-4-bromophenol	92
3-bromo-5-chloro-hydroxybenzoic acid	92
3-bromo-5-chlorosalicylic acid	92
2,6-dibromo-4-hydroxybenzaldehyde	92
2,6-dibromo-4-chlorophenol	92
2-bromo-4-nitrophenol	94
5-bromo-4-methylthiophene-2-carboxamide	94
2-bromoterephthalic acid	94
bromophthalic acid	94
dibromosalicylaldehyde	94
dibromonicotinic acid	94
2-acetylamino-3,5-dibromothiophene	94
dibromo-methoxybenzoic acid	94
dibromo-*N*,2-dihydroxybenzamide	94
4,5-dibromophthalic acid	94
2,2-dibromo-1-(4-methylthio)phenyl)ethenone	94
2,3,5-tribromo-1-H-pyridin-4-ol	94
3,5-dibromo-4-hydroxybenzenesulfonic acid	94
3,5-dibromo-alpha-oxo-4-pyridinaceticacidethylester	94
2-bromo-1-(5-bromo-2-hydroxy-3-nitrophenyl)ethenone	94
4,6-dibromo-3-hydroxy-2-nitrobenzoic acid	94
2,4,6-tribromo-resorcinol	94
2,4,6-tribromo-3-hydroxybenzoic acid	94
2-iodine-4,6-dibromophenol	94

bus(prop-2-enyl)3,4-dibromobenzene-1,2-dicarboxylate	94
2,4,6-tribromo-3-hydroxybenzenesulfonic acid	94
2-chlorophenylacetonitrile	95
3,4-dichlorophenylacetonitrile	95

5.6 References

(1) Kolpin, D. W.; Furlong, E. T.; Meyer, M. T.; Thurman, E. M.; Zaugg, S. D.; Barber, L. B.; Buxton, H. T.; Pharmaceuticals, hormones, and other organic wastewater contaminants in U.S. streams, 1999−2000: A national reconnaissance. *Environ. Sci. Technol.* **2002**, 36(6), 1202-1211.

(2) Schwarzenbach, R. P.; Escher, B. I.; Fenner, K.; Hofstetter, T. B.; Johnson, C. A.; von Gunten, U.; Wehrli, B.; The challenge of micropollutants in aquatic systems. *Science* **2006**, 313(5790), 1072-1077.

(3) Mompelat, S.; Thomas, O.; Le Bot, B.; Contamination levels of human pharmaceutical compounds in French surface and drinking water. *J. Environ. Monitor.* **2011**, 13(10), 2929-2939.

(4) Valcárcel, Y.; González Alonso, S.; Rodríguez-Gil, J. L.; Gil, A.; Catalá, M.; Detection of pharmaceutically active compounds in the rivers and tap water of the Madrid region (Spain) and potential ecotoxicological risk. *Chemosphere* **2011**, 84(10), 1336-1348.

(5) Kostich, M. S.; Batt, A. L.; Lazorchak, J. M.; Concentrations of prioritized pharmaceuticals in effluents from 50 large wastewater treatment plants in the us and implications for risk estimation. *Environ. Pollut.* **2014**, 184, 354-359.

(6) Stalter, D.; O'malley, E.; von Gunten, U.; Escher, B. I.; Fingerprinting the reactive toxicity pathways of 50 drinking water disinfection by-products. *Water Res.* **2016**, 91, 19-30.

(7) Walters, D. M.; Jardine, T. D.; Cade, B. S.; Kidd, K. A.; Muir, D. C.; Leipzig-Scott, P.; Trophic magnification of organic chemicals: A global synthesis. *Environ. Sci. Technol.* **2016**, 50(9), 4650-4658.

(8) Watts, M. J.; Linden, K. G.; Chlorine photolysis and subsequent •OH radical production during UV treatment of chlorinated water. *Water Res.* **2007**, 41(13), 2871-2878.

(9) Chuang, Y.-H.; Chen, S.; Chinn, C. J.; Mitch, W. A.; Comparing the UV/monochloramine and UV/free chlorine advanced oxidation processes (AOPs) to the UV/hydrogen peroxide AOP under scenarios relevant to potable reuse. *Environ. Sci. Technol.* **2017**, 51(23), 13859-13868.

(10) Li, W.; Jain, T.; Ishida, K.; Remucal, C. K.; Liu, H.; A mechanistic understanding of the degradation of trace organic contaminants by UV/hydrogen peroxide, UV/persulfate and UV/free chlorine for water reuse. *Environ. Sci.: Water Res. Technol.* **2017**, 3(1), 128-138.

(11) Bulman, D. M.; Mezyk, S. P.; Remucal, C. K.; The impact of pH and irradiation wavelength on the production of reactive oxidants during chlorine photolysis. *Environ. Sci. Technol.* **2019**, 53(8), 4450-4459.

(12) Buxton, G. V.; Subhani, M. S.; Radiation chemistry and photochemistry of oxychlorine ions. Part 1. Radiolysis of aqueous solutions of hypochlorite and chlorite ions. *J. Chem. Soc., Faraday Trans. 1* **1972**, 68, 947-957.

(13) Buxton, G. V.; Subhani, M. S.; Radiation chemistry and photochemistry of oxychlorine ions. Part 2. Photodecomposition of aqueous solutions of hypochlorite ions. *J. Chem. Soc., Faraday Trans. 1* **1972**, 68, 958-969.

(14) Nowell, L. H.; Hoigné, J.; Photolysis of aqueous chlorine at sunlight and ultraviolet wavelengths. 2. Hydroxyl radical production. *Water Res.* **1992**, 26(5), 599-605.

(15) Guo, K.; Zheng, S.; Zhang, X.; Zhao, L.; Ji, S.; Chen, C.; Wu, Z.; Wang, D.; Fang, J.; Roles of bromine radicals and hydroxyl radicals in the degradation of micropollutants by the UV/bromine process. *Environ Sci Technol* **2020**,

(16) Cheng, S.; Zhang, X.; Yang, X.; Shang, C.; Song, W.; Fang, J.; Pan, Y.; The multiple role of bromide ion in PPCPs degradation under UV/chlorine treatment. *Environ. Sci. Technol.* **2018**, 52(4), 1806-1816.
(17) Agus, E.; Voutchkov, N.; Sedlak, D. L.; Disinfection by-products and their potential impact on the quality of water produced by desalination systems: A literature review. *Desalination* **2009**, 237(1-3), 214-237.
(18) von Gunten, U.; Ozonation of drinking water: Part 2. Disinfection and by-product formation in presence of bromide, iodide, or chlorine. *Water Res.* **2003**, 37, 1469-1487.
(19) Heller-Grossman, L.; Manka, J.; Limoni-Relis, B.; Rebhun, M.; Thm, haloacetic acids and other organic DBPs formation in disinfection of bromide rich sea of Galilee (Lake Kinneret) water. *Water Sci. Technol. Water Supply* **2001**, 1(2), 259-266.
(20) Magazinovic, R. S.; Nicholson, B. C.; Mulcahy, D. E.; Davey, D. E.; Bromide levels in natural waters: Its relationship to levels of both chloride and total dissolved solids and the implications for water treatment. *Chemosphere* **2004**, 57(4), 329-335.
(21) Zhao, Q.; Shang, C.; Zhang, X.; Effects of bromide on UV/chlorine advanced oxidation process. *Water Sci. Technol.: Water Supply* **2009**, 9(6), 627-634.
(22) Treinin, A.; The photochemistry of oxyanions. *Isr. J. Chem.* **1970**, 8, 103-113.
(23) Zehavi, D.; Rabani, J.; Oxidation of aqueous bromide ions by hydroxyl radicals. Pulse radiolytic investigation. *J. Phys. Chem.* **1972**, 76(3), 312-319.
(24) Klaning, U. K.; Sehested, K.; Holcman, J.; Standard Gibbs energy of formation of the hydroxyl radical in aqueous solution. Rate constants for the reaction $ClO_2^- + O_3 = O_3^- + ClO_2$. *J. Phys. Chem.* **1985**, 89, 760-763.
(25) Kläning, U. K.; Sehested, K.; Wolff, T.; Ozone formation in laser flash photolysis of oxoacids and oxoanions of chlorine and bromine. *J. Chem. Soc., Faraday Trans. 1* **1984**, 80, 2969-2979.
(26) Zhang, K.; Parker, K. M.; Halogen radical oxidants in natural and engineered aquatic systems. *Environ. Sci. Technol.* **2018**, 52(17), 9579-9594.
(27) Allard, S.; Tan, J.; Joll, C. A.; von Gunten, U.; Mechanistic study on the formation of Cl-/Br-/I-trihalomethanes during chlorination/chloramination combined with a theoretical cytotoxicity evaluation. *Environ. Sci. Technol.* **2015**, 49(18), 11105-11114.
(28) Ding, S.; Deng, Y.; Bond, T.; Fang, C.; Cao, Z.; Chu, W.; Disinfection byproduct formation during drinking water treatment and distribution: A review of unintended effects of engineering agents and materials. *Water Res.* **2019**, 160, 313-329.
(29) Bulman, D. M.; Remucal, C. K.; The role of reactive halogen species in disinfection by-product formation during chlorine photolysis. *Environ. Sci. Technol.* **2020**, Accepted,
(30) Daiber, E. J.; Demarini, D. M.; Ravuri, S. A.; Liberatore, H. K.; Cuthbertson, A. A.; Thompson-Klemish, A.; Byer, J. D.; Schmid, J. E.; Afifi, M. Z.; Blatchley, E. R.; Richardson, S. D.; Progressive increase in disinfection byproducts and mutagenicity from source to tap to swimming pool and spa water: Impact of human inputs. *Environ. Sci. Technol.* **2016**, 50(13), 6652-6662.
(31) Plewa, M. J.; Wagner, E. D.; Richardson, S. D.; TIC-tox: A preliminary discussion on identifying the forcing agents of DBP-mediated toxicity of disinfected water. *J. Environ. Sci.* **2017**, 58, 208-216.
(32) Xu, J.; Kralles, Z. T.; Dai, N.; Effects of sunlight on the trichloronitromethane formation potential of wastewater effluents: Dependence on nitrite concentration. *Environ. Sci. Technol.* **2019**, 53(8), 4285-4294.

(33) Plewa, M. J.; Wagner, E. D.; Metz, D. H.; Kashinkunti, R.; Jamriska, K. J.; Meyer, M.; Differential toxicity of drinking water disinfected with combinations of ultraviolet radiation and chlorine. *Environ. Sci. Technol.* **2012**, 46(14), 7811-7817.
(34) Maizel, A. C.; Remucal, C. K.; Molecular composition and photochemical reactivity of size-fractionated dissolved organic matter. *Environ. Sci. Technol.* **2017**, 51(4), 2113-2123.
(35) Maizel, A. C.; Remucal, C. K.; The effect of advanced secondary municipal wastewater treatment on the molecular composition of dissolved organic matter. *Water Res.* **2017**, 122, 42-52.
(36) Berg, S. M.; Whiting, Q. T.; Herrli, J. A.; Winkels, R.; Wammer, K. H.; Remucal, C. K.; The role of dissolved organic matter composition in determining photochemical reactivity at the molecular level. *Environ. Sci. Technol.* **2019**, 53(20), 11725-11734.
(37) Gonsior, M.; Schmitt-Kopplin, P.; Stavklint, H.; Richardson, S. D.; Hertkorn, N.; Bastviken, D.; Changes in dissolved organic matter during the treatment processes of a drinking water plant in Sweden and formation of previously unknown disinfection byproducts. *Environ. Sci. Technol.* **2014**, 48(21), 12714-12722.
(38) U.S. E.P.A.; Stage 1 disinfectants and disinfection byproducts rule (Stage 1 DBPR) 63 FR 69390, December 16, 1998, 63(241). **1998**.
(39) U.S. E.P.A.; Contaminant candidate list 4. **2016**.
(40) Gan, W.; Huang, S.; Ge, Y.; Bond, T.; Westerhoff, P.; Zhai, J.; Yang, X.; Chlorite formation during clo_2 oxidation of model compounds having various functional groups and humic substances. *Water Res.* **2019**, 159, 348-357.
(41) Kläning, U. K.; Wolff, T.; Laser flash photolysis of HClO, ClO^-, HBrO, and BrO^- in aqueous solution. Reactions of Cl^- and Br^- atoms. *Ber. Bunsenges. Phys. Chem.* **1985**, 89, 243-245.
(42) Hoigné, J.; Bader, H.; Haag, W. R.; Staehelin, J.; Rate constants of reactions of ozone with organic and inorganic compounds in water III. Inorganic compounds and radicals. *Water Research* **1985**, 19(8), 993-1004.
(43) Hoigné, J.; Bader, H.; Kinetics of reactions of chlorine dioxide (OClO) in water I. Rate constants for inorganic and organic compounds. *Water Res.* **1994**, 28(1), 45-55.
(44) Hoigné, J.; Bader, H.; Kinetik typischer reaktionen von chlorodioxid mit wasserinhaltsstoffen. *Vom Wasser* **1982**, 59, 253-267.
(45) Guo, K.; Wu, Z.; Shang, C.; Yao, B.; Hou, S.; Yang, X.; Song, W.; Fang, J.; Radical chemistry and structural relationships of PPCP degradation by UV/chlorine treatment in simulated drinking water. *Environ. Sci. Technol.* **2017**, 51(18), 10431-10439.
(46) Sun, P.; Lee, W.-N.; Zhang, R.; Huang, C.-H.; Degradation of DEET and caffeine under UV/chlorine and simulated sunlight/chlorine conditions. *Environ. Sci. Technol.* **2016**, 50(24), 13265-13273.
(47) Buxton, G. V.; Subhani, M. S.; Radiation chemistry and photochemistry of oxychlorine ions. Part 3. Photodecomposition of aqueous solutions of chlorite ions. *J. Chem. Soc., Faraday Trans. 1* **1972**, 68, 970-977.
(48) Fischbacher, A.; Löppenberg, K.; von Sonntag, C.; Schmidt, T. C.; A new reaction pathway for bromite to bromate in the ozonation of bromide. *Environ. Sci. Technol.* **2015**, 49(19), 11714-11720.
(49) Chen, Z.; Li, X.; Zhang, S.; Jin, J.; Song, X.; Wang, X.; Tratnyek, P. G.; Overlooked role of peroxides as free radical precursors in advanced oxidation processes. *Environ. Sci. Technol.* **2019**, 53(4), 2054-2062.

(50) Fujii, M.; Dang, T. C.; Bligh, M. W.; Rose, A. L.; Waite, T. D.; Effect of natural organic matter on iron uptake by the freshwater cyanobacterium *microcystis aeruginosa*. *Environ. Sci. Technol.* **2014**, 48(1), 365-374.
(51) Liu, X.; Liu, R.; Zhu, B.; Ruan, T.; Jiang, G.; Characterization of carbonyl disinfection by-products during ozonation, chlorination, and chloramination of dissolved organic matters. *Environmental Science & Technology* **2020**, 54(4), 2218-2227
(52) Appiani, E.; Page, S. E.; Mcneill, K.; On the use of hydroxyl radical kinetics to assess the number-average molecular weight of dissolved organic matter. *Environ. Sci. Technol.* **2014**, 48 (20), 11794-11802.
(53) Harris, B. D.; Brown, T. A.; Mcgehee, J. L.; Houserova, D.; Jackson, B. A.; Buchel, B. C.; Krajewski, L. C.; Whelton, A. J.; Stenson, A. C.; Characterization of disinfection by-products from chromatographically isolated nom through high-resolution mass spectrometry. *Environ. Sci. Technol.* **2015**, 49(24), 14239-14248.
(54) Chu, W.; Gao, N.; Yin, D.; Krasner, S. W.; Mitch, W. A.; Impact of UV/H_2O_2 pre-oxidation on the formation of haloacetamides and other nitrogenous disinfection byproducts during chlorination. *Environ. Sci. Technol.* **2014**, 48(20), 12190-12198.
(55) Legrini, O.; Oliveros, E.; Braun, A. M.; Photochemical processes for water treatment. *Chem. Rev.* **1993**, 93(2), 671-698.
(56) Shah, A. D.; Dotson, A. D.; Linden, K. G.; Mitch, W. A.; Impact of UV disinfection combined with chlorination/chloramination on the formation of halonitromethanes and haloacetonitriles in drinking water. *Environ. Sci. Technol.* **2011**, 45(8), 3657-3664.
(57) Forsyth, J. E.; Zhou, P.; Mao, Q.; Asato, S. S.; Meschke, J. S.; Dodd, M. C.; Enhanced inactivation of bacillus subtilis spores during solar photolysis of free available chlorine. *Environ. Sci. Technol.* **2013**, 47(22), 12976-12984.
(58) Lau, S. S.; Dias, R. P.; Martin-Culet, K. R.; Race, N. A.; Schammel, M. H.; Reber, K. P.; Roberts, A. L.; Sivey, J. D.; 1, 3, 5-trimethoxybenzene (TMB) as a new quencher for preserving redox-labile disinfection byproducts and for quantifying free chlorine and free bromine. *Environ. Sci.: Water Res. Technol.* **2018**, 4(7), 926-941.
(59) Fang, J.; Fu, Y.; Shang, C.; The roles of reactive species in micropollutant degradation in the UV/free chlorine system. *Environ. Sci. Technol.* **2014**, 48(3), 1859-1868.
(60) Leitzke, A.; Reisz, E.; Flyunt, R.; von Sonntag, C.; The reactions of ozone with cinnamic acids: Formation and decay of 2-hydroperoxy-2-hydroxyacetic acid. *J. Chem. Soc., Perkin Trans. 2* **2001**, (5), 793-797.
(61) Weishaar, J. L.; Aiken, G. R.; Bergamaschi, B. A.; Fram, M. S.; Fujii, R.; Mopper, K.; Evaluation of specific ultraviolet absorbance as an indicator of the chemical composition and reactivity of dissolved organic carbon. *Environ. Sci. Technol.* **2003**, 37(20), 4702-4708.
(62) Helms, J. R.; Stubbins, A.; Ritchie, J. D.; Minor, E. C.; Kieber, D. J.; Mopper, K.; Absorption spectral slopes and slope ratios as indicators of molecular weight, source, and photobleaching of chromophoric dissolved organic matter. *Limnol. Oceanogr.* **2008**, 53(3), 955-969.
(63) Ziegler, G.; Gonsior, M.; Fisher, D. J.; Schmitt-Kopplin, P.; Tamburri, M. N.; Formation of brominated organic compounds and molecular transformations in dissolved organic matter (DOM) after ballast water treatment with sodium dichloroisocyanurate dihydrate (DICD). *Environ. Sci. Technol.* **2019**, 53(14), 8006-8016.
(64) Dittmar, T.; Koch, B.; Hertkorn, N.; Kattner, G.; A simple and efficient method for the solid-phase extraction of dissolved organic matter (SPE-DOM) from seawater. *Limnol. Oceanogr.: Methods* **2008**, 6, 230-235.

(65) Koch, B. P.; Dittmar, T.; Witt, M.; Kattner, G.; Fundamentals of molecular formula assignment to ultrahigh resolution mass data of natural organic matter. *Anal. Chem.* **2007**, 79(4), 1758-1763.
(66) Lavonen, E. E.; Kothawala, D. N.; Tranvik, L. J.; Gonsior, M.; Schmitt-Kopplin, P.; Köhler, S. J.; Tracking changes in the optical properties and molecular composition of dissolved organic matter during drinking water production. *Water Res.* **2015**, 85, 286-294.
(67) Zhang, H.; Zhang, Y.; Shi, Q.; Ren, S.; Yu, J.; Ji, F.; Luo, W.; Yang, M.; Characterization of low molecular weight dissolved natural organic matter along the treatment trait of a waterworks using Fourier transform ion cyclotron resonance mass spectrometry. *Water Res.* **2012**, 46(16), 5197-5204.
(68) Hodgeson, J. W.; Cohen, A. L.; Munch, D. J.; Hautman, D. P.; Method 551.1. Determination of chlorination disinfection byproducts, chlorinated solvents, and halogenated pesticides/herbicides in drinking water by liquid–liquid extractions and gas chromatography with electron capture detection. *U.S. Environmental Protection Agency, Cincinnati* **1995**,
(69) Hodgeson, J. W.; Collins, J.; Barth, R. E.; Munch, D. J.; Munch, J. W.; Pawlecki, A. M.; Method 552.2 determination of haloacetic acids and dalapon in drinking water by liquid-liquid extraction, derivatization and gas chromatography with electron capture detection. *U.S. Environmental Protection Agency, Cincinnati* **1995**,
(70) Jeong, C. H.; Wagner, E. D.; Siebert, V. R.; Anduri, S.; Richardson, S. D.; Daiber, E. J.; Mckague, A. B.; Kogevinas, M.; Villanueva, C. M.; Goslan, E. H.; Luo, W.; Isabelle, L. M.; Pankow, J. F.; Grazuleviciene, R.; Cordier, S.; Edwards, S. C.; Righi, E.; Nieuwenhuijsen, M. J.; Plewa, M. J.; Occurrence and toxicity of disinfection byproducts in european drinking waters in relation with the hiwate epidemiology study. *Environ. Sci. Technol.* **2012**, 46(21), 12120-12128.
(71) Grebel, J. E.; Pignatello, J. J.; Mitch, W. A.; Effect of halide ions and carbonates on organic contaminant degradation by hydroxyl radical-based advanced oxidation processes in saline waters. *Environ. Sci. Technol.* **2010**, 44(17), 6822-6828.
(72) Yang, Y.; Pignatello, J. J.; Ma, J.; Mitch, W. A.; Comparison of halide impacts on the efficiency of contaminant degradation by sulfate and hydroxyl radical-based advanced oxidation processes (AOPs). *Environ. Sci. Technol.* **2014**, 48(4), 2344-2351.
(73) Remucal, C. K.; Manley, D.; Emerging investigators series: The efficacy of chlorine photolysis as an advanced oxidation process for drinking water treatment. *Environ. Sci.: Water Res. Technol.* **2016**, 2(4), 565-579.
(74) Dodd, M. C.; Buffle, M.-O.; von Gunten, U.; Oxidation of antibacterial molecules by aqueous ozone: moiety-specific reaction kinetics and application to ozone-based wastewater treatment. *Environ. Sci. Technol.* **2006**, 40(6), 1969-1977.
(75) von Gunten, U.; Ozonation of drinking water: Part 1. Oxidation kinetics and products formation. *Water Res.* **2003**, 37, 1443-1467.
(76) Young, T. R.; Li, W.; Guo, A.; Korshin, G. V.; Dodd, M. C.; Characterization of disinfection byproduct formation and associated changes to dissolved organic matter during solar photolysis of free available chlorine. *Water Res.* **2018**, 146, 318-327.
(77) Li, C.; Wang, D.; Xu, X.; Wang, Z.; Formation of known and unknown disinfection by-products from natural organic matter fractions during chlorination, chloramination, and ozonation. *Sci. Total Environ.* **2017**, 587-588, 177-184.

(78) Phungsai, P.; Kurisu, F.; Kasuga, I.; Furumai, H.; Changes in dissolved organic matter composition and disinfection byproduct precursors in advanced drinking water treatment processes. *Environ. Sci. Technol.* **2018**, 52(6), 3392-3401.
(79) Varanasi, L.; Coscarelli, E.; Khaksari, M.; Mazzoleni, L. R.; Minakata, D.; Transformations of dissolved organic matter induced by UV photolysis, hydroxyl radicals, chlorine radicals, and sulfate radicals in aqueous-phase UV-based advanced oxidation processes. *Water Res.* **2018**, 135, 22-30.
(80) Lei, Y.; Cheng, S.; Luo, N.; Yang, X.; An, T.; Rate constants and mechanisms of the reactions of $Cl^{\bullet}$ and $Cl_2^{\bullet-}$ with trace organic contaminants. *Environ. Sci. Technol.* **2019**, 53(19), 11170-11182.
(81) Wols, B. A.; Hofman-Caris, C. H. M.; Review of photochemical reaction constants of organic micropollutants required for UV advanced oxidation processes in water. *Water Res.* **2012**, 46(9), 2815-2827.
(82) Richardson, S. D.; Ternes, T. A.; Water analysis: Emerging contaminants and current issues. *Anal. Chem.* **2011**, 83(12), 4614-4648.
(83) Richardson, S. D.; Ternes, T. A.; Water analysis: Emerging contaminants and current issues. *Anal. Chem.* **2018**, 90(1), 398-428.
(84) Yang, M.; Zhang, X.; Liang, Q.; Yang, B.; Application of (LC/)MS/MS precursor ion scan for evaluating the occurrence, formation and control of polar halogenated DBPs in disinfected waters: A review. *Water Res.* **2019**, 158, 322-337.
(85) Yang, M.; Zhang, X.; Comparative developmental toxicity of new aromatic halogenated DBPs in a chlorinated saline sewage effluent to the marine *polychaete platynereis dumerilii*. *Environ. Sci. Technol.* **2013**, 47(19), 10868-10876.
(86) Wang, D.; Bolton, J. R.; Andrews, S. A.; Hofmann, R.; Formation of disinfection by-products in the ultraviolet/chlorine advanced oxidation process. *Sci. Total Environ.* **2015**, 518-519, 49-57.
(87) Molina, M. J.; Ishiwata, T.; Molina, L. T.; Production of hydroxyl from photolysis of hypochlorous acid at 307-309 nm. *J.Phys. Chem.* **1980**, 84(8), 821-826.
(88) Kumar, K.; Margerum, D. W.; Kinetics and mechanism of general-acid-assisted oxidation of bromide by hypochlorite and hypochlorous acid. *Inorg. Chem.* **1987**, 26(16), 2706-2711.
(89) Merényi, G.; Lind, J.; Reaction mechanism of hydrogen abstraction by the bromine atom in water. *J.Am. Chem. Soc.* **1994**, 116, 7872-7876.
(90) Matthew, B. M.; Anastasio, C.; A chemical probe technique for the determination of reactive halogen species in aqueous solution: Part 1–bromide solutions. *Atmos. Chem. Phys.* **2006**, 6, 2423-2437.
(91) Donati, A. *Spectroscopic and kinetic investigations of halogen containing radicals in the tropospheric aquesous phase* (University of Leipzig, **2002**).
(92) Pan, Y.; Zhang, X.; Four groups of new aromatic halogenated disinfection byproducts: Effect of bromide concentration on their formation and speciation in chlorinated drinking water. *Environ. Sci. Technol.* **2013**, 47(3), 1265-1273.
(93) Jiang, J.; Zhang, X.; Zhu, X.; Li, Y.; Removal of intermediate aromatic halogenated DBPs by activated carbon adsorption: A new approach to controlling halogenated DBPs in chlorinated drinking water. *Environ. Sci. Technol.* **2017**, 51(6), 3435-3444.
(94) Wang, J.; Hao, Z.; Shi, F.; Yin, Y.; Cao, D.; Yao, Z.; Liu, J.; Characterization of brominated disinfection byproducts formed during the chlorination of aquaculture seawater. *Environ. Sci. Technol.* **2018**, 52(10), 5662-5670.

(95) Zhang, D.; Chu, W.; Yu, Y.; Krasner, S. W.; Pan, Y.; Shi, J.; Yin, D.; Gao, N.; Occurrence and stability of chlorophenylacetonitriles: A new class of nitrogenous aromatic DBPs in chlorinated and chloraminated drinking waters. *Environ. Sci. Tech. Lett.* **2018**, 5(6), 394-399.

Chapter 6

Conclusions

6.1 Summary of Findings

The purpose of this dissertation was to mechanistically investigate the formation of reactive oxidants, dissolved organic matter transformation, and the formation of high-molecular weight disinfection by-products during chlorine photolysis. The state of knowledge on chlorine photolysis is critically reviewed in Chapter 2. Chlorine photolysis has been shown to degrade many different organic contaminants in bench-scale studies. The impact of chlorine photolysis on disinfection by-product formation was not conclusive across studies with a variety of treatment conditions.

The formation of reactive oxidant was evaluated under different treatment conditions and experimental results were compared against a series of kinetic models (Chapter 3). We used kinetic probe experiments to measure the formation of $^{\bullet}OH$, $Cl^{\bullet}$, $Cl_2^{\bullet-}$, and O_3 during 254, 311, and 365 nm photolysis in buffered high purity water at pH 6-9. Radical steady-state concentrations were highest at low pH and wavelength due to the higher quantum yield of HOCl versus OCl^- and the higher molar absorptivity of both forms of chlorine at shorter wavelengths. Ozone formation was greatest at higher pH due to the importance of OCl^- in forming the O_3 precursor, $O(^3P)$. This study was the first to report the formation of ozone during 254 nm irradiation of chlorine. All previous studies have assumed that ozone does not form at shorter wavelengths, resulting in an overemphasis on other oxidants, such as $ClO^{\bullet}$, in contaminant degradation studies. The investigation of chlorine photolysis at 311 and 365 nm demonstrates that chlorine photolysis is viable for solar treatment applications.

The transformation of dissolved organic matter and the formation of disinfection by-products were evaluated using bulk and molecular techniques, in combination with probe measurements of reactive oxidant concentrations (Chapter 4). Reactive oxidant steady-state concentrations decrease in natural water, compared to high purity water, due to scavenging by organic and inorganic carbon. Reaction with organic carbon forms carbon-centered radicals as evidenced by the faster loss of chlorine in the presence of dissolved organic matter. Dissolved organic matter reacts with light, chlorine, and reactive oxidants to become more aliphatic and reduced in nature. Dissolved organic matter transformed during chlorine photolysis is more susceptible to dark reaction with chlorine, which may result in increased formation of potentially harmful disinfection by-products in the distribution system. Additionally, this work demonstrates that reactive chlorine species, namely $Cl^{\bullet}$ and $Cl_2^{\bullet-}$, react directly with dissolved organic matter to form novel high-molecular weight disinfection by-products.

A set of experiments were proposed to investigate the impact of bromide on oxidant formation, dissolved organic matter transformation, and disinfection by-product formation during chlorine photolysis (Chapter 5). Bromide reacts with free chlorine ($HOCl/OCl^-$) to form free bromine ($HOBr/OBr^-$). Free bromine can undergo photolysis to form reactive bromine species analogous to the formation of reactive chlorine species during chlorine photolysis. Free bromine is more reactive towards dissolved organic matter than free chlorine and can form brominated disinfection by-products that are more toxic than their chlorinated analogues. Investigations of free bromine photolysis of model organic compounds have shown that reactive bromine species are not important for direct halogenation reactions, but that transformed organic compounds can be brominated more readily by free bromine. There has been no previous investigation of high-

molecular weight disinfection by-product formation during chlorine photolysis in the presence of bromide.

Chlorine photolysis uses reactive oxidants to degrade organic contaminants in water. The primary oxidant, •OH, is produced most effectively at low pH and short irradiation wavelength so contaminant removal will be optimized under these conditions. However, the steady-state concentration of Cl• is also greatest under the same conditions and reactive chlorine species are important in forming novel high-molecular weight disinfection by-products. The human health risks of these high-molecular weight disinfection by-products have not been evaluated. Overall chlorine photolysis is an efficient way to produce •OH and degrade organic contaminants, both in engineered systems at 254 nm and in solar treatment applications. However, the human health risk of potentially harmful disinfection by-products may limit the utility of this process if total organic halogen or high-molecular weight disinfection by-products are regulated in drinking water.

6.2 Directions for Future Research

The degradation of organic contaminants during chlorine photolysis in engineered systems (i.e., at 254 nm) has been thoroughly investigated at the bench scale by many researchers around the world. Future work on chlorine photolysis in engineered systems should focus on scaling-up to full-scale treatment. Further research in the area of solar treatment could benefit developing regions without the necessary infrastructure for centralized drinking water treatment. There should be a deeper investigation into the use of cinnamic acid and 1,3,5-trimethoxybenzene as probe compounds during chlorine photolysis. Additionally, further investigation on the toxicity of high-molecular weight disinfection by-products and formation of nitrogen-containing disinfection by-products is warranted.

This research has shown that solar treatment applications are feasible for chlorine photolysis. There has been some previous investigation of specific contaminant degradation or pathogen inactivation in solar/free chlorine treatments,[1–4] but this area could be expanded as chlorine photolysis is the only potential photochemical advanced oxidation process that can be used in solar treatment. In addition to degrading organic contaminants, chlorine photolysis is effective in inactivating pathogens, including chlorine-resistant pathogens.[5] The implications of contaminant removal and pathogen inactivation using solar treatment are important in developing regions where the infrastructure for centralized drinking water treatment do not exist. Moving forward, there should be full-scale studies in developing regions where chlorine photolysis is used in individual households to treat drinking water.

Probe compounds are crucial in studying advanced oxidation processes and it is important to understand and evaluate any potential interferences. Cinnamic acid is a selective probe compound used to measure the formation of ozone. During experiments for Chapter 4, the formation of a direct photoproduct was discovered. This direct photoproduct can impact the measurement of benzaldehyde by high-performance liquid chromatography. Formation of a direct photoproduct means that some cinnamic acid is not available for reaction with ozone, which could impact the accuracy of the measurement. Similarly, 1,3,5-trimethoxybenzene (TMB) is used to measure the concentration of free chlorine and free bromine in solution. $Cl^{\bullet}$ is known to react with TMB to form the same chlorinated product as free chlorine. In this dissertation, TMB was used as a quencher and was not present during photolysis. However, TMB could be used *in situ* (e.g., during UV/H_2O_2 with elevated chloride or bromide) to measure the formation of reactive halogen species. The full utility of this probe has not been investigated.

The human health benefits of contaminant removal cannot be evaluated without determining the toxicity of the treated sample. The toxicity of high-molecular weight disinfection by-products is unknown but previously identified halogenated organic compounds are generally more toxic than small aliphatic disinfection by-products. Nitrogen-containing disinfection by-products often have increased toxicity relative to other halogenated disinfection by-products. The formation of fifteen novel high-molecular weight nitrogen-containing disinfection by-products was discovered in Chapter 4. The formation of these N-DBPs was attributed to reaction of reactive chlorine species, but further investigation into the mechanism of formation is needed.

6.3 References

(1) Chan, P. Y.; Gamal El-Din, M.; Bolton, J. R.; A solar-driven UV/chlorine advanced oxidation process. *Water Res.* **2012**, 46(17), 5672-5682.

(2) Hua, Z.; Guo, K.; Kong, X.; Lin, S.; Wu, Z.; Wang, L.; Huang, H.; Fang, J.; PPCP degradation and DBP formation in the solar/free chlorine system: Effects of pH and dissolved oxygen. *Water Res.* **2019**, 150, 77-85.

(3) Sun, P.; Lee, W.-N.; Zhang, R.; Huang, C.-H.; Degradation of DEET and caffeine under UV/chlorine and simulated sunlight/chlorine conditions. *Environ. Sci. Technol.* **2016**, 50(24), 13265-13273.

(4) Forsyth, J. E.; Zhou, P.; Mao, Q.; Asato, S. S.; Meschke, J. S.; Dodd, M. C.; Enhanced inactivation of *bacillus subtilis* spores during solar photolysis of free available chlorine. *Environ. Sci. Technol.* **2013**, 47(22), 12976-12984.

(5) Zhou, P.; Di Giovanni, G. D.; Meschke, J. S.; Dodd, M. C.; Enhanced inactivation of *Cryptosporidium parvum* oocysts during solar photolysis of free available chlorine. *Environ. Sci. Tech. Lett.* **2014**, 1(11), 453-458.

Appendix A

Supplementary Material for Chapter 2

A1. Supplementary Data

Tables A1-A4 summarize the experimental conditions for studies that quantified the formation of disinfection by-products (DBPs) by chlorine in the presence and absence of light. The type and fluence of the light source, the experimental duration (i.e., time between chlorine addition and DBP measurement), the free available chlorine (FAC) concentration, pH, and dissolved organic carbon (DOC) concentration are indicated for each data point. The difference between the concentration of DBP measured in the irradiated solutions and in dark control experiments is presented graphically in Figure 2.3 in the manuscript. Note that full-scale studies that pre-chlorinated water before any treatment are not included due to the elevated background DBP concentrations detected using that approach.

Table A1. Summary of experimental conditions for studies quantifying the formation of trihalomethanes (THMs) produced by chlorine in the presence and absence of light. The studies quantified either chloroform alone (denoted $CHCl_3$) or total trihalomethanes (denoted TTHM; the sum of bromodichloromethane, bromoform, chloroform, and dibromochloromethane).

DBPs Quantified	Light Source	Fluence (mJ/cm^2)	Duration (min)	pH	[FAC] (mg/L as Cl_2)	[DOC] (mg/L)	[DBP] in Irradiated Experiment (µg/L)	[DBP] in Dark Experiment (µg/L)	Reference
$CHCl_3$	Hg	N/A	60	8.1	2	4	4.2	9.5	1
				6.5			2.9	3.1	
	LP UV	60	4,320	7	7	5	122	87	2
				7		5	78	55	
				6.8		1.8	35	24	
				7		5	80	47	
	MP UV			7		5	92	87	
				7		5	77	55	
				6.8		1.8	40	24	
				7		5	86	47	
TTHM	LP UV	3,900	120	7.5	10	2.6	14	13	3
	UV-A	7,000					24	13	
	MP UV	1,820	1	6.5	2	3.5	7	4	4
					6		8	6	
					10		5	4	
				7.5	2		8	7	
					6		8	10	
					10		6	8	
				8.5	2		10	9	
					6		10	11	
					10		7	9	
			1,440	6.5	6.5		100	50	
				7.5			100	65	
				8.5			120	85	
	LP UV	800	120	7.2	1.5	3.2	15	31	5
			1,440				17	40	
			4,320				19	50	

Table A2. Summary of experimental conditions for studies quantifying the formation of haloacetic acids (HAAs) produced by chlorine in the presence and absence of light. The studies quantified the sum of dichloroacetic acid (DCAA) and trichloroacetic acid (TCAA; denoted DCAA + TCAA), the five regulated HAAs (denoted HAA5; the sum of bromoacetic acid, dibromoacetic acid, dichloroacetic acid, monochloroacetic acid, and trichloroacetic acid), or nine HAAs (denoted HAA9; the sum of HAA5, bromochloroacetic acid, bromodichloroacetic acid, chlorodibromoacetic acid, and tribromoacetic acid).

DBPs Quantified	Light Source	Fluence (mJ/cm^2)	Duration (min)	pH	[FAC] (mg/L as Cl_2)	[DOC] (mg/L)	[DBP] in Irradiated Experiment (µg/L)	[DBP] in Dark Experiment (µg/L)	Reference
DCAA + TCAA	LP UV	60	5	7	7	5	57	76	2
				7		5	118	108	
				7		5	80	68	
				6.8		1.8	48	37	
	MP UV			7		5	66	76	
				7		5	98	108	
				6.8		1.8	50	37	
				7		5	95	68	
HAA5	LP UV	3,900	120	7.5	10	2.6	37	17	3
	UV-A	7,000					31	17	
HAA9	LP UV	3,900					42	27	
	UV-A	7,000					47	27	
	MP UV	1,820	1	6.5	2	3.5	8	3	4
					6		7	3	
					10		4	2	
				7.5	2		13	3	
					6		9	3	
					10		5	3	
				8.5	2		15	3	
					6		8	3	
					10		5	2	
			1,440	6.5	6.5		140	70	
				7.5			100	75	
				8.5			70	60	
HAA5	LP UV	800	30	7.2	1.5	3.2	10	22	5
			120				12	25	
			1,440				18	34	
			4,320				22	39	

Table A3. Summary of experimental conditions for studies quantifying the formation of haloacetonitriles (HANs) produced by chlorine in the presence and absence of light. Both studies quantified the sum of bromochloroacetonitrile, dibromoacetonitrile, dichloroacetonitrile, and trichloroacetonitrile.

DBPs Quantified	Light Source	Fluence (mJ/cm^2)	Duration (min)	pH	[FAC] (mg/L as Cl_2)	[DOC] (mg/L)	[DBP] in Irradiated Experiment (µg/L)	[DBP] in Dark Experiment (µg/L)	Reference
HAN	MP UV	1,820	1	6.5	2	3.5	2.5	0	4
					6		2.5	0	
					10		1.5	0	
				7.5	2		4	0.5	
					6		3	0.5	
					10		1.5	0	
				8.5	2		5	0.5	
					6		3	0.5	
					10		1.5	0.5	
			1,440	6.5	6.5		30	9	
				7.5			16	8	
				8.5			4	3	
	LP UV	800	30	7.2	1.5	3.2	17	8	5
			120				22	11	
			1,440				26	14	
			4,320				40	20	

Table A4. Summary of experimental conditions for studies quantifying the formation of total organic halides (TOX) or adsorbable organic halides (AOX).

DBPs Quantified	Light Source	Fluence (mJ/cm^2)	Duration (min)	pH	[FAC] (mg/L as Cl_2)	[DOC] (mg/L)	[DBP] in Irradiated Experiment (µg/L)	[DBP] in Dark Experiment (µg/L)	Reference
TOX	LP UV	60	10	6.5	0.28	5	479.25	443.75	6
				8.5			390.5	319.5	
	MP UV			6.5			461.5	443.75	
				8.5			284	319.5	
	MP UV	220	10	6.5	0.28	5	301.75	337.25	7
							461.5	443.75	
	LP UV	300	4,320	8.6	1.7	1	111	113	8
	MP UV				2.2		147	113	
	LP UV	3,900	120	7.5	10	2.6	65	97	3
	UV-A	7,000					97	97	
AOX	MP UV	1,820	0.67	6.5	2	3.5	60	35	4
					6		40	40	
					10		25	35	
				7.5	2		70	35	
					6		50	35	
					10		30	35	
				8.5	2		90	42	
					6		70	35	
					10		40	35	
			1,440	6.5	6.5		300	200	
				7.5	6.5		225	200	
				8.5	6.5		210	200	

A2. References

(1) Nowell, L. H.; Hoigné, J.; Photolysis of aqueous chlorine at sunlight and ultraviolet wavelengths II. Hydroxyl radical production. *Water Res.* **1992**, 26(5), 599-605.

(2) Liu, W.; Cheung, L.-M.; Yang, X.; Shang, C.; THM, HAA and CNCl formation from UV irradiation and chlor(am)ination of selected organic waters. *Water Res.* **2006**, 40(10), 2033-2043.

(3) Pisarenko, A. N.; Stanford, B. D.; Snyder, S. A.; Rivera, S. B.; Boal, A. K.; Investigation of the use of chlorine based advanced oxidation in surface water: Oxidation of natural organic matter and formation of disinfection byproducts. *J. Adv. Oxid. Technol.* **2013**, 16(1), 137-150.

(4) Wang, D.; Bolton, J. R.; Andrews, S. A.; Hofmann, R.; Formation of disinfection by-products in the ultraviolet/chlorine advanced oxidation process. *Sci. Total Environ.* **2015**, 518-519(C), 49-57.

(5) Zhang, X.; Li, W.; Blatchley, I. I. I., Ernest R; Wang, X.; Ren, P.; UV/chlorine process for ammonia removal and disinfection by-product reduction: Comparison with chlorination. *Water Res.* **2015**, 68(C), 804-811.

(6) Zhao, Q.; Shang, C.; Zhang, X.; Effects of bromide on UV/chlorine advanced oxidation process. *Water Sci. Tech.* **2009**, 9(6), 627-634.

(7) Zhao, Q.; Shang, C.; Zhang, X.; Ding, G.; Yang, X.; Formation of halogenated organic byproducts during medium-pressure UV and chlorine co-exposure of model compounds, nom and bromide. *Water Res.* **2011**, 45(19), 6545-6554.

(8) Plewa, M. J.; Wagner, E. D.; Metz, D. H.; Kashinkunti, R.; Jamriska, K. J.; Meyer, M.; Differential toxicity of drinking water disinfected with combinations of ultraviolet radiation and chlorine. *Environ. Sci. Technol.* **2012**, 46(14), 7811-7817.

Appendix B

Supplementary Material for Chapter 3

B1. Materials

Acetonitrile (HPLC grade), formic acid (ACS, 88%), *ortho*-phosphoric acid (ACS, 98%), and sodium chloride (ACS, 100%) were purchased from Fisher Chemical. 2-Nitrobenzaldehyde (≥99%), *para*-nitroanisole (PNA, ≥99%), and sodium hypochlorite were purchased from Acros Organics. Boric acid (ACS) was purchased from Amresco, Inc. Pyridine (≥99%) was purchased from Alfa Aesar. Nitrobenzene (ACS, ≥99%), sodium benzoate (≥99%), *trans*-cinnamic acid (97%), benzaldehyde (ReagentPlus(R), 99%), sulfamethoxazole (≥99%), diclofenac (≥99%), sodium thiosulfate (ReagentPlus(R), 99%), 4-hydroxybenzoic acid (ReagentPlus(R), 99%), 3-hydroxybenzoic acid (ReagentPlus(R), 99%), 2-hydroxybenzoic acid (salicylic acid, ≥99%), 4-chlorobenzoic acid (ReagentPlus(R), 99%), 3-chlorobenzoic acid (ReagentPlus(R), 99%), 2-chlorobenzoic acid (98%), dibasic potassium phosphate (ACS, 98%), and monobasic potassium phosphate (ReagentPlus(R)) were purchased from Sigma Aldrich. All chemicals were used as received except for sodium hypochlorite, which was standardized using a Shimadzu UV-visible spectrometer (ε_{292} = 365 M^{-1} cm^{-1}).[1]

B2. Irradiation Parameters, Actinometry, and Controls

All photolysis experiments were conducted in a turn-table apparatus inside a photochemical reactor (Rayonet). Three different bulb configurations were used: four 254-nm bulbs with quartz test tubes (Southern New England Ultraviolet Co. RPR-2537 Å, λ_{max} = 254 nm, width at half-maximum ± 1 nm, fluence = 7.30 x 10^{-3} mE cm^{-1}), sixteen 311-nm bulbs with borosilicate glass test tubes (Southern New England Ultraviolet Co. RPR-3000 Å, λ_{max} = 311 nm, width at half-maximum ± 22 nm, fluence = 5.70 x 10^{-3} mE cm^{-1}), and sixteen 365-nm bulbs with borosilicate glass test tubes (Southern New England Ultraviolet Co. RPR-3500 Å, λ_{max} = 365 nm, width at half-maximum ± 10 nm, fluence = 6.36 x 10^{-2} mE cm^{-1}; Figure B1).

The intensities of the UV lamps used in this study were measured using chemical actinometry. The *p*-nitroanisole/pyridine actinometer was used at 365 nm as described previously ([pyridine] = 150 μM, [*p*-nitroanisole] = 10 μM; Φ = 0.29[pyridine] + 0.00029); this equation was determined using a solar simulator.[2–4] The loss of 2-nitrobenzaldehyde (initial concentration = 10 μM; Φ = 0.41) was used to quantify light intensity at 311 nm; this quantum yield is recommended for the 280 – 405 nm wavelength range, which encompasses the wavelenghts emitted by the bulbs (Figure B1).[5] Sulfamethoxazole and diclofenac were used at 254 nm in place of the traditional iodide/iodate actinometer due to high bulb intensity (concentration of each = 10 μM; Φ = 0.18 and 0.213, respectively).[6] The quantum yields for sulfamethoxazole and diclofenac were determined using a narrowband 254 nm light source, which is similar to the light spectrum emitted by the bulbs used in this study.

Both dark and irradiated control experiments were performed with nitrobenzene and benzoate. The dark control experiments had 4 mg-Cl_2/L and 10 μM of either nitrobenzene and benzoate. No probe loss was observed in the dark controls (Figure B2). Irradiated controls were

performed at each wavelength with 10 μM nitrobenzene and benzoate in the absence of chlorine. No irradiated loss was observed in the absence of chlorine (Figure B2). Similar control experiments were not performed for cinnamic acid as the reaction of cinnamic acid to form benzaldehyde is dependent on the presence of ozone.[12]

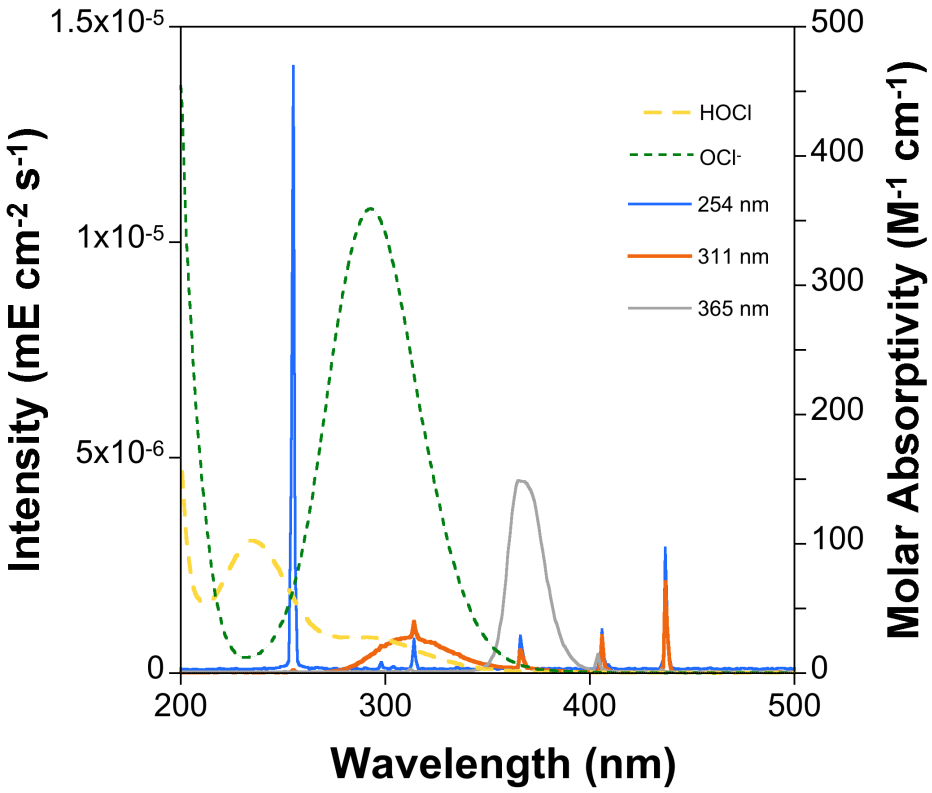

Figure B1. Rayonet bulb intensity for 254, 311, and 365 nm bulbs as a function of wavelength. Molar absorptivity of HOCl and OCl^- as a function of wavelength (second y-axis). Molar extinction coefficients are from the literature (HOCl: $\varepsilon_{max,235}$ = 98 – 101 M^{-1} cm^{-1}; OCl^-: $\varepsilon_{max,292}$ = 359 – 365 M^{-1} cm^{-1}).[7,8]

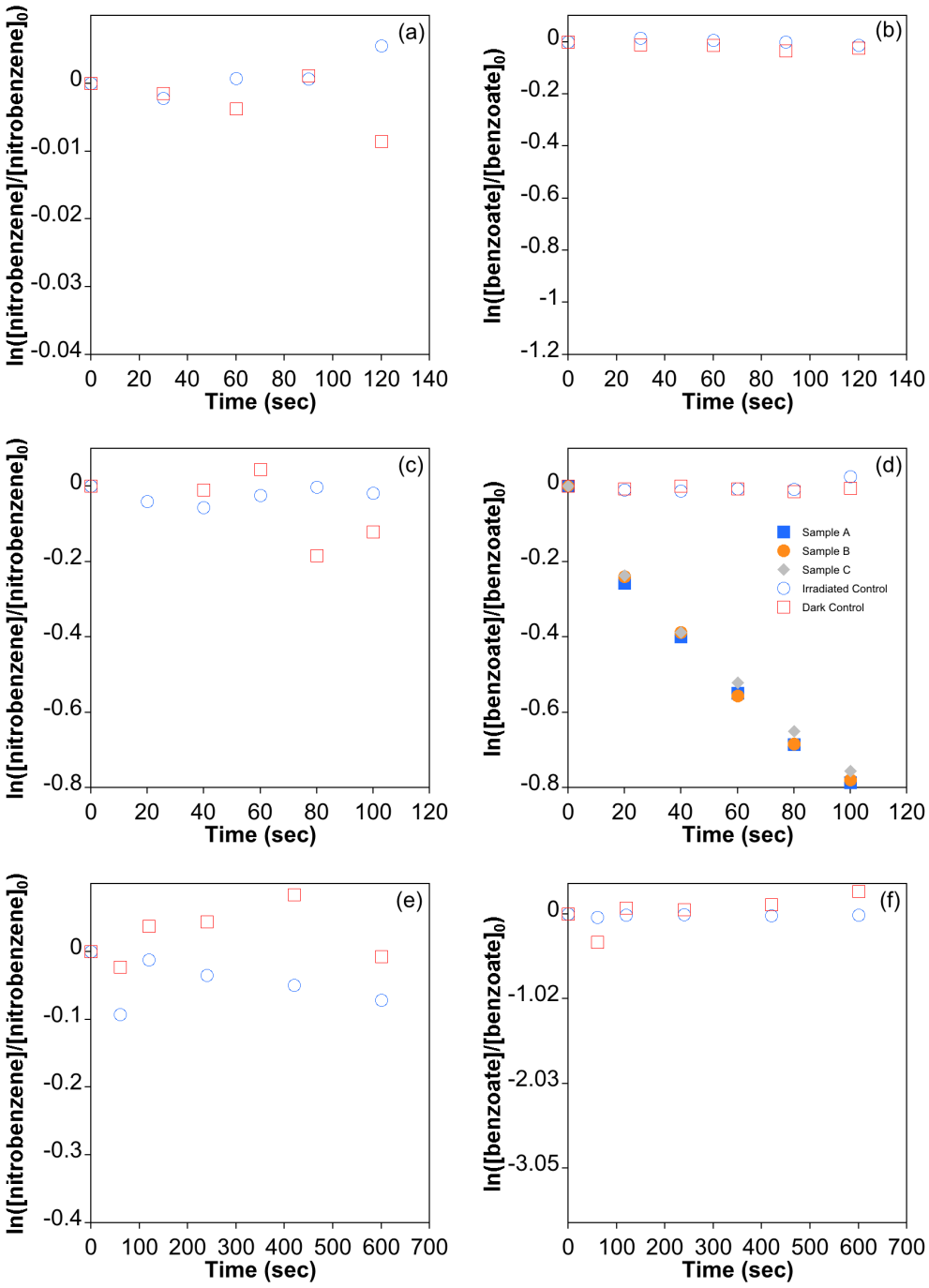

Figure B2. Controls of nitrobenzene and benzoate irradiated in the absence of chlorine (irradiated control) or reacted with 4 mg-Cl2/L in the dark (dark control) at pH 6 at (a, b) 254 nm, (c, d) 311 nm, and (e, f) 365 nm. (d) Example of the triplicate results for the first-order loss kinetics of benzoate seen during chlorine photolysis. Control experiments were completed under all pH and wavelength conditions. Data from pH 6 shown here as representative examples.

B3. Probe Validation and Steady-State Concentration Calculations

B3.1 Reaction of Probes with Ozone

Experiments were conducted in nitrogen-purged solutions to validate that reaction of nitrobenzene and benzoate with ozone is negligible under our experimental conditions, as expected based on their slow reaction rates with O_3 (k = 0.09 and 1.2 M^{-1} s^{-1}, respectively).[9] Removing oxygen from the reaction solution limits the reaction of the $O(^3P)$ excited state to form ozone (Reaction 9).[10,11] Buffered solutions of 4 mg-Cl_2/L chlorine and 10 μM nitrobenzene or benzoate and cinnamic acid were photolyzed at 311 nm after purging with nitrogen. Experiments were conducted in quartz test tubes with rubber sleeve-type stoppers. The reactors had a purged head-space. These experiments were conducted at pH 8 because only OCl^- is capable of forming $O(^3P)$ (Reaction 4).[10]

Degradation of the probe compounds does not change under nitrogen-purged conditions, confirming that ozone does not interfere with the measurement of $^{\bullet}OH$, $Cl^{\bullet}$, or $Cl_2^{\bullet-}$ (Figure B3b). We confirmed that purging the solution with nitrogen was effective in limiting the formation of ozone by measuring the formation of benzaldehyde, which is formed in a 1:1 molar ratio when cinnamic acid reacts with ozone.[12] The production of ozone in the purged solution was approximately 36% of the unpurged solution (Figure B3a). Complete prevention of ozone formation would likely be achieved in a fully anoxic environment.

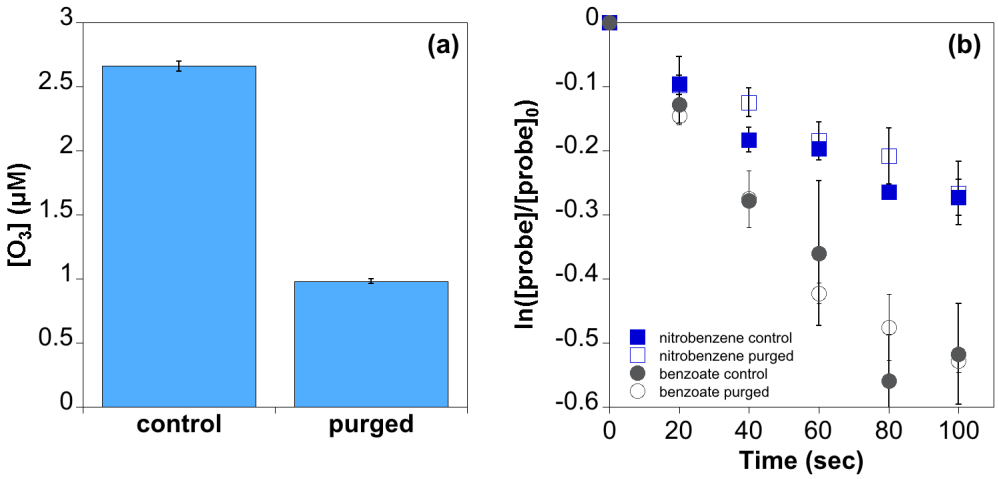

Figure B3. (a) Cumulative concentration of ozone produced during chlorine photolysis with and without purging with nitrogen. (b) Effect of reducing the production of ozone on the degradation of nitrobenzene and benzoate. All experiments were conducted at pH 8 with 4 mg-Cl_2/L and irradiation of 311 nm.

B3.2 Validation of Nitrobenzene Selectivity for •OH

Nitrobenzene is the primary probe compound used to measure the production of •OH during chlorine photolysis and is considered to be highly selective.[1,13–15] It is unreactive with HOCl[13] and not susceptible to direct photolysis between 254 and 365 nm (Figure B2).[1] Nitrobenzene is generally assumed to be unreactive towards Cl• and $Cl_2^{\bullet-}$ although there are no published rate constants for these reactions.[1,13,16] Therefore, in order to be confident that the observed nitrobenzene loss was only due to reaction with •OH, we validated the reactivity of nitrobenzene with Cl• by conducting experiments under highly acidic conditions (i.e., pH 0.25). The primary species of chlorine is Cl_2 under acidic conditions (Figure 3.2a in the manuscript), which photolyzes to produce two Cl• and no •OH.[13] As a result, photolysis of Cl_2 is considered to be a clean source of Cl•/$Cl_2^{\bullet-}$.[1,13] These experiments were conducted at pH 0.25, which was

adjusted with phosphoric acid to avoid introduction of additional chloride using 4 mg-Cl_2/L, 10 μM each of nitrobenzene or benzoic acid, and irradiation at 254 nm.

Nitrobenzene loss was observed when 4 mg-Cl_2/L was irradiated at 254 nm at pH 0.25 (Figure B4). While the pseudo-first order loss rate constant was a factor of 4.5 times slower than the rate constant at pH 6, it was similar to the rate constant measured at pH 9. At first glance, this result suggests that nitrobenzene does in fact react with $Cl^{\bullet}$ or $Cl_2^{\bullet-}$ since this low pH condition is considered to be a clean source of $Cl^{\bullet}$ or $Cl_2^{\bullet-}$.[13] However, a detailed investigation of chlorine speciation shows that, even though Cl_2 is the primary species of chlorine at low pH, there is still HOCl present in solution that could photolyze to produce $^{\bullet}OH$ (Figure 3.2a). For example, 0.71 mg-Cl_2/L HOCl is present in 4 mg-Cl_2/L total chlorine at pH 0.25 in the presence of 1.25 x 10^{-4} M chloride. Therefore, it is likely that $^{\bullet}OH$ is still produced, even at pH 0.25. The difference between literature results and the results of this study may be attributable to a higher concentration of chloride (not stated in past studies), which would increase the conversion of $^{\bullet}OH$ to $Cl^{\bullet}$ (Reaction 34).[1,13]

We conducted additional experiments to test the hypothesis that the $^{\bullet}OH$ produced by HOCl present at pH 0.25 is responsible for the observed nitrobenzene loss, rather than $Cl^{\bullet}$ or $Cl_2^{\bullet-}$ (Figure B5). We performed a series of chlorine variation experiments to determine the steady-state concentration of $^{\bullet}OH$ produced by HOCl at varied concentrations of chlorine at pH 6 (Figure B5). This allowed us to calculate the predicted degradation of nitrobenzene in the presence of 0.71 mg-Cl_2/L HOCl (i.e., the estimated [HOCl] present in 4 mg-Cl_2/L total chlorine at pH 0.25). This concentration of HOCl accounts for 88% of the observed nitrobenzene degradation at pH 0.25 (Figure B6). The remaining 12% of nitrobenzene loss may be attributable to other $^{\bullet}OH$ formation

pathways (e.g., formation of •OH from the reaction of Cl• with H_2O via Reactions 57 and 146) and the fact that only 96% of total chlorine is HOCl at pH 6.

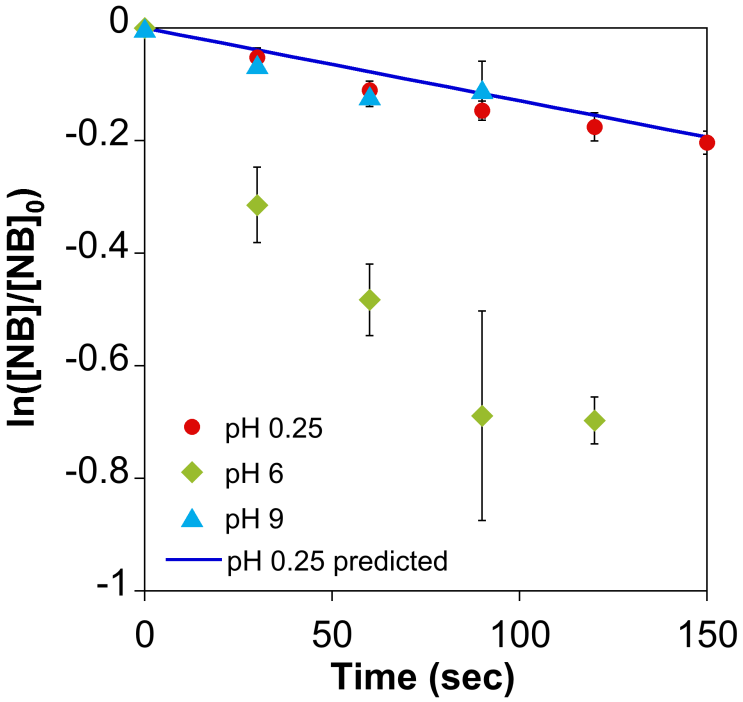

Figure B4. Nitrobenzene loss at different pH values (4 mg-Cl_2/L, 254 nm). The line represents the predicted loss of nitrobenzene at pH 0.25 based on the concentration of HOCl (0.71 mg-Cl_2/L) remaining in solution at 4 mg-Cl_2/L total chlorine.

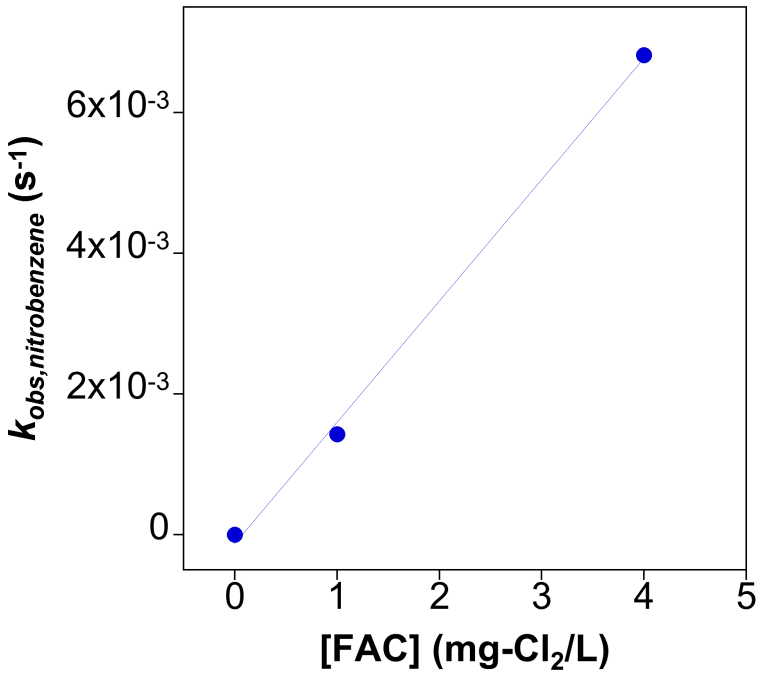

Figure B5. Observed nitrobenzene loss rate constant as a function of chlorine concentration at 254 nm, pH 6.

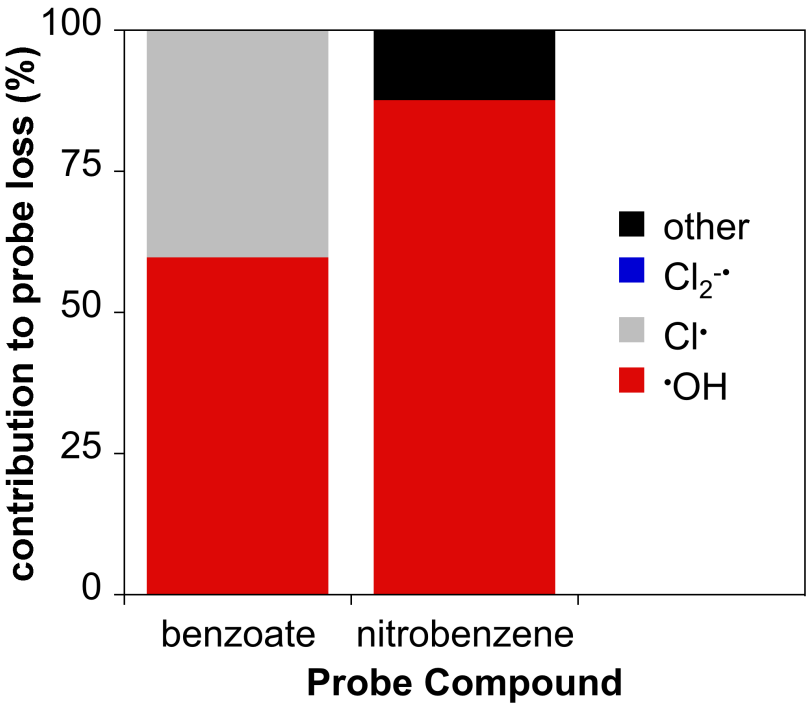

Figure B6. Contribution of oxidants to the degradation of benzoate and nitrobenzene at pH 0.25, 4 mg-Cl_2/L, 254 nm. The amount of nitrobenzene loss due to reaction with •OH was caluclated for the predicted $[^{\bullet}OH]_{ss}$ due to photolsis of 0.71 mg-Cl_2/L HOCl.

B.3.3 •OH Steady-State Concentration

After validating that nitrobenzene is selective for •OH under our experimental conditions, we calculated the steady-state concentration of •OH ($[^{\bullet}OH]_{ss}$) using the observed loss of nitrobenzene (Equation B1):

$$k_{obs,NB} = k_{NB}^{^{\bullet}OH} * [^{\bullet}OH]_{ss} \quad \text{(B1)}$$

where $k_{obs,NB}$ is the observed pseudo-first order rate constant of nitrobenzene loss (s^{-1}) and $k_{NB}^{^{\bullet}OH}$ is the literature rate constant of nitrobenzene and •OH (4.64×10^9 M^{-1} s^{-1};Reaction 162).

B.3.4 Benzoate Competition Kinetics

The reactivity of benzoate with reactive chlorine species was validated by quantifying the loss of benzoate (10 μM) in the presence of 0 – 500 μM of nitrobenzene (pH 6, 365 nm, 4 mg-Cl_2/L). During the competition kinetics experiments the predicted loss rate constant of benzoate was calculated according to the following equations:

$$f(^{\bullet}OH) = \frac{k_{obs,nitrobenzene}}{k^{^{\bullet}OH}_{nitrobenzene}}\left([HOCl]k^{^{\bullet}OH}_{HOCl} + [OCl^-]k^{^{\bullet}OH}_{OCl^-} + [Cl^-]k^{^{\bullet}OH}_{Cl^-}\right) \quad \text{(B2)}$$

$$[^{\bullet}OH]_{ss} = \frac{f(^{\bullet}OH)}{[HOCl]k^{^{\bullet}OH}_{HOCl} + [OCl^-]k^{^{\bullet}OH}_{OCl^-} + [Cl^-]k^{^{\bullet}OH}_{Cl^-} + [benzoate]k^{^{\bullet}OH}_{benzoate} + [nitrobenzene]k^{^{\bullet}OH}_{nitrobenzene}} \quad \text{(B3)}$$

$$k_{pred} = k^{^{\bullet}OH}_{BA}[^{\bullet}OH]_{ss} \quad \text{(B4)}$$

where f(•OH) is the formation rate of hydroxyl radical, $k_{obs,nitrobenzene}$ is the observed loss rate of nitrobenzene, k_{pred} is the predicted rate constant of benzoate, and $k^{\bullet OH}_X$ is the measured rate constant for the reaction of •OH with hypochlorous acid or hypochlorite (Section B6) or the literature rate constant for the reaction of •OH with chloride, nitrobenzene, or benzoate (Table B2). $[^{\bullet}OH]_{ss}$ was calculated based on the observed loss of nitrobenzene (Equation B1). These equations assume that benzoate only reacts with •OH and that nitrobenzene will increasingly compete for •OH as the concentration of nitrobenzene is increased. The difference between the predicted data assuming benzoate only reacts with •OH and the experimental measurements is attributed to the reaction of benzoate with reactive chlorine species.

Benzoate loss did not change as calculated with increasing nitrobenzene concentrations (Figure B7). For example, the predicted benzoate loss rate constant in the presence of 500 μM

assuming that benzoate only reacts with •OH was 54% of the observed rate. The difference between predicted and experimental results can be used to calculate the percent of benzoate reactivity that is due to •OH. The contribution of •OH to benzoate degradation decreases from 100 to 54% as nitrobenzene increases from 0 to 500 μM as nitrobenzene increasingly competes for •OH and the reactivity between benzoate and RCS increases. Potential light screening due to elevated concentrations of nitrobenzene can be neglected because nitrobenzene and benzoate are present in the same solution. Therefore, any potential decrease in $[^{\bullet}OH]_{ss}$ due to the competition for light between nitrobenzene and HOCl is reflected by the measured nitrobenzene loss rate constant. These data show that benzoate reacts with other non-•OH oxidant species, but does not allow for the identification of which oxidants are responsible.

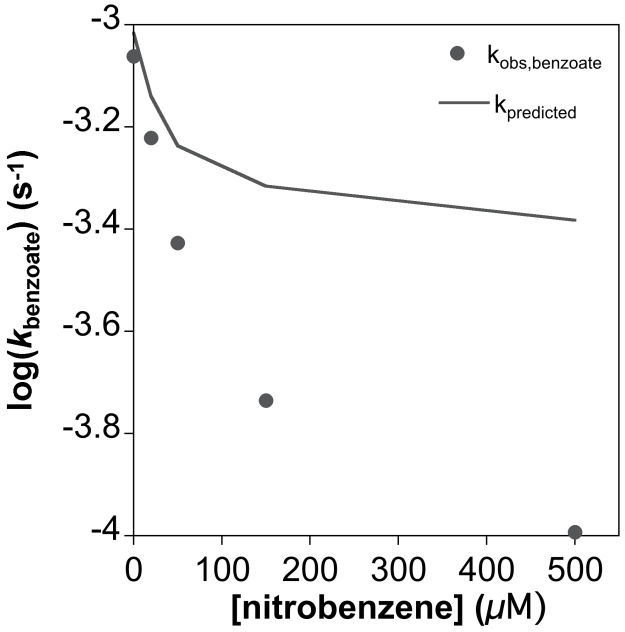

Figure B7. Predicted change in benzoate loss rate constant assuming only reaction with •OH as a function of nitrobenzene concentration compared with the experimental results of competition between nitrobenzene ([nitrobenzene] = 0 – 500 μM) and benzoate ([benzoate] = 10 μM) at pH 6 (4 mg-Cl_2/L; 365 nm irradiation).

B.3.5 Reactivity of Benzoate with $Cl^{\bullet}$, $Cl_2^{\bullet-}$, and $ClO^{\bullet}$

In order to identify which reactive chlorine species contribute to benzoate degradation, we conducted a series of chlorine and chloride concentration variation experiments. Both parameters were evaluated at pH 6 and 9 with 10 mM phosphate or borate buffer and 10 μM nitrobenzene or benzoate during irradiation at 254 nm. During chloride variation, the concentration of chlorine was held constant at 4 mg-Cl_2/L as the chloride concentration was varied from 0 – 500 mM added chloride. The chlorine concentration was varied from 0.4 – 100 mg-Cl_2/L and no chloride was added for the chlorine variation experiment. Increasing the chloride concentration allows for the evaluation of the effect of $Cl_2^{\bullet-}$ on benzoate with no added chloride. Increasing the chlorine concentration demonstrates the point at which $ClO^{\bullet}$ formation impacts benzoate degradation.

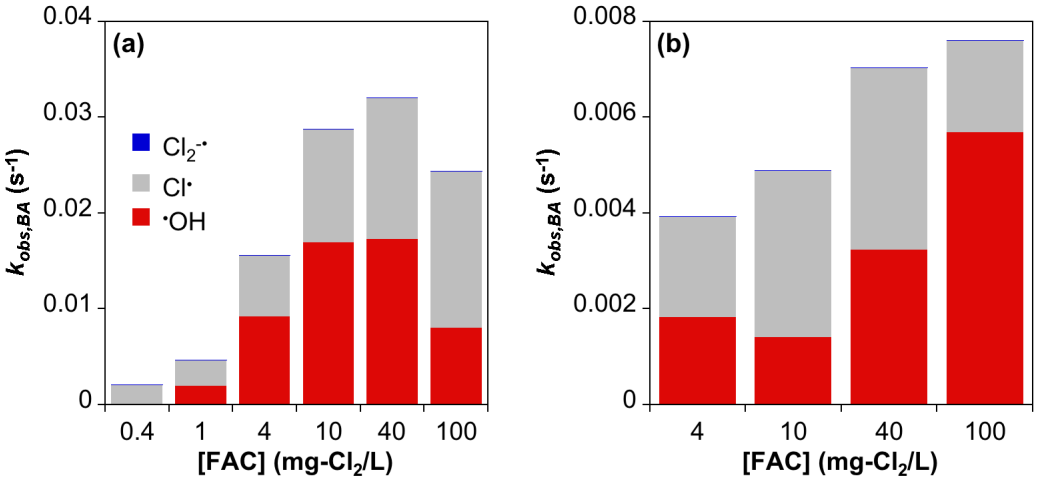

Figure B8. Contribution of oxidants ($^{\bullet}OH$, $Cl^{\bullet}$, and $Cl_2^{\bullet-}$) to benzoate loss at (a) pH 6 and (b) pH 9 as a function chlorine concentration. Experiments conducted at 254 nm.

Reaction with $ClO^{\bullet}$ was determined to be negligible for benzoate degradation via the chlorine variation experiments. As the concentration of chlorine increases, the production of $ClO^{\bullet}$ should increase due to quenching of $^{\bullet}OH$ and $Cl^{\bullet}$ by both chlorine species (Reactions 29, 37, 54,[17,18] and 55[17,19]). The reactivity of benzoate initially increases with chlorine concentration as

additional reactive species are produced at both pH values tested (Figure B8). At pH 6, when the concentration reaches 40 mg-Cl_2/L, $k_{obs,BA}$ decreases as $ClO^{\bullet}$ forms from the quenching of $^{\bullet}OH$ and $Cl^{\bullet}$ (Figure B8a). This decrease is not seen for the pH 9 chlorine variation (Figure B8b) because less $^{\bullet}OH$ is formed at high pH (Figure 3.1b). The decrease in benzoate degradation under conditions that favor $ClO^{\bullet}$ over $^{\bullet}OH$ and $Cl^{\bullet}$ indicate that reaction of benzoate with $ClO^{\bullet}$ is negligible under our experimental conditions. This is unsurprising given the slow reaction rate constant between benzoate and $ClO^{\bullet}$ (3 x 10^6 M^{-1} s^{-1}; Reaction 173).

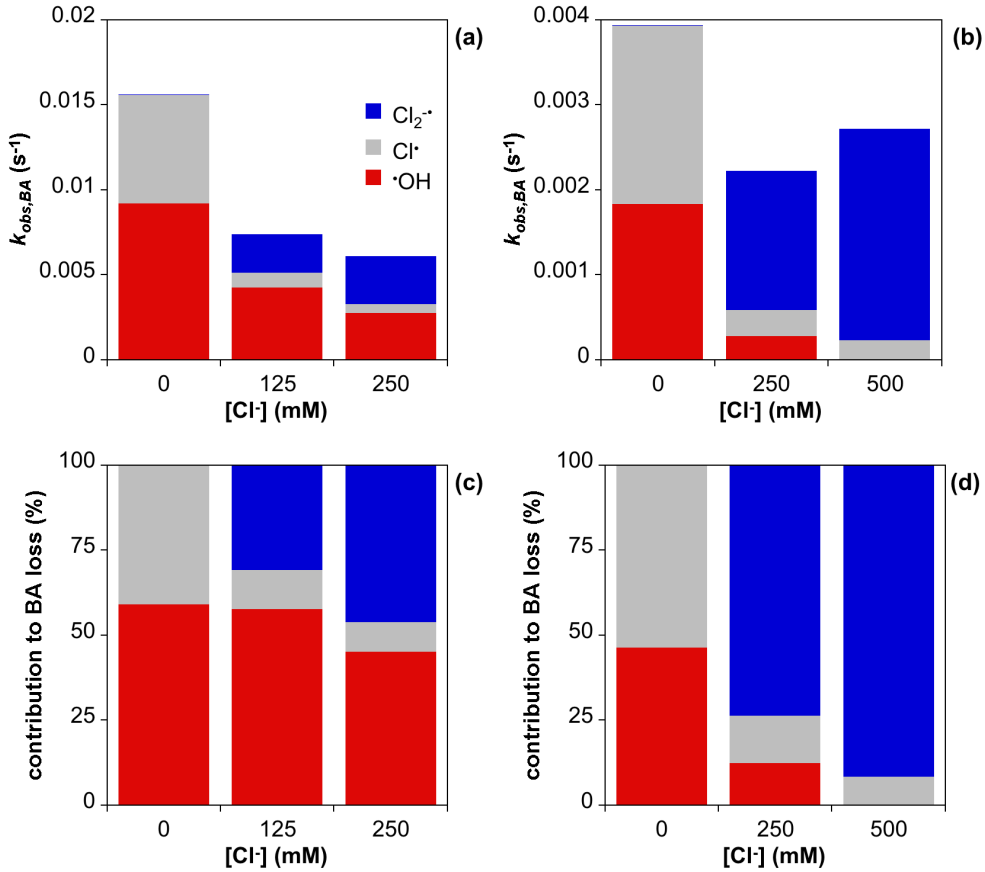

Figure B9. (a, b) Absolute and (c, d) percent contribution of oxidants ($^{\bullet}OH$, $Cl^{\bullet}$, and $Cl_2^{\bullet-}$) to benzoate loss at (a, c) pH 6 and (b, d) pH 9 as a function of chloride concentration. Experiments conducted at 254 nm.

Additional experiments were conducted with varied chloride in order to favor $Cl_2^{\bullet-}$ over $Cl^{\bullet}$. $Cl_2^{\bullet-}$ is four orders of magnitude less reactive with benzoate based on literature second order

rate constants (Reactions 170 and 172).[20,21] The contribution of $Cl^{\bullet}$ and $Cl_2^{\bullet-}$ to benzoate reactivity was determined by a system of equations described below. The observed benzoate loss rate constant decreases with increasing chloride concentration at both pH values due to the increased conversion of $Cl^{\bullet}$ to the less reactive $Cl_2^{\bullet-}$ (Figure B9). The decrease in benzoate reactivity with chloride shows that reaction between $Cl_2^{\bullet-}$ and benzoate is relatively less important in the absence of added chloride.

B.3.6 System of Equations Approach to Quantify $Cl^{\bullet}$ and $Cl_2^{\bullet-}$

The contribution of $Cl^{\bullet}$ and $Cl_2^{\bullet-}$ to benzoate degradation, as well as the steady-state concentrations of these species, were determined by combining measured nitrobenzene and benzoate loss rates, $Cl^{\bullet}/Cl_2^{\bullet-}$ equilibria, and chloride concentrations. We assumed equilibrium because the forward reaction is very fast (Reaction 69) and the reverse reaction will be forced because $Cl_2^{\bullet-}$ will accumulate (Reaction 59):

$$K_e = \frac{k_{rxn,69}}{k_{rxn,59}} = \frac{[Cl^{\bullet}]_{ss}[Cl^-]}{[Cl_2^{\bullet-}]_{ss}} \quad \text{(B5)}$$

where K_e is the equilibrium constant, $k_{rxn,69}$ is the forward rate constant of $Cl_2^{\bullet-}$ dissociation, and $k_{rxn,59}$ is the reverse rate constant of $Cl^{\bullet}$ reacting with Cl^-.

The degradation of benzoate is given by:

$$k_{obs,BA} = k_{BA}^{\bullet OH} * [^{\bullet}OH]_{ss} + k_{BA}^{Cl^{\bullet}} * [Cl^{\bullet}]_{ss} + k_{BA}^{Cl_2^{\bullet-}} * [Cl_2^{\bullet-}]_{ss} \quad \text{(B6)}$$

where $k_{obs,BA}$ is the observed loss rate constant of benzoate, $k_{BA}^{\bullet OH}$ is the literature rate constant of benzoate with $^{\bullet}OH$ (Reaction 169), $k_{BA}^{Cl^{\bullet}}$ is the literature rate constant of benzoate with $Cl^{\bullet}$ (Reaction 170), $k_{BA}^{Cl_2^{\bullet-}}$ is the literature rate constant of benzoate with $Cl_2^{\bullet-}$ (Reaction 172), and

$[^{\bullet}OH]_{ss}$ is calculated from nitrobenzene loss (Equation B1). Thus, it is possible to simultaneously calculate $[Cl^{\bullet}]_{ss}$ and $[Cl_2^{\bullet-}]_{ss}$ using equations S5 and S6 if the chloride concentration is known.

The assumption that $Cl_2^{-\bullet}$ contribution is negligible to benzoate degradation with no added Cl^- was validated by calculating the contribution of $Cl_2^{\bullet-}$ and Cl^- at varying added chloride concentrations (Figure B9). While $Cl_2^{\bullet-}$ does form with no added Cl^-, the concentration (8.7 x 10^{-12} M) is so low that the contribution to benzoate loss is negligible because the rate constant of $Cl_2^{\bullet-}$ with benzoate is four orders of magnitude slower than the reaction of $Cl^{\bullet}$ with benzoate. Thus, under our ambient conditions (i.e., $[Cl^-]$ = 1.25 x 10^{-4} M), we used a simplified approach to calculate the steady-state concentration of $Cl^{\bullet}$:

$$k_{obs,BA} = k_{BA}^{^{\bullet}OH} * [^{\bullet}OH]_{ss} + k_{BA}^{Cl^{\bullet}} * [Cl^{\bullet}]_{ss} \quad \text{(B7)}$$

The use of two probes (i.e., nitrobenzene and benzoate) enables the quantitative determination of $^{\bullet}OH$, $Cl^{\bullet}$, and $Cl_2^{\bullet-}$. However, this approach does have limitations in situations where $k_{obs,NB}$ and $k_{obs,BA}$ are similar because small differences in reactivity between the two probes can lead to uncertainty in measurements when Equation B1 is substituted into Equation B7. In other words, this approach is best suited for conditions with relatively high $[Cl^{\bullet}]_{ss}$ and/or $[Cl_2^{\bullet-}]_{ss}$.

B4. Analytical Methods

All probe compounds and actinometers were analyzed using an Agilent 1260 Infinity high-performance liquid chromatograph (HPLC) with either a diode-array or variable wavelength detector. All separations were achieved using an Agilent Poroshell 120 EC-C18 column (3.0 x 50 mm, 2.7 μm) with 10 mM phosphate buffer (10% acetonitrile v/v) and acetonitrile as the aqueous and organic phases, respectively, at a flow rate of 0.5 mL/min. All compounds were eluted using isocratic methods and detected at a single analysis wavelength (Table B1).

Table B1. Chromatography parameters for analysis of probe compounds and actinometers.

Compound	% Aqueous	Retention Time (min)	Detection Wavelength (nm)	Purpose
benzaldehyde	75	1.89	250	product of ozone probe reaction
benzoate	100	1.86	197	$^{\bullet}$OH and RCS probe
diclofenac	30	1.25	220	254 nm actinometer
p-nitroanisole	50	1.19	314	365 nm actinometer
2-nitrobenzaldehyde	80	2.86	226	311 nm actinometer
nitrobenzene	70	4.26	265	$^{\bullet}$OH probe
sulfamethoxazole	95	1.16	266	254 nm actinometer

B5. Kinetic Model

Photolysis rates of HOCl and OCl^- were calculated using the following equations:

$$A_{\lambda,FAC} = \left(\varepsilon_{HOCl,\lambda} * [HOCl] + \varepsilon_{OCl^-,\lambda} * [OCl^-]\right) * \ell \quad \text{(B8)}$$

$$[FAC] = [HOCl] + [OCl^-] \quad \text{(B9)}$$

$$R_{abs,\lambda} = \frac{2.303 * I_\lambda * A_{\lambda,FAC} * S_\lambda}{\ell * [FAC]} \quad \text{(B10)}$$

$$S_\lambda = \frac{1 - 10^{-A_\lambda}}{2.303 * A_\lambda} \quad \text{(B11)}$$

where $A_{\lambda,FAC}$ is the theoretical absorbance of chlorine at a given pH and wavelength (versus A_λ which is the absorbance of the sample solution including buffer and probe compounds), $\varepsilon_{HOCl,,\lambda}$ and $\varepsilon_{OCl\text{-},\lambda}$ are the molar absorptivities of HOCl and OCl^-, respectively, *l* is the pathlength, I_λ is the relative bulb intensity, R_{abs} is the rate of light absorbance, and S_λ is the solution screening factor that calculates the amount of light blocked by the solution based on the experimental sample absorbance.[3,22] Integrations were from 200 – 500 nm.

Photolysis rate constants of H_2O_2, HO_2^-, and O_3 were calculated using the molar absorptivity and predicted concentrations, rather than the experimental concentration, because we assumed no initial concentrations, using the following equation:

$$k_{abs} = 2.303 * I_\lambda * \varepsilon_\lambda * S_\lambda \quad \text{(B12)}$$

where ε_λ is the molar absorptivity of H_2O_2, HO_2^-, or O_3 (Figure B10).

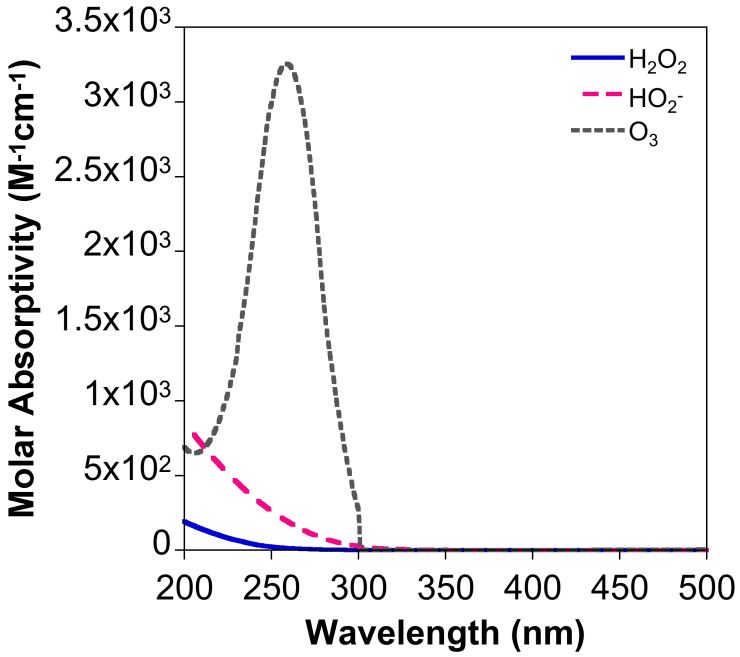

Figure B10. Molar absorptivities of H_2O_2, HO_2^-,[23] and O_3[24] as a function of wavelength.

Initial conditions in the kinetic model were based on experimental measurements and empirical assumptions. The concentration of water was assumed to be 55 M and the concentration of dissolved oxygen was assumed to be 250 µM.[25] Experimental parameters included the initial concentration of chlorine and the pH, along with chloride concentration.

Table B2. Reactions and rate constants included in the kinetic models used in this study. The reactions included in the literature models, as well as the rate constants used in the models, are indicated. XX refers to reactions included in the model with reaction rates calculated using molar absorptivity and quantum yields.

Reaction Number	Reaction	This Study	Chuang et al. 2017[14]	Fang et al. 2014[141]	Guo et al. 2017[41]	Li et al. 2017[15]	Sun et al. 2016[38]	Units	Ref. for *k*
Photolysis Reactions									
1	$HOCl + h\nu \rightarrow {}^{\bullet}OH + Cl^{\bullet}$	XX	XX	XX	XX	XX	XX	s^{-1}	
2	$OCl^- + h\nu \rightarrow O^{-\bullet} + Cl^{\bullet}$	XX	XX	XX	XX	XX	XX	s^{-1}	10
3	$OCl^- + h\nu \rightarrow O(^1D) + Cl^-$	XX						s^{-1}	10
4	$OCl^- + h\nu \rightarrow O(^3P) + Cl^-$	XX						s^{-1}	10
5	$H_2O_2 + h\nu \rightarrow {}^{\bullet}OH + {}^{\bullet}OH$	XX	XX					s^{-1}	14
6	$HO_2^- + h\nu \rightarrow {}^{\bullet}OH + O^{-\bullet}$	XX	XX					s^{-1}	14
7	$O_3 + h\nu \rightarrow O(^1D) + O_2$	XX						s^{-1}	26–28
Reactions of Excited States of Oxygen									
8	$O(^1D) + H_2O \rightarrow {}^{\bullet}OH + {}^{\bullet}OH$	1.2×10^{11}						$M^{-1}\ s^{-1}$	10
9	$O(^3P) + O_2 \rightarrow O_3$	4.0×10^{9}						$M^{-1}\ s^{-1}$	10,29
10	$O(^3P) + OCl^- \rightarrow ClO_2^-$	9.4×10^{9}						$M^{-1}\ s^{-1}$	29,30
11	$O(^3P) + H_2O_2 \rightarrow {}^{\bullet}OH + HO_2^{\bullet}$	1.6×10^{9}						$M^{-1}\ s^{-1}$	31
12	$O(^3P) + HO_2^- \rightarrow {}^{\bullet}OH + O_2^{-\bullet}$	5.3×10^{9}						$M^{-1}\ s^{-1}$	31
13	$O(^3P) + ClO_4^- \rightarrow$ products	6.0×10^{5}						$M^{-1}\ s^{-1}$	32
14	$O(^3P) + OH^- \rightarrow HO_2^-$	4.2×10^{8}						$M^{-1}\ s^{-1}$	31
15	$O_3 \rightarrow O_2 + O(^3P)$	4.5×10^{-6}						s^{-1}	33,34
Speciation Reactions									
16	$HOCl \rightarrow H^+ + OCl^-$	1.41×10^{3}	1.41×10^{3}	1.41×10^{3}	1.6×10^{3}		1.4×10^{3}	s^{-1}	35,36
17	$H^+ + OCl^- \rightarrow HOCl$	5.0×10^{10}	5.0×10^{10}	5.0×10^{10}	5.0×10^{10}		5.0×10^{10}	$M^{-1}\ s^{-1}$	35,36

18	$HOCl + Cl^- + H^+ \rightarrow Cl_2 + H_2O$	2.14×10^{-2}			1.82×10^{-1}		1.82×10^{-1}	$M^{-1} s^{-1}$	37
19	$HOCl + Cl^- \rightarrow Cl_2OH^-$	1.5×10^{4}				1.5×10^{4}		$M^{-1} s^{-1}$	37
20	$H_2O \rightarrow H^+ + OH^-$	1.0×10^{-3}	1.0×10^{-3}		1.0×10^{-3}	1.0×10^{-3}	1.0×10^{-3}	s^{-1}	35,36
21	$H^+ + OH^- \rightarrow H_2O$	1.0×10^{11}	1.0×10^{11}		1.0×10^{11}	1.0×10^{11}	1.0×10^{11}	$M^{-1} s^{-1}$	35,36
22	$Cl_2 + H_2O \rightarrow HOCl + Cl^- + H^+$	2.23×10^{1}	1.5×10^{1}		2.7×10^{-1}	2.2	2.7×10^{-1}	$M^{-1} s^{-1}$	37
23	$Cl_2 + OH^- \rightarrow HOCl + Cl^-$	1.0×10^{9}			1.0×10^{9}			$M^{-1} s^{-1}$	38
24	$Cl_2O_2 + H_2O \rightarrow ClO_2^- + HOCl + H^+$	1.0×10^{4}	1.0×10^{4}					$M^{-1} s^{-1}$	39
25	$HCl \rightarrow H^+ + Cl^-$	8.6×10^{16}	8.6×10^{16}		8.6×10^{16}	8.6×10^{16}	8.6×10^{16}	s^{-1}	35,36
26	$H^+ + Cl^- \rightarrow HCl$	5.0×10^{10}	5.0×10^{10}		5.0×10^{10}	5.0×10^{10}	5.0×10^{10}	$M^{-1} s^{-1}$	35,36
27	$H_2O_2 \rightarrow H^+ + HO_2^-$	1.26×10^{-1}	1.26×10^{-1}		1.3×10^{-1}	1.3×10^{-1}	1.3×10^{-1}	s^{-1}	35,36
28	$H^+ + HO_2^- \rightarrow H_2O_2$	5.0×10^{10}	5.0×10^{10}		5.0×10^{10}	5.0×10^{10}	5.0×10^{10}	$M^{-1} s^{-1}$	35,36
Reactions of Hydroxyl Radical									
29	$^{\bullet}OH + HOCl \rightarrow ClO^{\bullet} + H_2O$	1.21×10^{9}	5.0×10^{8}	2.0×10^{9}	2.0×10^{9}	2.0×10^{9}	2.0×10^{9}	$M^{-1} s^{-1}$	this study
30	$^{\bullet}OH + {}^{\bullet}OH \rightarrow H_2O_2$	5.5×10^{9}	5.5×10^{9}	5.5×10^{9}	5.5×10^{9}	3.6×10^{9}	5.5×10^{9}	$M^{-1} s^{-1}$	36,40
31	$^{\bullet}OH + ClO^{\bullet} \rightarrow ClO_2^- + H^+$	1.0×10^{9}			1.0×10^{9}			$M^{-1} s^{-1}$	41
32	$^{\bullet}OH + H_2O_2 \rightarrow HO_2^{\bullet} + H_2O$	2.7×10^{7}	2.7×10^{7}		2.7×10^{7}	2.7×10^{7}	2.7×10^{7}	$M^{-1} s^{-1}$	40,42
33	$^{\bullet}OH + O_2^{-\bullet} \rightarrow O_2 + OH^-$	8.5×10^{9}	7.0×10^{9}		1.0×10^{10}	7.0×10^{9}	7.0×10^{9}	$M^{-1} s^{-1}$	43,44
34	$^{\bullet}OH + Cl^- \rightarrow Cl^{\bullet} + OH^-$	1.1×10^{9}					4.3×10^{9}	$M^{-1} s^{-1}$	45
35	$^{\bullet}OH + Cl_2^{-\bullet} \rightarrow HOCl + Cl^-$	1.0×10^{9}	1.0×10^{9}			1.0×10^{9}		$M^{-1} s^{-1}$	46
36	$^{\bullet}OH + Cl_2 \rightarrow HOCl + Cl^-$						1.0×10^{9}	$M^{-1} s^{-1}$	N/A
37	$^{\bullet}OH + OCl^- \rightarrow ClO^{\bullet} + OH^-$	6.37×10^{9}	1.85×10^{9}	8.8×10^{9}	8.8×10^{9}	8.8×10^{9}	8.8×10^{9}	$M^{-1} s^{-1}$	this study
38	$^{\bullet}OH + HO_2^{\bullet} \rightarrow O_2 + H_2O$	7.53×10^{9}	6.6×10^{9}		7.1×10^{9}	6.6×10^{9}	6.6×10^{9}	$M^{-1} s^{-1}$	43,47, 48
39	$^{\bullet}OH + Cl^- \rightarrow HOCl^{-\bullet}$	3.65×10^{9}	4.3×10^{9}	4.3×10^{9}	4.3×10^{9}	4.3×10^{9}		$M^{-1} s^{-1}$	19,49

40	$^{\bullet}OH + ClO_2^- \rightarrow OH^- + ClO_2^{\bullet}$	4.5×10^9	7.0×10^9		6.3×10^9			$M^{-1} s^{-1}$	50,51
41	$^{\bullet}OH + ClO_3^- \rightarrow$ products	1.0×10^6	1.0×10^6					$M^{-1} s^{-1}$	40,51
42	$^{\bullet}OH + HO_2^- \rightarrow H_2O + O_2^{-\bullet}$	7.05×10^9						$M^{-1} s^{-1}$	42,52–54
43	$^{\bullet}OH + HO_2^- \rightarrow HO_2^{\bullet} + OH^-$		7.5×10^9		7.5×10^9	7.5×10^9	7.5×10^9	$M^{-1} s^{-1}$	36,42,55
44	$^{\bullet}OH + O^{-\bullet} \rightarrow HO_2^-$	2.0×10^{10}				1.0×10^{10}		$M^{-1} s^{-1}$	56
45	$^{\bullet}OH + OH^- \rightarrow H_2O + O^{-\bullet}$	1.25×10^{10}	1.2×10^{10}	1.3×10^{10}		1.2×10^{10}		$M^{-1} s^{-1}$	40,57
46	$^{\bullet}OH + H_2 \rightarrow H_2O + H^{\bullet}$	4.58×10^7						$M^{-1} s^{-1}$	58–62
47	$^{\bullet}OH + O_3^{-\bullet} \rightarrow HO_2^{\bullet} + O_2^{-\bullet}$	8.5×10^9						$M^{-1} s^{-1}$	63
48	$^{\bullet}OH + H^{\bullet} \rightarrow H_2O$	7.0×10^9						$M^{-1} s^{-1}$	61
49	$^{\bullet}OH + H_2O_2^{+\bullet} \rightarrow O_2 + H^+ + H_2O$	1.2×10^{10}						$M^{-1} s^{-1}$	47
50	$^{\bullet}OH + ClO_2^{\bullet} \rightarrow ClO_3^- + H^+$	4.0×10^9	4.0×10^9		4.0×10^9			$M^{-1} s^{-1}$	17,45
51	$^{\bullet}OH + O_3 \rightarrow O_2 + HO_2^{\bullet}$	1.05×10^8						$M^{-1} s^{-1}$	64
Reactions of Chlorine Radical									
52	$Cl^{\bullet} + H_2O_2 \rightarrow HO_2^{\bullet} + Cl^- + H^+$	2.0×10^9	2.0×10^9		2.0×10^9	2.0×10^9	2.0×10^9	$M^{-1} s^{-1}$	36,65
53	$Cl^{\bullet} + Cl_2^{-\bullet} \rightarrow Cl_2 + Cl^-$	2.1×10^9	2.1×10^9		2.1×10^9	2.1×10^9	2.1×10^9	$M^{-1} s^{-1}$	38,65
54	$Cl^{\bullet} + HOCl \rightarrow Cl^- + ClO^{\bullet} + H^+$	3.0×10^9	3.0×10^9	3.0×10^9	3.0×10^9	3.0×10^9	3.0×10^9	$M^{-1} s^{-1}$	17,18
55	$Cl^{\bullet} + OCl^- \rightarrow Cl^- + ClO^{\bullet}$	8.25×10^9	8.3×10^9	8.2×10^9	8.3×10^9	8.3×10^9	8.3×10^9	$M^{-1} s^{-1}$	17
56	$Cl^{\bullet} + Cl_2 \rightarrow Cl_3^{\bullet}$	5.3×10^8				5.3×10^8		$M^{-1} s^{-1}$	19,66
57	$Cl^{\bullet} + H_2O \rightarrow HOCl^{-\bullet} + H^+$	2.05×10^5	2.5×10^5		4.5×10^3	2.5×10^5	4.5×10^3	$M^{-1} s^{-1}$	17,67
58	$Cl^{\bullet} + Cl^{\bullet} \rightarrow Cl_2$	8.8×10^7	8.8×10^7		8.8×10^7	8.8×10^7	8.8×10^7	$M^{-1} s^{-1}$	68
59	$Cl^{\bullet} + Cl^- \rightarrow Cl_2^{-\bullet}$	1.18×10^{10}	8.0×10^9	6.5×10^9	8.5×10^9	8.5×10^9	8.5×10^9	$M^{-1} s^{-1}$	17,69,70
60	$Cl^{\bullet} + OH^- \rightarrow HOCl^{-\bullet}$	1.8×10^{10}	1.8×10^{10}	1.8×10^{10}	1.8×10^{10}	1.8×10^{10}	1.8×10^{10}	$M^{-1} s^{-1}$	17

61	$Cl^{\bullet} + ClO_3^- \rightarrow$ products	1.0×10^6	1.0×10^6					$M^{-1} s^{-1}$	14
62	$Cl^{\bullet} + ClO_2^{\bullet} \rightarrow$ products	1.0×10^9	1.0×10^9					$M^{-1} s^{-1}$	39
63	$Cl^{\bullet} + ClO_2^- \rightarrow ClO_2^{\bullet} + Cl^-$	7.0×10^9	7.0×10^9					$M^{-1} s^{-1}$	14
Reactions of Chlorine Radical Anion									
64	$Cl_2^{-\bullet} + Cl_2^{-\bullet} \rightarrow Cl_2 + Cl^- + Cl^-$	9.0×10^8	9.0×10^8		8.3×10^8	9.0×10^8	9.0×10^8	$M^{-1} s^{-1}$	70
65	$Cl_2^{-\bullet} + Cl_2^{-\bullet} \rightarrow Cl_3^- + Cl^-$	4.07×10^9						$M^{-1} s^{-1}$	67,71–85
66	$Cl_2^{-\bullet} + H_2O_2 \rightarrow HO_2^{\bullet} + Cl^- + Cl^- + H^+$	1.4×10^5	1.4×10^5		1.4×10^5	1.4×10^5	1.4×10^5	$M^{-1} s^{-1}$	21
67	$Cl_2^{-\bullet} + OH^- \rightarrow HOCl^{-\bullet} + Cl^-$	4.5×10^7	4.5×10^7	4.5×10^7	4.5×10^7	4.5×10^7	4.5×10^7	$M^{-1} s^{-1}$	49
68	$Cl_2^{-\bullet} + OCl^- \rightarrow Cl^- + Cl^- + ClO^{\bullet}$	2.9×10^8						$M^{-1} s^{-1}$	86
69	$Cl_2^{-\bullet} \rightarrow Cl^{\bullet} + Cl^-$	6.0×10^4	6.0×10^4	1.1×10^5	6.0×10^4	6.0×10^4	6.0×10^4	s^{-1}	36,65
70	$Cl_2^{-\bullet} + H_2O \rightarrow H_2OCl^{\bullet} + Cl^-$	1.3×10^3				1.3×10^3		$M^{-1} s^{-1}$	67
71	$Cl_2^{-\bullet} + H_2O \rightarrow Cl^- + HOCl^{-\bullet}$		1.3×10^3		2.34×10^1			$M^{-1} s^{-1}$	N/A
72	$Cl_2^{-\bullet} + HO_2^{\bullet} \rightarrow O_2 + Cl^- + Cl^- + H^+$	2.83×10^9	3.0×10^9		3.0×10^9	3.1×10^9	3.0×10^9	$M^{-1} s^{-1}$	75,76,87
73	$Cl_2^{-\bullet} + HO_2^{\bullet} \rightarrow Cl^- + H_2OCl$						2.34×10^1	$M^{-1} s^{-1}$	N/A
74	$Cl_2^{-\bullet} + H^{\bullet} \rightarrow Cl^- + Cl^- + H^+$	7.5×10^9						$M^{-1} s^{-1}$	74,76
75	$Cl_2^{-\bullet} + O_2^{-\bullet} \rightarrow O_2 + Cl^- + Cl^-$	2.0×10^9	2.0×10^9		1.0×10^9	2.0×10^9	2.0×10^9	$M^{-1} s^{-1}$	80
76	$Cl_2^{-\bullet} + ClO_2^{\bullet} \rightarrow$ products	1.0×10^9			1.3×10^8			$M^{-1} s^{-1}$	39
Reactions of $ClO^{\bullet}$ Radical									
77	$ClO^{\bullet} + ClO^{\bullet} + H_2O + OH^- \rightarrow HOCl + HClO_2$	2.5×10^9			2.5×10^9			$M^{-2} s^{-1}$	17
78	$ClO^{\bullet} + ClO^{\bullet} + H_2O \rightarrow HOCl + H^+ + ClO_2^-$	2.5×10^9			2.5×10^9			$M^{-1} s^{-1}$	17
79	$ClO^{\bullet} + ClO_2^- \rightarrow ClO_2^{\bullet} + OCl^-$	9.4×10^8	9.4×10^8		9.4×10^8			$M^{-1} s^{-1}$	88
80	$ClO^{\bullet} + ClO^{\bullet} \rightarrow Cl_2O_2$	5.0×10^9	2.5×10^9		2.5×10^9		2.5×10^9	$M^{-1} s^{-1}$	17,51

Reaction of Ozone									
81	$O_3 + OH^- \rightarrow O_2 + HO_2^-$	7.0×10^1						$M^{-1} s^{-1}$	89
82	$O_3 + HO_2^- \rightarrow O_3^{-\bullet} + HO_2^\bullet$	5.5×10^6						$M^{-1} s^{-1}$	89
83	$O_3 + HO_2^\bullet \rightarrow H^+ + O_2 + O_3^{-\bullet}$	1.6×10^9						$M^{-1} s^{-1}$	assumed from 90
84	$O_3 + OCl^- \rightarrow O_2 + O_2 + Cl^-$	1.1×10^2						$M^{-1} s^{-1}$	91
85	$O_3 + OCl^- \rightarrow O_2 + ClO_2^-$	3.0×10^1						$M^{-1} s^{-1}$	91
86	$O_3 + Cl^- \rightarrow O_2 + OCl^-$	1.6×10^{-3}						$M^{-1} s^{-1}$	34,92
87	$O_3 + H_2O_2 \rightarrow O_2 + {}^\bullet OH + HO_2^\bullet$	2.72×10^{-2}						$M^{-1} s^{-1}$	33,89, 93
88	$O_3 + HO_2^- \rightarrow O_2 + {}^\bullet OH + O_2^{-\bullet}$	5.5×10^6						$M^{-1} s^{-1}$	89
89	$O_3 + H^\bullet \rightarrow O_2 + {}^\bullet OH$	2.2×10^{10}						$M^{-1} s^{-1}$	94
90	$O_3 + Cl_2^{-\bullet} \rightarrow$ products	9.0×10^7						$M^{-1} s^{-1}$	95
91	$O_3 + O_2^{-\bullet} \rightarrow O_2 + O_3^{-\bullet}$	1.55×10^9						$M^{-1} s^{-1}$	94,96
92	$O_3 + ClO_2^\bullet \rightarrow O_2 + ClO_3^\bullet$	1.23×10^3						$M^{-1} s^{-1}$	34,45, 97,98
93	$O_3 + ClO_2^- \rightarrow O_3^{-\bullet} + ClO_2^\bullet$	2.01×10^6						$M^{-1} s^{-1}$	34,45
94	$O_3 + ClO_3^- \rightarrow$ products	1.0×10^{-4}						$M^{-1} s^{-1}$	34
95	$O_3 + ClO_4^- \rightarrow$ products	2.0×10^{-5}						$M^{-1} s^{-1}$	34
96	$O_3 + H^+ \rightarrow$ products	4.0×10^{-4}						$M^{-1} s^{-1}$	89
Reactions of Reactive Oxygen Species									
97	$H_2O_2 + Cl_2 \rightarrow HCl + HCl + O_2$	1.3×10^4	1.3×10^4		1.3×10^4	1.3×10^4	1.3×10^4	$M^{-1} s^{-1}$	36,99
98	$H_2O_2 + HOCl \rightarrow HCl + H_2O + O_2$	1.1×10^4	1.1×10^4		1.1×10^4	1.1×10^4	1.1×10^4	$M^{-1} s^{-1}$	36,100
99	$H_2O_2 + OCl^- \rightarrow Cl^- + H_2O + O_2$	1.7×10^5	1.7×10^5		1.7×10^5	1.7×10^5	1.7×10^5	$M^{-1} s^{-1}$	36,100

100	$H_2O_2 + HO_2^\bullet \rightarrow O_2 + {}^\bullet OH + H_2O$	3.0	3.0		3.0	3.0	3.0	$M^{-1}\ s^{-1}$	101
101	$H_2O_2 + O^{-\bullet} \rightarrow O_2^{-\bullet} + H_2O$	4.0×10^8				4.0×10^8		$M^{-1}\ s^{-1}$	40
102	$H_2O_2 + H^\bullet \rightarrow H_2O + {}^\bullet OH$	5.87×10^8						$M^{-1}\ s^{-1}$	102–104
103	$H_2O_2 + O_2^{-\bullet} \rightarrow O_2 + {}^\bullet OH + OH^-$	6.65×10^{-1}	1.3×10^{-1}		1.3×10^{-1}	1.3×10^{-1}	1.3×10^{-1}	$M^{-1}\ s^{-1}$	105–108
104	$HO_2^- + O^{-\bullet} + H_2O \rightarrow HO_2^\bullet + OH^- + OH^-$	5.0×10^8						$M^{-1}\ s^{-1}$	40
105	$HO_2^- + H^\bullet \rightarrow {}^\bullet OH + OH^-$	1.2×10^9						$M^{-1}\ s^{-1}$	103
106	$HO_2^- + O^{-\bullet} \rightarrow {}^\bullet OH + O_2^{-\bullet}$	4.0×10^8				4.0×10^8		$M^{-1}\ s^{-1}$	40
107	$HO_2^- + O_2^{-\bullet} \rightarrow O_2 + H_2O_2$	2.0					9.7×10^7	$M^{-1}\ s^{-1}$	109
108	$HO_2^- + ClO_2^\bullet \rightarrow HO_2^\bullet + ClO_2^-$	9.57×10^4						$M^{-1}\ s^{-1}$	50,97,110
109	$HO_2^\bullet + HOCl \rightarrow Cl^\bullet + OH^- + O_2 + H^+$	7.5×10^6	7.5×10^6		7.5×10^6	7.5×10^6	7.5×10^6	$M^{-1}\ s^{-1}$	36,99
110	$HO_2^\bullet + Cl_3^- \rightarrow Cl_2^{-\bullet} + HCl + O_2$	1.0×10^9	1.0×10^9		1.0×10^9	1.0×10^9	1.0×10^9	$M^{-1}\ s^{-1}$	36,111
111	$HO_2^\bullet + Cl_2 \rightarrow Cl_2^{-\bullet} + H^+ + O_2$	1.0×10^9	1.0×10^9		1.0×10^9	1.0×10^9	1.0×10^9	$M^{-1}\ s^{-1}$	111
112	$HO_2^\bullet \rightarrow H^+ + O_2^{-\bullet}$	1.6×10^5			7.0×10^5	1.6×10^5	7.9×10^5	s^{-1}	112
113	$HO_2^\bullet + H^\bullet \rightarrow H_2O_2$	1.5×10^{10}						$M^{-1}\ s^{-1}$	48
114	$HO_2^\bullet + H_2 \rightarrow H_2O_2 + H^\bullet$	1.0						$M^{-1}\ s^{-1}$	113
115	$HO_2^\bullet + O_2^{-\bullet} + H_2O \rightarrow H_2O_2 + O_2 + OH^-$	9.7×10^7						$M^{-1}\ s^{-1}$	112
116	$HO_2^\bullet + O_2^{-\bullet} \rightarrow HO_2^- + O_2$		9.7×10^7		9.7×10^7	9.7×10^7		$M^{-1}\ s^{-1}$	N/A
117	$HO_2^\bullet + HO_2^\bullet \rightarrow H_2O_2 + O_2$	1.19×10^7	8.3×10^5		8.3×10^9	8.3×10^5	8.3×10^9	$M^{-1}\ s^{-1}$	112,114
118	$HO_2^\bullet + ClO_2^\bullet \rightarrow$ products	1.0×10^6						$M^{-1}\ s^{-1}$	115
119	$O_2^{-\bullet} + HOCl \rightarrow Cl^\bullet + OH^- + O_2$	7.5×10^6	7.5×10^6		7.5×10^6	7.5×10^6	7.5×10^6	$M^{-1}\ s^{-1}$	36,99,116
120	$O_2^{-\bullet} + HOCl \rightarrow Cl^- + {}^\bullet OH + O_2$	7.5×10^6						$M^{-1}\ s^{-1}$	116

121	$O_2^{-\bullet} + OCl^- + H_2O \rightarrow Cl^\bullet + OH^- + OH^- + O_2$	2.0×10^8	2.0×10^8		2.0×10^8	2.0×10^8	2.0×10^8	$M^{-1} s^{-1}$	36,99
122	$O_2^{-\bullet} + Cl_3^- \rightarrow Cl_2^{-\bullet} + Cl^- + O_2$	3.8×10^9	3.8×10^9		3.8×10^9	3.8×10^9	3.8×10^9	$M^{-1} s^{-1}$	36,99
123	$O_2^{-\bullet} + Cl_2 \rightarrow Cl_2^{-\bullet} + O_2$	1.0×10^9	1.0×10^9		1.0×10^9	1.0×10^9	1.0×10^9	$M^{-1} s^{-1}$	36,99
124	$O_2^{-\bullet} + O^{-\bullet} + H_2O \rightarrow O_2 + OH^- + OH^-$	6.0×10^8						$M^{-1} s^{-1}$	117
125	$O_2^{-\bullet} + O^{-\bullet} + H^+ \rightarrow OH^- + O_2$					6.0×10^8		$M^{-2} s^{-1}$	N/A
126	$O_2^{-\bullet} + Cl^- \rightarrow$ products	1.4×10^2						$M^{-1} s^{-1}$	116
127	$O_2^{-\bullet} + ClO_2^\bullet \rightarrow O_2 + ClO_2^-$	3.15×10^9						$M^{-1} s^{-1}$	50
128	$O_2^{-\bullet} + ClO_2^- \rightarrow$ products	4.0×10^1						$M^{-1} s^{-1}$	115,116
129	$O_2^{-\bullet} + H^+ \rightarrow HO_2^\bullet$	5.67×10^{10}			5.0×10^{10}	5.0×10^{10}	5.0×10^{10}	$M^{-1} s^{-1}$	36,113,118
130	$O_2^{-\bullet} + ClO_3^- \rightarrow$ products	3.0×10^{-3}				3.2×10^3		$M^{-1} s^{-1}$	116
131	$O_3^{-\bullet} \rightarrow O_2 + O^{-\bullet}$	4.28×10^3				3.2×10^3		s^{-1}	119–122
132	$O_3^{-\bullet} + ClO^\bullet \rightarrow OCl^- + O_3$	1.0×10^9						$M^{-1} s^{-1}$	29
133	$O_3^{-\bullet} + H^+ \rightarrow O_2 + {}^\bullet OH$	9.0×10^{10}						$M^{-1} s^{-1}$	63
134	$O_3^{-\bullet} + O^{-\bullet} \rightarrow O_4^{2-}$	7.0×10^8						$M^{-1} s^{-1}$	121
135	$O_3^{-\bullet} + O^{-\bullet} \rightarrow O_2^{-\bullet} + O_2^{-\bullet}$	7.0×10^8						$M^{-1} s^{-1}$	117
136	$O_3^{-\bullet} + ClO_2^\bullet \rightarrow O_2 + ClO_3^-$	1.8×10^5						$M^{-1} s^{-1}$	45
137	$O_3^{-\bullet} + H^+ \rightarrow HO_3^\bullet$	5.2×10^{10}						$M^{-1} s^{-1}$	96
138	$O_3^{-\bullet} + O_3^{-\bullet} \rightarrow$ products	9.0×10^8						$M^{-1} s^{-1}$	123
139	$O_3^{-\bullet} + ClO_2^\bullet \rightarrow ClO_2^- + O_3$	3.15×10^9						$M^{-1} s^{-1}$	45
140	$O^{-\bullet} + OCl^- + H_2O \rightarrow ClO^\bullet + OH^- + OH^-$	2.3×10^8						$M^{-1} s^{-1}$	51
141	$O^{-\bullet} + H_2O \rightarrow {}^\bullet OH + OH^-$	9.35×10^7		1.8×10^6	1.8×10^6	1.8×10^5	1.8×10^6	$M^{-1} s^{-1}$	18,57

142	$O^{-\bullet} + O_2 \rightarrow O_3^{-\bullet}$	3.5×10^9				3.6×10^9		$M^{-1} s^{-1}$	40,53, 56,119 ,124,1 25
143	$O^{-\bullet} + ClO_2^- \rightarrow OH^- + ClO_2^{\bullet}$	1.95×10^8						$M^{-1} s^{-1}$	50,51
144	$O^{-\bullet} + O^{-\bullet} \rightarrow O_2^{2-}$	4.65×10^9						$M^{-1} s^{-1}$	56,125
145	$O^{-\bullet} + ClO_2^{\bullet} \rightarrow ClO_3^-$	2.7×10^9						$M^{-1} s^{-1}$	45
Reactions of Other Chlorine Species									
146	$HOCl^{-\bullet} \rightarrow Cl^- + {}^{\bullet}OH$	6.1×10^9	6.1×10^9	6.1×10^9	6.1×10^9	6.1×10^9	6.1×10^9	s^{-1}	19
147	$HOCl^{-\bullet} + H^+ \rightarrow Cl^{\bullet} + H_2O$	2.1×10^{10}	2.1×10^{10}	2.1×10^{10}	2.1×10^{10}	2.1×10^{10}	2.1×10^{10}	$M^{-1} s^{-1}$	17,19, 36
148	$HOCl^{-\bullet} + Cl^- \rightarrow OH^- + Cl_2^{-\bullet}$	1.0×10^4	1.0×10^4	1.0×10^5	1.0×10^5	1.0×10^4		$M^{-1} s^{-1}$	49
149	$Cl_2 + Cl^- \rightarrow Cl_3^-$	2.0×10^4	2.0×10^4		2.0×10^4	2.0×10^4	2.0×10^4	$M^{-1} s^{-1}$	36,126
150	$H_2ClO^{\bullet} \rightarrow HOCl^{-\bullet} + H^+$	1.0×10^8	1.0×10^8		1.0×10^8	1.0×10^8	1.0×10^8	s^{-1}	67
151	$H_2ClO^{\bullet} + Cl^- \rightarrow Cl_2^{-\bullet} + H_2O$	5.0×10^9			5.0×10^9	5.0×10^9	5.0×10^9	$M^{-1} s^{-1}$	36,67
152	$H_2ClO^{\bullet} \rightarrow Cl^{\bullet} + H_2O$	1.0×10^2			1.0×10^2	1.0×10^2	1.0×10^2	s^{-1}	36,67
153	$Cl_2OH^- \rightarrow HOCl + Cl^-$	5.5×10^9				5.5×10^9		s^{-1}	37
154	$ClO_2^{\bullet} \rightarrow O_2 + Cl^{\bullet}$	6.7×10^9						s^{-1}	127
155	$Cl^- + H^{\bullet} \rightarrow$ products	1.0×10^5						$M^{-1} s^{-1}$	128
156	$Cl_3^- + H^{\bullet} \rightarrow Cl^- + Cl_2^{-\bullet} + H^+$	3.0×10^{10}						$M^{-1} s^{-1}$	75
157	$Cl_3^- \rightarrow Cl_2 + Cl^-$	1.1×10^5	1.1×10^5		1.1×10^5	1.1×10^5	1.1×10^5	s^{-1}	36,126
Reactions of Hydrogen Radical									
158	$H^{\bullet} + HOCl \rightarrow H_2O + Cl^{\bullet}$	5.0×10^{-12}						$M^{-1} s^{-1}$	129
159	$H^{\bullet} + H_2O \rightarrow {}^{\bullet}OH + H_2$	5.5×10^2						$M^{-1} s^{-1}$	130

160	$H^{\bullet} + O_2 \rightarrow HO_2^{\bullet}$	1.43×10^{10}						$M^{-1} s^{-1}$	40,102,131,132
161	$H^{\bullet} + H^{\bullet} \rightarrow H_2$	7.76×10^{9}						$M^{-1} s^{-1}$	40,133–136
Reactions with Probes									
162	$^{\bullet}OH$ + nitrobenzene → n-nitrophenol + $H^{\bullet}$	4.64×10^{9}		3.9×10^{9}				$M^{-1} s^{-1}$	40,137–139
163	$H^{\bullet}$ + nitrobenzene → nitrobenzene radical + H_2O	1.65×10^{9}						$M^{-1} s^{-1}$	140
164	O_3 + nitrobenzene → products	9.0×10^{-2}						$M^{-1} s^{-1}$	9
165	$Cl^{\bullet}$ + benzoic acid → n-chlorobenzoic acid + $H^{\bullet}$	1.8×10^{10}	1.8×10^{10}	1.8×10^{10}				$M^{-1} s^{-1}$	141
166	$^{\bullet}OH$ + benzoic acid → products	3.27×10^{9}	4.3×10^{9}					$M^{-1} s^{-1}$	137,142
167	$Cl_2^{-\bullet}$ + benzoic acid → products		1.5×10^{6}					$M^{-1} s^{-1}$	N/A
168	$H^{\bullet}$ + benzoic acid → products	9.2×10^{8}						$M^{-1} s^{-1}$	40
169	$^{\bullet}OH$ + benzoate → products	5.27×10^{9}	5.9×10^{9}	5.9×10^{9}				$M^{-1} s^{-1}$	40,137,138,143–145
170	$Cl^{\bullet}$ + benzoate → products	1.8×10^{10}	1.8×10^{10}	1.8×10^{10}				$M^{-1} s^{-1}$	20
171	$O^{-\bullet}$ + benzoate → products	4.0×10^{7}	4.0×10^{7}	4.0×10^{7}				$M^{-1} s^{-1}$	40
172	$Cl_2^{-\bullet}$ + benzoate → products	2.0×10^{6}	2.0×10^{6}	2.0×10^{6}				$M^{-1} s^{-1}$	21
173	$ClO^{\bullet}$ + benzoate → products	3.0×10^{6}						$M^{-1} s^{-1}$	88
174	$H^{\bullet}$ + benzoate → products	1.08×10^{9}						$M^{-1} s^{-1}$	140
175	O_3 + benzoate → products	1.2						$M^{-1} s^{-1}$	9
176	O_3 + cinnamic acid → benzaldehyde + glyoxylic acid + H_2O_2	3.8×10^{5}						$M^{-1} s^{-1}$	12

Reactions with Buffer									
177	$^{\bullet}OH + HPO_4^{2-} \rightarrow HPO_4^{-\bullet} + OH^-$	1.5×10^5	1.5×10^5		1.5×10^5		1.5×10^5	$M^{-1} s^{-1}$	36,55
178	$^{\bullet}OH + H_2PO_4^- \rightarrow HPO_4^{-\bullet} + H_2O$	2.0×10^4	2.0×10^4		2.0×10^4		2.0×10^4	$M^{-1} s^{-1}$	55
179	$^{\bullet}OH + H_3PO_4 \rightarrow H_2PO_4^{\bullet} + H_2O$	1.37×10^6						$M^{-1} s^{-1}$	146,147
180	$H_2O_2 + HPO_4^{-\bullet} \rightarrow H_2PO_4^- + HO_2^{\bullet}$	2.7×10^7	2.7×10^7		2.7×10^7		2.7×10^7	$M^{-1} s^{-1}$	148
181	$H_2O_2 + H_2PO_4^{\bullet} \rightarrow H_2PO_4^- + H^+ + H^+ + O_2^{-\bullet}$	5.5×10^7						$M^{-1} s^{-1}$	148
182	$O^{-\bullet} + HPO_4^{2-} \rightarrow$ products	3.5×10^6						$M^{-1} s^{-1}$	146
183	$O_3 + H_2PO_4^- \rightarrow$ products	2.0×10^{-4}						$M^{-1} s^{-1}$	34
184	$H_3PO_4 + O_3 \rightarrow$ products	2.0×10^{-2}						$M^{-1} s^{-1}$	34
185	$O_3^{-\bullet} + H_2PO_4^- \rightarrow HPO_4^{2-} + HO_3^{\bullet}$	9.1×10^7						$M^{-1} s^{-1}$	96
186	$H_2O + H_2PO_4^{\bullet} \rightarrow H_3PO_4 + {}^{\bullet}OH$	1.3×10^5						$M^{-1} s^{-1}$	147
187	$Cl^- + H_2PO_4^{\bullet} \rightarrow H_2PO_4^- + Cl^{\bullet}$	2.2×10^6						$M^{-1} s^{-1}$	149
188	$H_2PO_4^{\bullet} + Cl^- + H^+ \rightarrow H_3PO_4 + Cl^{\bullet}$	1.9×10^9						$M^{-1} s^{-1}$	147
189	$Cl^- + HPO_4^{-\bullet} \rightarrow$ products	1.0×10^4						$M^{-1} s^{-1}$	149
190	$H^{\bullet} + H_3PO_4 \rightarrow H_2PO_4^{\bullet} + H_2$	5.0×10^5						$M^{-1} s^{-1}$	146
191	$H^{\bullet} + H_2PO_4^- \rightarrow HPO_4^{-\bullet} + H_2$	5.0×10^5						$M^{-1} s^{-1}$	146
192	$H^{\bullet} + HPO_4^{2-} \rightarrow PO_4^{2-\bullet} + H_2$	5.0×10^4						$M^{-1} s^{-1}$	146
193	$HPO_4^{-\bullet} + HPO_4^{-\bullet} \rightarrow P_2O_8^{4-} + H^+ + H^+$	3.0×10^8						$M^{-1} s^{-1}$	150,151
194	$H_2PO_4^{\bullet}$ + benzoic acid → benzoic acid$^{+\bullet}$ + $H_2PO_4^-$	2.4×10^8						$M^{-1} s^{-1}$	152
195	$H_2PO_4^- + H^+ \rightarrow H_3PO_4$	5.0×10^{10}			5.0×10^{10}		5.0×10^{10}	$M^{-1} s^{-1}$	36
196	$H_3PO_4 \rightarrow H^+ + H_2PO_4^-$	3.97×10^8			3.87×10^8		3.97×10^8	$M^{-1} s^{-1}$	36
197	$HPO_4^{2-} + H^+ \rightarrow H_2PO_4^-$	5.0×10^{10}			5.0×10^{10}		5.0×10^{10}	$M^{-1} s^{-1}$	36

198	$H_2PO_4^- \rightarrow HPO_4^{2-} + H^+$	3.2×10^3			3.15×10^3		3.2×10^3	s^{-1}	36
199	$PO_4^{3-} + H^+ \rightarrow HPO_4^{2-}$	5.0×10^{10}			5.0×10^{10}		5.0×10^{10}	$M^{-1} s^{-1}$	36
200	$HPO_4^{2-} \rightarrow PO_4^{3-} + H^+$	2.5×10^{-2}			2.5×10^{-2}		2.5×10^{-2}	s^{-1}	36
201	$^{\bullet}OH + H_3BO_3 \rightarrow H_2BO_3^{\bullet} + H_2O$	5.0×10^4						$M^{-1} s^{-1}$	153
202	$O_3 + H_2BO_3^- \rightarrow$ products	4.0×10^{-3}						$M^{-1} s^{-1}$	34
203	$HBO_3^{2-} + O_3 \rightarrow$ products	6.0×10^{-2}						$M^{-1} s^{-1}$	34

B6. Measurement of Second-Order Rate Constants

The second-order rate constants of •OH with HOCl and OCl^- were measured using electron pulse radiolysis and transient absorption spectroscopy. Experiments were conducted on the linear accelerator (LINAC) electron pulse radiolysis system at the Notre Dame Radiation Laboratory. Rate constants were measured by pulsing hypochlorite samples solutions and observing the rate of formation of the ClO• radical at λ = 280 nm. The rate constant of OCl^- with •OH was measured by pulsing a solution of 10 mM phosphate buffer (pH 10; KOH) and 0.1 – 1.0 mM hypochlorite. The rate constant of HOCl with •OH was similarly measured with 10 mM phosphate buffer (pH 5; perchloric acid) and 1 mM hypochlorous acid and 100 μM KSCN, which was added to slow the reaction.

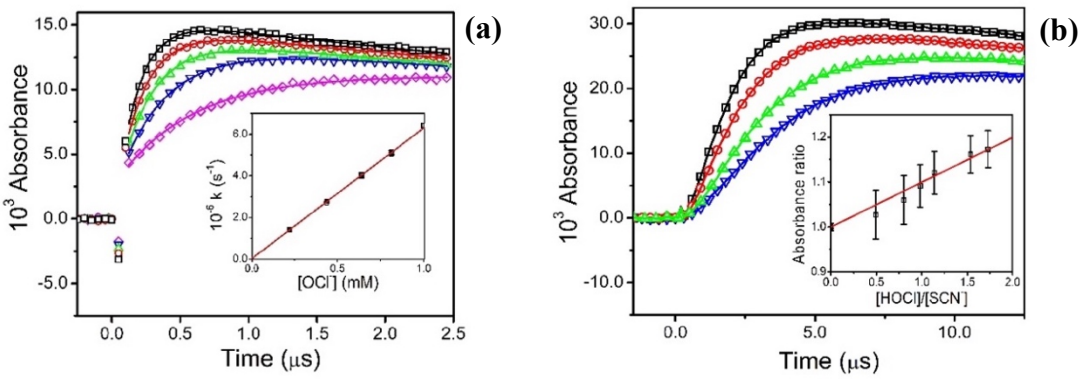

Figure B11. (a). Direct measurement of •OH reaction with OCl^- in N_2O-saturated 10 mM phosphate buffered pH 10 solution at 280 nm and 22°C for 1.0 mM (□), 812 μM (**O**), 638 μM (Δ), 313 μM (∇) and 262 μM (◊) added NaOCl. Solid lines are exponential growth and decay fits. Inset: Second order determination from fitted growth kinetics for reaction. Solid linear fit corresponds to reaction rate constant of $k_{37} = (6.37 \pm 0.06) \times 10^9\ M^{-1}\ s^{-1}$. (b). Competition kinetics-based determination for the reaction of •OH radical with HOCl in N_2O-saturated 10 mM phosphate buffered pH 5 solution by monitoring the $(SCN)_2^{-\bullet}$ transient at 475 nm. 101.4 μM KSCN was used throughout. Solid lines correspond to exponential growth and decay fits, from which limiting absorbance for zero (□), 237 μM (**O**), 116 μM (Δ) and 82 μM (∇) added HOCl. Inset: Competition kinetics plot for limiting absorbance values at different HOCl concentrations. Slope of solid line corresponds to reaction rate constants of $k_{29} = (1.21 \pm 0.08) \times 10^9\ M^{-1}\ s^{-1}$.

B7. Direct and Indirect Photolysis of Chlorine

Table B3. The ratios of the experimentally observed chlorine loss rate constant ($k_{obs,FAC}$) at pH 10 (>99% OCl^-) to pH 6 (96% HOCl) and the ratio of the molar absorptivity of chlorine at pH 10 to pH 6.

	Ratio of chlorine loss rate constant at pH 10 to pH 6	**Ratio of molar absorptivity at pH 10 to pH 6**
365 nm	2.18	3.99
311 nm	7.21	9.15
254 nm	1.32	0.96

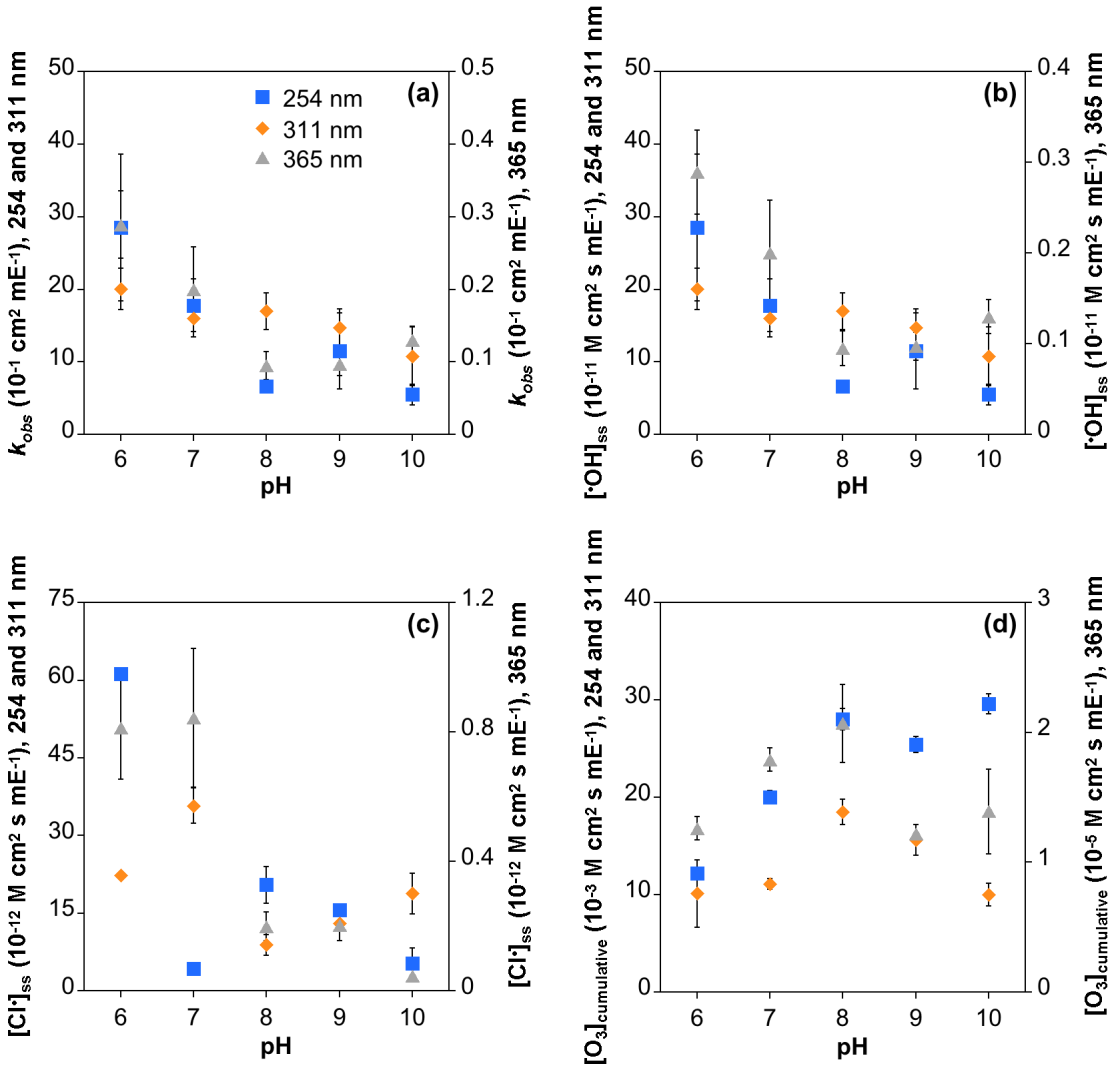

Figure B12. Fluence-normalized (a) observed free chlorine loss rate constant, (b) hydroxyl radical steady-state concentration, (c) chlorine radical steady-state concentration, and (d) cumulative ozone production as a function of pH during irradiation at 254, 311, and 365 nm (secondary axis).

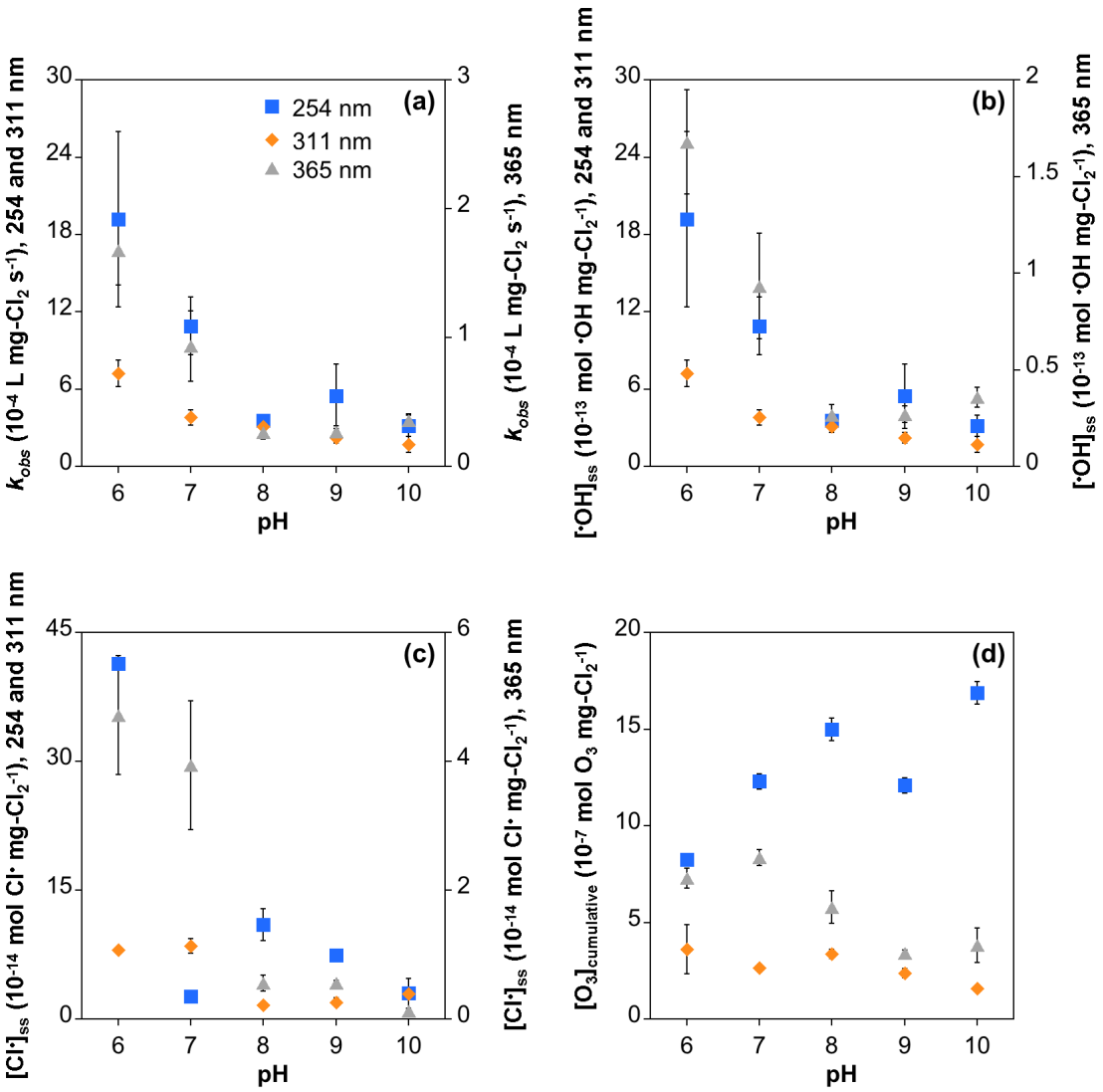

Figure B13. Total chlorine loss-normalized (a) observed free chlorine loss rate constant, (b) hydroxyl radical steady-state concentration, (c) chlorine radical steady-state concentration, and (d) cumulative ozone production as a function of pH during irradiation at 254, 311, and 365 nm (secondary axis).

B8. Literature Model Comparison

Table B4. Summary of the literature models included in this study.

Study	pH range	added chloride range	chlorine range	buffer used	main goals of the study	number of reactions
This Study	6 - 10	0 - 500 mM	4 mg-Cl_2/L	phosphate and borate	Measurement of oxidants across a range of pH and irradiation wavelengths.	196
Chuang et al. 2017[14]	7	0 - 20 mM	70 µM (5 mg-Cl_2/L)	phosphate	To predict oxidant loss and separate radicals generated from photolysis and those generated by radical chain reactions.	77
Fang et al. 2014[141]	6 - 9	0 - 1 mM	70 µM (5 mg-Cl_2/L)	none in model, phosphate experimentally	To identify the primary species responsible for contaminant degradation.	25
Guo et al. 2017[41]	6 - 8	none	10 µM (0.71 mg-Cl_2/L)	phosphate	To predict contaminant degradation and identify the main species responsible.	78
Li et al. 2017[15]	5.8	80 uM	2 mM (142 mg-Cl_2/L)	none in the model, ambient conditions experimentally	Modeling chlorine photolysis of reverse osmosis permeate.	69
Sun et al. 2016[38]	7	420 mM	7 - 28 mg-Cl_2/L	phosphate	To model the degradation of organic contaminants in saltwater. Experiments were conducted at both 254 nm and under simulated sunlight but only 254 nm was modeled	70

Table B5. Comparison of literature reported radical steady-state concentrations and steady-state concentrations modeled in this study using the first principles models from Table B2 and inputs as described in Section B5.

Model built for:	Result from:	$[^{\bullet}OH]_{ss}$ (M)	$[Cl^{\bullet}]_{ss}$ (M)	$[Cl_2^{-\bullet}]_{ss}$ (M)	$[ClO^{\bullet}]_{ss}$ (M)
This Study	This Study	8.01×10^{-13} - 6.40×10^{-12}	1.92×10^{-14} - 9.32×10^{-14}	2.03×10^{-13} - 1.05×10^{-12}	5.40×10^{-9} - 5.97×10^{-9}
Chuang et al. 2017[14]	This Study	1.15×10^{-13} - 1.25×10^{-11}	6.93×10^{-15} - 9.18×10^{-15}	5.27×10^{-14} - 6.96×10^{-14}	1.12×10^{-9} - 4.71×10^{-9}
	Chuang et al. 2017	1.1×10^{-13} - 1.5×10^{-13}	1.5×10^{-15} - 1×10^{-14}	1.4×10^{-15} - 4.1×10^{-12}	1.1×10^{-9}
Fang et al. 2014[141]	This Study	6.99×10^{-13} - 2.15×10^{-12}	2.14×10^{-14} - 8.29×10^{-13}	1.00×10^{-20} - 3.34×10^{-20}	2.27×10^{-5} - 2.98×10^{-5}
	Fang et al. 2014	2.73×10^{-14} - 1.04×10^{-13}	1.46×10^{-14} - 6.45×10^{-14}	6.44×10^{-14} - 4.10×10^{-12}	nr
Guo et al. 2017[41]	This Study	7.66×10^{-14} - 2.72×10^{-12}	1.26×10^{-14} - 3.23×10^{-13}	2.20×10^{-13} - 6.47×10^{-12}	1.63×10^{-10} - 6.33×10^{-10}
	Guo et al. 2017	7.48×10^{-14} - 2.55×10^{-13}	5.32×10^{-15} - 1.75×10^{-14}	3.22×10^{-15} - 4.87×10^{-14}	1.23×10^{-10} - 1.72×10^{-10} *
Li et al. 2017[15]	This Study	8.50×10^{-13} - 4.41×10^{-12}	3.24×10^{-15} - 4.22×10^{-15}	2.82×10^{-14} - 3.80×10^{-14}	2.25×10^{-5} - 2.97×10^{-5}
	Li et al. 2017	2.6×10^{-12}	4.9×10^{-13}	5.5×10^{-12}	nr
Sun et al. 2016[38]	This Study	7.00×10^{-14} - 4.10×10^{-12}	1.19×10^{-14} - 1.90×10^{-13}	2.12×10^{-13} - 3.76×10^{-12}	1.42×10^{-9} - 4.70×10^{-9}
	Sun et al. 2016	3.7×10^{-13} - 4.8×10^{-13}	9.0×10^{-14} - 1.8×10^{-13}	1.1×10^{-12} - 1.1×10^{-9}	4.0×10^{-9} - 8.1×10^{-9}

nr: not reported, *this study also reported $[ClO^{\bullet}]_{ss}$ of ~10^{-13} in the presence of NOM.

Table B6. Root-mean-square error of each model as a function of pH as compared to experimental data. Red boxes indicate the most accurate model.

Model	Root Mean Square Error of:			
	$k_{obs,FAC}$	•OH	Cl•	O_3
This Study	4.17×10^{-3}	2.87×10^{-12}	1.66×10^{-13}	1.48×10^{-6}
Chuang et al. 2017[14]	2.06×10^{-3}	6.39×10^{-12}	2.07×10^{-13}	1.65×10^{-6}
Fang et al. 2014[141]	8.17×10^{-3}	6.41×10^{-13}	3.19×10^{-13}	1.65×10^{-6}
Guo et al. 2017[41]	3.15×10^{-3}	1.09×10^{-12}	1.43×10^{-13}	1.65×10^{-6}
Li et al. 2017[15]	8.54×10^{-3}	1.99×10^{-12}	2.10×10^{-13}	1.65×10^{-6}
Sun et al. 2016[38]	7.09×10^{-3}	1.99×10^{-12}	1.28×10^{-13}	1.65×10^{-6}

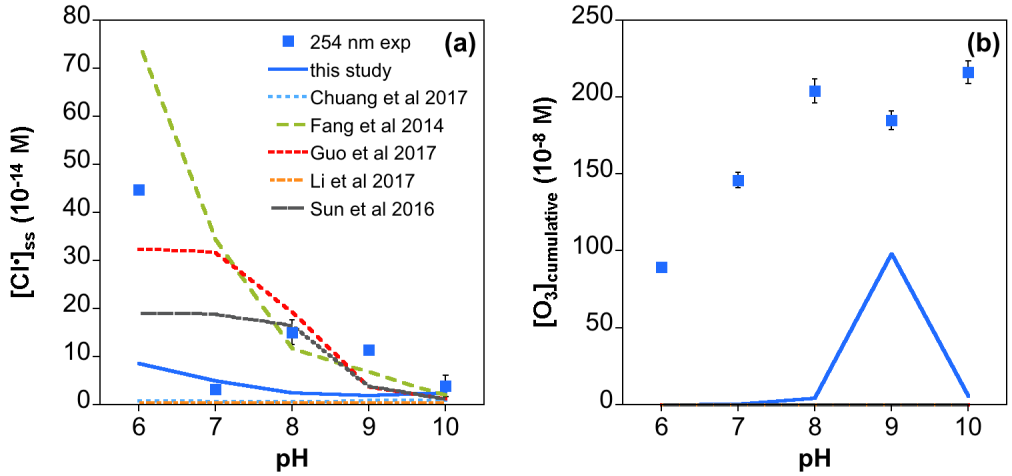

Figure B14. Comparison of experimental data with model output from the model developed in this study along with literature models for (a) chlorine radical steady-state concentration and (b) cumulative ozone concentration as a function of pH during irradiation at 254 nm.

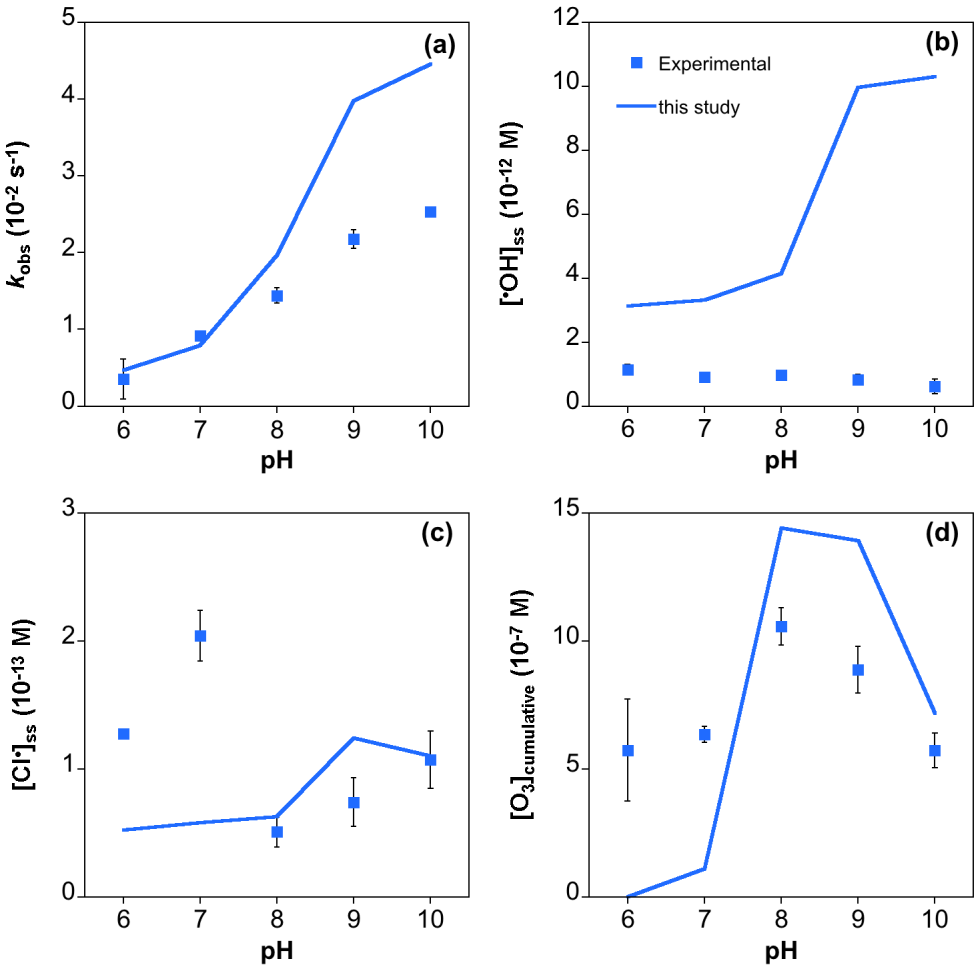

Figure B15. Comparison of experimental data with model output from the model developed in this study for the (a) observed free chlorine loss rate constant, (b) hydroxyl radical steady-state concentration, (c) chlorine radical steady-state concentration, and (d) cumulative ozone concentration as a function of pH during irradiation of 4 mg-Cl_2/L at 311 nm.

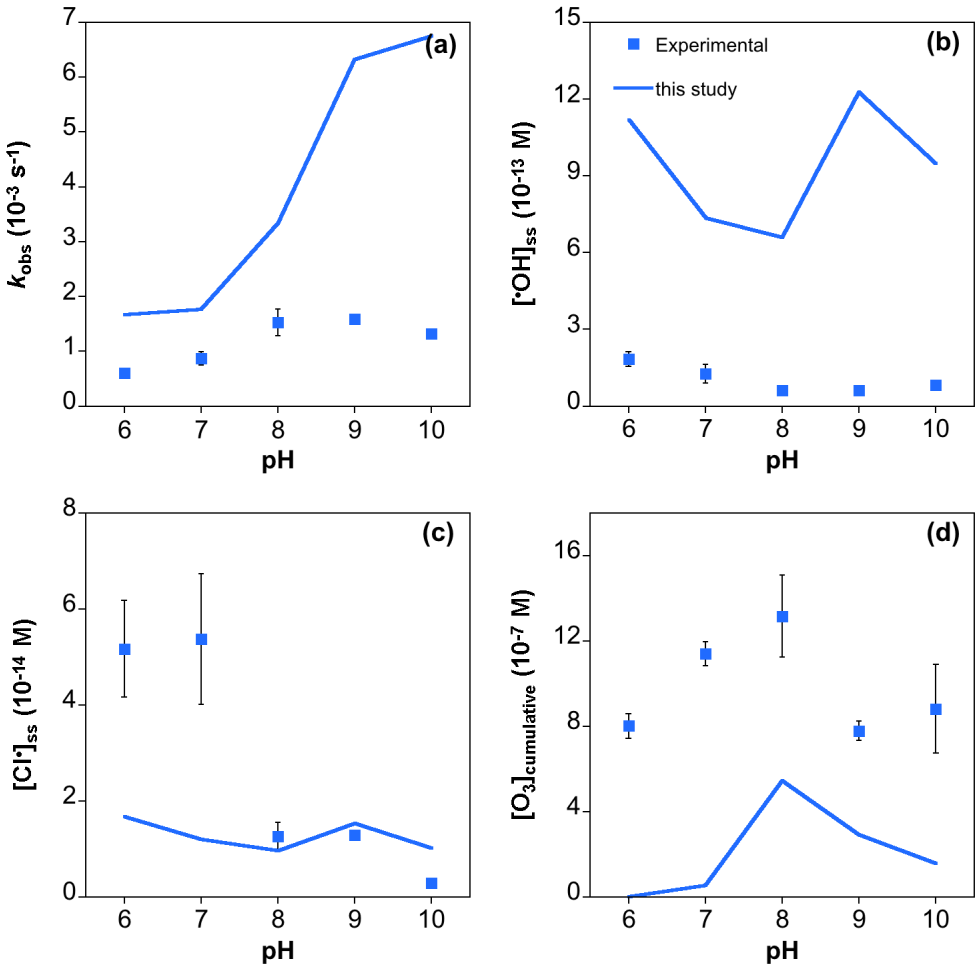

Figure B16. Comparison of experimental data with model output from the model developed in this study for the (a) observed free chlorine loss rate constant, (b) hydroxyl radical steady-state concentration, (c) chlorine radical steady-state concentration, and (d) cumulative ozone concentration as a function of pH during irradiation of 4 mg-Cl_2/L at 365 nm.

B9. References

(1) Watts, M. J.; Linden, K. G.; Chlorine photolysis and subsequent •OH radical production during UV treatment of chlorinated water. *Water Res.* **2007**, 41(13), 2871-2878.

(2) Laszakovits, J. R.; Berg, S. M.; Anderson, B. G.; O'Brien, J. E.; Wammer, K. H.; Sharpless, C. M.; *p*-Nitroanisole/pyridine and *p*-nitroacetophenone/pyridine actinometers revisited: Quantum yield in comparison to ferrioxalate. *Environ. Sci. Technol. Lett.* **2017**, 4(1), 11-14.

(3) McConville, M. B.; Hubert, T. D.; Remucal, C. K.; Direct photolysis rates and transformation pathways of the lampricides TFM and niclosamide in simulated sunlight. *Environ. Sci. Technol.* **2016**, 50(18), 9998-10006.

(4) Maizel, A. C.; Li, J.; Remucal, C. K.; Relationships between dissolved organic matter composition and photochemistry in lakes of diverse trophic status. *Environ. Sci. Technol.* **2017**, 51(17), 9624-9632.

(5) Galbavy, E. S.; Ram, K.; Anastasio, C.; 2-Nitrobenzaldehyde as a chemical actinometer for solution and ice photochemistry. *Photochem. Photobio. A* **2010**, 209(2-3), 186-192.

(6) Baeza, C.; Knappe, D. R. U.; Transformation kinetics of biochemically active compounds in low-pressure UV photolysis and UV/H_2O_2 advanced oxidation processes. *Water Res.* **2011**, 45(15), 4531-4543.

(7) Wang, D.; Bolton, J. R.; Hofmann, R.; Medium pressure UV combined with chlorine advanced oxidation for trichloroethylene destruction in a model water. *Water Res.* **2012**, 46(15), 4677-4686.

(8) Feng, Y.; Smith, D. W.; Bolton, J. R.; Photolysis of aqueous free chlorine species (HOCl and OCl^-) with 254 nm ultraviolet light. *J. Environ. Eng. Sci.* **2007**, 6(3), 277-284.

(9) Hoigné, J.; Bader, H.; Rate constants of reactions of ozone with organic and inorganic compounds in water-I: Non-dissociating organic compounds. *Water Res.* **1983**, 17, 173-183.

(10) Buxton, G. V.; Subhani, M. S.; Radiation chemistry and photochemistry of oxychlorine ions Part 2. Photodecomposition of aqueous solutions of hypochlorite ions. *J. Chem. Soc., Faraday Trans.* **1972**, 68, 958-969.

(11) Young, T. R.; Li, W.; Guo, A.; Korshin, G. V.; Dodd, M. C.; Characterization of disinfection byproduct formation and associated changes to dissolved organic matter during solar photolysis of free available chlorine. *Water Res.* **2018**, 146, 318-327.

(12) Leitzke, A.; Reisz, E.; Flyunt, R.; Von Sonntag, C.; The reactions of ozone with cinnamic acids: Formation and decay of 2-hydroperoxy-2-hydroxyacetic acid. *J. Chem. Soc., Perkin Trans. 2* **2001**, (5), 793-797.

(13) Nowell, L. H.; Hoigné, J.; Photolysis of aqueous chlorine at sunlight and ultraviolet wavelengths II. Hydroxyl radical production. *Water Res.* **1992**, 5, 599-605.

(14) Chuang, Y. H.; Chen, S.; Chinn, C. J.; Mitch, W. A.; Comparing the UV/monochloramine and UV/free chlorine advanced oxidation processes (AOPs) to the UV/hydrogen peroxide AOP under scenarios relevant to potable reuse. *Environ. Sci. Technol.* **2017**, 51(23), 13859-13868.

(15) Li, W.; Jain, T.; Ishida, K.; Remucal, C. K.; Liu, H.; A mechanistic understanding of the degradation of trace organic contaminants by UV/hydrogen peroxide, UV/persulfate and UV/free chlorine for water reuse. *Environ. Sci.: Water Res. Tech.* **2017**, 3(1), 128-138.

(16) Remucal, C. K.; Manley, D.; Emerging investigators series: The efficacy of chlorine photolysis as an advanced oxidation process for drinking water treatment. *Environ. Sci.: Water Res. Tech.* **2016**, 2 (4), 565-579.
(17) Kläning, U. K.; Wolff, T.; Laser flash photolysis of HClO, ClO^-, HBrO, and BrO^- in aqueous solution. Reactions of Cl and Br atoms. *Ber. Bunsenges. Phys. Chem.* **1985**, 89, 243-245.
(18) Zehavi, D.; Rabani, J.; Pulse radiolytic investigation of O_{aq}^- radical ions. *J. Phys. Chem.* **1971**, 75 (11), 1738-1744.
(19) Jayson, G. G.; Parsons, B. J.; Swallow, A. J.; Some simple, highly reactive, inorganic chlorine derivatives in aqueous solution. *J. Chem. Soc., Faraday Trans. 1* **1973**, 69, 1597-1607.
(20) Mártire, D. O.; Rosso, J. A.; Bertolotti, S.; Le Roux, G. C.; Braun, A. M.; Gonzalez, M. C.; Kinetic study of the reactions of chlorine atoms and $Cl_2^{\bullet-}$ radical anions in aqueous solutions. II. Toluene, benzoic acid, and chlorobenzene. *J. Phys. Chem. A* **2001**, 105(22), 5385-5392.
(21) Hasegawa, K.; Neta, P.; Rate constants and mechanisms of reaction of chloride (Cl_2^-) radicals. *J. Phys. Chem.* **1978**, 82(8), 854-857.
(22) Leifer, A. *The kinetics of environmental aquatic photochemistry: Theory and practice* (American Chemical Society, Washington DC, 1988).
(23) Morgan, M. S.; Van Trieste, P. F.; Garlick, S. M.; Mahon, M. J.; Smith, A. L.; Ultraviolet molar absorptivities of aqueous hydrogen peroxide and hydroperoxyl ion. *Anal. Chim. Acta* **1988**, 215, 325-329.
(24) Hart, E. J.; Sehested, K.; Holcman, J.; Molar absorptivities of ultraviolet and visible bands of ozone in aqueous solutions. *Anal. Chem.* **1983**, 55, 46-49.
(25) Eaton, A. D.; Clesceri, L. S.; Greenberg, A. E., Eds. *Standard Methods for the Examination of Water and Wastewater*, ed.; United Book Press, Inc., Baltimore, 1995.
(26) Armerding, W.; Comes, F. J.; Schülke, B.; $O(^1D)$ quantum yields of ozone photolysis in the UV from 300 nm to its threshold and at 355 nm. *J. Phys. Chem.* **1995**, 99, 3137-3143.
(27) Takahashi, K.; Quantum yields of $O(^1D)$ formation in the photolysis of ozone between 230 and 308 nm. *J. Geophys. Res.* **2002**, 107(D20), ACH 11-1.
(28) Moortgat, G. K.; Warneck, P.; Relative $O(^1D)$ quantum yields in the near UV photolysis of ozone at 298 K. *Zeitschrift für Naturforschung A* **1975**, 30 (6-7), 835-844.
(29) Kläning, U. K.; Sehested, K.; Wolff, T.; Ozone formation in laser flash photolysis of oxoacids and oxoanions of chlorine and bromine. *J. Chem. Soc., Faraday Trans. 1* **1984**, 80, 2969-2979.
(30) Buxton, G. V.; Subhani, M. S.; Radiation chemistry and photochemistry of oxychlorine ions Part 3. Photodecomposition of aqueous solutions of chloride ions. *J. Chem. Soc., Faraday Trans.* **1972**, 68, 970-977.
(31) Sauer Jr., M. C.; Brown, W. G.; Hart, E. J.; $O(^3P)$ atom formation by the photolysis of hydrogen peroxide in alkaline aqueous solutions. *J Phys. Chem.* **1984**, 88, 1398-1400.
(32) Hart, E. J.; Brown, W. G.; $O(^3P)$ atom formation in gamma and 184.9-nm-irradiated aqueous perchlorate solutions. *J. Phys. Chem.* **1980**, 84, 2237-2240.
(33) Sehested, K.; Corfitzen, H.; Holcman, J.; Hart, E. J.; Decomposition of ozone in aqueous acetic acid solutions (pH 0-4). *J. Phys. Chem.* **1992**, 96, 1005-1009.

(34) Hoigné, J.; Bader, H.; Haag, W. R.; Staehelin, J.; Rate constants of reactions of ozone with organic and inorganic compounds in water III. Inorganic compounds and radicals. *Water Res.* **1985**, 19 (8), 993-1004.
(35) Yang, Y.; Pignatello, J. J.; Ma, J.; Mitch, W. A.; Comparison of halide impacts on the efficiency of contaminant degradation by sulfate and hydroxyl radical-based advanced oxidation processes (AOPs). *Environ. Sci. Technol.* **2014**, 48(4), 2344-2351.
(36) Grebel, J. E.; Pignatello, J. J.; Mitch, W. A.; Effect of halide ions and carbonates on organic contaminant degradation by hydroxyl radical-based advanced oxidation processes in saline waters. *Environ. Sci. Technol.* **2010**, 44(17), 6822-6828.
(37) Wang, T. X.; Margerum, D. W.; Kinetics of reversible chlorine hydrolysis: Temperature dependence and general acid/base assisted mechanisms. *Inorg. Chem.* **1994**, 33, 1050-1055.
(38) Sun, P.; Lee, W. N.; Zhang, R.; Huang, C. H.; Degradation of DEET and caffeine under UV/chlorine and simulated sunlight/chlorine conditions. *Environ. Sci. Technol.* **2016**, 50(24), 13265-13273.
(39) Mialocq, J. C.; Barat, F.; Gilles, L.; Hickel, B.; Lesigne, B.; Flash photolysis of chlorine dioxide in aqueous solution. *J. Phys. Chem.* **1973**, 77 (6), 742-749.
(40) Buxton, G. V.; Greenstock, C. L.; Helman, W. P.; Ross, A. B.; Critical review of rate constants for reactions of hydrated electrons, hydrogen atoms and hydroxyl radicals (OH/ O^-) in aqueous solution. *J. Phys. Chem. Ref. Data* **1988**, 17 (2), 513-886.
(41) Guo, K.; Wu, Z.; Shang, C.; Yao, B.; Hou, S.; Yang, X.; Song, W.; Fang, J.; Radical chemistry and structural relationships of PPCP degradation by UV/chlorine treatment in simulated drinking water. *Environ. Sci. Technol.* **2017**, 51(18), 10431-10439.
(42) Christensen, H.; Sehested, K.; Corfitzen, H.; Reactions of hydroxyl radicals with hydrogen peroxide at ambient and elevated temperatures. *J. Phys. Chem.* **1982**, 86, 1588-1590.
(43) Elliot, A. J.; Buxton, G. V.; Temperature dependence of the reactions OH + O_2^- and OH + HO_2 in water up to 200 ºC. *J. Chem. Soc., Faraday Trans.* **1992**, 88 (17), 2465-2470.
(44) Beck, G.; Elektrische leitfähigkeitsmessungen zum nachweis geladener zwischenprodukte der pulsradiolyse. *Int. J. Radiat. Phys. Chem.* **1969**, 1, 361-371.
(45) Kläning, U. K.; Sehested, K.; Holcman, J.; Standard Gibbs energy of formation of the hydroxyl radical in aqueous solution. Rate constants for the reaction ClO_2^- + O_3 = O_3^- + ClO_2. *J. Phys. Chem.* **1985**, 89, 760-763.
(46) Wagner, I.; Karthäuser, J.; Strehlow, H.; On the decay of the dichloride anion in Cl_2^- in aqueous solution. *Ber. Bunsenges. Phys. Chem.* **1986**, 90, 861-867.
(47) Sehested, K.; Rasmussen, O. L.; Fricke, H.; Rate constants of OH with HO_2, O_2^-, and $H_2O_2^+$ from hydrogen peroxide formation in pulse-irradiated oxygenated water. *J. Phys. Chem.* **1968**, 72 (2), 626-631.
(48) Thomas, J. K.; The rate constant for H atom reactions in aqueous solutions. *J. Am. Chem. Soc.* **1963**, 67, 2593-2595.
(49) Grigor'ev, A. E.; Makarov, I. E.; Pikaev, A. K.; Formation of Cl_2^- in the bulk solution during the radiolysis of concentrated aqueous solutions of chlorides. *High Energy Chem.* **1987**, 21, 99-102.
(50) Eriksen, T. E.; Lind, J.; Merényi, G.; Generation of chlorine dioxide from ClO_2^- by pulse radiolysis. *J. Chem. Soc., Faraday Trans. 1* **1981**, 77, 2115-2123.

(51) Buxton, G. V.; Subhani, M. S.; Radiation chemistry and photochemistry of oxychlorine ions part 1.-radiolysis of aqueous solutions of hypochlorite and chlorite ions. *J. Chem. Soc., Faraday Trans. 1* **1972**, 68 (0), 947-957.
(52) Merényi, G.; Lind, J. S.; Role of a peroxide intermediate in the chemiluminesence of luminol. A mechanistic study. *J. Am. Chem. Soc.* **1980**, 102, 5830-5835.
(53) Buxton, G. V.; Pulse radiolysis of aqueous solutions. *Trans. Faraday Soc.* **1969**, 65, 2150-2158.
(54) Rabani, J. Pulse radiolysis of alkaline solutions. In *Radiation Chemistry*; 1968; pp 131
(55) Crittenden, J. C.; Hu, S.; Hand, D. W.; Green, S. A.; A kinetic model for H_2O_2/UV process in a completely mixed batch reactor. *Water Res.* **1999**, 33 (10), 2315-2328.
(56) Rabani, J.; Matheson, M. S.; The pulse radiolysis of aqueous solutions of potassium ferrocyanide. *J. Phys. Chem.* **1966**, 70 (3), 761-769.
(57) Buxton, G. V.; Pulse radiolysis of aqueous solutions: Rate of reaction of OH with OH^-. *Trans. Faraday Soc.* **1970**, 66, 1656-1660.
(58) Christensen, H.; Sehested, K.; Reaction of hydroxyl radicals with hydrogen at elevated temperatures. Determination of the activation energy. *J. Phys. Chem.* **1983**, 87(1), 118-120.
(59) Schmidt, K. H.; Measurement of the activation energy for the reaction of the hydroxyl radical with hydrogen in aqueous solution. *J. Phys. Chem.* **1977**, 81(13), 1257-1263.
(60) Thomas, J. K.; Rabani, J.; Matheson, M. S.; Hart, E. J.; Gordon, S.; Absorption spectrum of the hydroxyl radical. *J. Phys. Chem.* **1966**, 70(7), 2409-2410.
(61) Thomas, J. K.; Rates of reaction of the hydroxyl radical. *Trans. Faraday Soc.* **1965**, 61, 702-707.
(62) Bunn, D.; Dainton, F. S.; Salmon, G. A.; Hardwick, T. J.; The reactivity of hydroxyl radicals in aqueous solution. Part 2. Relative reactivities with hydrogen, deuterium and hydrogen deuteride. *J. Chem. Soc., Faraday Trans.* **1959**, 55, 1760-1767.
(63) Sehested, K.; Holcman, J.; Bjergbakke, E.; Hart, E. J.; Formation of ozone in the reaction of OH with O_3^- and the decay of the ozonide ion radical at pH 10-13. *J. Phys. Chem* **1984**, 88, 269-273.
(64) Sehested, K.; Holcman, J.; Bjergbakke, E.; Hart, E. J.; A pulse radiolytic study of the reaction OH + O_3 in aqueous medium. *J. Phys. Chem.* **1984**, 88, 4144-4147.
(65) Yu, X.-Y.; Barker, J. R.; Hydrogen peroxide photolysis in acidic aqueous solutions containing chloride ions. II. Quantum yield of $HO^{\bullet}_{(aq)}$ radicals. *J. Phys. Chem. A* **2003**, 107(9), 1325-1332.
(66) Bunce, N. J.; Ingold, K. U.; Landers, J. P.; Lusztyk, J.; Scaiano, J. C.; Kinetic study of the photochlorination of 2,3-dimethylbutane and other alkanes in solution in the presence of benzene. First measurements of the absolute rate constants for hydrogen abstraction by the "free" chlorine atom and the chlorine atom-benzene pi-complex. Identification of these two species as the only hydrogen abstractors in these systems. *J. Am. Chem. Soc.* **1985**, 107, 5464-5472.
(67) Mcelroy, W. J.; A laser photolysis study of the reaction of SO_4^- with Cl^- and the subsequent decay of Cl_2^- in aqueous solution. *J. Phys. Chem.* **1990**, 94, 2435-2441.
(68) Wu, D.; Wong, D.; Di Bartolo, B.; Evolution of Cl_2^- in aqueous NaCl solutions. *J. Photochem.* **1980**, 14, 303-310.
(69) Nagarajan, V.; Fessenden, R. W.; Flash photolysis of transient radicals. X_2^- with x = Cl, Br, I, and SCN. *J. Phys. Chem.* **1985**, 89, 2330-2335.

(70) Yu, X.-Y.; Barker, J. R.; Hydrogen peroxide photolysis in acidic aqueous solutions containing chloride ions. I. Chemical mechanism. *J. Phys. Chem. A* **2003**, 107(9), 1313-1324.
(71) Ferraudi, G.; Magnetic field effects on the rates of Cl_2^- and Br_2^- reactions: The dependence of the rates of radical disproportionation and oxidation of Mn(II) complexes on field intensity. *J. Phys. Chem.* **1993**, 97, 2793-2797.
(72) Huie, R. E.; Clifton, C. L.; Temperature dependence of the rate constants for reactions of the sulfate radical, SO_4^-, with anions. *J. Phys. Chem.* **1990**, 94, 8561-8567.
(73) Hynes, A. J.; Wine, P. H.; Time-resolved resonance Raman study of the spectroscopy and kinetics of the Cl_2^- radical anion in aqueous solution. *J. Chem. Phys.* **1988**, 89(6), 3565-3572.
(74) Lierse, C.; Sullivan, J. C.; Schmidt, K. H.; Rates of oxidation of selected actinides by $Cl_2^{\bullet-}$ *Inorg Chem.* **1987**, 26, 1408-1410.
(75) Gogolev, A. V.; Makarov, I. E.; Pikaev, A. K.; Pulsed radiolysis of concentrated hydrochloric acid. *Khimiya Vysokikh Energii* **1984**, 18(6), 496-501.
(76) Navaratnam, S.; Parsons, B. J.; Swallow, A. J.; Some reactions of the dichloride anion radical. *Radiat. Phys. Chem.* **1980**, 15, 159-161.
(77) Zansokhova, A. A.; Kabakchi, S. A.; Pikaev, A. K.; Mechanism of Cl_2^- formation in the pulse radiolysis of neutral aqueous solutions of alkali metal chlorides. *High Energy Chem.* **1977**, 11, 50-54.
(78) Broszkiewicz, R. K.; On the effect of Br^- on formation of Cl_2^- in the pulse radiolysis of the aqueous chlorine solutions. *Bull. Polish Acad. Sci., Series Sci. Chem.* **1976**, 24, 123-131.
(79) Woods, R. J.; Lesigne, B.; Gilles, L.; Ferradini, C.; Pucheault, J.; Pulse radiolysis of aqueous lithium chloride solutions. *J. Phys. Chem.* **1975**, 79 (24), 2700-2704.
(80) Zhestkova, T. P.; Pikaev, A. K.; Destruction rate of Cl_2^- anion-radicals during pulse radiolysis of concentrated aqueous lithium chloride solutions. *Izvestiya Akademii Nauk SSSR, Seriya Kimiya* **1974**, 23(4), 913-914.
(81) Broszkiewicz, R. K.; Pulse radiolysis studies on chloro-complexes of palladium. *Int. J. Radiat. Phys. Chem.* **1974**, 6, 249-258.
(82) Thornton, A. T.; Laurence, G. S.; Kinetics of oxidation of transition-metal ions by halogen radical anions. Part I. The oxidation of iron(II) by dibromide and dichloride generated by flash photolysis. *J. Chem. Soc., Dalton Trans.* **1973**, 0 (8), 804-813.
(83) Patterson, L. K.; Bansal, K. M.; Bogan, G.; Infante, G. A.; Fendler, E. J.; Fendler, J. H.; Micellar effects on Cl_2^- reactivity. Reactions with surfactants and pyrimidines. *J. Am. Chem. Soc.* **1972**, 94 (26), 9028-9032.
(84) Ward, J. F.; Kuo, I. Steady state and pulse radiolysis of aqueous chloride solutions of nucleic acid components. In *Radiation Chemistry*; 1968; pp 368
(85) Langmuir, M. E.; Hayon, E.; Flash photolysis study of mercury(II) halide complexes in aqueous solution. Rates of reaction of X_2^- radical anions. *J. Phys. Chem.* **1967**, 71(12), 3808-3814.
(86) Treinin, A.; The photochemistry of oxyanions. *Israel J. Chem.* **1970**, 8, 103-113.
(87) Gilbert, C. W.; Ingalls, R. B.; Swallow, A. J.; Pulse irradiation of aqueous solutions containing ferrous and chloride ions: Reactions between Cl_2^- and $HO_2^{\cdot}$ *Radiat. Phys. Chem.* **1977**, 10, 221-225.
(88) Alfassi, Z. B.; Huie, R. E.; Mosseri, S.; Neta, P.; Kinetics of one-electron oxidation by the ClO radical. *Radiat. Phys. Chem.* **1988**, 32 (1), 85-88.

(89) Staehelin, J.; Hoigné, J.; Decomposition of ozone in water: Rate initiation by hydroxide ions and hydrogen peroxide. *Environ. Sci. Technol.* **1982**, 16, 676-681.
(90) Fischbacher, A.; Löppenberg, K.; Von Sonntag, C.; Schmidt, T. C.; A new reaction pathway for bromite to bromate in the ozonation of bromide. *Environ. Sci. Technol.* **2015**, 49(19), 11714-11720.
(91) Haag, W. R.; Hoigné, J.; Ozonation of water containing chlorine or chloramines: Reaction products and kinetics. *Water Res.* **1983**, 17 (10), 1397-1402.
(92) Yeatts Jr., L. R. B.; Taube, H.; The kinetics of the reaction of ozone and chloride ion in acid aqueous solution. *J. Am. Chem. Soc.* **1949**, 71 (12), 4100-4105.
(93) Taube, H.; Bray, W. C.; Chain reactions in aqueous solutions containing ozone, hydrogen peroxide and acid. *J. Am. Chem. Soc.* **1940**, 62, 3357-3373.
(94) Sehested, K.; Holcman, J.; Hart, E. J.; Rate constants and products of the reactions of e^-_{aq}, O_2^-, and H with ozone in aqueous solutions. *J. Phys. Chem.* **1983**, 87, 1951-1954.
(95) Bielski, B. H. J.; A pulse radiolysis study of the reaction of ozone with Cl_2^- in aqueous solutions. *Radiat. Phys. Chem.* **1993**, 41 (3), 527-530.
(96) Bühler, R. E.; Staehelin, J.; Hoigné, J.; Ozone decomposition in water studied by pulse radiolysis. 1. HO_2/O_2^- and HO_3/O_3^- as intermediates. *J. Phys. Chem.* **1984**, 88, 2560-2564.
(97) Hoigné, J.; Bader, H.; Kinetics of reactions of chlorine dioxide (OClO) in water I. Rate constants for inorganic and organic compounds. *Water Res.* **1994**, 28 (1), 45-55.
(98) Hoigné, J.; Bader, H.; Kinetik typischer reaktionen von chlordioxid mit wasserinhaltssoffen. *Vom Wasser* **1982**, 59, 253-267.
(99) Matthew, B. M.; Anastasio, C.; A chemical probe technique for the determination of reactive halogen species in aqueous solution. Part 1: Bromide solutions. *Atmos. Chem. Phys.* **2006**, 6, 2423-2437.
(100) Connick, R. E.; The interaction of hydrogen peroxide and hypochlorous acid in acidic solutions containing chloride ion. *J. Am. Chem. Soc.* **1947**, 69 (6), 1509-1514.
(101) Koppenol, W. H.; Butler, J.; Van Leeuwen, J. W.; The Haber-Weiss cycle. *Photochem. Photobio.* **1978**, 28, 655-660.
(102) Elliot, A. J.; A pulse radiolysis study of the temperature dependence of reactions involving H, OH and e^-_{aq} in aqueous solution. *Radiat. Phys. Chem.* **1989**, 34 (5), 753-758.
(103) Mezyk, S. P.; Bartels, D. M.; Direct EPR measurement of Arrhenius parameters for the reactions of H atoms with H_2O_2 and D atoms with D_2O_2 in aqueous solution. *J. Chem. Soc., Faraday Trans.* **1995**, 91 (18), 3127-3132.
(104) Sweet, J. P.; Thomas, J. K.; Absolute rate constants for H atom reactions in aqueous solutions. *J. Phys. Chem.* **1984**, 68 (6), 1363-1368.
(105) Weinstein, J.; Bielski, B. H. J.; Kinetics of the interaction of HO_2 and O_2^- radials with hydrogen peroxide, the Haber-Weiss reaction. *J. Am. Chem. Soc.* **1979**, 101 (1), 58-62.
(106) Melhuish, W. H.; Sutton, H. C.; Study of the Haber-Weiss reaction using a sensitive method for detection of OH radicals. *J. Chem. Soc., Chem. Commun.* **1978**, 0 (22), 970-971.
(107) Ferradini, C.; Foos, J.; Houee, C.; Pucheault, J.; The reaction between superoxide anion and hydrogen peroxide. *Photochem. Photobio.* **1978**, 28, 697-700.
(108) Rigo, A.; Stevanato, R.; Finazzi-Agro, A.; Rotilio, G.; An attempt to evaluate the rate of the Haber-Weiss reaction by using OH radical scavengers. *FEBS Letters* **1977**, 80 (1), 130-132.

(109) Marklund, S.; Spectrophotometric study of spontaneous disproportionation of superoxide anion radical and sensitive direct assay for superoxide dismutase. *J. Biol. Chem.* **1976**, 251(23), 7504-7507.
(110) Kozlov, Y. N.; Purmal', A. P.; Uskov, A. M.; Oxidation of one and two electron donors by chlorine dioxide. *Zhurnal Fizicheskoi Khimii* **1985**, 59(6), 1567-1570.
(111) Bjergbakke, E.; Navaratnam, S.; Parsons, B. J.; Swallow, A. J.; Reaction between HO_2 and chlorine in aqueous solution. *J. Am. Chem. Soc.* **1981**, 103, 5926-5928.
(112) Bielski, B. H. J.; Cabelli, D. E.; Arudi, R. L.; Ross, A. B.; Reactivity of HO_2/O_2^- radicals in aqueous solution. *J. Phys. Chem. Ref. Data* **1985**, 14(4), 1041-1100.
(113) Field, R. J.; Noyes, R. M.; Postlethwaite, D.; Photoreduction of hydrogen peroxide by hydrogen. *J. Phys. Chem.* **1976**, 80 (3), 223-229.
(114) Christensen, H.; Sehested, K.; HO_2 and O_2^- radicals at elevated temperatures. *J. Phys. Chem.* **1988**, 92 (10), 3007-3011.
(115) Huie, R. E.; Neta, P.; Kinetics of one-electron transfer reactions involving ClO_2 and NO_2. *J. Phys. Chem.* **1986**, 90, 1193-1198.
(116) Long, C. A.; Bielski, B. H. J.; Rate of reaction of superoxide radical with chloride containing species. *J. Phys. Chem.* **1980**, 84 (5), 555-557.
(117) Sehested, K.; Holcman, J.; Bjergbakke, E.; Hart, E. J.; Ultraviolet spectrum and decay of the ozonide ion radical O_3^-, in strong alkaline solution. *J. Phys. Chem.* **1982**, 86, 2066-2069.
(118) Ilan, Y.; Rabani, J.; On some fundamental reactions in radiation chemistry: Nanosecond pulse radiolysis. *Int. J. Radiat. Phys. Chem* **1976**, 8, 609-611.
(119) Elliot, A. J.; Mccracken, D. R.; Effect of temperature on O^- reactions and equilibria: A pulse radiolysis study. *Radiat. Phys. Chem.* **1989**, 33 (1), 69-74.
(120) Bobrowski, K.; Suwalski, J. P.; Zagorski, Z. P.; Pulse radiolysis study on tetraalkylammonium hydroxides in alkaline solutions containing O_2 and N_2O. *Int. J. Radiat. Phys. Chem.* **1976**, 8, 527-531.
(121) Gall, B. L.; Dorfman, L. M.; Pulse radiolysis studies. XV. Reactivity of the oxide radical ion and of the ozonide ion in aqueous solution. *J. Am. Chem. Soc.* **1969**, 91 (9), 2199-2204.
(122) Behar, D.; Czapski, G.; Flash photolysis of hydrogen peroxide I: The reaction of ozonide with hydrogen peroxide. *Israel Journal of Chemistry* **1968**, 6, 43-51.
(123) Subhani, M. S.; Kauser, Z.; Flash photolysis decomposition of sulphate and sulphite anions in aqueous solution. *Revue Roumaine de Chimie* **1978**, 23 (7), 1129-1137.
(124) Kläning, U. K.; Sehested, K.; Wolff, T.; Laser flash photolysis and pulse radiolysis of iodate and periodate in aqueous solution. *J. Chem. Soc., Faraday Trans. 1* **1981**, 77, 1707-1718.
(125) Adams, G. E.; Boag, J. W.; Michael, B. D.; Transient species produced in irradiated water and aqueous solutions containing oxygen. *Proc. R. Soc. Lond. A, Math. Phys. Sci.* **1966**, 289 (1418), 321-341.
(126) Ershov, B. G.; Kinetics, mechanism and intermediates of some radiation-induces reaction in aqueous solutions. *Russian Chemical Reviews* **2004**, 73 (1), 101-113.
(127) Dunn, R. C.; Simon, J. D.; Excited-state photoreactions of chlorine dioxide in water. *J. Am. Chem. Soc.* **1992**, 114, 4856-4860.
(128) Draganić, Z. D.; Draganić, I. G.; Studies on the formation of primary hydrogen atom yield (Gh) in the gamma radiolysis of water. *J. Phys. Chem.* **1972**, 76 (19), 2733-2737.

(129) Vogt, R.; Schindler, R. N.; Product channels in the photolysis of HOCl. *Photochem. Photobio. A* **1992**, 66, 133-140.
(130) Hartig, K. J.; Getoff, N.; Reactivity of hydrogen atoms with liquid water. *J. Photochem.* **1982**, 18, 29-38.
(131) Elliot, A. J.; Mccracken, D. R.; Buxton, G. V.; Wood, N. D.; Estimation of rate constants for near-diffusion-controlled reactions in water at high temperatures. *J. Chem. Soc., Faraday Trans.* **1990**, 86 (9), 1539-1547.
(132) Gordon, S.; Hart, E. J.; Thomas, J. K.; The ultraviolet spectra of transients produced in the radiolysis of aqueous solutions. *J. Phys. Chem.* **1964**, 68 (5), 1262-1264.
(133) Sehested, K.; Christensen, H.; The rate constant of the biomolecular reaction of hydrogen atom at elevated temperatures. *Radiat. Phys. Chem.* **1990**, 36 (3), 499-500.
(134) Beckert, D.; Mehler, K.; Investigation of hydrogen atom addition to vinyl monomers by time resolved ESR spectroscopy. *Ber. Bunsenges. Phys. Chem.* **1983**, 87, 587-591.
(135) Fessenden, R. W.; Verma, N. C.; Studies of the reactions of hydrogen atoms by time-resolved E.S.R. Spectroscopy. *Faraday Discuss. Chem. Soc.* **1977**, 63, 104-111.
(136) Pagsberg, P.; Christensen, H.; Rabani, J.; Nilsson, G.; Fenger, J.; Nielsen, S. O.; Far-ultraviolet spectra of hydrogen and hydroxyl radicals from pulse radiolysis of aqueous solutions. Direct measurement of the rate of H + H. *J. Phys. Chem.* **1969**, 73 (4), 1029-1038.
(137) Ashton, L.; Buxton, G. V.; Stuart, C. R.; Temperature dependence of the rate of reaction of OH with some aromatic compounds in aqueous solution. *J. Chem. Soc., Faraday Trans.* **1995**, 91 (11), 1631-1633.
(138) Neta, P.; Dorfman, L. M. Pulse radiolysis studies. XIII. Rate constants for the reaction of hydroxyl radicals with aromatic compounds in aqueous solutions. In *Advances in Chemistry: Radiation Chemistry*; eds.; American Chemical Society: Washington, D. C., 1968; pp 222
(139) Asmus, K. D.; Cercek, B.; Ebert, M.; Henglin, A.; Wigger, A.; Pulse radiolysis of nitrobenzene solutions. *Trans. Faraday Soc.* **1967**, 63, 2435-2442.
(140) Neta, P.; Dorfman, L. M.; Pulse-radiolysis studies. XIV. Rate constants for the reactions of hydrogen atom with aromatic compounds in aqueous solution. *J. Phys. Chem.* **1969**, 73 (2), 413-417.
(141) Fang, J.; Fu, Y.; Shang, C.; The roles of reactive species in micropollutant degradation in the UV/free chlorine system. *Environ. Sci. Technol.* **2014**, 48(3), 1859-1868.
(142) Wander, R.; Neta, P.; Dorfman, L. M.; Pulse radiolysis studies. XII. Kinetics and spectra of the cyclokexadienyl radicals in aqueous benzoic acid solution. *J. Phys. Chem.* **1968**, 72 (8), 2946-2949.
(143) Wolfenden, B. S.; Willson, R. L.; Radical-cations as reference chromogens in kinetic studies of one-electron transfer reaction: Pulse radiolysis studies of 2,2'-azinobis-(3-ethylbenzthiazoline-6-sulphonate). *J. Chem. Soc., Perkins Trans. 2* **1982**, 0 (7), 805-812.
(144) Willson, R. L.; Greenstock, C. L.; Adams, G. E.; Wageman, R.; Dorfman, L. M.; The standardization of hydroxyl radical rate data from radiation chemistry. *Int. J. Radiat. Phys. Chem.* **1971**, 3, 211-220.
(145) Cohen, H.; Meyerstein, D.; Oxidation of benzoatopentaamminecobalt(III) by hydroxyl radicals. *J. Am. Chem. Soc.* **1971**, 93 (17), 4179-4183.

(146) Grabner, G.; Getoff, N.; Schwörer, F.; Pulseradiolyse von H_3PO_4, $H_2PO_4^-$, HPO_4^{2-} und $P_2O_7^{4-}$ in wässriger lösung-I. Geschwindigkeitskonstanten der reaktionen mit den primärprodukten der wasserradiolyse. *Int. J. Radiat. Phys. Chem.* **1973**, 5, 393-403.

(147) Jiang, P.-Y.; Katsumura, Y.; Domae, M.; Ishikawa, K.; Nagaishi, R.; Yoshida, Y.; Pulse radiolysis study of concentration phosphoric acid solutions. *J. Chem. Soc., Faraday Trans.* **1992**, 88 (22), 3319-3322.

(148) Nakashima, M.; Hayon, E.; Rates of reaction of inorganic phosphate radicals in solution. *J. Phys. Chem.* **1970**, 74 (17), 3290-3291.

(149) Maruthamuthu, P.; Neta, P.; Phosphate radicals. Spectra, acid-base equilibria, and reactions with inorganic compounds. *J. Phys. Chem.* **1978**, 82 (6), 710-713.

(150) Grabner, G.; Getoff, N.; Schwörer, F.; Pulseradiolyse von H_3PO_4, $H_2PO_4^-$, HPO_4^{2-} und $P_2O_7^{4-}$ in wässriger lösung-II. Spektren und kinetik der zwischenprodukte. *Int. J. Radiat. Phys. Chem.* **1973**, 5, 405-417.

(151) Black, E. D.; Hayon, E.; Pulse radiolysis of phosphate anions $H_2PO_4^-$, HPO_4^{2-}, PO_4^{3-}, and $P_2O_7^{4-}$ in aqueous solutions. *J. Phys. Chem.* **1970**, 74 (17), 3199-3203.

(152) Maruthamuthu, P.; Neta, P.; Reactions of phosphate radicals with organic compounds. *J. Phys. Chem.* **1977**, 81 (17), 1622-1625.

(153) Buxton, G. V.; Sellers, R. M.; Reactivity of the hydrated electron and the hydroxyl radical with boric acid in aqueous solutions. *Radiat. Phys. Chem.* **1987**, 29 (2), 137-140.

Appendix C

Supplementary Material for Chapter 4

C1. Materials

Acetonitrile (HPLC grade), formic acid (ACS, 88%), sodium bicarbonate (Certified ACS Grade), sulfuric acid (Trace Metal Grade), dichloroacetic acid (98%, premade 1000 µg/mL in MtBE), monochloroacetic acid (99.0+%), and *ortho*-phosphoric acid (ACS, 98%) were purchased from Fisher Chemical. 2-Nitrobenzaldehyde (≥99%), *para*-nitroanisole (PNA, ≥99%), 1,3,5-timethoxybenzene (99.0%), copper II sulfate pentahydrate (99%), tribromomethane (bromoform, 99+%), and sodium hypochlorite were purchased from Acros Organics. Sodium borate buffer (ACS) was purchased from Amresco, Inc. Pyridine (≥99%), hydrogen peroxide (ACS, 29-32%), dibromochloromethane (98%), dibromoacetonitrile (94%), dichloroacetonitrile (98+%), trichloroacetonitrile (98%), and monobromoacetic acid (98+%) were purchased from Alfa Aesar. Nitrobenzene (ACS, ≥99%), sodium benzoate (≥99%), *trans*-cinnamic acid (97%), benzaldehyde (ReagentPlus(R), 99%), sulfamethoxazole (≥99%), diclofenac (≥99%), methanol (MeOH, ACS Reagent Grade, ≥99.8%), methyl *tert*-butyl ether (MtBE, GC Grade, >99.5%), 2-chloro-1,3,5-trimethoxybenzene, bromodichloromethane (≥97%), 1,2,3-trichloropropane (99%), sodium thiosulfate (ReagentPlus(R), 99%), dibasic potassium phosphate (ACS, 98%), and monobasic potassium phosphate (ReagentPlus(R)) were purchased from Sigma Aldrich. *Tert*-butanol (*t*-BuOH, ACS Reagent Grade, ≥99.7%) was purchased from Honeywell. Sodium sulfate (ACS Grade) was purchased from Dot Scientific. Tribromoacetic acid (99%, premade 1000 µg/mL in MeOH) was purchased from SPEXOrganics. Decafluorobiphenyl (98%) was purchased from Matric Scientific. 1-bromo-4-fluorobenzene was purchased from Oakwood Chemical. 2,3-

Dibromopropionoic acid (98%) was purchased from BeanTown Chemical. Trichloromethane (chloroform, GC-FIC Grade, 99.99%) was purchased from MP Biomedicals. Bromochloroacetonitrile (1000 µg/mL in MeOH), bromochloroacetic acid (1000 µg/mL in MtBE), and dibromoacetic acid (1000 µg/mL in MtBE) were purchased from Ultra Scientific. Bromodichloroacetic acid (0.1 mg/mL in MtBE) and chlorodibromoacetic acid (1 mg/mL in MtBE) were purchased from Crescent Chemical. Trichloroacetic acid (ACS Reagent Grade) was purchased from Merck. All chemicals were used as received except for sodium hypochlorite, which was standardized using a Shimadzu UV-visible spectrometer (λ_{292} = 365 M^{-1} cm^{-1}).[1]

C2. Water Quality and Photochemistry Parameters

All photolysis experiments were conducted in a turn-table apparatus inside a photochemical reactor (Rayonet). Three different bulb configurations were used: four 254-nm bulbs with quartz test tubes (Southern New England Ultraviolet Co. RPR-2537 Å, λ_{max} = 254 nm, width at half-maximum ± 1 nm, irradiance = 6.08 x 10^{-5} mE cm^{-2} s^{-1}), sixteen 311-nm bulbs with borosilicate glass test tubes (Southern New England Ultraviolet Co. RPR-3000 Å, λ_{max} = 311 nm, width at half-maximum ± 22 nm, irradiance = 5.70 x 10^{-5} mE cm^{-2} s^{-1}), and sixteen 365-nm bulbs with borosilicate glass test tubes (Southern New England Ultraviolet Co. RPR-3500 Å, λ_{max} = 365 nm, width at half-maximum ± 10 nm, irradiance = 1.60 x 10^{-4} mE cm^{-2} s^{-1}). Based on the experiment times of six (254 nm), five (311 nm), and thirty (365 nm) minutes, the fluence was calculated to be 8.59 x 10^3 mJ/cm^2, 6.24 x 10^3 mJ/cm^2, and 6.24 x 10^4 mJ/cm^2, respectively.

Photochemical experiments were carried out in borosilicate glass (i.d. 1.4 cm) or quartz (i.d. 1 cm) test tubes. The solution was mixed prior to taking each sample. The photon intensity was measured in the same test tubes via chemical actinometry as described below and was

representative of both direct and incident light within the reactor. There are bulbs evenly spaced around the reactor with a mirror on the outside of that to reflect all light towards the center of the reactor, except for the 254 nm case where two pairs of bulbs sit on opposite sides of the reactor.

The intensities of the UV lamps used in this study were measured using chemical actinometry. The *p*-nitroanisole/pyridine actinometer was used at 365 nm as described previously ([pyridine] = 150 μM, [*p*-nitroanisole] = 10 μM; $\Phi = 0.29[\text{pyridine}] + 0.00029$); this equation was determined using a solar simulator.[2–4] The loss of 2-nitrobenzaldehyde (initial concentration = 10 μM; $\Phi = 0.41$) was used to quantify light intensity at 311 nm; this quantum yield is recommended for the 280 – 405 nm wavelength range, which encompasses the wavelenghts emitted by the bulbs.[5] Sulfamethoxazole and diclofenac were used at 254 nm in place of the traditional iodide/iodate actinometer due to high bulb intensity (concentration of each = 10 μM; $\Phi = 0.18$ and 0.213, respectively).[6] The quantum yields for sulfamethoxazole and diclofenac were determined using a narrowband 254 nm light source, which is similar to the light spectrum emitted by the bulbs used in this study.[6]

Table C1. Concentrations of anions and cations in the first treated Mendota Water sample collected March 8, 2019 (TMW) and the second treated Mendota Water sample collected October 31, 2019 (TMW2).

Constituent	TMW	TMW2
$[Ca^{2+}]$ (ppm)	54.1 ± 1.2	129.9 ± 1.7
$[Fe]_{total}$ (ppb)	34.0 ± 9.0	<10
$[K^{+}]$ (ppm)	3.4 ± 0.5	3.5 ± 0.7
$[Mg^{2+}]$ (ppm)	39.5 ± 0.3	73.8 ± 0.4
$[Mn]_{total}$ (ppb)	35.1 ± 4.5	<10
$[Na^{+}]$ (ppm)	28.3 ± 0.1	101.8 ± 0.3
$[Cl^{-}]$ (ppm)	220	351
$[NO_2^{-}]$ (ppm)	22.0	32.4
$[SO_4^{2-}]$ (ppm)	75.2	131
$[Br^{-}]$ (ppm)	0.44	0.89
$[NO_3^{-}]$ (ppm)	1.8	3.5
Alkalinity (mg-$CaCO_3$/L)	27.9	30.1
[DOC] (mg-C/L)	1.71 ± 0.24	1.84 ± 0.17

Table C2. Intensity-weighted screening factor and light absorbance rates (R_{abs}) for each solution condition.

Treatment Condition	Water	Intensity Weighted Screening Factor	R_{abs} (mE cm^{-3} s^{-1})
254 nm pH 6.5	TMW	0.96	3.35×10^{-7}
	MQ	1.0	3.24×10^{-8}
254 nm pH 8.5	TMW	0.96	3.26×10^{-7}
	MQ	1.0	3.71×10^{-8}
311 nm pH 6.5	TMW	0.99	1.46×10^{-8}
	MQ	1.0	2.56×10^{-9}
311 nm pH 8.5	TMW	0.99	1.26×10^{-8}
	MQ	1.0	2.19×10^{-8}
365 nm pH 6.5	TMW	0.99	2.40×10^{-8}
	MQ	1.0	1.21×10^{-9}
365 nm pH 8.5	TMW	0.99	1.97×10^{-8}
	MQ	1.0	3.88×10^{-9}

C3. Chlorine Photolysis Chemistry

The formation of reactive oxidant species during chlorine photolysis is a function of pH and wavelength.[1,3,7] The environmentally relevant pK_a of hypochlorous acid (HOCl, pK_a = 7.5) causes the distinct photochemistry of both HOCl and hypochlorite (OCl^-) to influence the system.[3] Both chlorine species and reactive chlorine species can react with naturally occurring dissolved organic matter (DOM) to form halogenated disinfection by-products (DBPs).[8] Schematic C1 illustrates the formation pathways of the oxidants measured in this study, as well as which species are likely to react with DOM to form halogenated DBPs.

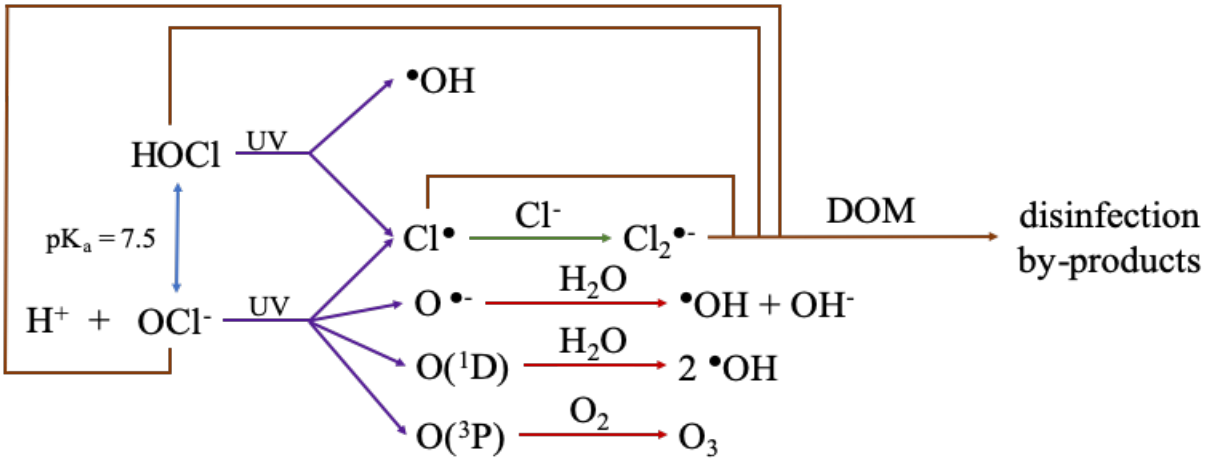

Schematic C1. Formation of hydroxyl radical (•OH), chlorine radical (Cl•), dichloride radical anion ($Cl_2^{\bullet-}$), and ozone (O_3) during chlorine photolysis. $O^{\bullet-}$ is the conjugate base of •OH, and $O(^1D)$ and $O(^3P)$ are excited states of oxygen.[9]

C4. Analytical Methods

Dissolved organic carbon concentrations ([DOC]) were measured using a total organic carbon analyzer (GE Sievers M5310 C series Laboratory TOC Analyzer). Anions were quantified using ion chromatography (Dionex ICS-1100 series ion chromatograph). Optical properties of DOM were collected using a Shimadzu UV-visible spectrometer against a Milli-Q water blank.

All probe compounds and actinometers were quantified using an Agilent 1260 Infinity high-performance liquid chromatograph (HPLC) with either a diode-array or variable wavelength detector. All separations were achieved using an Agilent Poroshell 120 EC-C18 column (3.0 x 50 mm, 2.7 μm) with 0.1 % formic acid v/v (10% acetonitrile v/v) and acetonitrile as the aqueous and organic phases, respectively, at a flow rate of 0.5 mL/min. All compounds were eluted using isocratic methods and detected at a single analysis wavelength (Table C3).

Table C3. Chromatography parameters for analysis of probe compounds and actinometers.

Compound	% Aqueous	Retention Time (min)	Detection Wavelength (nm)	Purpose
benzaldehyde	75	4.63	250	product of ozone probe reaction
benzoate	100	3.24	197	$^{\bullet}OH$, $Cl^{\bullet}$, and $Cl_2^{\bullet-}$ probe
diclofenac	30	1.25	220	254 nm actinometer
p-nitroanisole	50	1.19	314	365 nm actinometer
2-nitrobenzaldehyde	80	2.86	226	311 nm actinometer
nitrobenzene	70	2.59	265	$^{\bullet}OH$ probe
sulfamethoxazole	95	1.16	266	254 nm actinometer
2-chloro-1,3,5-trimethoxybenzene	75	5.90	264	chlorine probe

C5. Reactive Oxidant Species

Reactive oxidant concentrations were measured at pH 6.5 and pH 8.5 in treated Mendota water (TMW) and Milli-Q water (MQ) during chlorine photolysis at 254, 311, and 365 nm. Data for $k_{obs,chlorine}$, $^{\bullet}OH$, $Cl^{\bullet}$, and O_3 at pH 6.5 are shown in the manuscript (Figure 4.1a-d). Data for $k_{obs,chlorine}$, $^{\bullet}OH$, $Cl^{\bullet}$, and O_3 at pH 8.5 are shown below (Figure C1a-d) along with the data for $Cl_2^{\bullet-}$ (Figure C1e) and fluence-normalized $k_{obs,chlorine}$ (Figure C1f). Temperature changes can have an effect on reaction kinetics, but no change in temperature was measured over the course of the reactions with each of the three sets of bulbs.

Probe experiment controls are presented in Figure C2. Probes were validated in MQ in a previous study.[3] Probes were validated in TMW during dark chlorination and under direct photolysis at all three experimental wavelengths. Neither RCS is measured at high pH in TMW due to the low rate constant of $Cl_2^{\bullet-}$ with benzoate[10] relative to $Cl^{\bullet}$[11] and the small measured difference in reactivity between benzoate and nitrobenzene. Formation of $^{\bullet}OH$ during photolysis of TMW in the absence of chlorine (Figure C2d) is due to photolysis of DOM and other water constituents.

Cinnamic acid reacts with O_3 selectively to form benzaldehyde. Benzaldehyde concentration was used to quantify cumulative O_3 production. Direct photolysis of benzaldehyde results in the formation of a direct photoproduct (Figure C3a) that is characterized by a maximum absorption at 266 nm (Figure C3b). Care was taken to ensure separation of this photoproduct from benzaldehyde at the maximum absorption of benzaldehyde at 250 nm. Representative O_3 control measurements are show in Figure C3c.

The branching ratio of radical reaction with organic and inorganic carbon species was calculated as the percent oxidant scavenging by natural water constituents (Equation C1). R is the radical of interest (i.e., •OH or Cl•) and S is the scavenger.

$$\%\ oxidant\ scavenged = \frac{k_S^R[S]}{k_{DOM}^R[DOC] + k_{HCO_3^-}^R[HCO_3^-] + k_{CO_3^{2-}}^R[CO_3^{2-}]} * 100 \qquad \text{(Equation C1)}$$

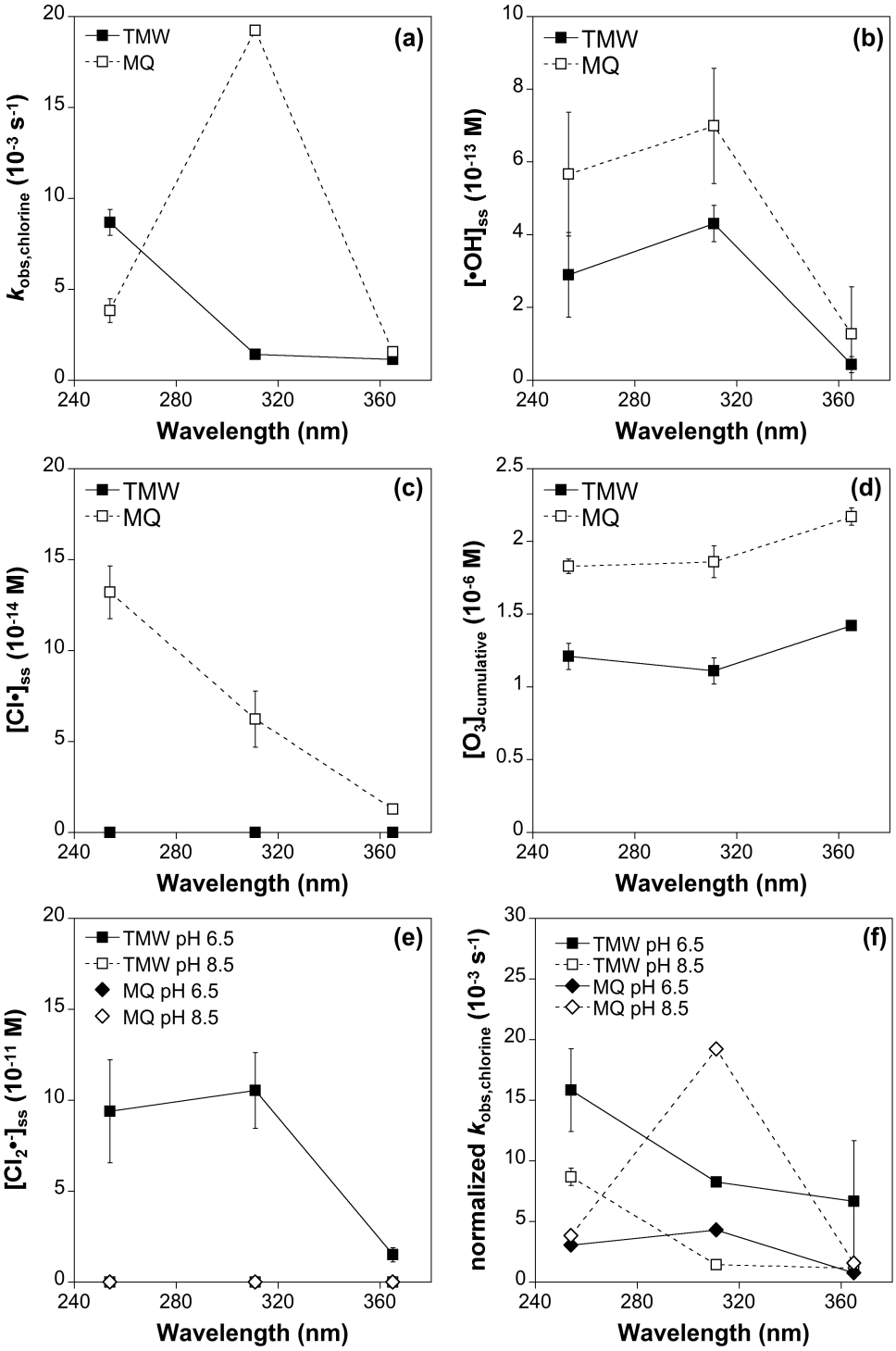

Figure C1. (a) Observed chlorine loss rate constant ($k_{obs,chlorine}$), (b) •OH steady-state concentration, (c) Cl• steady-state concentration, and (d) cumulative ozone concentration at pH 8.5 in Milli-Q water or treated Mendota water irradiated using 254, 311, and 365 nm light. (e) $Cl_2•^-$ steady-state concentration and (f) screening factor-normalized $k_{obs,chlorine}$ at pH 6.5 and pH 8.5 in MQ or TMW at 254, 311, and 365 nm.

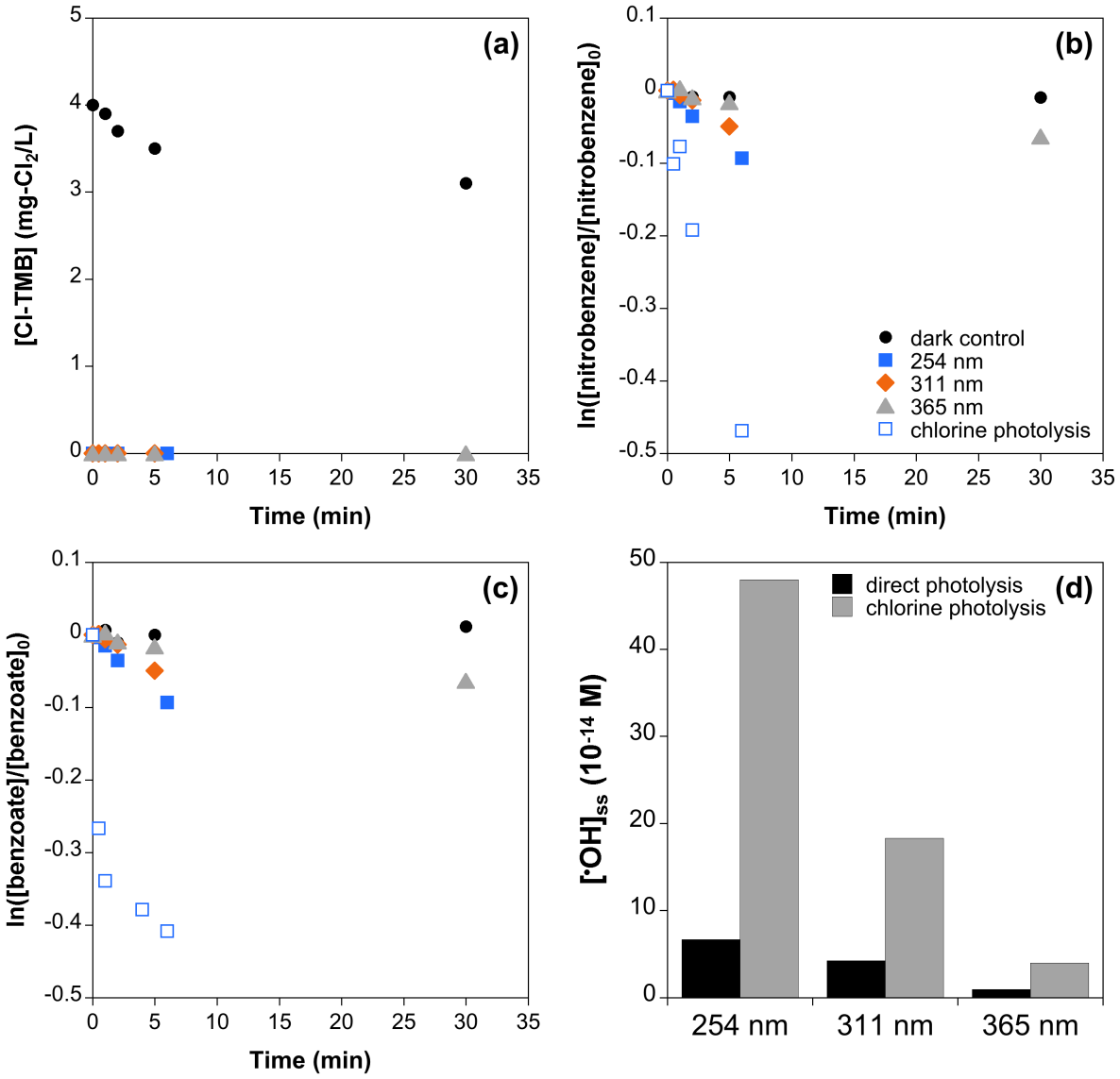

Figure C2. (a) Dark chlorine and irradiated controls of trimethoxybenzene (TMB) in TMW at pH 6.5, 254, 311, and 365 nm. Dark chlorination control shows formation of 2-chloro-1,3,5-trimethoxybenzene (Cl-TMB; black data points). Direct photolysis of natural waters in the presence of TMB does not result in formation of Cl-TMB (colored data points). (b) Dark chlorine and irradiated controls of nitrobenzene in TMW at pH 6.5, 254, 311, and 365 nm, with pseudo-first-order loss kinetics of nitrobenzene during chlorine photolysis (pH 6.5, 254 nm) shown for comparision. (c) Dark chlorine and irradiated controls of benzoate in TMW at pH 6.5, 254, 311, and 365 nm, with pseudo-first-order loss kinetics of nitrobenzene during chlorine photolysis (pH 6.5, 254 nm) shown for comparision. (d) $[^{\bullet}OH]_{ss}$ during photolysis of pH 6.5 TMW and chlorine photolysis of pH 6.5 TMW. Analogous control experiments were completed under all pH and wavelength conditions.

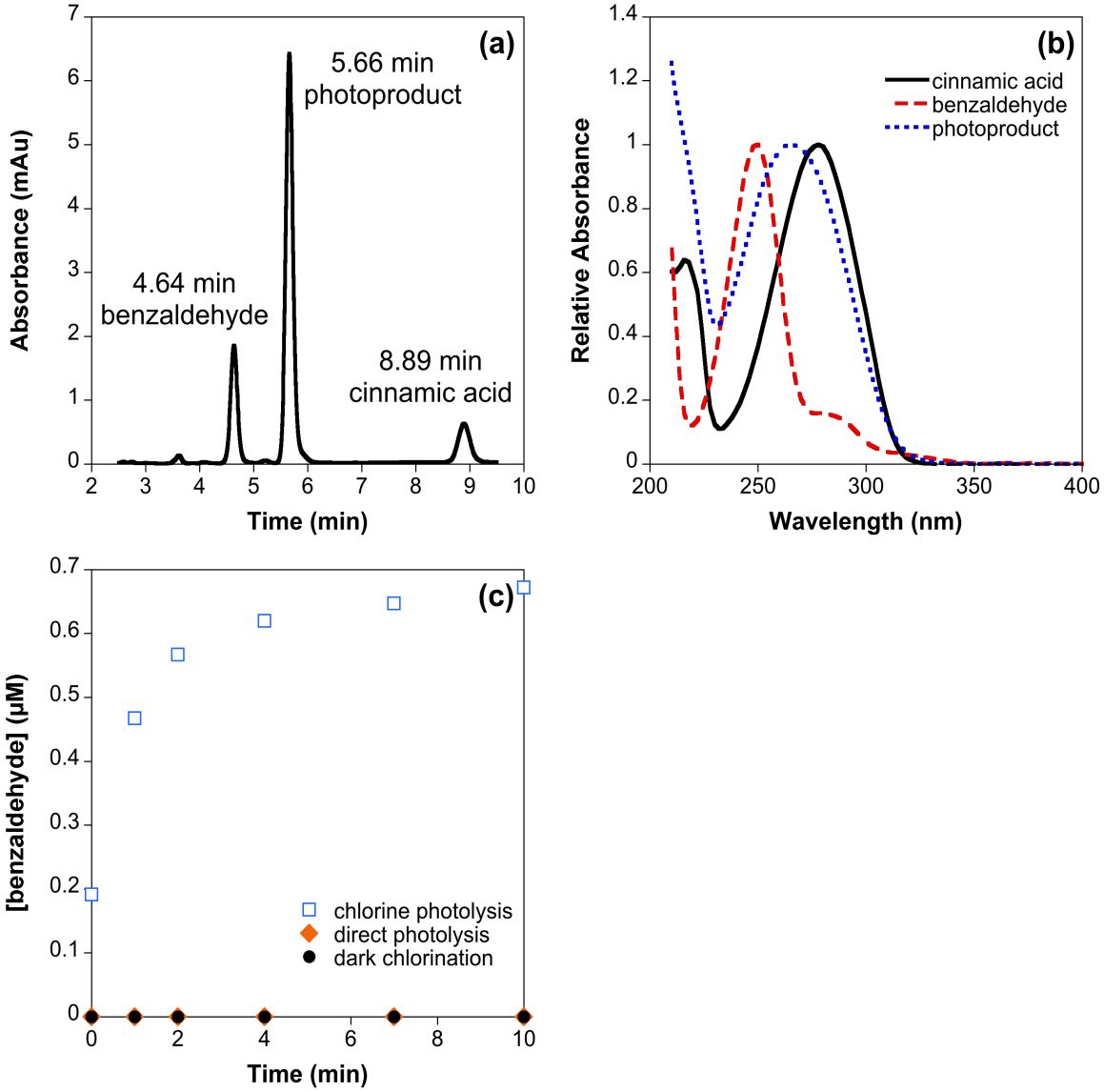

Figure C3. (a) Representative HPLC chromatogram of a chlorine photolysis sample in the presence of cinnamic acid (l = 250 nm). (b) Relative absorbance spectra of cinnamic acid, benzaldehyde, and the direct photoproduct of cinnamic acid. (c) Control of benzaldehyde formation during dark chlorination and direct photolysis at pH 6.5 at 254 nm, chlorine photolysis shown for comparison. Analgous control experiments were completed under all pH and wavelength conditions.

Table C4. Percent decrease in oxidant concentration in the presence of TMW as compared with MQ.

Oxidant	pH	254 nm	311 nm	365 nm
$[^{\cdot}OH]_{ss}$	6.5	72.5	80.3	74.4
	8.5	48.9	38.4	66.3
$[Cl^{\cdot}]_{ss}$	6.5	67.9	48.0	76.7
	8.5	100	100	100
$[O_3]_{cumulative}$	6.5	20.6	45.1	54.7
	8.5	33.9	40.5	34.6

Table C5. Branching ratio of $^{\bullet}OH$ scavenging by naturally ocurring carbon at pH 6.5 and 8.5.

pH	% DOC	% HCO_3^-	% CO_3^{2-}
6.5	95.06	4.90	0.04
8.5	93.71	6.29	0.00

Table C6. Branching ratio of $Cl^{\bullet}$ scavenging by naturally occuring carbon at pH 6.5 and 8.5.

pH	% DOC	% HCO_3^-	% CO_3^{2-}
6.5	28.03	71.94	0.03
8.5	23.05	76.95	0.00

Table C7. Branching ratio of O_3 scavenging by naturally ocurring carbon at pH 6.5 and 8.5.

pH	% DOC	% HCO_3^-	% CO_3^{2-}
6.5	100.0	0.00	0.00
8.5	100.0	0.00	0.00

Table C8. Literature rate constants of reactions between oxidants and scavengers present in natural waters. Reference in brackets.

Water Constituent	$^{\bullet}OH$	$Cl^{\bullet}$	O_3
DOM (L mg-C^{-1} s^{-1})	2.5×10^4 [12]	1.3×10^4 [12]	1.5×10^3 [13,14]
Cl^- (M^{-1} s^{-1})	3.65×10^9 [15,16]	1.18×10^{10} [17–19]	2.0×10^{-4} [20]
HCO_3^- (M^{-1} s^{-1})	8.5×10^6 [6]	2.2×10^8 [12]	1.0×10^{-3} [21]
CO_3^{2-} (M^{-1} s^{-1})	3.9×10^8 [6]	5.0×10^8 [22]	1.0×10^{-1} [21]
HOCl (M^{-1} s^{-1})	1.21×10^9 [3]	3.0×10^9 [17,23]	0 [24]
OCl^- (M^{-1} s^{-1})	6.37×10^9 [3]	8.25×10^9 [17]	1.1×10^2 [24]
t-BuOH (M^{-1} s^{-1})	6.00×10^8 [25]	3.00×10^8 [26]	2.50×10^6 [27]

C6. Targeted Disinfection By-Products

Targeted DBPs including THMs (chloroform, bromoform, bromodichloromethane, and dibromochloromethane), HAAs (bromochloroacetic acid, bromodichloroacetic acid, chlorodibromoacetic acid, dibromoacetic acid, dichloroacetic acid, monobromoacetic acid, monochloroacetic acid, tribromoacetic acid, and trichloroacetic acid), and HANs (bromochloroacetonitrile, dibromoacetonitrile, dichloroacetonitrile, and trichloroacetonitrile) were quantified using EPA methods 551.1 (THMs and HANs)[28] and 552.2 (HAAs).[29] Extracted samples were analyzed using gas-chromatography with electron-capture detection (Shimadzu GC-2010 gas chromatograph with ECD-2010 detector; Table C9).[28,29]

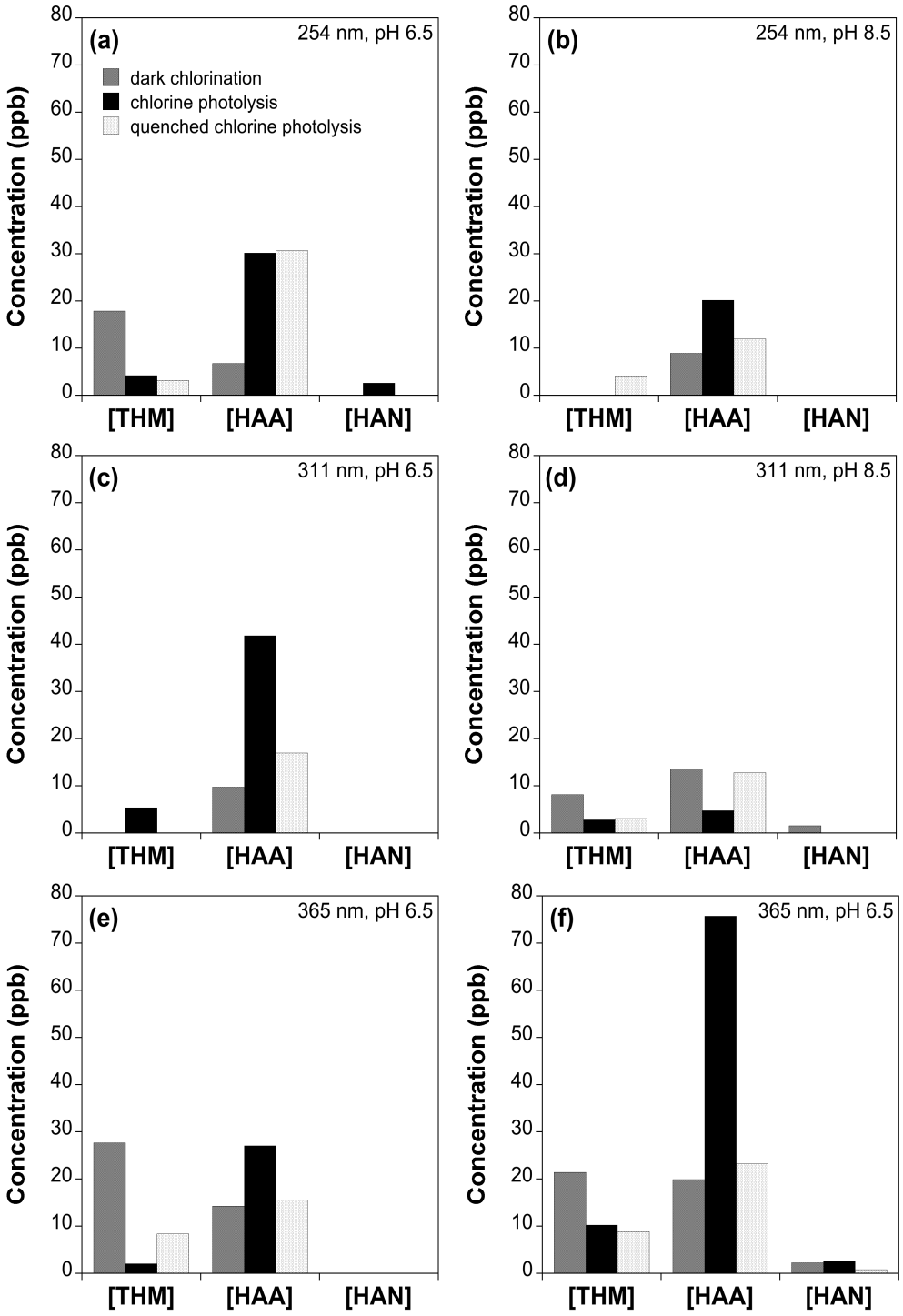

Figure C4. Concentration of total THMs, HAAs, and HANs during dark chlorination, chlorine photolysis, and quenched chlorine photolysis at (a) 254 nm, pH 6.5, (b) 254 nm, pH 8.5, (c) 311 nm, pH 6.5, (d) 311 nm, pH 8.5, (e) 365 nm, pH 6.5, and (f) 365 nm, pH 8.5. Panel (a) is presented as Figure 4.3b in chapter 4 and included here for comparison.

Table C9. Retention times and column information of measured disinfection by-products.

Compound	Retention Time (min)
551.1 compounds - column Agilent DB - 5.625	
trichloromethane (chloroform, TCM)	7.44
trichloroacetonitrile (TCACN)	11.41
dichloroacetonitrile (DCACN)	13.30
bromodichloromethane (BDCM)	13.75
dibromochloromethane (DBCM)	24.93
tribromomethane (bromoform, TBM)	29.47
dibromoacetonitrile (DBACN)	29.66
bromochloroacetonitrile (BCACN)	30.66
internal standard (bromofluorobenzene, IS 1.1)	31.06
surrogate standard (decafluorobiphenyl, SS 1.1)	35.98
552.2 compounds - column Agilent DB - 1	
monobromoacetic acid (MBAA)	13.08
dichloroacetic acid (DCAA)	13.82
tribromoacetic acid (TBAA)	16.55
dibromoacetic acid (DBAA)	17.82
trichloroacetic acid (TCAA)	17.97
bromochloroacetic acid (BCAA)	18.15
internal standard (1,2,3-trichloropropane, IS 2.2)	18.37
monochloroacetic acid (MCAA)	22.25
bromodichloroacetic acid (BDCAA)	23.16
chlorodibromoacetic acid (CDBAA)	32.26
surrogate standard (2,3-dibromopropionic acid, SS 2.2)	32.55

Table C10. Concentrations of all trihalomethanes measured in initial and treated samples (ppb). (n.b. is not buffered).

Wavelength	pH	Treatment	[TCM]	[BDCM]	[DBCM]	[TBM]	[TTHM]
n/a	n.b.	raw TMW	0	0	0	0	0
	6.5	initial	0	0	0	0	0
	8.5	initial	0	0	0	0	0
254 nm	6.5	dark chlorination	**7.25**	**6.36**	**4.22**	0	**17.82**
		direct photolysis	0	0	0	0	0
		chlorine photolysis	**4.15**	0	0	0	**4.15**
		quenched chlorine photolysis	**3.08**	0	0	0	**3.08**
	8.5	dark chlorination	0	0	0	0	0
		direct photolysis	0	0	0	0	0
		chlorine photolysis	0	0	0	0	0
		quenched chlorine photolysis	**4.11**	0	0	0	**4.11**
311 nm	6.5	dark chlorination	0	0	0	0	0
		direct photolysis	0	0	0	0	0
		chlorine photolysis	**5.32**	0	0	0	**5.32**
		quenched chlorine photolysis	0	0	0	0	0
	8.5	dark chlorination	**4.44**	**3.68**	0	0	**8.12**
		direct photolysis	0	0	0	0	0
		chlorine photolysis	**2.75**	0	0	0	**2.75**
		quenched chlorine photolysis	**3.06**	0	0	0	**3.06**
365 nm	6.5	dark chlorination	**8.45**	**7.77**	**5.18**	0	**21.40**
		direct photolysis	0	0	0	0	0
		chlorine photolysis	**4.61**	**3.77**	**1.79**	0	**10.17**
		quenched chlorine photolysis	**3.77**	0	**5.05**	0	**8.81**
	8.5	dark chlorination	**15.66**	**11.99**	0	0	**27.64**
		direct photolysis	0	0	0	0	0
		chlorine photolysis	**2.04**	0	0	0	**2.04**
		quenched chlorine photolysis	**4.41**	**3.88**	0	0	**8.29**

Table C11. Concentrations of all haloacetic acids measured in initial and treated samples (ppb). (n.b. is not buffered).

λ_{irr}	pH	Treatment	[MBAA]	[DCAA]	[DBAA]	[TCAA]	[BCAA]	[TBAA]	[MCAA]	[BDCAA]	[CDBAA]	[HAA_9]
n/a	n.b.	raw TMW	0	0	0	0	0	0	0	0	0	0
	6.5	initial	0	0	0	0	0	0	0	0	0	0
	8.5	initial	0	0	0	0	0	0	0	0	0	0
254 nm	6.5	dark chlorination	0	**6.71**	0	0	0	0	0	0	0	**6.71**
		direct photolysis	0	0	0	0	0	0	0	0	0	0
		chlorine photolysis	**3.73**	**20.50**	**5.87**	0	0	0	0	0	0	**30.11**
		quenched chlorine photolysis	**3.04**	**21.46**	**6.15**	0	0	0	0	0	0	**30.65**
	8.5	dark chlorination	0	**8.90**	0	0	0	0	0	0	0	**8.90**
		direct photolysis	0	0	0	0	0	0	0	0	0	0
		chlorine photolysis	0	**14.22**	**5.88**	0	0	0	0	0	0	**20.10**
		quenched chlorine photolysis	0	**8.53**	**3.41**	0	0	0	0	0	0	**11.94**
311 nm	6.5	dark chlorination	0	**9.69**	0	0	0	0	0	0	0	**9.69**
		direct photolysis	0	0	0	0	0	0	0	0	0	0
		chlorine photolysis	0	**35.44**	**6.34**	0	0	0	0	0	0	**41.78**
		quenched chlorine photolysis	0	**13.19**	**3.73**	0	0	0	0	0	0	**16.92**
	8.5	dark chlorination	0	**13.56**	0	0	0	0	0	0	0	**13.56**
		direct photolysis	0	0	0	0	0	0	0	0	0	0
		chlorine photolysis	0	**4.70**	0	0	0	0	0	0	0	**4.70**
		quenched chlorine photolysis	0	**12.75**	0	0	0	0	0	0	0	**12.75**
365 nm	6.5	dark chlorination	**4.79**	**12.48**	**2.55**	0	0	0	0	0	0	**19.82**
		direct photolysis	0	0	0	0	0	0	0	0	0	0
		chlorine photolysis	**16.70**	**56.24**	**2.76**	0	0	0	0	0	0	**75.70**
		quenched chlorine photolysis	0	**23.18**	0	0	0	0	0	0	0	**23.18**
	8.5	dark chlorination	0	**14.21**	0	0	0	0	0	0	0	**14.21**
		direct photolysis	0	0	0	0	0	0	0	0	0	0
		chlorine photolysis	0	**22.76**	**4.26**	0	0	0	0	0	0	**27.02**
		quenched chlorine photolysis	0	**15.45**	0	0	0	0	0	0	0	**15.45**

Table C12. Concentrations of all haloacetonitriles measured in initial and treated samples (ppb). (n.b. is not buffered).

Wavelength	pH	Treatment	[TCACN]	[DBACN]	[BCACN]	[DCACN]	[HAN]
n/a	n.b.	raw TMW	0	0	0	0	0
	6.5	initial	0	0	0	0	0
	8.5	initial	0	0	0	0	0
254 nm	6.5	dark chlorination	0	0	0	0	0
		direct photolysis	0	0	0	0	0
		chlorine photolysis	0	0	0	**2.58**	**2.58**
		quenched chlorine photolysis	0	0	0	0	0
	8.5	dark chlorination	0	0	0	0	0
		direct photolysis	0	0	0	0	0
		chlorine photolysis	0	0	0	**3.18**	**3.18**
		quenched chlorine photolysis	0	0	0	0	0
311 nm	6.5	dark chlorination	0	0	0	0	0
		direct photolysis	0	0	0	0	0
		chlorine photolysis	0	0	0	0	0
		quenched chlorine photolysis	0	0	0	0	0
	8.5	dark chlorination	0	0	0	**1.51**	**1.51**
		direct photolysis	0	0	0	0	0
		chlorine photolysis	0	0	0	0	0
		quenched chlorine photolysis	0	0	0	0	0
365 nm	6.5	dark chlorination	0	0	0	**2.24**	**2.24**
		direct photolysis	0	0	0	0	0
		chlorine photolysis	0	0	0	**2.64**	**2.64**
		quenched chlorine photolysis	0	0	0	**0.78**	**0.78**
	8.5	dark chlorination	0	0	0	0	0
		direct photolysis	0	0	0	0	0
		chlorine photolysis	0	0	0	0	0
		quenched chlorine photolysis	0	0	0	0	0

C7. Dissolved Organic Matter Transformation

Samples were extracted for the analysis of DOM using solid-phase extraction.[30,31,32] BondElut PPL cartridges were activated with 5 mL of methanol prior to extraction. 500 mL of sample was acidified to pH <2.5 with formic acid then loaded onto the cartridges. The cartridges were then rinsed with 20 mL of 0.1% formic acid to remove any remaining salts and extracted with 5 mL of methanol. Methanol extracts were diluted 100-fold in 1:1 ACN:Milli-Q water and analyzed using Fourier transform-ion cyclotron resonance mass-spectrometry (FT-ICR MS; SolariX XR 12T). Data was collected using negative mode electrospray ionization as the average of 350 scans with a 1 second accumulation time. Blanks of both methanol and the 1:1 ACN:Milli-Q solution were run as controls for solvent contamination. Additional blanks were run periodically between samples to ensure that there was no carry-over between samples.

All *m/z* peaks detected by FT-ICR MS with a S/N > 3 were converted to neutral mass and calibrated using common DOM formulas as described previously.[4,33,34] Molecular formulas with $C_{0\text{-}80}H_{0\text{-}140}O_{0\text{-}80}N_{0\text{-}1}S_{0\text{-}1}P_{0\text{-}1}Cl_{0\text{-}3}{}^{13}C_{0\text{-}1}$ were considered. Molecular formulas were assigned within a mass error of 0.5 ppm and were required to be part of a $+CH_2$ or CH_4 versus O homologous series with 3 or more members. In addition, all masses matched to a chlorine containing formula were required to have a ^{37}Cl isotopologue.

Bulk DOM properties including $H:C_w$, $O:C_w$, and carbon-normalized double bond equivalents (DBE/C_w) were calculated as relative intensity weighted averages from the assigned molecular formulas.[4,33,35] The number of total matched formulas, CHO-containing formulas, and CHOCl containing formulas, along with the $H:C_w$, $O:C_w$, and DBE/C_w data are tabulated in Table C13. van Krevelen diagrams are used to visualize the high-resolution mass spectrometry data.[36-40]

Bray-Curtis dissimilarity analysis was conducted in *R* and compared all initial and treated samples (Figure C7). Overall, the Bray-Curtis dissimilarity does not show clear separation of treatment types. The initial samples group together and are separate from all treated samples. The 254 nm and 311 nm direct photolysis samples group together, as do the chlorine photolysis samples at those wavelengths. The quenched chlorine photolysis samples generally do not group with the chlorine photolysis samples.

Principal-component analysis was done on all samples at 254 and 311 nm and separately on the 365 nm samples based on the similarity in Bray-Curtis analysis. For the 254 and 311 nm PCA analysis, the first two components explained 95.1% of the variance in the data, while 98.5% of the variance in the 365 nm samples was explained by the first two components. In both PCA plots, the initial samples group separately from the treated samples (Figures 4.2f and C8). For treatments at 365 nm, all treated samples group together (Figure C8). For treatments at 254 and 311 nm, all treatments move in the same direction relative to the initial. Samples group by treatment type in this plot and the quenched chlorine photolysis samples fall between the dark chlorination and chlorine photolysis samples (Figure 4.2f).

Formulas that consistently increase or decrease in intensity during treatment are visualized by first identifying formulas that are common to all pH 6.5 samples. Formulas that increase or decrease in intensity in all samples for a given treatment type (e.g., formulas that decrease in intensity in the 254, 311, and 365 nm, pH 6.5 chlorine photolysis samples) were plotted on a van Krevelen diagram. The color of these points corresponds to the percent change in relative intensity of that formula compared to the initial relative intensity of the same formula in the control sample (Figures C9 and C10).

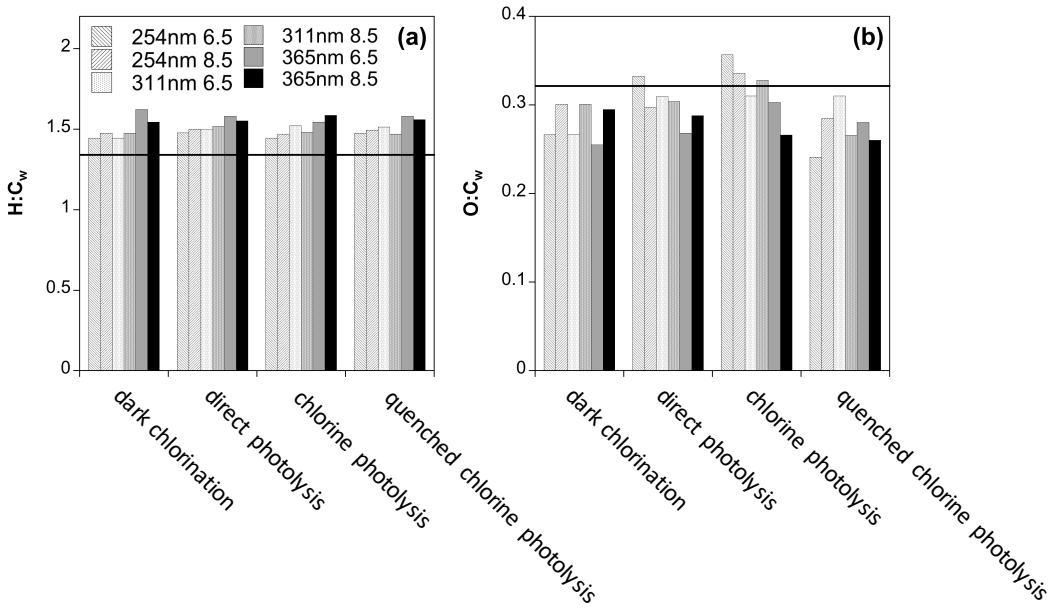

Figure C5. (a) H:C_w and (b) O:C_w of matched formulas grouped by treatment type. The solid line in each panel represents the corresponding value in the initial sample.

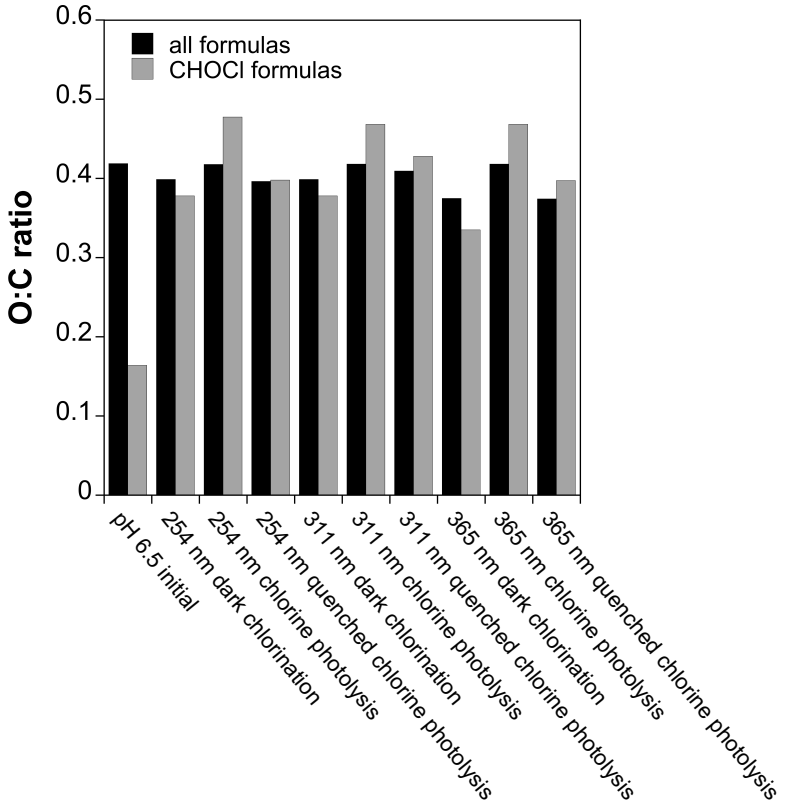

Figure C6. Average O:C ratio of all matched formulas or CHOCl formulas for different treatments. Data shown for pH 6.5, TMW sample only.

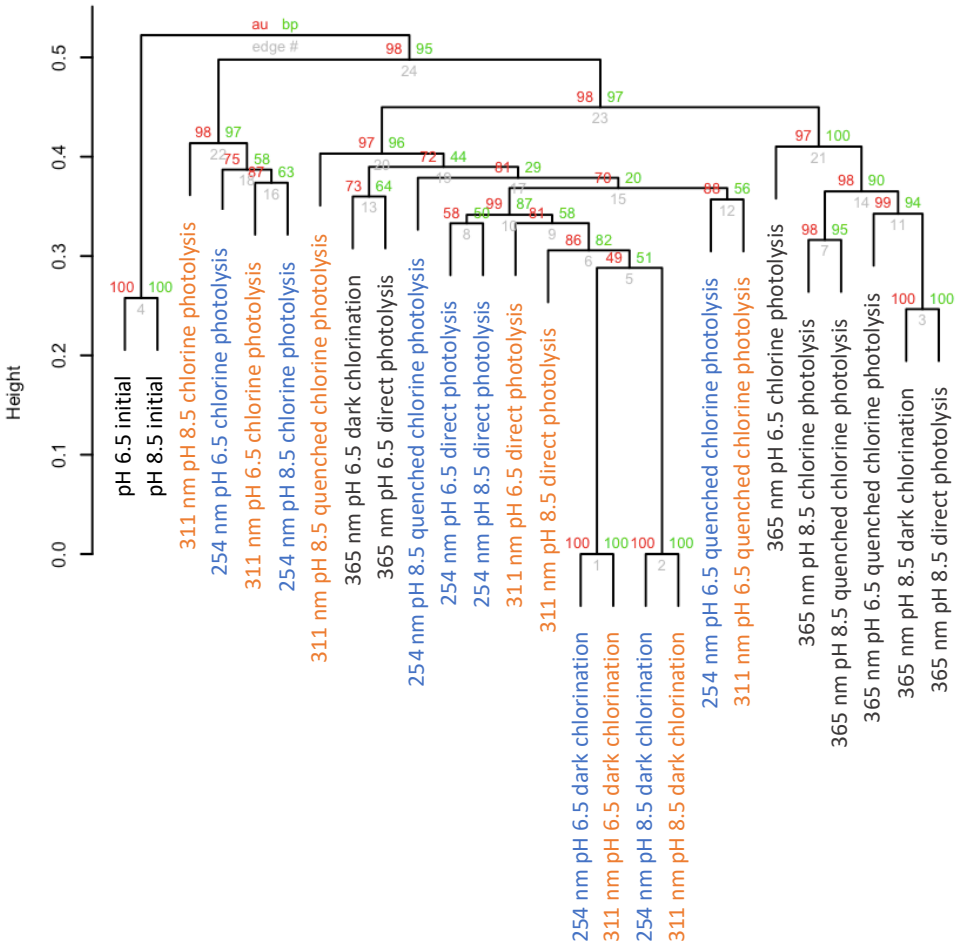

Figure C7. Bray-Curtis dissimilarity analysis of initial and treated samples in TMW based on formulas identified using FT-ICR MS.

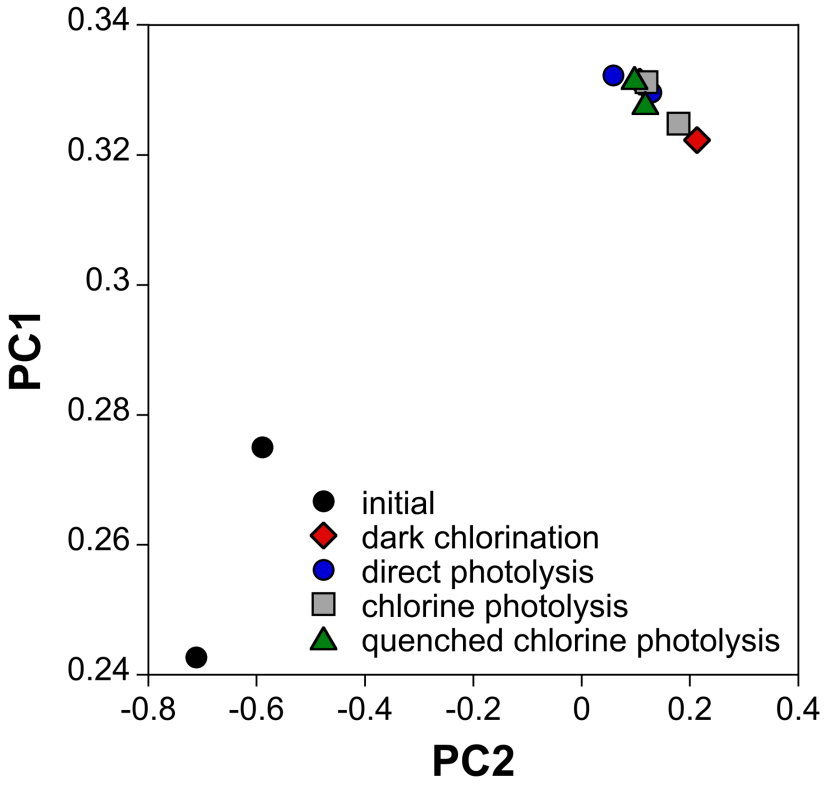

Figure C8. Principal component analysis of initial samples and 365 nm treated samples.

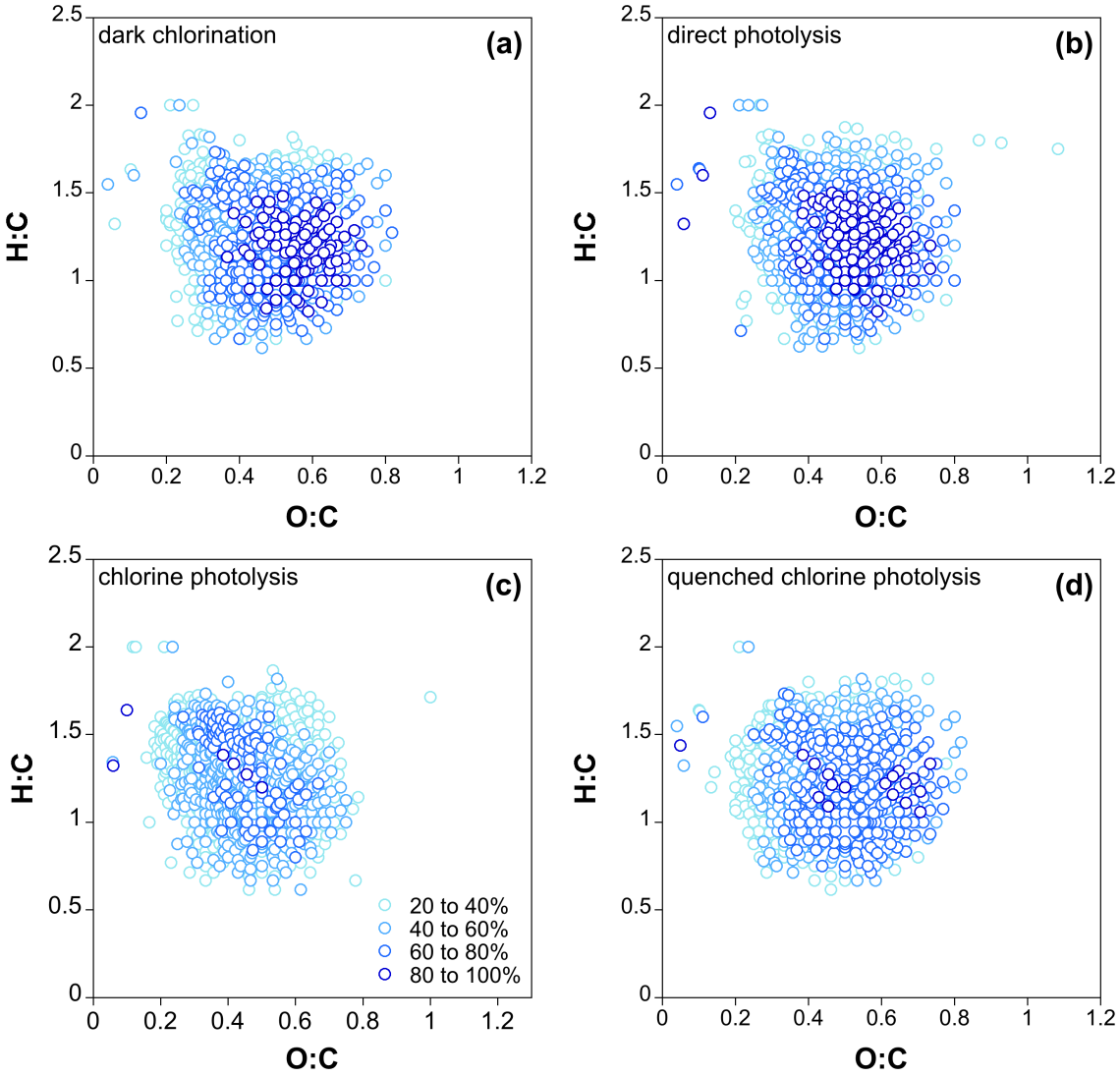

Figure C9. van Krevelen diagrams of formulas that consistently decrease in intensity during treatment. Formulas are present in the initial sample and samples irradiated using all three wavelengths at pH 6.5. Points are color coded based on the average percent decrease in relative intensity during treatment as compared to the initial sample. Treatments are (a) dark chlorination, (b) direct photolysis, (c) chlorine photolysis, and (d) quenched chlorine photolysis. Panel (c) is included as Figure 4.2c in Chapter 4 and shown here for comparison.

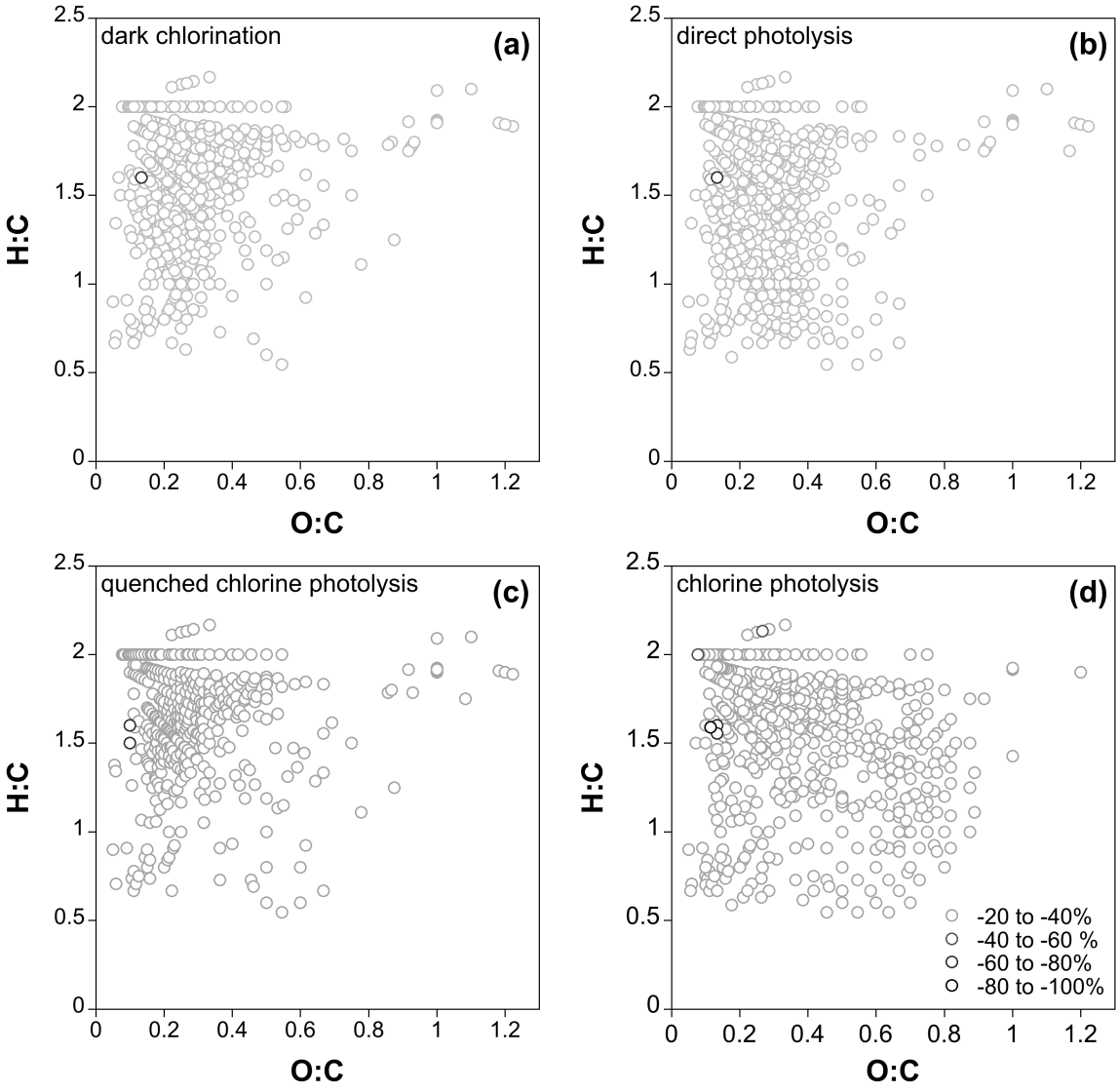

Figure C10. van Krevelen diagrams of formulas that consistently increase in intensity during treatment. Formulas are present in the initial sample and samples irradiated using all three wavelengths at pH 6.5. Points are color coded based on the average percent decrease in relative intensity during treatment as compared to the initial sample. Treatments are (a) dark chlorination, (b) direct photolysis, (c) chlorine photolysis, and (d) quenched chlorine photolysis. Panel (c) is included as Figure 4.2d in Chapter 4 and shown here for comparison. Note that nearly all points in all panels fall within the -20 to -40% range.

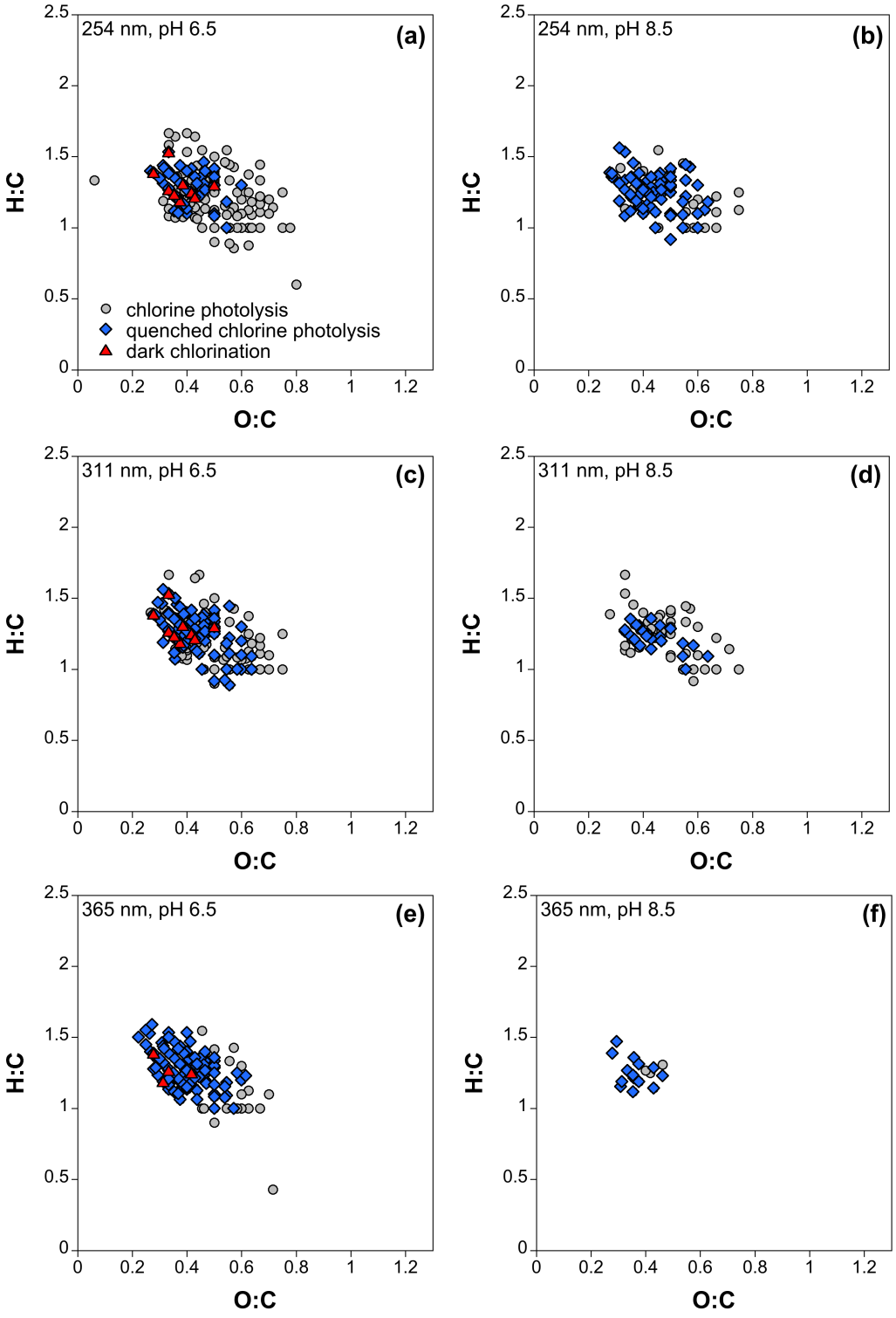

Figure C11. CHOCl formulas formed during dark chlorination, chlorine photolysis, or quenched chlorine photolysis under different treatment conditions: (a) 254 nm, pH 6.5, (b) 254 nm, pH 8.5, (c) 311 nm, pH 6.5, (d) 311 nm pH 8.5, (e) 365 nm pH 6.5, (f) 365 nm pH 8.5.

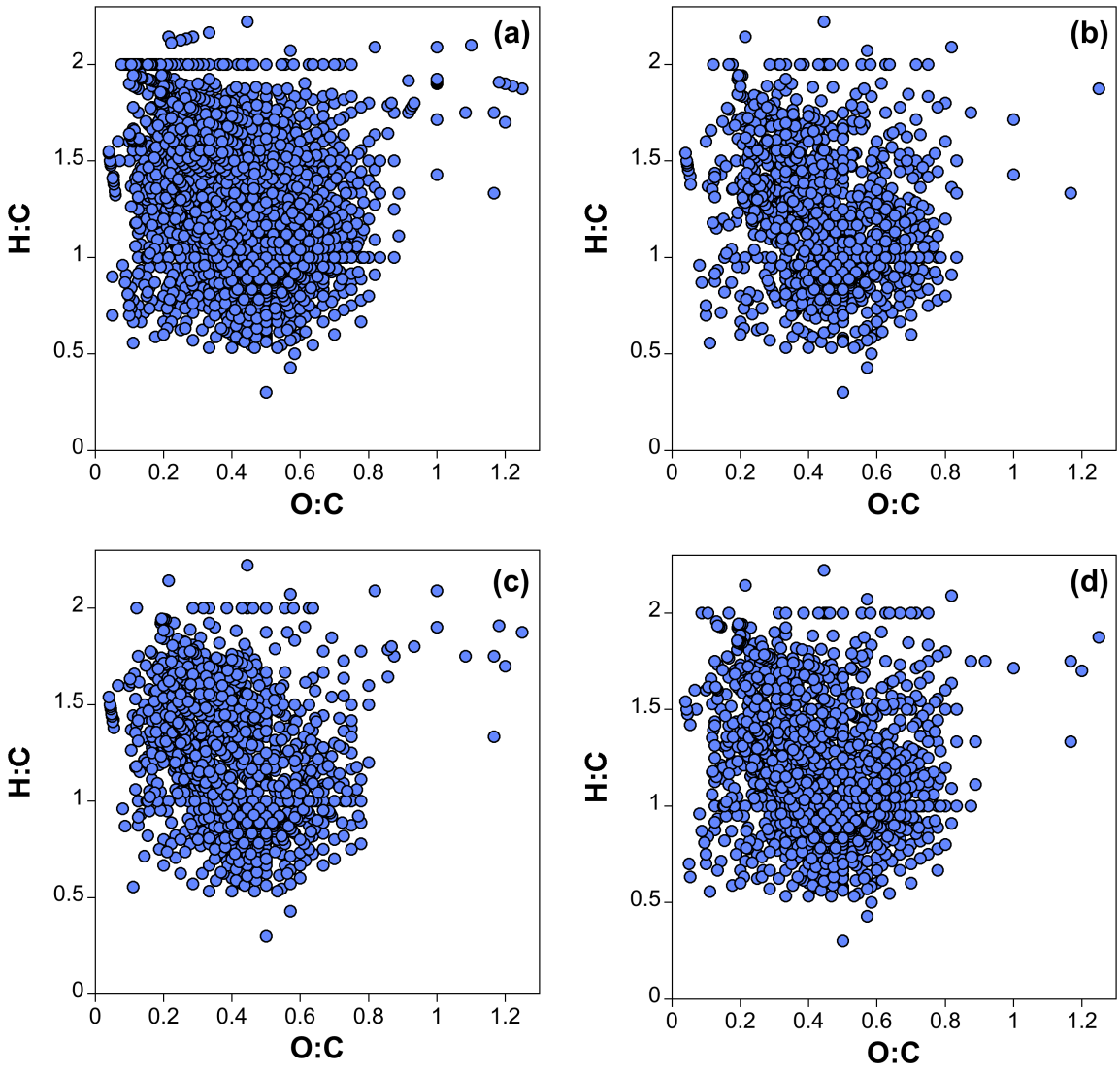

Figure C12. van Krevelen diagrams of formulas removed during treatment at pH 6.5 at all wavelengths (i.e., present in the initial sample, but not in the treated sample). Treatments are (a) dark chlorination, (b) direct photolysis, (c) chlorine photolysis, and (d) quenched chlorine photolysis.

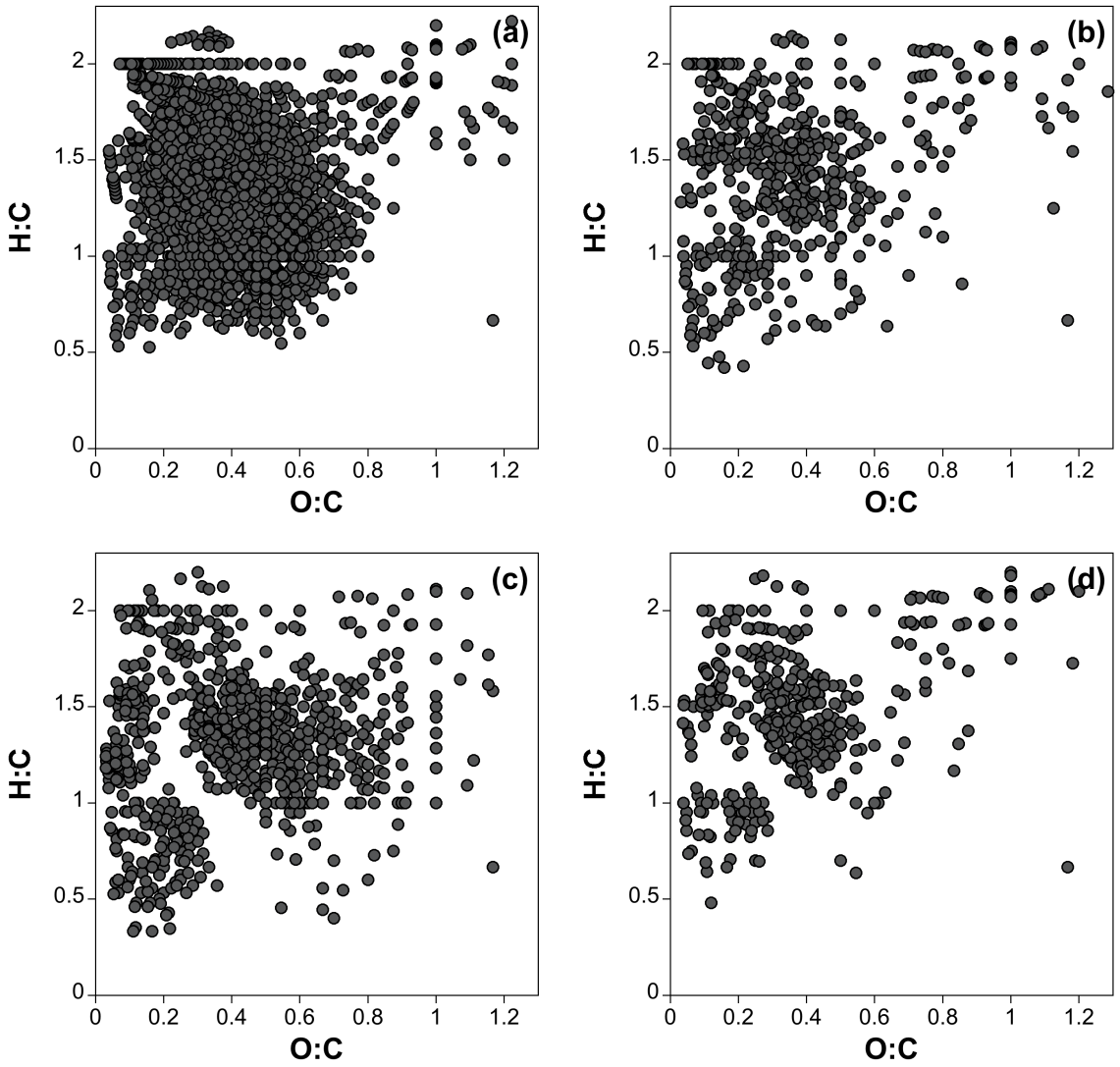

Figure C13. van Krevelen diagrams of formulas formed during treatment at pH 6.5 at all wavelengths (i.e., present in the treated sample, but not in the initial). Treatments are (a) dark chlorination, (b) direct photolysis, (c) chlorine photolysis, and (d) quenched chlorine photolysis.

Table C13. Total number of matched formulas, number of formulas with heteroatoms, and intensity weighted averages of H:C ($H:C_w$), O:C ($O:C_w$), and double-bond equivalents per carbon (DBE/C_w) for initial and treated TMW samples.

pH	wavelength	treatment	total formulas	CHO formulas	CHON formulas	CHOS formulas	CHOP formulas	CHOCl formulas	$H:C_w$	$O:C_w$	DBE/C_w
6.5	n/a	initial	3215	1907	721	638	37	0	1.38	0.32	0.36
	254 nm	dark chlorination	2661	1688	496	409	85	9	1.44	0.27	0.33
		direct photolysis	2728	1668	502	555	79	0	1.48	0.33	0.32
		chlorine photolysis	2871	1692	583	434	93	138	1.44	0.36	0.34
		quenched chlorine photolysis	2269	1489	317	358	78	55	1.48	0.24	0.32
	311 nm	direct photolysis	2711	1659	517	496	108	0	1.50	0.31	0.31
		chlorine photolysis	2749	1607	542	457	73	127	1.52	0.31	0.30
		quenched chlorine photolysis	2575	1569	467	423	92	80	1.51	0.31	0.30
	365 nm	dark chlorination	2297	1572	320	369	50	4	1.62	0.26	0.25
		direct photolysis	2768	1879	403	451	80	0	1.58	0.27	0.27
		chlorine photolysis	3218	2086	629	405	64	89	1.54	0.30	0.29
		quenched chlorine photolysis	2797	1816	443	387	97	98	1.58	0.28	0.27
8.5	n/a	initial	3167	1874	717	614	56	0	1.39	0.31	0.36
	254 nm	dark chlorination	2538	1627	461	400	97	0	1.48	0.30	0.32
		direct photolysis	2868	1706	594	549	95	0	1.50	0.30	0.31
		chlorine photolysis	2735	1583	564	475	104	81	1.49	0.34	0.33
		quenched chlorine photolysis	2948	1764	633	453	72	67	1.49	0.28	0.31
	311 nm	direct photolysis	2458	1672	290	460	77	0	1.52	0.30	0.30
		chlorine photolysis	2737	1650	493	530	91	59	1.48	0.33	0.32
		quenched chlorine photolysis	2728	1718	481	454	94	25	1.47	0.27	0.32
	365 nm	dark chlorination	2273	1575	320	324	68	0	1.54	0.29	0.29
		direct photolysis	2607	1781	373	417	78	0	1.55	0.29	0.28
		chlorine photolysis	2656	1798	486	327	52	9	1.59	0.27	0.26
		quenched chlorine photolysis	2762	1825	485	397	71	14	1.56	0.26	0.28

Table C14. [DOC], and $SUVA_{254}$ for each treatment condition. [DOC] is only reported for the initial, photolysis, and chlorine photolysis samples due to the potential interference of HOCl and *t*-BuOH on the measurement of [DOC]. $SUVA_{254}$ values for dark chlorination and quenched chlorine photolysis samples were calculated using the average of the initial [DOC] at the same pH and the [DOC] of the other two samples at the same pH and wavelength.

pH	wavelength	treatment	[DOC] (mg-C L^{-1})	$SUVA_{254}$ (L mg-C^{-1} m^{-1})
6.5	n/a	initial	1.71 ± 0.16	2.01 ± 0
	254 nm	dark chlorination	n.r.	1.84 ± 0.03
		direct photolysis	1.84 ± 0.10	2.19 ± 0.05
		chlorine photolysis	1.78 ± 0.10	1.78 ± 0.22
		quenched chlorine photolysis	n.r.	2.21 ± 0.01
	311 nm	dark chlorination	n.r.	1.84 ± 0.03
		direct photolysis	1.95 ± 0.16	1.98 ± 0.11
		chlorine photolysis	1.71 ± 0.10	1.44 ±0.01
		quenched chlorine photolysis	n.r.	1.51 ± 0.13
	365 nm	dark chlorination	n.r.	1.91 ± 0.05
		direct photolysis	1.98 ± 0.17	1.93 ± 0.16
		chlorine photolysis	2.01 ± 0.20	1.44 ± 0.08
		quenched chlorine photolysis	n.r.	1.64 ± 0.21
8.5	n/a	initial	1.84 ± 0.17	2.00 ± 0.01
	254 nm	dark chlorination	n.r.	1.86 ± 0.05
		direct photolysis	1.65 ± 0.31	2.25 ± 0.17
		chlorine photolysis	1.60 ± 0.27	1.73 ± 0.23
		quenched chlorine photolysis	n.r.	1.65 ± 0.06
	311 nm	dark chlorination	n.r.	1.86 ± 0.05
		direct photolysis	2.04 ± 0.10	2.09 ± 0.02
		chlorine photolysis	1.87 ± 0.16	1.44 ± 0.18
		quenched chlorine photolysis	n.r.	1.74 ± 0.02
	365 nm	dark chlorination	n.r.	2.00 ± 0.07
		direct photolysis	2.01 ± 0.20	2.18 ± 0.02
		chlorine photolysis	2.14 ± 0.20	1.58 ± 0.01
		quenched chlorine photolysis	n.r.	1.73 ± 0.03

Table C15. log relative intensity, relative to the intensity of all matched formulas, of common CHONCl formulas identified via FT-ICR MS.

Formula Mass (Da)	Chemical Formula	initial	dark chlorine	direct photolysis	chlorine photolysis						quenched chlorine photolysis					
					254 nm		311 nm		365 nm		254 nm		311 nm		365 nm	
					pH 6.5	pH 8.5	pH 6.5	pH 8.5	pH 6.5	pH 8.5	pH 6.5	pH 8.5	pH 6.5	pH 8.5	pH 6.5	pH 8.5
219.0298	$C_8H_{10}O_4N_1Cl_1$	0	0	0	0	0	0	0	0	0	0	0	-4.50	0	0	0
235.0247	$C_8H_{10}O_5N_1Cl_1$	0	0	0	-4.52	0	-4.42	0	0	0	0	0	0	0	0	0
247.0611	$C_{10}H_{14}O_4N_1Cl_1$	0	0	0	-4.27	0	0	0	0	0	0	0	-4.32	0	0	0
249.0404	$C_9H_{12}O_5N_1Cl_1$	0	0	0	-4.28	0	-4.30	-4.24	-4.49	0	0	-4.44	0	0	0	0
255.0429	$C_9H_{15}O_3N_1Cl_2$	0	0	0	0	0	0	-4.37	0	0	0	0	0	0	0	0
261.0768	$C_{11}H_{16}O_4N_1Cl_1$	0	0	0	0	0	-4.62	-4.63	0	0	0	-4.66	-4.52	0	0	0
271.0378	$C_9H_{15}O_4N_1Cl_2$	0	0	0	0	0	-4.82	0	0	0	0	0	0	0	0	0
273.0768	$C_{12}H_{16}O_4N_1Cl_1$	0	0	0	0	0	0	0	0	0	0	-4.53	0	0	0	0
275.0924	$C_{12}H_{18}O_4N_1Cl_1$	0	0	0	0	0	0	0	-4.91	0	0	0	0	0	0	0
289.0353	$C_{11}H_{12}O_6N_1Cl_1$	0	0	0	0	0	-4.37	0	-4.36	0	0	0	0	0	0	0
303.0510	$C_{12}H_{14}O_6N_1Cl_1$	0	0	0	0	0	0	0	0	0	0	0	0	0	-4.28	0
303.0874	$C_{12}H_{18}O_5N_1Cl_1$	0	0	0	0	0	0	0	0	0	0	-4.56	0	0	0	0
325.0120	$C_{11}H_{13}O_6N_1Cl_2$	0	0	0	0	0	-4.37	0	0	0	0	0	0	0	0	0
349.0564	$C_{13}H_{16}O_8N_1Cl_1$	0	0	0	0	0	0	0	0	0	0	0	0	0	-4.34	0
521.3061	$C_{33}H_{44}O_2N_1Cl_1$	0	0	0	-3.73	0	0	0	0	0	0	0	0	0	0	0

C8. Oxygen Addition

Oxidation was investigated at the molecular level by identifying formulas in treated samples that had a mass equivalent one or two oxygen atoms greater than the mass of a formula in the initial sample. To conduct this analysis, a mass list was created by taking all the matched masses from the initial sample and adding the mass of one or two oxygen atoms. In some cases, the oxygen addition mass could be the result of addition of either one or two oxygen atoms (e.g., $C_{20}H_{21}O_{11}N_1$ could result from the addition of 1O to $C_{20}H_{21}O_{10}N_1$ or 2O to $C_{20}H_{21}O_9N_1$). In these cases, the masses were categorized as "+1O/+2O". Treated samples were then analyzed for the presence of these oxygen-addition formulas after verifying that the same formulas were not in the initial sample (i.e., they are unique to the treated samples).

Table C16. Number of oxygen addition formulas formed during chlorine photolysis or quenched chlorine photolysis at pH 6.5 for 254, 311, and 365 nm.

pH	wavelength	treatment	+1O	+2O	+1O/+2O
6.5	254 nm	dark chlorination	33	43	43
		direct photolysis	21	21	278
		chlorine photolysis	39	98	93
		quenched chlorine photolysis	15	39	31
	311 nm	dark chlorination	33	43	43
		direct photolysis	21	33	30
		chlorine photolysis	44	84	83
		quenched chlorine photolysis	36	61	47
	365 nm	dark chlorination	31	27	26
		direct photolysis	39	36	32
		chlorine photolysis	64	90	66
		quenched chlorine photolysis	58	61	52

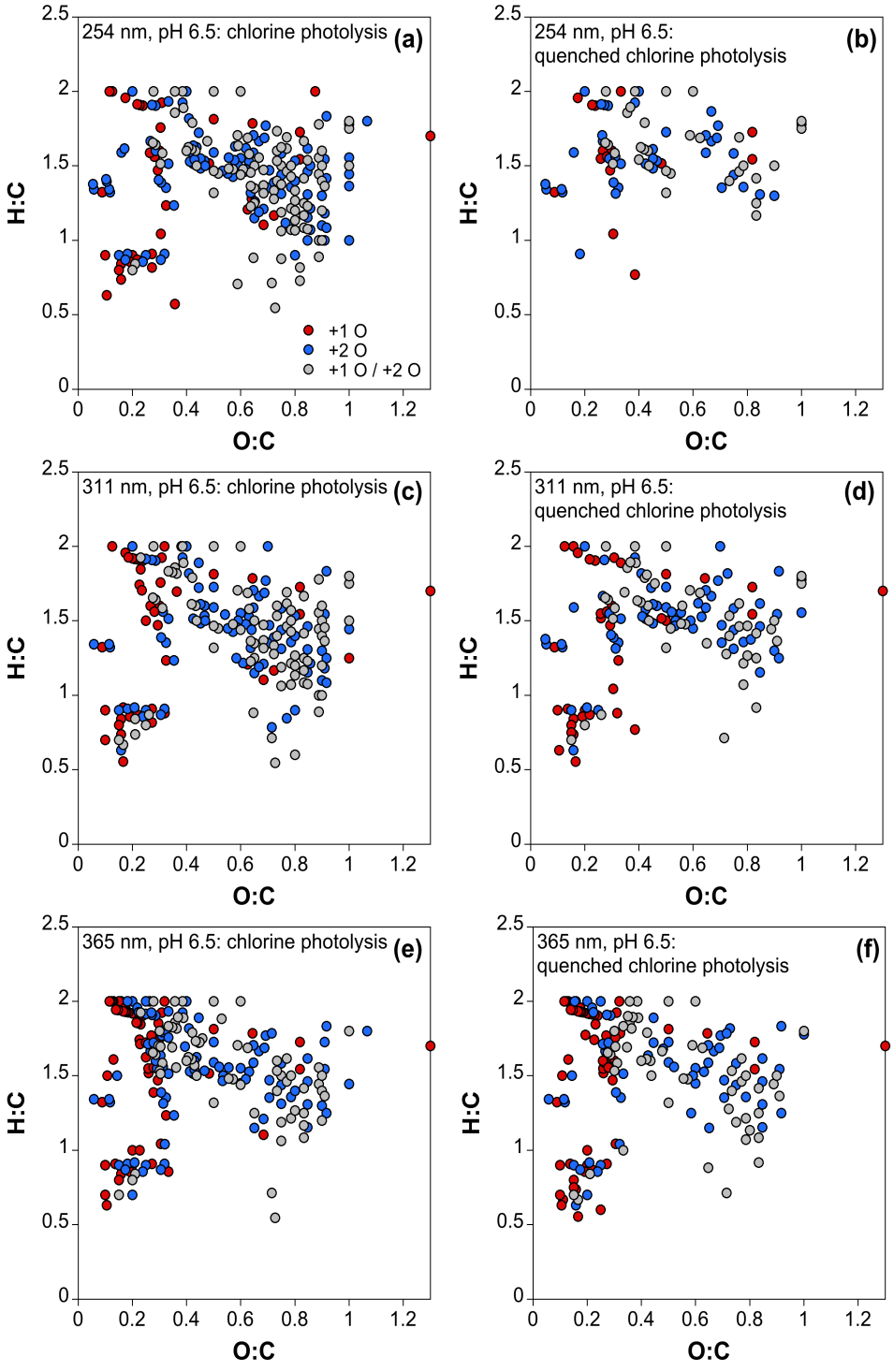

Figure C14. van Krevelen diagrams of formulas found in the treated sample that are +1O (red), +2O (blue), or +1O/+2O (grey) compared to formulas in the initial sample. (a) 254 nm, pH 6.5 chlorine photolysis, (b) 254 nm, pH 6.5 quenched chlorine photolysis, (c) 311 nm, pH 6.5 chlorine photolysis, (d) 311 nm pH 6.5 quenched chlorine photolysis, (e) 365 nm pH 6.5 chlorine photolysis, (f) 365 nm pH 6.5 quenched chlorine photolysis.

C9. Sequential Treatment Experiment

A second TMW (TMW2) sample was collected to conduct the sequential treatment experiments due to sample volume limitations from the initial sample. This sample was treated with dark chlorination, direct photolysis, dark H_2O_2, chlorine photolysis, H_2O_2 photolysis, direct photolysis followed by dark chlorination, or H_2O_2 photolysis followed by dark chlorination (**Schematic C2**). All photolysis experiments were 6 minutes followed by 0 or 6 minutes of dark chlorination. UV/H_2O_2 is a hydroxyl radical control.[41] UV/H_2O_2 experiments were conducted at 254 nm and were dosed with 40 μM H_2O_2 in order to achieve the same hydroxyl radical steady-state concentration as the chlorine photolysis experiments. This concentration was determined by varying the concentration of H_2O_2 and measuring $[^{\bullet}OH]_{ss}$ (**Figure C15**).

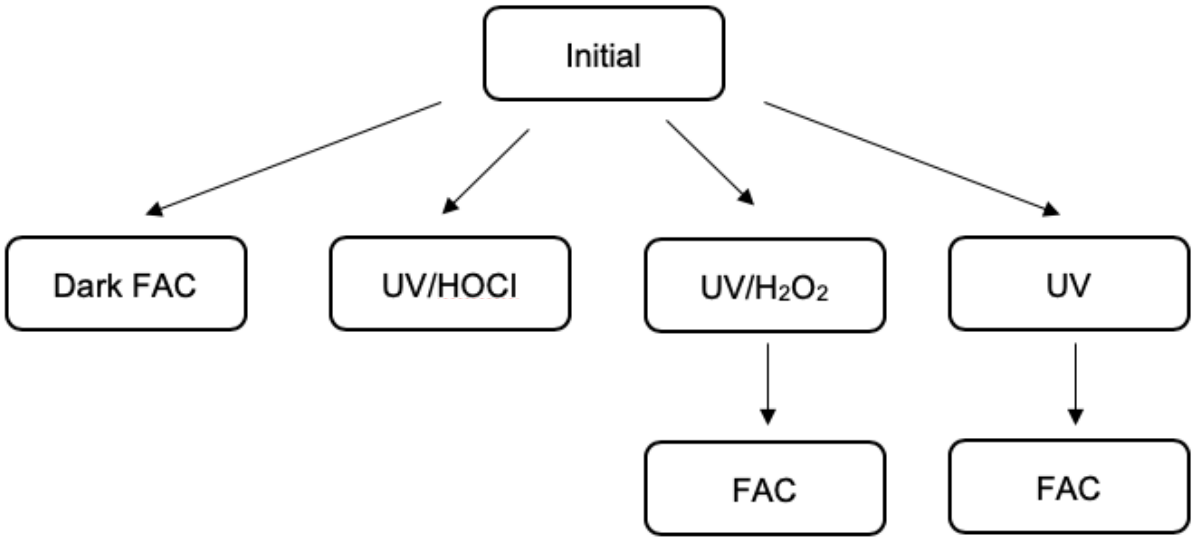

Schematic C2. Samples generated during the sequential treatment experiment.

Table C17. Total number of matched formulas, number of formulas with heteroatoms, and intensity weighted averages of H:C ($H:C_w$), O:C ($O:C_w$), and double-bond equivalents per carbon (DBE/C_w) for initial and treated TMW2 samples.

treatment	total formulas	CHO formulas	CHON formulas	CHOS formulas	CHOP formulas	CHOCl formulas	$H:C_w$	$O:C_w$	DBE/C_w
initial	3580	2149	748	704	50	2	1.33	0.40	7.60
direct photolysis	3685	2157	749	831	65	1	1.35	0.40	7.08
dark chlorination	3370	2088	652	647	24	4	1.36	0.38	7.17
dark H_2O_2	2871	1743	435	615	165	1	1.48	0.32	5.75
chlorine photolysis	3157	1890	542	690	131	124	1.44	0.34	6.04
H_2O_2 photolysis	3001	1884	447	670	90	0	1.45	0.36	5.84
direct photolysis + dark chlorination	2545	1566	212	699	126	32	1.51	0.31	5.35
H_2O_2 photolysis + dark chlorination	3413	1971	666	789	60	27	1.34	0.45	7.13

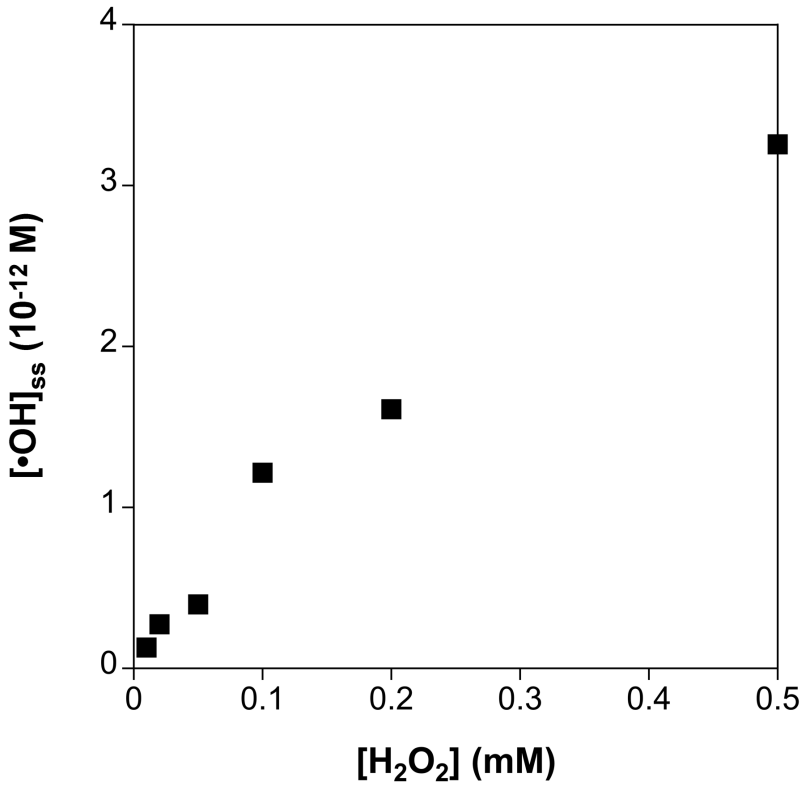

Figure C15. [•OH]$_{ss}$ during H_2O_2 photolysis at 254 nm pH 6.5 as a function of H_2O_2 concentration.

C10. References

(1) Watts, M. J.; Linden, K. G.; Chlorine photolysis and subsequent $^{\bullet}OH$ radical production during UV treatment of chlorinated water. *Water Res.* **2007**, 41(13), 2871-2878.

(2) Laszakovits, J. R.; Berg, S. M.; Anderson, B. G.; O'Brien, J. E.; Wammer, K. H.; Sharpless, C. M.; *p*-Nitroanisole/pyridine and *p*-nitroacetophenone/pyridine actinometers revisited: Quantum yield in comparison to ferrioxalate. *Environ. Sci. Technol. Lett.* **2017**, 4(1), 11-14.

(3) Bulman, D. M.; Mezyk, S. P.; Remucal, C. K.; The impact of pH and irradiation wavelength on the production of reactive oxidants during chlorine photolysis. *Environ. Sci. Technol.* **2019**, 53(8), 4450-4459.

(4) Berg, S. M.; Whiting, Q. T.; Herrli, J. A.; Winkels, R.; Wammer, K. H.; Remucal, C. K.; The role of dissolved organic matter composition in determining photochemical reactivity at the molecular level. *Environ. Sci. Technol.* **2019**, 53(20), 11725-11734.

(5) Galbavy, E. S.; Ram, K.; Anastasio, C.; 2-Nitrobenzaldehyde as a chemical actinometer for solution and ice photochemistry. *J. Photochem. Photobio. A* **2010**, 209(2-3), 186-192.

(6) Baeza, C.; Knappe, D. R.; Transformation kinetics of biochemically active compounds in low-pressure UV photolysis and UV/H_2O_2 advanced oxidation processes. *Water Res.* **2011**, 45(15), 4531-4543.

(7) Buxton, G. V.; Subhani, M. S.; Radiation chemistry and photochemistry of oxychlorine ions. Part 2. Photodecomposition of aqueous solutions of hypochlorite ions. *J. Chem. Soc. Faraday Trans. 1* **1972**, 68, 958-969.

(8) Ding, S.; Deng, Y.; Bond, T.; Fang, C.; Cao, Z.; Chu, W.; Disinfection byproduct formation during drinking water treatment and distribution: A review of unintended effects of engineering agents and materials. *Water Res.* **2019**, 160, 313-329.

(9) Remucal, C. K.; Manley, D.; Emerging investigators series: The efficacy of chlorine photolysis as an advanced oxidation process for drinking water treatment. *Environ. Sci. Water Res. Tech.* **2016**, 2(4), 565-579.

(10) Hasegawa, K.; Neta, P.; Rate constants and mechanisms of reaction of chloride ($Cl_2^{\bullet-}$) radicals. *J. Phys. Chem.* **1978**, 82(8), 854-857.

(11) Mártire, D. O.; Rosso, J. A.; Bertolotti, S.; Le Roux, G. C.; Braun, A. M.; Gonzalez, M. C.; Kinetic study of the reactions of chlorine atoms and $Cl_2^{\bullet-}$ radical anions in aqueous solutions. II. Toluene, benzoic acid, and chlorobenzene. *J. Phys. Chem. A* **2001**, 105(22), 5385-5392.

(12) Fang, J.; Fu, Y.; Shang, C.; The roles of reactive species in micropollutant degradation in the UV/free chlorine system. *Environ. Sci. Technol.* **2014**, 48(3), 1859-1868.

(13) Von Sonntag, C.; von Gunten, U. *Chemistry of ozone in water and wastewater treatment* (IWA publishing, **2012**).

(14) Elovitz, M. S.; von Gunten, U.; Kaiser, H.-P. The influence of dissolved organic matter character on ozone decomposition rates and R_{ct}. Barrett, Sylvia E.; Krasner, Stuart W.; Amy, Gary L.; eds.; ACS Publications: **2000**.

(15) Grigor'ev, A. E.; Makarov, I. E.; Pikaev, A. K.; Formation of $Cl_2^{\bullet-}$ in the bulk of solution during radiolysis of concentrated aqueous solutions of chlorides. *Khimiya Vysokikh Ehnergij* **1987**, 21(2), 99-102.

(16) Jayson, G. G.; Parsons, B. J.; Swallow, A. J.; Some simple, highly reactive, inorganic chlorine derivatives in aqueous solution. *J. Chem. Soc. Faraday Trans. 1* **1973**, 69, 1597-1607.

(17) Kläning, U. K.; Wolff, T.; Laser flash photolysis of HClO, ClO^-, HBrO, and BrO^- in aqueous solution. Reactions of Cl^- and Br^- atoms. *Ber. Bunsen. Ges. Phys. Chem.* **1985**, 89, 243-245.

(18) Nagarajan, V.; Fessenden, R. W.; Flash photolysis of transient radicals. 1. X_2^- with X = Cl, Br, I, and SCN. *J. Phys. Chem.* **1985**, 89(11), 2330-2335.

(19) Yu, X.-Y.; Barker, J. R.; Hydrogen peroxide photolysis in acidic aqueous solutions containing chloride ions. I. Chemical mechanism. *J. Phys. Chem. A* **2003**, 107(9), 1313-1324.

(20) Yeatts Jr., L. R. B.; Taube, H.; The kinetics of the reaction of ozone and chloride ion in acid aqueous solution. *J. Am. Chem. Soc.* **1949**, 71(12), 4100-4105.

(21) Hoigné, J.; Bader, H.; Haag, W. R.; Staehelin, J.; Rate constants of reactions of ozone with organic and inorganic compounds in water—III. Inorganic compounds and radicals. *Water Res.* **1985**, 19(8), 993-1004.

(22) Li, W.; Jain, T.; Ishida, K.; Remucal, C. K.; Liu, H.; A mechanistic understanding of the degradation of trace organic contaminants by UV/hydrogen peroxide, UV/persulfate and UV/free chlorine for water reuse. *Environ. Sci. Water Res. Technol.* **2017**, 3(1), 128-138.

(23) Zehavi, D.; Rabani, J.; Pulse radiolytic investigation of O_{aq}^- radical ions. *J. Phys. Chem.* **1971**, 75(11), 1738-1744.

(24) Haag, W. R.; Hoigné, J.; Ozonation of water containing chlorine of chloramines: Reaction products and kinetics. *Water Res.* **1983**, 17(10), 1397-1402.

(25) Buxton, G. V.; Greenstock, C. L.; Helman, W. P.; Ross, A. B.; Critical review of rate constants for reactions of hydrated electrons, hydrogen atoms and hydroxyl radicals ($^{\bullet}OH$/ $O^{\bullet-}$) in aqueous solution. *J. Phys. Chem. Ref. Data* **1988**, 17(2), 513-886.

(26) Mertens, R.; Von Sonntag, C.; Photolysis (λ= 254 nm) of tetrachloroethene in aqueous solutions. *J. Photochem. Photobio. A* **1995**, 85, 1-9.

(27) Forsyth, J. E.; Zhou, P.; Mao, Q.; Asato, S. S.; Meschke, J. S.; Dodd, M. C.; Enhanced inactivation of *Bacillus subtilis* spores during solar photolysis of free available chlorine. *Environ. Sci. Technol.* **2013**, 47(22), 12976-12984.

(28) Hodgeson, J. W.; Cohen, A. L.; Munch, D. J.; Hautman, D. P.; Method 551.1. Determination of chlorination disinfection byproducts, chlorinated solvents, and halogenated pesticides/herbicides in drinking water by liquid-liquid extractions and gas chromatography with electron capture detection. *U.S. Environmental Protection Agency, Cincinnati* **1995**.

(29) Hodgeson, J. W.; Collins, J.; Barth, R. E.; Munch, D. J.; Munch, J. W.; Pawlecki, A. M.; Method 552.2 determination of haloacetic acids and dalapon in drinking water by liquid-liquid extraction, derivatization and gas chromatography with electron capture detection. *U.S. Environmental Protection Agency, Cincinnati* **1995**.

(30) Maizel, A. C.; Remucal, C. K.; The effect of advanced secondary municipal wastewater treatment on the molecular composition of dissolved organic matter. *Water Res.* **2017**, 122, 42-52.

(31) Ziegler, G.; Gonsior, M.; Fisher, D. J.; Schmitt-Kopplin, P.; Tamburri, M. N.; Formation of brominated organic compounds and molecular transformations in dissolved organic matter (DOM) after ballast water treatment with sodium dichloroisocyanurate dihydrate (DICD). *Environ. Sci. Technol.* **2019**, 53(14), 8006-8016.

(32) Dittmar, T.; Koch, B.; Hertkorn, N.; Kattner, G.; A simple and efficient method for the solid-phase extraction of dissolved organic matter (SPE-DOM) from seawater. *Limnol. Oceanogr. Methods* **2008**, 6, 230-235.

(33) Koch, B. P.; Dittmar, T.; Witt, M.; Kattner, G.; Fundamentals of molecular formula assignment to ultrahigh resolution mass data of natural organic matter. *Anal. Chem.* **2007**, 79(4), 1758-1763.

(34) Maizel, A. C.; Li, J.; Remucal, C. K.; Relationships between dissolved organic matter composition and photochemistry in lakes of diverse trophic status. *Environ. Sci. Technol.* **2017**, 51(17), 9624-9632.

(35) Maizel, A. C.; Remucal, C. K.; Molecular composition and photochemical reactivity of size-fractionated dissolved organic matter. *Environ. Sci. Technol.* **2017**, 51(4), 2113-2123.

(36) Sleighter, R. L.; Hatcher, P. G.; Molecular characterization of dissolved organic matter (DOM) along a river to ocean transect of the lower chesapeake bay by ultrahigh resolution electrospray ionization fourier transform ion cyclotron resonance mass spectrometry. *Marine Chem.* **2008**, 110(3-4), 140-152.

(37) Hockaday, W. C.; Purcell, J. M.; Marshall, A. G.; Baldock, J. A.; Hatcher, P. G.; Electrospray and photoionization mass spectrometry for the characterization of organic matter in natural waters: A qualitative assessment. *Limnol. Oceanograph. Methods* **2009**, 7(1), 81-95.

(38) Kujawinski, E. B.; Longnecker, K.; Blough, N. V.; Vecchio, R. D.; Finlay, L.; Kitner, J. B.; Giovannoni, S. J.; Identification of possible source markers in marine dissolved organic matter using ultrahigh resolution mass spectrometry. *Geochim. Cosmochim. Acta* **2009**, 73(15), 4384-4399.

(39) Sleighter, R. L.; Hatcher, P. G.; The application of electrospray ionization coupled to ultrahigh resolution mass spectrometry for the molecular characterization of natural organic matter. *J. Mass Spectrom.* **2007**, 42(5), 559-574.

(40) Kim, S.; Kramer, R. W.; Hatcher, P. G.; Graphical method for analysis of ultrahigh-resolution broadband mass spectra of natural organic matter, the van Krevelen diagram. *Anal. Chem.* **2003**, 75(20), 5336-5344.

(41) Chuang, Y.-H.; Chen, S.; Chinn, C. J.; Mitch, W. A.; Comparing the UV/monochloramine and UV/free chlorine advanced oxidation processes (AOPs) to the UV/hydrogen peroxide AOP under scenarios relevant to potable reuse. *Environ. Sci. Technol.* **2017**, 51(23), 13859-13868.